UNIVERSITY OF SOUTHAMPTON

Faculty of Engineering, Science and Mathematics

School of Chemistry

A quantitative characterisation of phospholipid composition and biosynthesis in HeLa cells and nuclei - a mass spectrometry study

by

Charlotte Victoria Hague MChem (Hons)

Submitted for the degree of Doctor of Philosophy

November 2009

UNIVERSITY OF SOUTHAMPTON
Faculty of Engineering, Science and Mathematics
School of Chemistry

Doctor of Philosophy

ABSTRACT

A quantitative characterisation of phospholipid composition and biosynthesis in HeLa cells and nuclei - a mass spectrometry study

by Charlotte Victoria Hague

Nuclei from Human cells have been shown to contain a pool of endonuclear phospholipid that is distinct from the nuclear membrane. It has been suggested that this endonuclear phospholipid is involved in the regulation of nuclear processes such as transcription.

This study utilised tandem electrospray ionisation mass spectrometry to determine, quantitatively, the phospholipid content of cultured HeLa (Human cervical carcinoma) cells and their isolated naked nuclei. Endonuclear PC, DAG and PI was found to be enriched in disaturated molecular species with respect to the whole cell.

Whole cell and endonuclear phospholipid content was monitored throughout the cell cycle following treatment with the cell cycle blocking agent mimosine. The molecular species composition of both whole cell and nuclei was found to differ to that of cells which had not been treated with mimosine. These compositional differences between synchronous and asynchronous cell populations were found to relate to the saturation level of the molecular species.

Using a combination of ESI-MS and stable isotope labelling, the biosynthesis of PC was monitored in both whole cells and nuclei. The molecular species composition of newly synthesised PC closely resembled that of endogenous PC. Biosynthesis of PC was found to continue in nuclei that had been removed from the cell and stripped of their nuclear envelope.

Contents

List of Figures

Conventions and notation

Abbreviation	Term
ESI-MS	Electrospray Ionisation Mass spectrometry
CID	Collision Induced Dissociation
Choline-d9	9-deuterated methylcholine
Q-TOF MS	Quadrupole Time of Flight Mass spectrometry
PC	Phosphatidylcholine
PE	Phosphatidylethanolamine
PA	Phosphatic acid
PS	Phosphatidylserine
PI	Phosphatidylinositol
DAG	Diacylglycerol
PG	Phosphatidylglycerol
DMEM	Dulbeccos modifed Eagle's medium
FBS	Fetal Bovine Serum
PIPES	piperazine-N,N'-bis(2-ethanesulfonic acid)
HBSS	Hanks balanced Salt Solution
PBS	Phosphate Buffered Saline
DPBS	Dulbeccos Phosphate Buffered Saline
FACS	Fluorescence-activated cell sorting (Flow cytometry)
TEM	Transmission Electron Microscopy

Declaration

This thesis is the result of work undertaken whilst registered as a postgraduate student at the University of Southampton. The thesis and the work presented in the thesis are both my own and have been generated by me as the result of my own original research. Where I have consulted the published work of others, this is always clearly attributed. I have acknowledged all main sources of help. None of this work has been published before submission.

Charlotte Hague

Acknowledgements

I would like to thank the following people for their guidance, help and support throughout my PhD;

- Prof. George Attard
- Dr Marcus Dymond
- Prof. Tony Postle
- Dr Grielof Koster
- Dr Alan Hunt

I would also like to thank;

- Southampton Biomedical Imaging Unit for their help with TEM
- Dr David Holmes and Dr John Lowry (BD Biosciences) for their help with Flow Cytometry
- Dr Nefeli Tsaloglou for help with radiation experiments
- Rosemary Bell of the University Radiation Protection Service
- The EU neonuclei project for funding

Special thanks to my parents.

Chapter 1

Introduction

1.1 Motivation - the neonuclei project

The eukaryotic cell nucleus was the first organelle to be discovered and is often referred to as the control centre of the cell as it contains all the cell's chromosomal DNA. The nucleus is separated from the cell cytoplasm by the nuclear envelope, a double membrane structure, which is contiguous with the endoplasmic reticulum. Unlike prokaryotic cells, DNA transcription occurs in the nucleus and is separate to translation which occurs in the cytoplasm [1, 2, 3].

The European Commission funded Neonuclei project was a collaborative research programme between five EU Universities. The overall aim of the Neonuclei project was to produce synthetic analogues of cell nuclei which are transcription-competent in the presence of the necessary transcription factors. These neonuclei could be interfaced with systems such as cell-free protein expression [4] to synthesise complex biological molecules on demand. To guide the design and preparation of neonuclei it was necessary to study and understand the components and biological processes of real nuclei. It was also important to identify suitable systems for mimicking the properties of real nuclei. Consequently two approaches were adopted; a top down approach to better understand nuclear structure and a bottom up approach to investigate the use of synthetic systems to replicate nuclear function.

The work presented in this thesis formed part of the top down approach to understanding real nuclei. The aim of this study was to investigate the composition and role of endonuclear phospholipids in eukaryotic cells. Using HeLa cells as the

basis for this work, mass spectrometry was utilised to elucidate and quantify both whole cell and endonuclear phospholipid content. The remainder of this chapter introduces some background information which is relevant to this research.

1.2 Phospholipids

Lipids are a large and diverse group of compounds which include classes such as fatty acids, sterols and eicosanoids. The structure and biological function of different lipid types can vary significantly. In this thesis, however, discussion is limited to phospholipids (also termed glycerophospholipids). The general structure of phospholipids is shown in Figure 1.1. They consist of a glycerol backbone to which a polar phosphate headgroup and two non-polar fatty acid chains are connected. Phospholipids are typically classified by their headgroup structure, examples of which are shown in Figure 1.1.

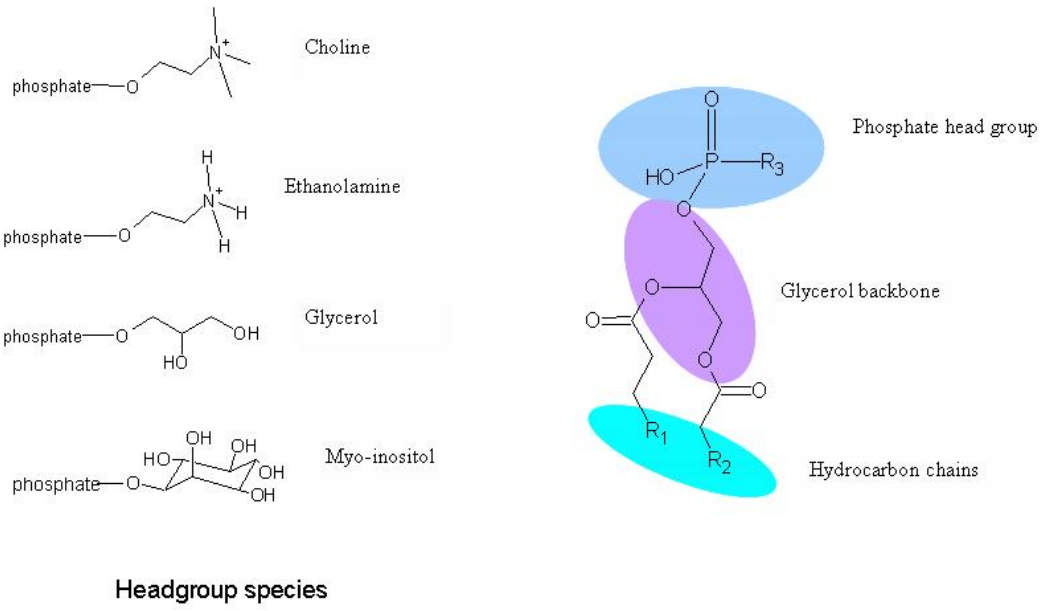

Figure 1.1: Chemical structure of a typical phospholipid and examples of typical head groups.

The number of possible chain lengths and degree of saturation of the fatty acids creates a large number of different molecular species within each headgroup class. Within this thesis the following nomenclature is used to denote the structure of

a phospholipid; PC16:0/18:1 where PC indicates the head group species (in this example, phosphatidylcholine), 16 represents the number of carbons in the fatty acid chain and 0 the number of double bonds. The numbers after the forward slash indicate the number of carbons and double bonds for the second fatty acid chain if it is present. The letter 'a' can be included after the numbers to denote that the fatty acid chain has an alkyl rather than acyl linkage.

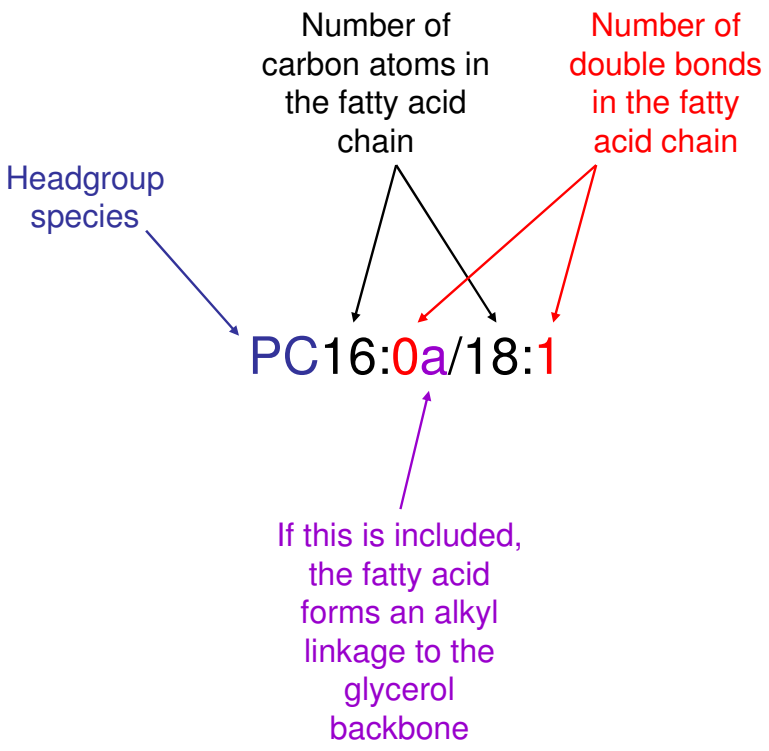

Figure 1.2: Nomenclature for phospholipids

All membrane lipids are amphiphilic and therefore tend to form aggregates in an aqueous environment. Phospholipids are are essential components of biological membranes and form a bilayer with the hydrophilic headgroups oriented towards the aqeous medium and the hydrophobic fatty acid chains towards the centre of the bilayer [1].

Phospholipids are not, however, simply the building blocks of biological membranes whose main function is cellular compartmentalisation. They are now known to perform a diverse range of roles within the cell from signal transduction to cytoskeletal support [5, 6, 7]. Indeed the biochemical and biophysical properties of membranes, which are affected by their phospholipid composition, play an impor-

tant role in the cell. The activity of some proteins for instance can be altered by interaction with a membrane. CTP:phosphocholine cytidyltransferase (CCT) is a rate limiting enzyme involved in biosynthesis of phosphatidylcholine and its activity is mediated by membrane association. CCT membrane binding (and therefore its activity) is thought to be modulated through a physical feedback signal due to the stored elastic stress (torque tension) of the bilayer, a property which is related to its lipid composition [8, 9].

Phospholipids and their derivatives are important signalling molecules involved in cellular processes such as apoptosis [7]. The phosphoinositide system for example plays a role in the release of intracellular calcium stores. Although it can not be described as a phospholipid, DAG (glycerol with two hydroxyl groups esterified to a fatty acid) is also discussed throughout this thesis as is is an important intermediate in the metabolism of phospholipids. DAG functions as a second messenger (a molecule that transfers signals from cell surface receptors to target molecules within the cell) and is involved in many cellular processes through its interaction with protein kinase C [10].

1.2.1 Phospholipids in the cell nucleus

The presence of phospholipids within the nucleus, but distinct from the nuclear envelope, has been demonstrated by several histochemical and biochemical techniques. Using gold-conjugated phospholipases, amorphous lipoprotein complexes were identified in the interchromatin of the nucleus, co-located with ribonucleoproteins [11]. Radioiodination of rat liver nuclear phospholipids demonstrated that phospholipids extracted from the chromatin were indeed present and not simply due to contamination from nuclear membranes [12]. More recently lipid mass spectrometry has been employed to determine the molecular species composition of certain phospholipids within the nuclear compartment [13].

Membranous structures within the nucleus have yet to be identified therefore the precise molecular organisation of these endonuclear phospholipids is still unclear [13, 14]. Many studies, however, indicate that endonuclear phospholipids are located with the chromatin domains and may play important roles in events such as gene transcription, DNA replication and passage through the cell cycle [13].

Enzymes necessary for phospholipid metabolism have also been found within the endonuclear compartment suggesting the presence of a separate nuclear metabolism [15, 16, 17]. Lipids are known to play an important role in cell signalling by generating bioactive metabolites in response to stimuli. Endonuclear phospholipid signalling, independent of that at the plasma membrane is therefore a possibility [13, 18, 19, 20].

1.3 The cell cycle

The process by which cells reproduce is described by the cell division cycle. In each cell division cycle a cell divides producing two genetically identical daughter cells. Figure 1.3 shows the phases of a standard eukaryotic cell cycle. The M phase (mitosis) is where cell division occurs and usually accounts for only a small fraction of the cell cycle. The remaining phases are known collectively as interphase during which the cell grows and prepares for cell division. During G1, the cell grows and at a certain point commits to transversing the entire cycle. Prior to this restriction point during the G1 phase, cells can also enter a resting state termed G0 in which they can remain for an unspecified time period before resuming their progress through the cell cycle [21, 22]. DNA replication occurs during the S phase leading to a doubling of the cellular DNA content. G2 provides additional time for growth before mitosis [23, 1, 10].

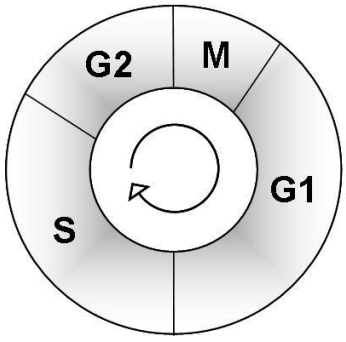

Figure 1.3: The phases of a standard eukaryotic cell cycle. The cell goes through phases of growth (G1 and G2 phases) and DNA synthesis (S phase) before undergoing mitosis (M phase) to produce two genetically identical daughter cells.

Although the cell cycle can be considered simply as four phases, in reality a large number of complex and coordinated events are required for successfull cell cycle progression. The transition from one stage to another is regulated by a group of proteins called the cyclin-dependent kinases. Activation of these kinases by another group of proteins called cyclins triggers the events which allow the cell to transverse the cell cycle. Checkpoints monitor events such as DNA replication so that mutations can be avoided. If a checkpoint is activated it sends a signal that delays cell cycle progression until the problem has been rectified [23, 24].

1.3.1 Phospholipids and the cell cycle

The creation of daughter cells during mitosis requires a doubling of the membrane phospholipid. If this did not occur it would result in cells of abnormal size and internal membrane surface. Changes in phospholipid metabolism are thought to be coordinated with events of the cell cycle. In the G1 phase, phospholipids are rapidly synthesised and degraded (turn over). It is possible that this metabolism, which can generate lipid second messengers, is required for further cell cycle progression [25]. Continued phospholipid synthesis coupled with reduced turnover during the S phase leads to a doubling of the phospholipid mass. Phospholipid metabolisim is thought to cease during the G2/M phase although this may not be true for all cell types [26, 27, 28]. It seems that phospholipid metabolism is linked to the cell cycle but it is unclear whether the phospholipid content can also effect cell cycle progression [29].

1.3.2 Cell cycle synchronisation

A normal cell population contains cells which are distributed randomly between all the phases of the cell cycle and is thus termed asynchronous. To investigate a particular part of the cell cycle, it is therefore necessary to bring the cell population into phase. Several methods of synchronisation are commonly used and are summarised in Table 1.1.

Method of synchronisation	Cell cycle phase	Mode of action
Serum starvation	G0/G1	Withdrawal of growth factors
Lovastatin	G0/G1	HMG-CoA reductase
Mimosine	G1/S	Ribonucelase reductase
Thymidine	S	dNTP synthesis
Aphidicolin	S	DNA polymerase
Nocodazole	G2/M	Destabilises microtubules
Mitotic shake off	G2/M	Selection of mitotic cells which detach from culture substrate
FACS	any	DNA content
Centrifugal elutriation	any	Cell size

Table 1.1: Methods of cell cycle synchronisation and the phase during which they act.

Chemical inhibitors such as mimosine or nocodazole reversibly arrest the cell cycle at a certain point. Cells continue to cycle until they reach this point after which their progression is halted. On release of the block the cell population resumes progression through the cell cycle with a high proportion of cells in phase. Application of these methods tends to be simple and results in a high degree of synchrony [30]. Non-chemical methods such as mitotic shake off, centrifugal elutriation and FACS can also be used and offer the advantage that normal progression of the cell through the cell cycle is not perturbed. Mitotic shake off relies on the observation that adherant cells become rounded and less firmly attached to the surface during mitosis and is thus only applicable to adherant cell lines. Centrifugal elutriation separates cells based on their size, a characteristic which tends to correlate to position in the cell cycle [30]. FACS allows cells to be sorted according to their DNA content after staining with a fluorescent DNA probe. FACS is discussed in more detail in section 1.4. Although these methods may reduce the risk of unexpected side effects caused by perturbing the normal cell cycle, they are less convenient when a large number of cells is required and can yield populations which are not sufficiently

synchronous [31].

Serum starvation induces synchronisation by removing a nutrient source which is required for cell division. The cells stop growing and enter a resting state called G0 phase or quiescence where they can remain until the nutrient source is replenished. The cells will then resume proliferation and continue cycling synchronously [32, 1]. This method can however alter the rate of progression through the cell cycle and questions have been raised regarding the entry of cells into a G0 phase [33, 34].

1.4 Flow cytometry

Flow cytometry is a technique which allows certain physical characteristics of particles, such as cells, to be determined as they flow in a stream of liquid through a beam of light. The particles are suspended in a fluid called the sheath fluid and carried through to the illumination point. At this point the particles scatter the incident laser light and emit fluorescence (if labelled with a fluorescent compound). Light scattered at small angles is called forward scatter (FSC) and is proportional to the size of the particle. Side scattered light (SSC) is collected perpendicular to the laser beam and gives an indication of the internal structure of the cell [35, 36]. Interaction of the laser with a fluorescently labelled particle will lead to emission of light at a specific wavelength (fluorescence) which can be detected by the flow cytometer. This technique can be used to measure the DNA content of a cell and thus determine the proportion of cells within each cell cycle phase. Fluorescent dyes such as propidium iodide are allowed to stoichiometrically bind to the DNA. Cells with more DNA will bind more of the dye and therefore fluoresce more strongly than those cells with less DNA. As the DNA content varies depending on the phase of the cell cycle it is therefore possible to determine the proportion of cells in each phase from the level of fluorescence [37, 38].

Some flow cytometers can also be used to sort particles on the basis of their measured characteristics. These are termed fluorescence activated cell sorters (FACS) however this term is often applied to flow cytometers that do not have this capability.

1.5 Mass spectrometry

A mass spectrometer allows the mass of a chemical compound to be determined by separating molecular ions according to their mass to charge ratio. Although many different types of mass spectrometer exist they all consist of three basic components; an ion source, a mass analyser and a detector [39].

The advent of 'soft ionisation' techniques such as electrospray and matrix-assisted laser desorption/ionisation have greatly improved the analysis of biological samples by mass spectrometry. These techniques avoid the problem of sample decompostion which can occur with electron ionisation. Electrospray ionisation (ESI) forms a spray of charged droplets from the tip of a needle to which a potential difference has been applied. The droplets undergo desolvation at atmospheric pressure until the ions are released and transferred into the mass analyser [39, 40, 41]. Two mechanisms by which ions are released from the droplet have been proposed - 'Coulomb explosion' and 'Ion evaporation'. This remains a topic for further research but is beyond the scope of this study [42, 43].

A mass analyser measures the mass to charge ratio of the gas phase ion produced by the ion source. Quadrupole mass analysers are made up of four parallel rods to which a fixed DC potential and an alternating radio frequency (RF) is applied. Opposite rods have a potential of

$$\phi_0 = +(U - V\cos\omega t) \text{ and } -\phi_0 = -(U - V\cos\omega t)$$

where 'U' is the applied direct potential and '$V\cos\omega t$' is the applied RF with frequency ω and amplitude 'V'. Ions entering along the z axis of the quadrupole will be subject to the electric field of the rods. Certain combinations of the direct and alternating potentials will allow specific ions to maintain a stable trajectory through the centre of the quadrapole. Other ions will be unstable in the electric field, hit the rods and therefore not be detected [44].

Quadrupoles can be placed in series to perform tandem mass analysis. An instrument consisting of three quadrupoles is depicted in figure 1.4. The second quadrupole acts as a collision cell producing fragments by colliding the ions with an inert gas such as argon. Several possible scan types are shown.

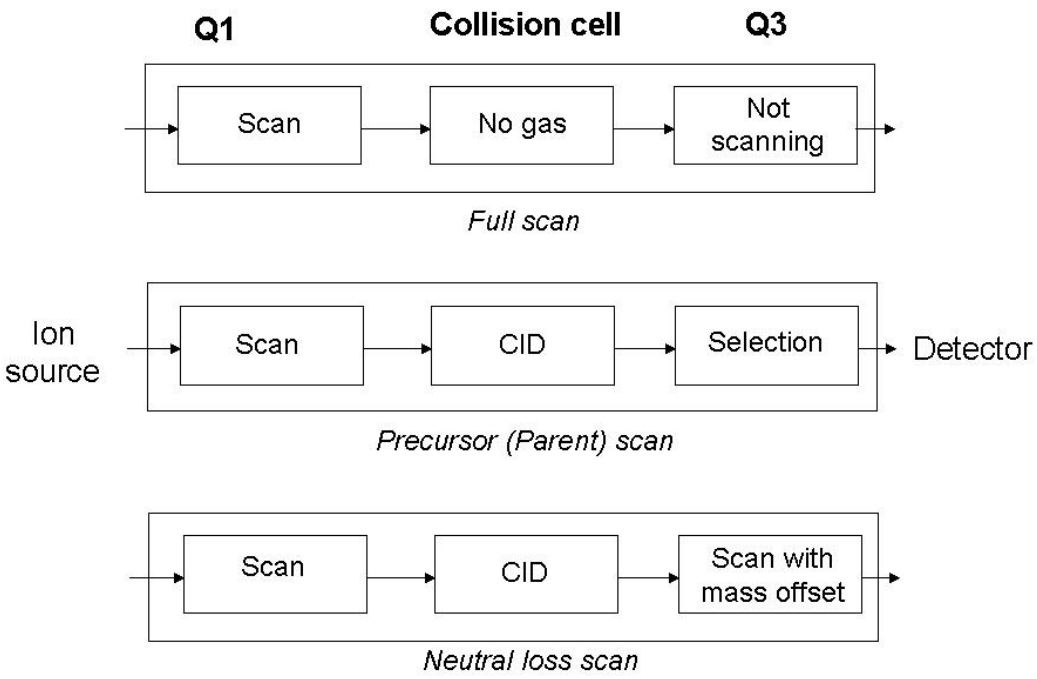

Figure 1.4: In the full scan mode ions are scanned in the first quadrupole (Q1) and allowed to pass through the remaining quardrupoles without fragmentation. This allows detection of all molecular ion species. If Q3 is set to detect a certain ion and Q1 scans all masses, all the ions that produce the selected ion after fragmentaion (CID) are detected - this is called a precursor scan. If Q1 and Q3 are scanned together but with a constant mass offset this is called a neutral loss scan. An ion is detected if it has given a fragment of mass equal to the mass offset between the two quadrupoles.

1.5.1 Mass spectrometry of phospholipids

Analysis of phospholipids has conventionally relied mainly on techniques such as thin layer chromatography (TLC) and gas chromatography. These techniques can be time consuming and require a large amount of sample [7, 5, 45]. Only since the advent of soft ionisation techniques (section 1.5) has mass spectrometry been widely used for the study of lipids. Mass spectrometry (ESI triple quadrupole MS) offers a good alternative to traditional methods due to its sensitivity and ability to identify different lipid species without prior separation by chromatography [46, 47]. The precursor and neutral loss scanning ability of triple quadrupole mass spectrometers enables detection of molecular species for each phospholipid class from a crude mixture thus allowing direct analysis of a cellular extract.

In addition to the relative abundance of molecular species for a certain phospholipid class, inclusion of internal standards allows quantitative analysis. Internal standards are phospholipid species of a known quantity that are not normally found in the cell line of interest. Comparision of the relative intensity of the species of interest to that of the internal standard allows absolute quantification [5].
The use of stable isotope labelling also allows dynamic studies of lipid synthesis to be undertaken [48]. In this study choline-d9 is used to follow the synthesis of PC. An excess of the deuterated choline causes the phosphocholine-d9 headgroup to be incorporated in any newly synthesised PC. This newly synthesised PC can then be distinguished from endogenous PC by ESI-MS as it produces an analogous fragment nine mass units higher. The same method can be applied to other phospholipid species [49].

1.6 HeLa cell culture

The culture of human cells *in vitro* has been invaluable to the research of fundamental cellular processess as it offers a relatively easy system for such research. One of the most widely used and well-known immortalised cell lines is HeLa. This cell line was derived from the cervical cancer cells of Henrietta Lacks and first cultured by George Gey in 1951. HeLa cells grow extremely well under cell culture conditions and are surprisingly resilient. This has, in many cases, led to cross-contamination of other cell lines with HeLa [50, 51, 52].
In this study we use a stably transfected HeLa cell line in which the histone H2B gene has been fused to the gene encoding for green fluorescent protein (GFP) from the jellyfish *Aequorea victoria*. This offers an alternative to DNA stains such as DAPI for live microscopy of nuclear chromatin structure [53, 54]. This cell line was used as a basis for the work described in this study as it was decided that a standard cell line should be used for studies by all members of the neonuclei project.

1.7 Thesis aims and overview

As described in section 1.1, the work presented in this thesis is an investigation into the composition and role of endonuclear phospholipids in eukaryotic cells. The purpose of this work was to further the understanding of components and processes present in real nuclei and thus contribute to the overall neonuclei project aim of producing synthetic analogues of cell nuclei.

Previous studies have provided strong evidence for the presence of endonuclear phospholipids in several cell lines (see section 1.2.1). The molecular species composition of some endonuclear phospholipid classes has also previously been determined by mass spectrometry [48]. The work presented in this thesis considerably extends these mass spectrometry studies by providing a quantitative determination of the endonuclear molecular species composition for all phospholipid classes and DAG in HeLa cells. Furthermore this work aims to determine any link between whole cell and endonuclear phospholipid composition and the cell cycle. This extends both the scope of previous mass spectrometry studies and also provides additional information to that obtained from previous studies using techniques such as chromatography [26].

As described in section 1.5.1 the biosynthesis of phospholipids can be followed by stable isotope labelling. Previous studies have determined the molecular species composition of newly synthesised endonuclear PC [55, 56]. In this study PC synthesis is followed using both stable and radio-isotope methods throughout the cell cycle. In addition, this study aimed to determine if naked nuclei (nuclei stripped of their nuclear envelope) are capable PC synthesis.

Although previously reported methods and protocols were initially followed, this thesis describes the process of modification and optimisation applied to these protocols to best address the requirements of the study. Method developments were applied to both sample preparation and data analysis protocols for mass spectrometry.

Chapter 2 describes the development and optimisation of experimental techniques used in this study. The compositional analysis of whole cell and endonuclear phospholipids, in relation to the cell cycle, is detailed in chapters 3 and 4 respectively. Chapter 5 describes the use of stable and radio-isotope methods to determine

the biosynthetic dynamics of phosphatidylcholine. Conclusions and experimental details are presented in chapters 6 and 7.

References

[1] B. Alberts, D. Bray, J. Lewis, M. Raff, K. Roberts, and J. Watson. *Molecular Biology of The Cell*. Garland Publishing, third edition, 1994.

[2] D. L. Spector. Macromolecular domains within the cell nucleus. *Anu. Rev. Cell. Biol*, 9:265–315, 1993.

[3] M. Dundr and T. Misteli. Functional architecture in the cell nucleus. *Biochem. J*, 356:297–310, 2001.

[4] F. Katzen, G. Chang, and W. Kudlicki. The past, present and future of cell-free protein synthesis. *Trends in Biotechnology*, 23(3):150–156, 2005.

[5] M. Pulfer and R. C. Murphy. Electrospray mass spectrometry of phospholipids. *Mass Spectrometry Reviews*, 22:332–264, 2003.

[6] J.S. Forrester, S.B. Milne, P.T. Ivanova, and H.A. Brown. Computational lipidomics: A multiplexed analysis of dynamic changes in membrane lipid composition during signal transduction. *Mol Pharmacol*, 65(4):813–821, 2004.

[7] S. Milne, P. Ivanova, J. Forrester, and H. A. Brown. Lipidomics: An analysis of cellular lipids by ESI-MS. *Methods*, 39:92–103, 2006.

[8] G. Attard, R. Templer, W. Smith, A. Hunt, and S. Jackowski. Modulation of CTP:phosphocholine cytidyltransferase by membrane curvature elastic stress. *PNAS*, 97(16):39032–9036, 2000.

[9] J. Beard, G. S. Attard, and M. J. Cheetham. Integrative feedback and robustness in a lipid biosynthetic network. *Journal of the Royal Society Interface*, 5:533–543, 2008.

[10] C. Mathews, K. van Holde, and K. Ahern. *Biochemistry.* Addison Wesley Longman, third edition, 2000.

[11] N. M. Maraldi, G. Mazzotti, S. Capitani, R. Rizzoli, N. Zini, S. Squarzoni, and F. Manzoli. Morphological evidence of function-related localisation of phospholipids in the cell nucleus. *Advan. Enzyme Regul.*, 32:73–90, 1992.

[12] E. Albi, M. Mersel, M.L Tomassoni, and M.P. Viola Magni. Rat liver chromatin phospholipids. *Lipids*, 29(10):715–719, 1994.

[13] A. Hunt, G. T. Clark, G. S. Attard, and A. D. Postle. Highly saturated endonuclear phosphatidylcholine is synthesized in situ and colocated with CDP-choline pathway enzymes. *The Journal of Biological Chemistry*, 276(11):8492–8499, 2001.

[14] J. D. Lewis and D. Tollervey. Like attracts like: Getting RNA processing together in the nucleus. *Science*, 288:1385–1389, 2000.

[15] E. Albi, M. Micheli, and M.P. Viola Magni. Phospholipids and nuclear RNA. *Cell Biology International*, 20(6):407–412, 1996.

[16] E. Albi and M.P. Viola Magni. The role of intranuclear lipids. *Biology of the Cell*, 96:657–667, 2004.

[17] A.V. Alessenko and E.B Burlakova. Functional role of phospholipids in the nuclear events. *Bioelectrochemistry*, 58:13–21, 2002.

[18] A. Hunt and A.D. Postle. Phosphatidylcholine biosynthesis inside the nucleus: is it involved in regulating cell proliferation? *Advan. Enzyme Regul.*, 44:173–186, 2004.

[19] K. Tamiya-Koizumi. Nuclear lipid metabolism and signalling. *Journal of Biochemistry*, 132:13–22, 2002.

[20] C.S D'Santos, J.H. Clarke, and N. Divecha. Phospholipid signalling in the nucleus. *Biochemica et Biophysica Acta*, 1436:201–232, 1998.

[21] A.B.Pardee. A restriction point for control of normal animal cell proliferation. *Proc.Nat.Acad.Sci.*, 64(4):1286–1290, 1974.

[22] K.Vermeulen, D.R.Van Bockstaele, and Z.N.Berneman. The cell cycle: a review of regulation, deregulation and therapeutic targets in cancer. *Cell Prolif.*, 36:131–149, 2003.

[23] K. Collins, T. Jacks, and N. Pavletich. The cell cycle and cancer. *PNAS*, 94:2776–2778, 1997.

[24] L. H. Hartwell and T. A. Weinert. Checkpoints: Controls that ensure the order of cell cycle events. *Science*, 246:629–634, 1989.

[25] F. Terce, H. Brun, and D. Vance. Requirement of phosphatidylcholine for normal progression through the cell cycle in C3H/10T1/2 fibroblasts. *Journal of Lipid Research*, 35:2130–2142, 1994.

[26] S. Jackowski. Coordination of membrane phospholipid synthesis with the cell cycle. *The Journal of Biological Chemistry*, 269:3858–3867, 1994.

[27] W. Lin and G. Arthur. Phospholipids are synthesised in the G2/M phase of the cell cycle. *IJBCB*, 39:579–605, 2007.

[28] K. Yokoyama *et al.* Changes in composition of newly synthesised sphingolipids of HeLa cells during the cell cycle. *Eur J Biochem*, 249:450–455, 1997.

[29] S. Jackowski. Cell cycle regulation of membrane phospholipid metabolism. *The Journal of Biological Chemistry*, 271:20219–20222, 1996.

[30] A. Kurose, T. Tanaka, X. Huang, F. Traganos, and Z. Darzynkiewicz. Synchronization in the cell cycle by inhibitors of DNA replication induces histone H2AX phosphorylation: an indication of DNA damage. *Cell Prolif.*, 39:231–240, 2006.

[31] S. Tate and P. Ko Ferrigno. *Cell Cycle: Synchronisation at various stages.* John Wiley and sons, 2005.

[32] M. Griffin. Synchroniszation of some Human cell strains by serum and calcium starvation. *In Vitro*, 12(5):393–398, 1976.

[33] S. Cooper. On the proposal of a G0 phase and the restriction point. *FASEB Journal*, 12:367–373, 1998.

[34] S. Cooper. Rethinking synchronisation of mammalian cells for cell cycle analysis. *Cell. Mol. Life Sci*, 60:1099–1106, 2003.

[35] A. Longobardi Givan. *Flow cytometry first principles.* Wiley-Liss, second edition, 2001.

[36] BD Biosciences. *Introduction to Flow cytometry: A Learning Guide*, 11-11.32-01 edition, 2000.

[37] J. W. Gray, F. Dolbeare, M. G. Pallavicini, W. Beisker, and F. Waldman. Cell cycle analysis using flow cytometry. *Int. J. Radiat. Biol*, 49(2):237–255, 1986.

[38] J. Lawry. DNA staining for flow cytometry. *Proceedings RMS*, 36(1):61–65, 2001.

[39] G. Siuzdak. *Mass spectrometry for Biotechnology.* Academic Press, first edition, 1996.

[40] G. Siuzdak. *The Expanding Role of Mass Spectrometry in Biotechnology.* MCC Press, second edition, 2006.

[41] T. Covey. Atmospheric Pressure Ionisation. BMSS LC/MS Short Course, 2007.

[42] P. Kebarle and L. Tang. From ions in solution to ions in the gas phase - the mechanism of electrospray mass spectrometry. *Analytical Chemistry*, 65(22):972–986, 1993.

[43] S.Gaskell. Electrospray: Principles and practice. *Journal of Mass Spectrometry*, 32:677–688, 1997.

[44] E. de Hoffmann and V. Stroobant. *Mass spectrometry, Principles and Applications.* Wiley, second edition, 2001.

[45] B. Brügger, G. Erben, R. Sandhoff, F. T. Wieland, and W. D. Lehmann. Quantitative analysis of biological membrane lipids at the low picomole level by nano-electrospray ionisation tandem mass spectrometry. *PNAS*, 94:2339–2344, 1997.

[46] X. Han and R. Gross. Global analyses of cellular lipidomes directly from crude extracts of biological samples by ESI mass spectrometry: a bridge to lipidomics. *Journal of Lipid Research*, 44:1071–1079, 2003.

[47] M. Koivusalo, P. Haimi, L. Heikinheimo, R. Kostiainen, and P. Somerharju. Quantitative determination of phospholipid compositions by ESI-MS: effects of acyl chain length, unsaturation, and lipid concentration on instrument response. *J. Lipid Res.*, 42(4):663–672, 2001.

[48] A. Hunt and A.D. Postle. Mass spectrometry determination of endonuclear phospholipid composition and dynamics. *Methods*, 39:104–111, 2006.

[49] A. Hunt. *Nuclear Matrix phosphatidylcholine biosynthesis: Why is it essential, why is there so much and why is it so saturated?*, pages 47–61. Research Signpost, 2003.

[50] J. Masters. HeLa cells 50 years on: the good, the bad and the ugly. *Nature Reviews*, 2:315–319, 2002.

[51] A. Cardenas T. Shimahara J. Segura-Aguilar P. Caviedes D. D. Allen, R. Caviedes. Cell lines as in vitro models for drug screening and toxicity studies. *Drug Development and Industrial Pharmacy*, 31:757–768, 2005.

[52] S. Gartler. Apparent HeLa cell contamination of Human heteroploid cell lines. *Nature*, 217:750–751, 1968.

[53] D. Zink, N. Sadoni, and E. Stelzer. Visualizing chromatin and chromosomes in living cells. *Methods*, 29:42–50, 2003.

[54] G. Wahl T. Kanda, K. Sullivan. Histone-GFP fusion protein enables sensitive analysis of chromosome dynamics in living mammalian cells. *Current Biology*, 8:377–385, 1998.

[55] A. Hunt. Dynamic lipidomics of the nucleus. *Journal of Cellular Biochemistry*, 97:244–251, 2006.

[56] A. Hunt. Completing the cycles; the dynamics of endonuclear lipidomics. *BBA*, 1761:577–587, 2006.

Chapter 2

Method development

2.1 Introduction

Experimental and analytical techniques descibed in this thesis have been optimised to best address the requirements of this study. The development of these methods is detailed in this chapter.

2.2 Development of Biological methods

Before analysis of phospholipid composition by mass spectrometry can take place, the biological sample must be prepared. Figure 2.1 shows the process followed to obtain a phospholipid sample from cells in culture (a synchronised population). To assess the endonuclear phospholipid composition, it is first necessary to isolate nuclei that are free from nuclear envelope. The method of isolating these nuclei is discussed in detail in section 2.2.1. Quantitative analysis of both whole cells and nuclei requires an assessment of cell/nuclei number. Section 2.2.2 describes the current technique for this analysis and proposes an alternative method. The process of cell cycle synchronisation is discussed in Chapter 3.

2.2.1 Isolation of naked nuclei

As introduced in section 1.2.1, endonuclear phospholipids are distinct from those in the nuclear envelope. Complete removal of the nuclear envelope is therefore es-

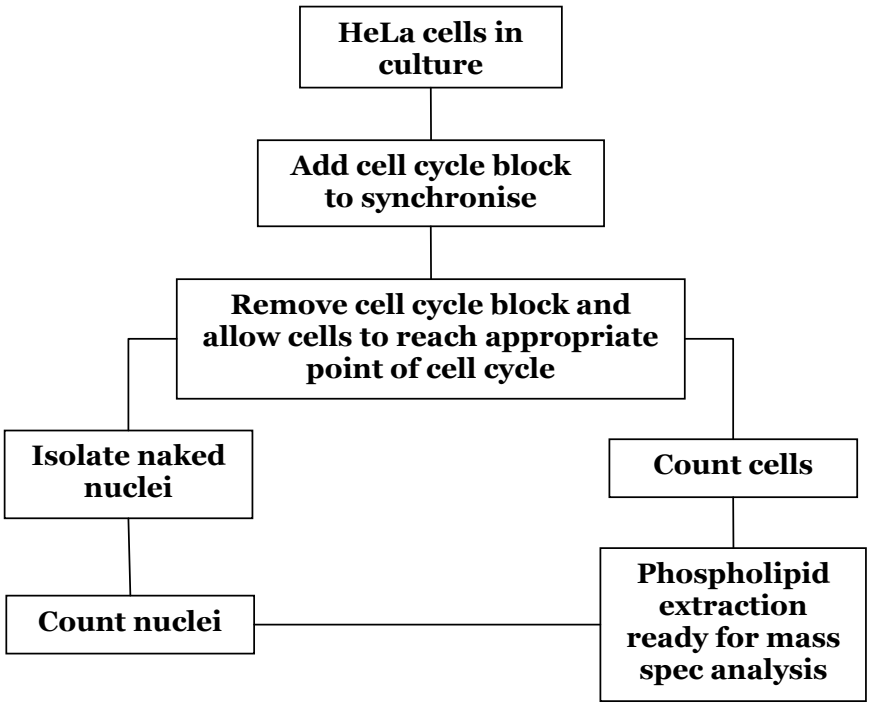

Figure 2.1: Process of preparing cells for analysis. Once the synchronised cell population has reached an appropriate cell cycle point, the culture medium is removed and the cells counted before phospholipid extraction. If nuclei are required, these are extracted prior to counting and phospholipid extraction.

sential to avoid contamination of the endonuclear phospholipid pool and thus allow accurate compositional analysis. Detergents can be used to solubilise membranes and release cellular components. Section 7.3 describes the protocol whereby these cellular components are separated through a sucrose density gradient. The nuclear fraction forms a pellet which is easily separated from the other less dense cellular components. The resultant nuclei are free from nuclear envelope and are therefore termed 'naked nuclei'.

Previous studies have indicated that complete nuclear envelope removal can be achieved with the detergent Triton-X-100 [1]. Unfortunately residual detergent contamination of the naked nuclei can be carried through during phospholipid extraction. Triton-X-100 is easily detected by mass spectrometry under positive ionisation conditions and fragmentaion of the molecule leads to peaks at 44 mass unit intervals in the P193 spectra (Table 7.2) as shown in Figure 2.2. These peaks can obscure those of the species of interest and lead to signal reduction through ion supression [2].

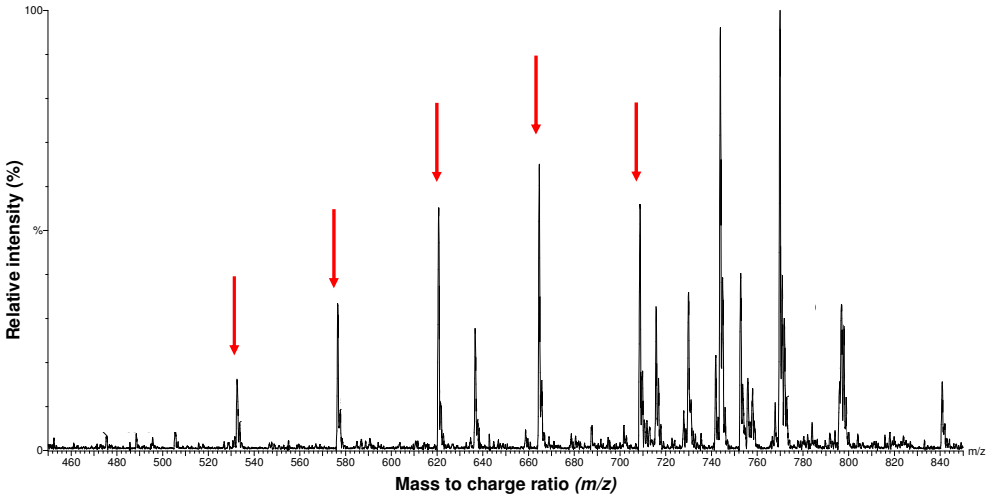

Figure 2.2: A typical P193 spectrum with detergent contamination. Peaks marked with arrows arise from the Triton-X-100 contamination.

Solid phase extraction cartridges can be used to separate the phospholipid into neutral, acidic, PC and PE fractions (section 7.7.1) [1, 3]. Triton-X-100 contaminant is eluted with the neutral fraction, removing the problem of detergent peaks in the P193 spectrum. Although this method can be used to remove Triton-X-100, some loss of sample during the procedure is likely. This is significant due to the small quantity of phospholipid which can be extracted from the endonuclear compartment.

Alternative surfactants to Triton-X-100 were investigated with the aim of successfully isolating naked nuclei whilst removing the problem of artefactual mass spectrometry results. Table 2.1 summarises the results from several detergents. Use of the ionic detergents (SDS and CTAB) did not result in intact nuclei even at low concentrations. The non-ionic detergents all gave intact nuclei, however, only n-Decyl β-D-Maltopyranoside allowed extraction of the nuclear fraction without causing experimental or analytical difficulties.

Detergent	Comments
SDS	Caused complete cell lysis. No nuclei obtained.
CTAB	Caused complete cell lysis. No nuclei obtained.
n-Decyl β-D-Maltopyranoside	Nuclei were isolated. No detergent peaks visible when analysed by mass spectrometry.
Nonidet P-40	Nuclei were isolated. Detergent peaks detected when analysed by mass spectrometry.
n-Octyl α-D-Glucopyranoside	Nuclei were extracted. Detergent easily crystallised out of solution, limiting the viability of the extraction procedure.

Table 2.1: Detergents investigated as alternatives to Triton-X-100 for the isolation of naked nuclei. Initially the same concentration as used for Triton-X-100 was used in each case (section 7.3). The procedure was repeated with a reduced concentration of detergent but the results remained the same.

Transmission electron microscopy (TEM) was used to assess the effectiveness of n-Decyl β-D-Maltopyranoside for nuclear envelope removal. Figure 2.3 shows TEM pictures of a whole cell, a n-Decyl β-D-Maltopyranoside extracted nucleus and a Triton-X-100 extracted nucleus. The double membrane, 'track-like', morphology of the nuclear envelope is visible in the whole cell however there is no evidence of this structure in either of the nuclear samples. These results strongly indicate that n-Decyl β-D-Maltopyranoside is a suitable alternative to Triton-X-100 for naked nuclei preparation.

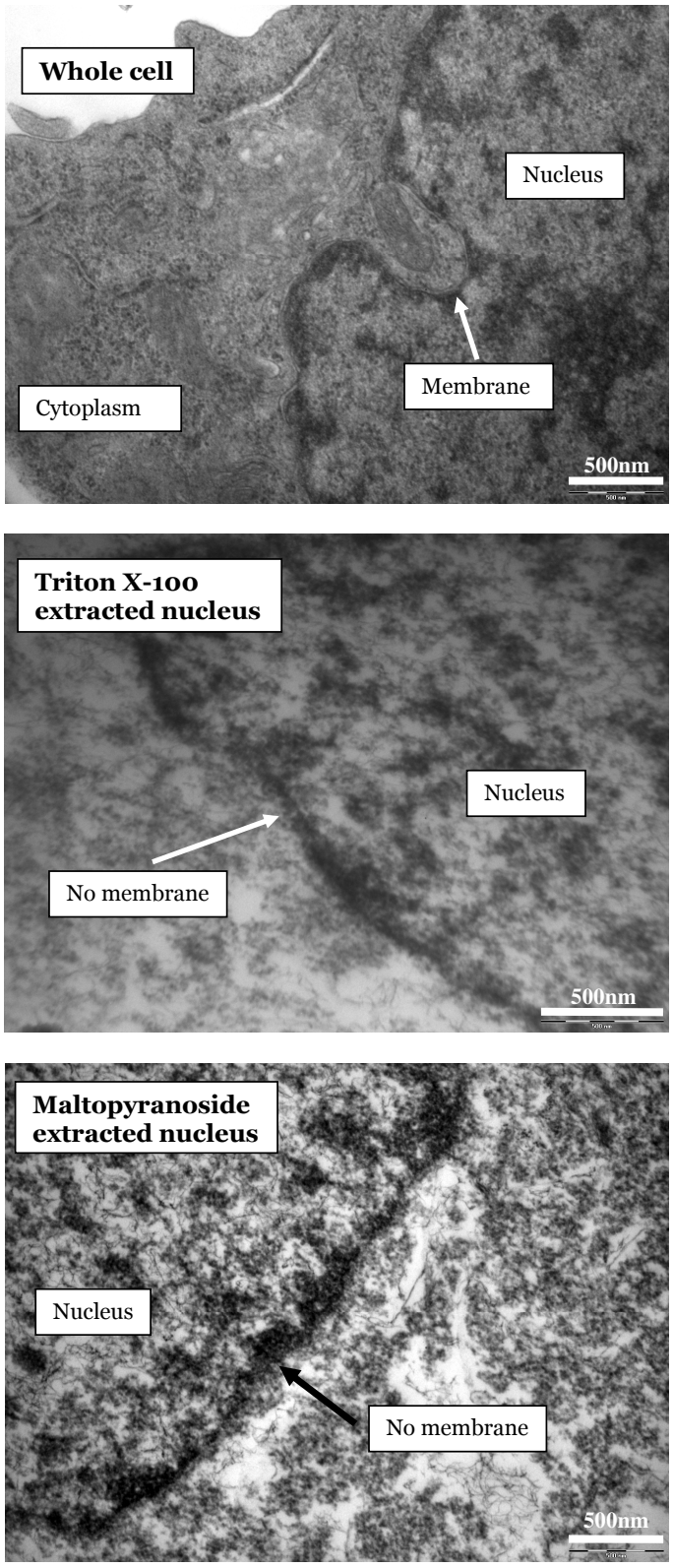

Figure 2.3: TEM image of whole cells and nuclei isolated with n-Decyl β-D-Maltopyranoside and Triton-X-100. The double membrane of the nuclear envelope is visible in the the whole cell but not in either nuclei sample. In this figure n-Decyl β-D-Maltopyranoside has been shortened to 'maltopyranoside'.

2.2.2 Cell counting

Phospholipid quantification requires an accurate estimate of the number of cells per sample. Haemocytometer counting was used (section 7.4.2) as this is simple, relatively quick and requires very little sample. Assessment of the number of naked nuclei by this method is however more challenging than for intact cells. Rather than forming a uniform suspension in buffer, naked nuclei can become clumped making it extremely difficult to obtain an accurate count.

The feasablility of using DNA content per sample as an indicator of naked nuclei number was investigated. When phospholipid is extracted using the Bligh Dyer protocol the DNA content of the cells remains in the aqueous layer. This DNA can be isolated and quantified as described in section 7.10. The DNA from several whole cell samples was quantified and compared to the haemocytometer count (Figure 2.4). As DNA content is dependent on cell cycle position, synchronised cell populations were used (discussed in more detail in section 3.3). The 6hr and 9hr synchronised cells show a clear increase in DNA content with cell number but this is not apparent for those at 3hrs and 12hrs. A clear trend is not obvious for all data sets indicating that the DNA method does not offer a significant improvement on haemocytometer counting. This data is however preliminary and with further improvement could provide a valuable alternative.

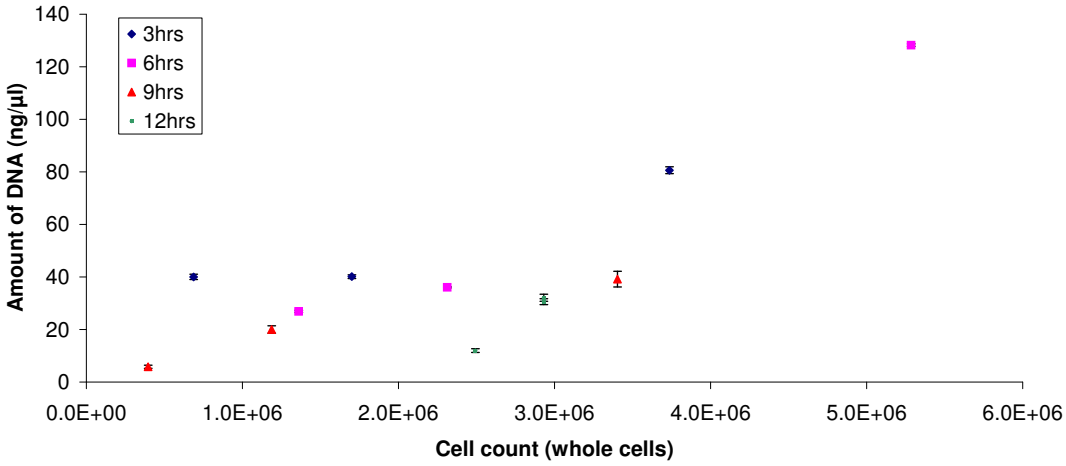

Figure 2.4: The DNA content of whole cells at various cell cycle points compared to the cell count obtained by haemocytometer counting.

2.3 Development of data analysis protocols for mass spectrometry

To produce a final data set from ESI-MS measurements, a number of processes are applied in sequence to the raw results. These processes, as summarised in Figure 2.5, correct for instrumental noise, isotope effects and measurement errors.

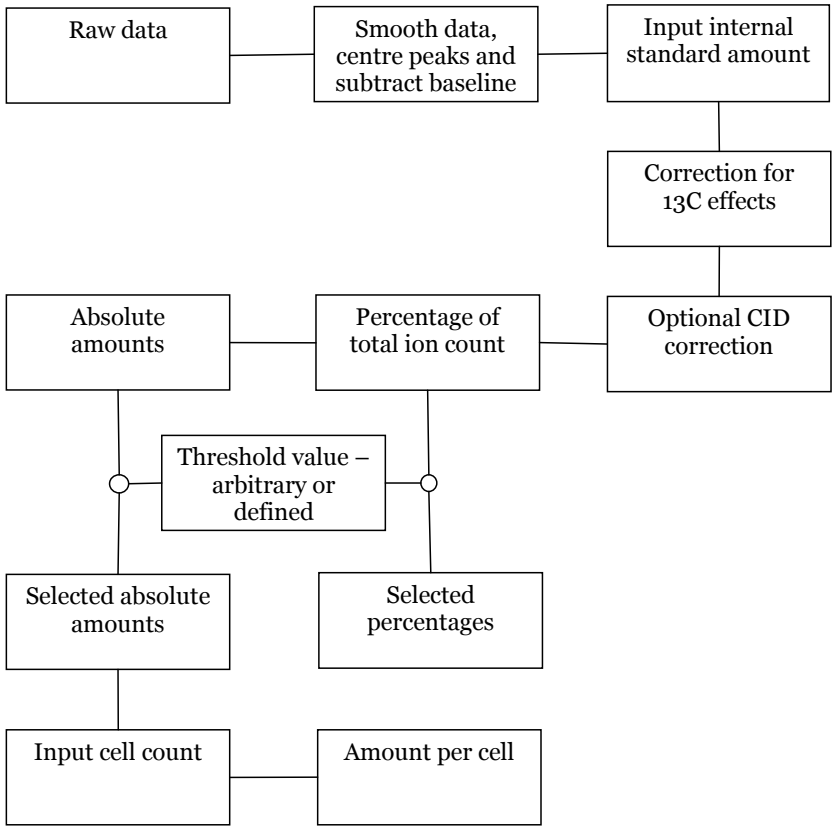

Figure 2.5: Process of analysing mass spectrometry data. The raw data is smoothed to remove noise and converted to centroid format following baseline subtraction. The data is then corrected for isotope effects and collision induced dissociation (CID) error. The species are expressed as a percentage of the total ion count. The absolute amount of each species is determined by comparison with the internal standard ion count. Species above a chosen threshold value (below which data can not be distinguished from noise) are selected and presented as a percentage of the total ion count of the selected species. The same threshold is applied to the absolute amounts and following input of cell count, the amount of each species per cell is determined.

The CID correction and threshold value can be affected by instrument settings, enviromental conditions and the nature of the sample. To avoid arbitrary assignment of correction values, a method to assess these processes was adopted and is discussed further in sections 2.3.2 and 2.3.3.
The reproducibility of the final results are dependent not only on the accuracy of the data processing but also on the stability of the mass spectrometer. Section 2.3.5 provides a detailed assessment of spectrometer reproducibility and its effect.

2.3.1 Standard mixture

Natural variations and small differences in the method of collection, preparation and storage can lead to inconsistencies between biological samples. An accurate assessment of instrument stability and also the corrections applied to mass spectrometry results however requires measurement of identical samples. Any inconsistencies between measurements are thus not attributable to the sample being measured. A standard mixture of known phospholipids at known concentrations was therefore prepared. Table 2.2 shows the constituents of this standard mixture and their concentrations. Section 7.4.5 details the preparation of the standard mixture and how it was aliquoted to give identical samples. The use of this standard mixture is discussed further in sections 2.3.3 and 2.3.5.

Phospholipid class	Molecular species	Concentration
PC	18:1/18:1	10 nM
PC	16:0/16:0	10 nM
PC	16:0/14:0	10 nM
PC	20:0/20:0	10 nM
DG	16:0/18:1	2 nM
DG	12:0/12:0	2 nM
PS	16:0/16:0	2 nM
PS	18:1/18:1	2 nM
PS	14:0/14:0	2 nM
PA	18:1/18:1	2 nM
PA	16:0/16:0	2 nM
PA	14:0/14:0	2 nM
PE	18:1/18:1	2 nM
PE	14:0/14:0	2 nM

Table 2.2: Standard mixture compostition. This mixture was prepared accurately to give many identical samples which could be run to assess instrument stability and the effect of applied corrections.

2.3.2 Error due to CID

In the collision cell of the mass spectrometer sample molecules collide with argon gas and are fragmented (collision induced dissociation or CID). The energy required to break up these molecules is related to their size with larger molecules requiring more energy. Lighter molecules tend to scatter more following collision and are often lost outside the quadrupole field. The efficiency at which fragments are transferred through the mass spectrometer is related to the combination of both these effects [4]. The mass spectrometer is optimised to produce a maximum transfer efficiency at a particular m/z value, usually in the middle of the chosen range. The further away the molecule of interest is from the optimised mass, the less the transfer efficiency. A correction for this effect has been previously reported on, however the value is dependent on the instrument settings at that time [1]. A

full scan allows all ions to pass through the mass spectrometer without collision and is therefore not affected by this transfer efficiency. Comparision of the breakdown scan with the full scan therefore allows the magnitude of this effect to be assessed. Figure 2.6 shows an example of this assessment under current settings. The ratio of precursor scan values to full positive scan values is constant across the mass range indicating that the correction needed is minimal.

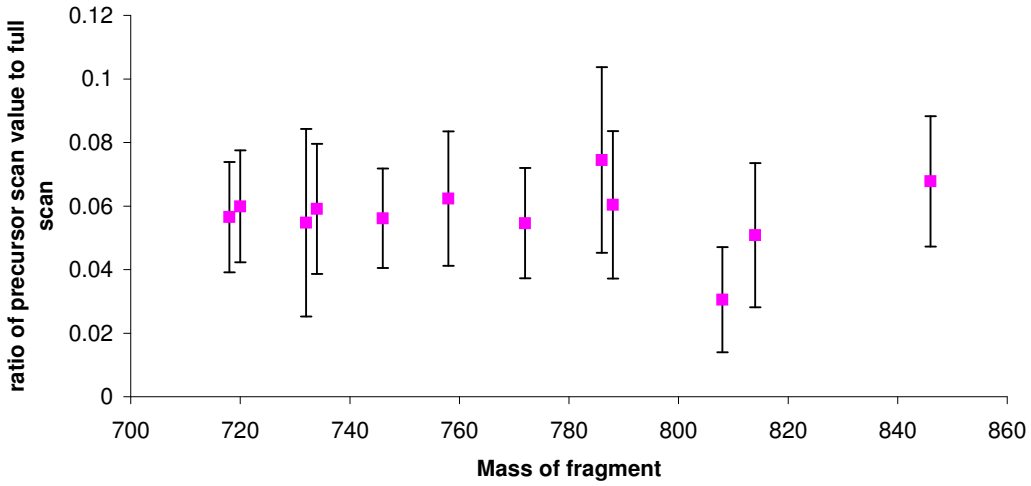

Figure 2.6: Ratio of P184 scan to the full positive scan. This comparison indicates that the response is very similar across the mass range for this species under current settings.

2.3.3 Peak selection

All peaks from a mass spectrum are expressed as a percentage of the total ion count, however some of these peaks are a result of background fluctuations. During the analysis of mass spectrometry data it is important to select only sample peaks and not those that are due to this background noise. A threshold value is therefore chosen below which sample peaks are not distinguishable from noise. Any data points which fall below this threshold value are not included in any further analysis steps. The remaining 'selected' species are expressed as a percentage of the total ion count for those selected species.

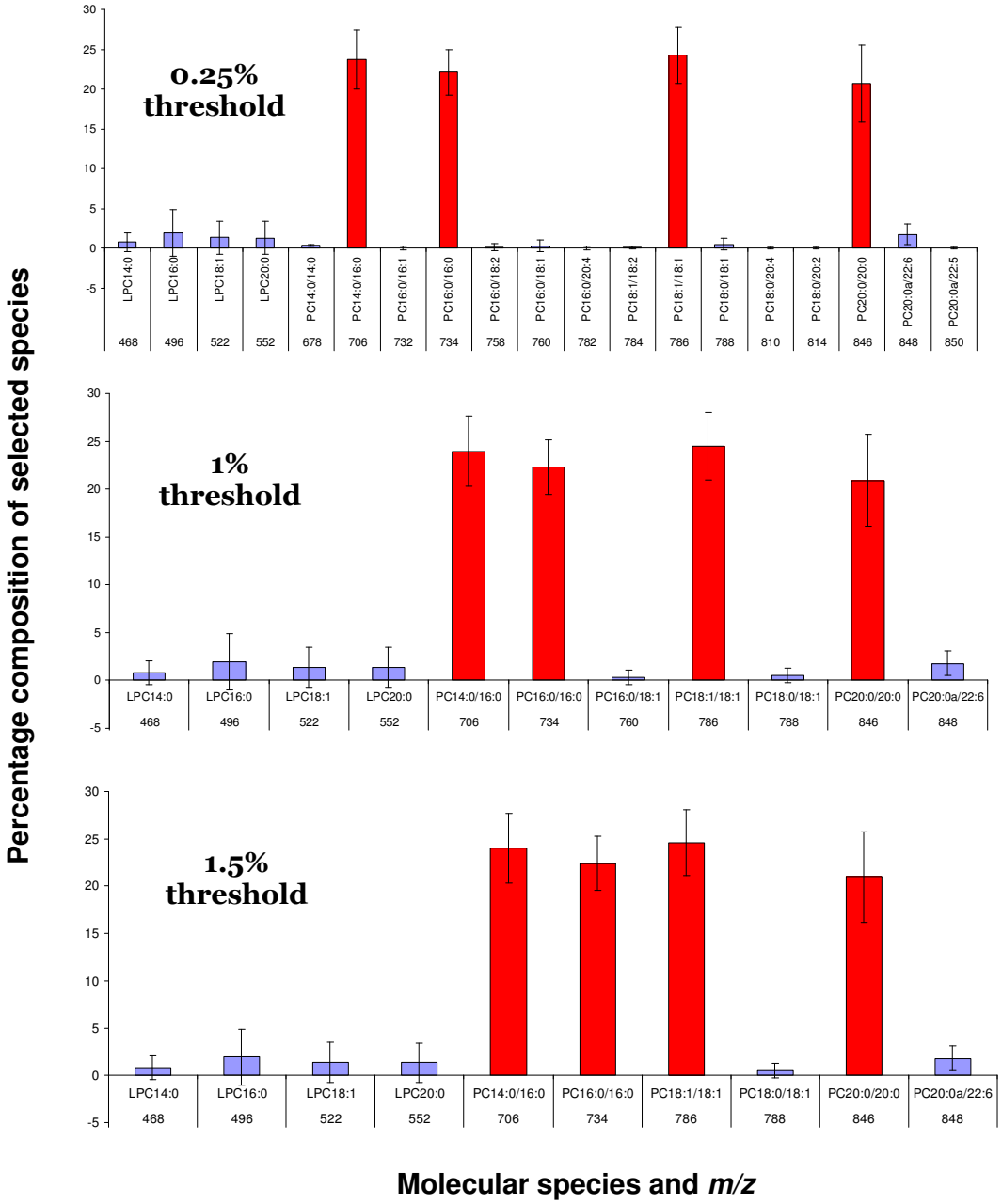

Figure 2.7: Peak selections with different threshold values. The species shown in red are those present in the standard mixture. The lyso PC species which remain at 1.5 % threshold are probably due to breakdown of the species in the collision cell. Error bars represent the first standard deviation of 58 independent measurements and therefore include instrument instability.

As the standard mixture composition is known (section 2.3.1), it was used to provide an estimate of this threshold value. If species which are not present in the mixture remain following the selection process then the threshold value is too low. If however species known to be present are removed then the threshold is too high. Figure 2.7 shows the result of three different threshold values for the PC headgroup species in the standard mixture. A similar analysis was performed for all headgroup classes and the results are summarised in Table 2.3. PI was not included in the standard mixture as this was not readily available therefore the threshold for this species was estimated to be 1.5%.

Phospholipid class	**Threshold value (%)**
PC	1.5
PE	1.5
DG	4.0
PA	2.5
PS	2.0

Table 2.3: Threshold values below which sample peaks are not distinguishable from noise

2.3.4 Accuracy of internal standards

Inclusion of internal standards allows the amount (moles) of phospholipid in a sample to be quantified (section 1.5.1). The intensity of the signal from the species of interest is compared to that of the internal standard to provide an estimate of the amount of the sample species. The internal standard must be prepared carefully to allow an accurate quantification of the sample species (section 7.4.4).

A colorimetric method based on the formation of a complex between phospholipids and ammonium ferrothiocyantate was used to assess the accuracy of prepared internal standards [5]. For each phospholipid species a calibration curve of concentration versus optical density was prepared, an example of which is shown in Figure 2.8 (see also section 7.5).

Following the same method, the absorbance of the internal standard was deter-

mined and compared to the calibration curve to determine its concentration. The concentration of the internal standards found by this method agreed well with their expected value from calculation indicating that they were accurately prepared.

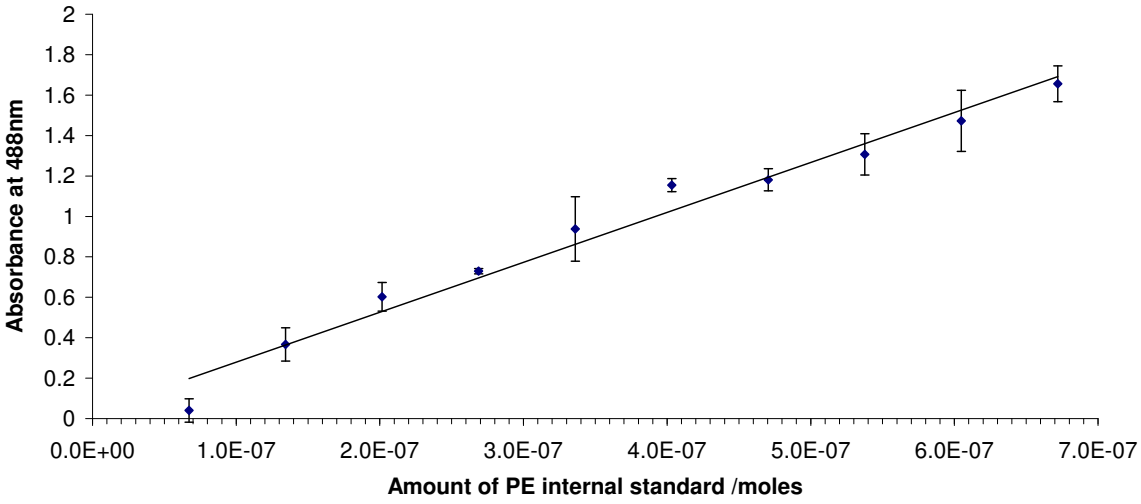

Figure 2.8: A colorimetric method based on the formation of a complex between phospholipids and ammonium ferrothiocyantate used to assess the accuracy of prepared internal standards. This figure represents a calibration curve of absorbance at 488nm versus the amount of PE species.

2.3.5 Instrument stability

Mass spectrometric analysis of a complete sample set can require data acquisition over a number of hours or days. As described in section 2.3.2, the efficiency at which fragments are transferred through the mass spectrometer following CID is dependent on the quadrupole field and the pressure of the collision cell. Variations in instrument settings, source conditions and collision cell gas pressure which may arise between measurements can therefore lead to changes in the resultant spectrum [6]. A distinction must therefore be made between real results and artefacts resulting from spectrometer instability.

The standard mixture of known phospholipids (sections 2.3.1 and 7.4.5) was used to assess inter-session reproducibility of mass spectrometry results. Figure 2.9A shows the percentage composition of PC molecular species in the standard mixture

when measured by mass spectrometry on three separate occasions over a period of three months. Results from the same day incur a very small error (represented by the error bars) however there is a noticeable variation between measurements. The PC20:0/20:0 (m/z 846) species was used as an internal standard and the resulting quantified data is shown in Figure 2.9B. The error in percentage composition of the internal standard molecular species is carried through for this analysis, therefore the variation between data sets is greater.

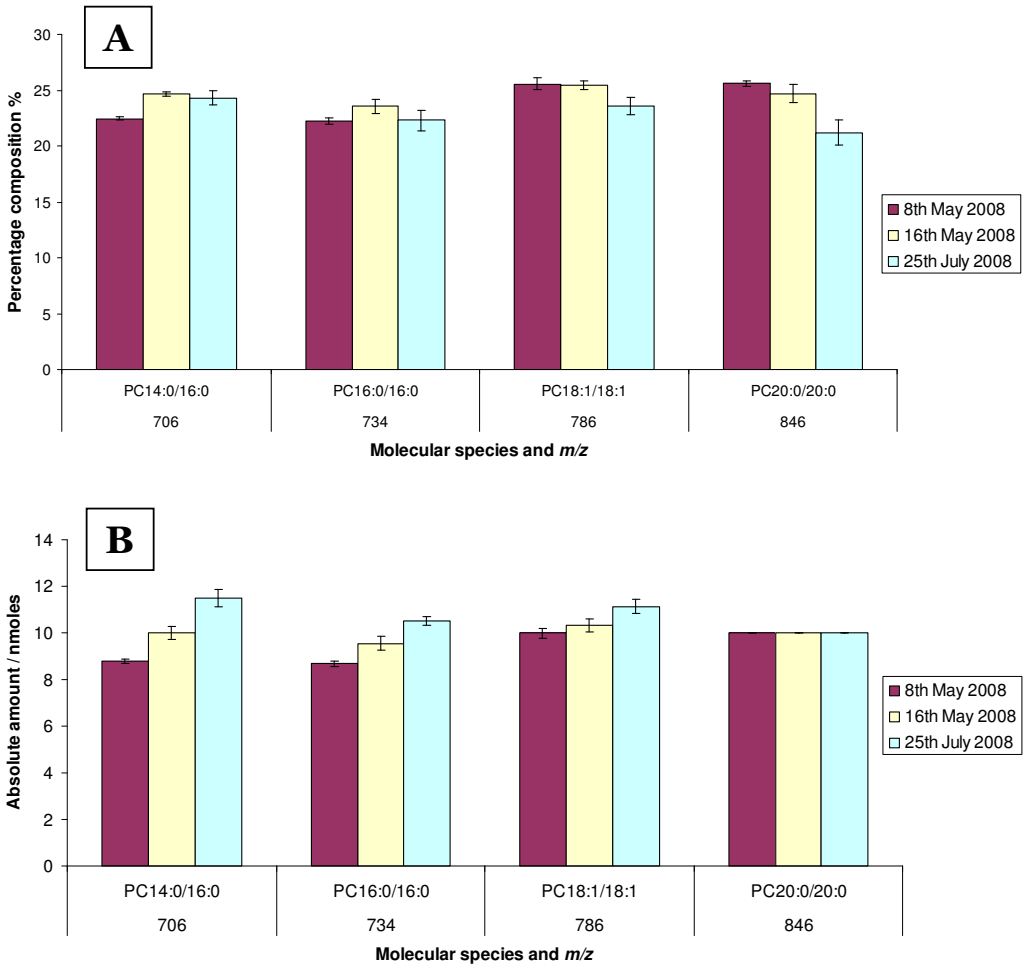

Figure 2.9: A: Percentage composition of PC molecular species in the standard mixture, measured on three occasions over a period of three months. B: The amount per cell of the PC molecular species in the standard mixture determined by using PC20:0/20:0 as the internal standard. Error bars represent the first standard deviation of three measurements on the same day.

The coefficient of variance is defined as the ratio of the standard deviation to the mean. It allows variability to be determined even when comparing between datasets with markedly different means. Figure 2.10 shows the coefficient of variance (CV) for percentage composition measurements of the PC standard mixture. The CV for data obtained over a long period of time is indeed larger than that of data obtained during the same session.

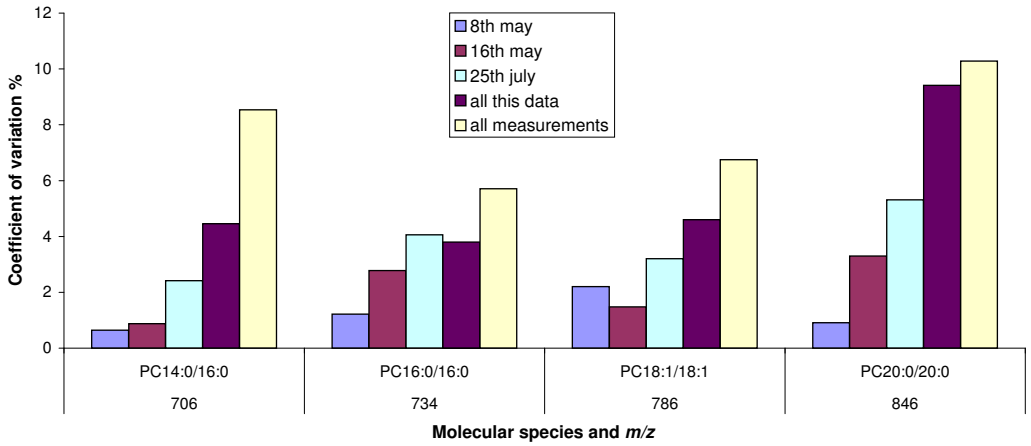

Figure 2.10: Coefficient of variance for the standard mixture PC percentage composition results. The CV for each time point in figure 2.9, the total CV for these points and the overall CV for every standard mixture measurement (spanning from May 2007 to December 2008) is shown.

The same analysis was applied to the standard mixture data for PA and is shown in Figure 2.11. In this case, the CV for data obtained during the same session is not significantly smaller than that obtained over a longer period of time. Similar analysis was applied to all phospholipid species in the standard mixture and is presented in Appendix A (figures A.1 to A.3). The CV of percentage composition measurements for each phospholipid species is summarised in Table 2.4.

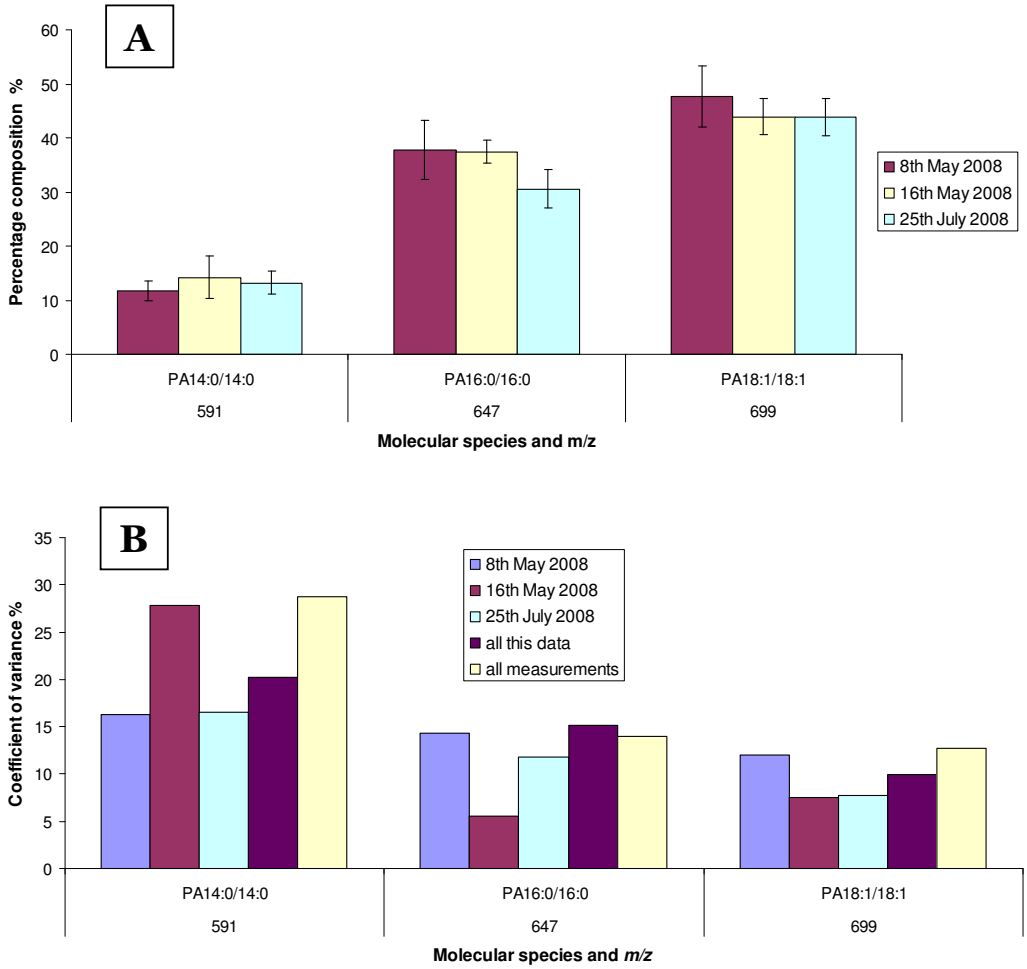

Figure 2.11: A: Percentage composition of PA molecular species in the standard mixture measured on three occasions over a period of three months. B: Coefficient of variance for the standard mixture PA percentage composition results

		Maximum coefficient of variance/ %		
Phospholipid class	**Molecular species**	**Day**	**3 months**	**All measurements**
PC	14:0/16:0	2.4	4.5	8.5
	16:0/16:0	4.1	3.8	5.7
	18:1/18:1	3.2	4.6	6.8
	20:0/20:0	5.3	9.4	10.3
PE	14:0/14:0	7.2	19.3	15.2
	18:1/18:1	3.7	9.6	8.9
PS	14:0/14:0	20.4	25.0	19.7
	16:0/16:0	13.0	10.3	9.5
	18:1/18:1	19.2	14.8	20.5
PA	14:0/14:0	27.8	20.2	28.8
	16:0/16:0	14.3	15.2	14.0
	18:1/18:1	12.0	9.9	12.7
DG	12:0/12:0	9.6	11.1	22.8
	16:0/18:1	7.1	10.3	12.4

Table 2.4: Maximum CV for percentage composition measurements of each phospholipid species in the standard mixture

To minimise the effect of this instrument variability, data sets should be as far as possible collected on the same day. When comparing between data sets measured on different occasions the possibility of instrument instability must be noted. Although a direct comparison of values may be affected by such instability, consistent patterns between data sets can still be considered as real.

2.3.6 Q-TOF

Time of flight mass spectrometry can also be used to characterise lipid species. In a time of flight analyser, ions are accelerated into a tube which is field free. Ions of lower m/z reach a higher velocity than those of higher m/z therefore the time it takes for ions to travel a set distance is a measure of m/z. In this study the time of flight analyser is used in tandem with a quadrupole to allow species selection.

Ions are introduced into the quadrupole where a particular mass is selected. These ions are then fragmented in the collision cell and all possible fragments are detected in the time of flight analyser. This procedure is repeated for other masses until a spectrum of all the possible fragments for each species is acquired. This information could be obtained by running a series of product ion (daughter) scans on the triple quadrupole ESI-MS however this would be a long process. The advantage of using the TOF-MS is that all the possible fragments are detected at one time [7].

Normally the peaks from the ESI triple quadrupole MS spectrum are assigned according to the most likely molecular species for each mass. Several different molecular species can however have the same mass therefore making correct assignments difficult. Q-TOF allows the complete fatty acid chain composition of each phospholipid class to be determined and thus allows a more accurate assignment of molecular species. Figure 2.12 shows the PC molecular species of whole cells and nuclei which were found to be present by Q-TOF for each mass. The same analysis was applied to the other phospholipid species and is presented in Appendix A, Figures A.4 to A.8.

Mass	Originally assigned species	Species found to be present by TOF analysis. In order of intensity (most intense first)						
		whole cells			nuclei			
706	PC14:0/16:0	16:0/14:0			16:0/14:0			
718	PC16:0a/16:1	16:0a/16:1	16:1a/16:0		16:0a/16:1	16:1a/16:0	14:0a/18:1	
720	PC16:0a/16:0	16:0a/16:0	18:0a/14:0		16:0a/16:0	18:0a/14:0		
732	PC16:0/16:1	16:0/16:1	14:0/18:1		16:0/16:1	14:0/18:1		
734	PC16:0/16:0	16:0/16:0			16:0/16:0			
744	PC16:0a/18:2	16:1a/18:1	16:0a/18:2	18:1a/16:1	16:1a/18:1	16:0a/18:2	16:1/18:1a	
746	PC16:0a/18:1	16:0a/18:1	18:1a/16:0	16:1a/18:0	16:0a/18:1	18:1a/16:0	18:0a/16:1	
748	PC16:0a/18:0	18:0a/16:0	16:0a/18:0		18:0a/16:0	16:0a/18:0		
758	PC16:0/18:2	16:0/18:2	16:1/18:1		16:1/18:1	16:0/18:2		
760	PC16:0/18:1	16:0/18:1	16:1/18:0		16:0/18:1			
772	PC18:0a/18:2	18:1a/18:1	18:0a/18:2		18:1a/18:1	18:0a/18:2		
774	PC18:0a/18:1	18:0a/18:1	18:1a/18:0		18:0a/18:1	18:1a/18:0		
782	PC16:0/20:4	20:4/16:0	18:1/18:3		16:0/20:4	18:1/18:3		
784	PC18:1/18:2	18:1/18:2	20:3/16:0		18:1/18:2	16:0/20:3	18:0/18:3	16:1/20:2
786	PC18:1/18:1	18:1/18:1	18:0/18:2	16:0/20:2	18:1/18:1	16:0/20:2	18:0/18:2	16:1/20:1
788	PC18:0/18:1	18:0/18:1	20:1/16:0		18:0/18:1	16:0/20:1		
794	PC18:1a/20:4	18:1a/20:4	20:4a/18:1		18:1a/20:4	20:4a/18:1		
808	PC18:1/20:4	18:1/20:4	22:5/16:0	20:5/18:0	20:4/18:1	16:0/22:5	18:0/20:5	20:3/18:2
810	PC18:0/20:4	18:0/20:4	20:3/18:1		18:1/20:3	18:0/20:4	16:0/22:4	
812	PC18:0/20:3	20:2/18:1	18:2/20:1		20:2/18:1	20:1/18:2	18:0/20:3	
814	PC18:0/20:2	20:1/18:1	16:0/22:2	18:0/20:2	20:1/18:1	16:0/22:2	18:0/20:2	
848	PC20:0a/22:6	24:5a/18:1	24:6a/18:0		24:5a/18:1	22.5a/20:1		

Figure 2.12: The PC molecular species assignment for whole cells and nuclei determined by Q-TOF. The species are presented in order of decreasing intensity. The proportion of each species for a particular mass cannot be quantified.

2.4 Summary

This chapter has described the development of experimental and analytical techniques used in this study including the process of preparing biological samples and the process of analysing mass spectrometry data.

The preparation of nuclei free from nuclear envelope contamination is essential for the accurate analysis of endonuclear phospholipid composition by mass spectrometry. Complete nuclear envelope removal can be achieved with the detergent Triton-X-100, however, residual contamination of the resulting naked nuclei can lead to artefactual peaks arising in the P193 spectrum. Alternatives to Triton-X-100 were investigated and n-Decyl β-D-Maltopyranoside was found to successfully isolate naked nuclei without leading to difficulties with mass spectrometry analysis (section 2.2.1).

Preliminary experiments to determine the feasability of using DNA content as an indicator of naked nuclei number were described. Naked nuclei can become clumped, rather than forming a uniform suspension, thus making an accurate assessment of their number challenging. The amount of DNA isolated from the aqueous layer following Bligh Dyer phospholipid extraction of synchronised cell populations was compared to the count obtained from the haemocytometer method. The DNA method did not offer an improvement on haemocytometer counting, however further development of the method could provide a viable alternative (section 2.2.2).

The mass spectrometer is optimised to produce a maximum transfer efficiency of fragments at a particular m/z. The transfer efficiency is reduced the further away the molecule of interest is from the optimised mass. A method to assess the magnitude of this effect was described and it was found to be minimal under current settings (section 2.3.2).

A method to determine threshold values below which sample peaks are not distinguishable from noise was described. Using a carefully prepared mixture of phospholipids at a known concentration, termed the 'standard mixture', the threshold value was set to only allow selection of molecular species which were present in the standard mixture (section 2.3.3).

Accurate preparation of internal standards is required for an accurate assessment

of the absolute amount of each phospholipid species. A colorimetric method based on the formation of a complex between phospholipids and ammonium ferrothiocyanate was described to assess the accuracy of prepared internal standards (section 2.3.4).

Using the standard mixture, an assessment of mass spectrometer stability over time was described. Variations in the results for identical samples can occur between different measurement sessions. It was noted that data sets should be, as far as possible, collected on the same day (section 2.3.5).

Several molecular species of a particular phospholipid class can have the same mass. Q-TOF mass spectrometry was used to allow the correct assignment of molecular species for each mass. The method and results of this analysis were described (section 2.3.6).

References

[1] A. Hunt, G. T. Clark, G. S. Attard, and A. D. Postle. Highly saturated endonuclear phosphatidylcholine is synthesized in situ and colocated with CDP-choline pathway enzymes. *The Journal of Biological Chemistry*, 276(11):8492–8499, 2001.

[2] A. Hunt and A.D. Postle. Mass spectrometry determination of endonuclear phospholipid composition and dynamics. *Methods*, 39:104–111, 2006.

[3] P. Caesar, S. Wilson, C. Normand, and A. D. Postle. A comparison of the specificity of phosphatidylcholine synthesis by Human fetal lung maintained in either organ or organotypic culture. *Biochemical Journal*, 253(2):451–457, 1988.

[4] G. Koster. Lipid Mass Spectrometry course. 2004.

[5] J.C.M. Stewart. Colorimetric determination of phospholipids with ammonium ferrothiocyanate. *Biochemistry*, 104:10–14, 1980.

[6] R. Pelikan, W. Bigbee, D. Malehorn, J. Lyons-Weiler, and M. Hauskrecht. Intersession reproducibility of mass spectrometry profiles and its effect on accuracy of multivariate classification models. *Bioinformatics*, 23:3065–3072, 2007.

[7] K. Ekroos, I. V. Chemushevich, K. Simons, and A. Shevchenko. Quantitative profiling of phospholipids by multiple precursor ion scanning on a hybrid quadrupole time-of-flight mass spectrometer. *Analytical Chemistry*, 74(5):941–949, 2002.

Chapter 3

Phospholipid composition of intact HeLa cells - an analysis by ESI-MS

3.1 Introduction

This chapter describes the use of ESI-MS to analyse and quantify the phospholipid composition of intact, also termed whole, HeLa cells. Section 3.2 details the molecular species composition and overall composition of the main phospholipid classes in the whole cells. This composition is then monitored over the cell cycle using a population of synchronised cells, the results of which are presented in section 3.3. The findings of this analysis not only give a detailed description of the phospholipid composition of HeLa-GFP cells but also provide a control for comparison with the nuclei data described in Chapter 4.

3.2 Non-synchronised whole cells

Non-synchronised whole cells are representative of a normal cell population when grown under standard cell culture conditions. As introduced in section 1.3.2, the cells of a non-synchronised population are distributed randomly between the phases of the cell cycle and are therefore termed asynchronous. As such they pro-

vide a basis for comparison to populations which have been partially synchronised by the addition of agents such as mimosine that lead to cell cycle inhibition. The cells were prepared for analysis by mass spectrometry following the techniques described in sections 7.1, 7.4.2, 7.4.3 and 7.6.

3.2.1 Molecular species percentage composition

The results presented in this section (Figures 3.1 to 3.6) show the molecular species composition of each headgroup class in intact HeLa-GFP cells. The molecular species composition presented is an average of measurements obtained over six different days. On each day the composition of phospholipid extracted from three separate flasks of cells was measured. The error bars shown on the data represent the first standard deviation of all these measurements (18 samples in total). The reported stardard deviation therefore includes error resulting from both biological variability and instrument instability.

The molecular species composition of the PC headgroup class is shown in Figure 3.1. PC is composed mainly of monounsaturated molecular species, the most abundant of which are 16:0/18:1 (m/z 760) at 28.2% of the total and 18:1/18:1 (m/z 786) at 16.5% of the total. Species 16:0a/18:1 (m/z 746), 16:0/16:1 (m/z 732) and 18:0/18:1 (m/z 788) comprise 8.7%, 6.8% and 6.4% respectively. The remaining species comprise between 2% and 5% each.

Although a similar study of HeLa cell phospholipid composition was not found in the literature, these results are comparable with previous studies by ESI-MS of the Human neuroblastoma cell line IMR-32 [1] and the Human promyelocytic leukemia cell line HL-60 [2]. In the IMR-32 cell line 16:0/18:1 is also the most abundant molecular species, comprising approximately 23% of the total. Unlike HeLa cells however, species 18:1/18:1 only comprises approximately 6% of the total and species containing polyunsaturated chains were also detected in IMR-32 cells. HL-60 cells show a very similar composition to that of the HeLa cells with the most abundant species, 16:0/18:1 (m/z 760), 18:1/18:1 (m/z 786), 18:0/18:1 (m/z 788), 16:0a/18:1 (m/z 746) and 16:0/16:1 (m/z 732) comprising approximately 20%, 16%, 8%, 7% and 6% respectively. The differences between these cell lines most probably reflects the different roles of each cell type.

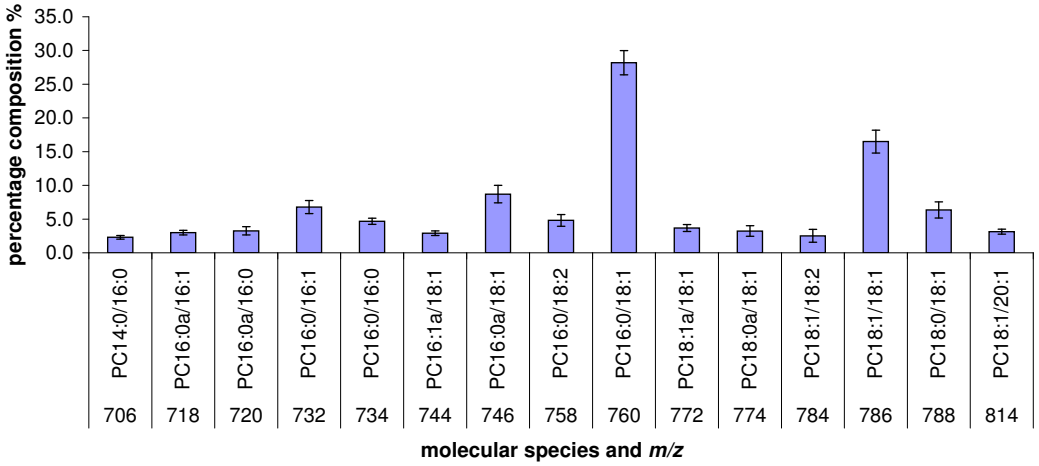

Figure 3.1: Molecular species percentage composition of PC for asynchronous whole cells (average of 6 triplicate measurements of phospholipid composition). The error bars represent the first standard deviation of this data and include errors arising from biological variability and instrument instability.

The most abundant molecular species of the PE headgroup class are 18:1/18:1 (m/z 744), 18:0/18:1 (m/z 746) and 16:0/18:1 (m/z 718) which comprise 23.8%, 15.7% and 10.8% respectively (Figure 3.2). Despite the high abundance of these monounsaturated species, there is also a large proportion of highly unsaturated molecular species such as 18:1/20:4 (m/z 766) at 7.5% of the total and 18:0/22:6 (m/z 792) at 5.6% of the total.

The PE of IMR-32 cells [1] was also found to contain a large proportion of highly unsaturated species. Molecular species containing polyunsaturated chains were however found to contribute to approximately 80% of the total in contrast to 37% in the HeLa cells. For IMR-32 cells 18:0/20:4 and 18:1/20:4 were the most abundant molecular species. The two most abundant molecular species in HL-60 cells were, as described for HeLa, 18:1/18:1 and 18:0/18:1 although these were found to comprise only 7.6% and 7% of the total respectively [2].

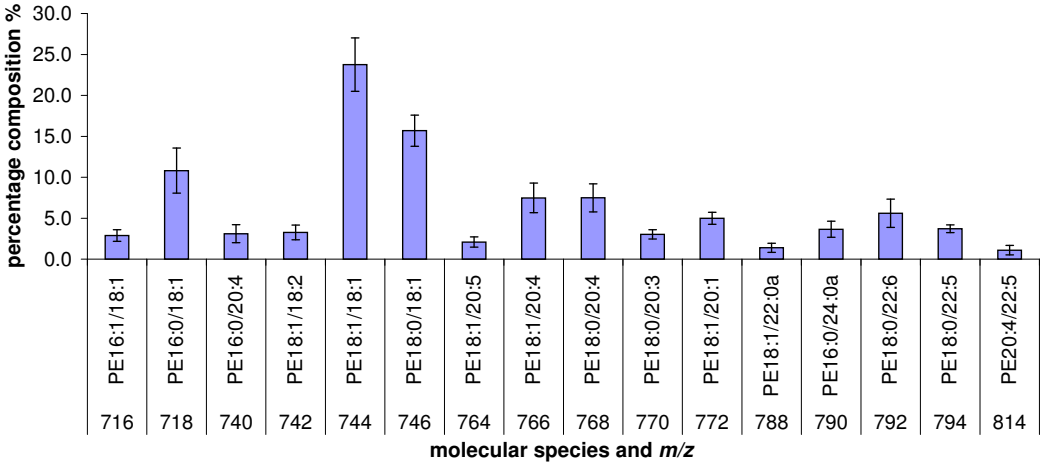

Figure 3.2: Molecular species percentage composition of PE for asynchronous whole cells (average of 6 triplicate measurements of phospholipid composition). The error bars represent the first standard deviation of this data and include errors arising from biological variability and instrument instability.

DAG is composed mainly of molecular species with saturated or monounsaturated chains, the most abundant of which are 16:0/18:1 (m/z 612) at 31.3% of the total and 18:1/18:1 (m/z 638) at 18% of the total (Figure 3.3). This molecular species composition closely resembles that of PC which is probably due to the interconversion between PC and DAG (figure A.9). DAG is synthesised from PC by the action of phospholipase C (PLC) and PC can be generated from DAG by the enzyme DAG-cholinephosphotransferase [3].

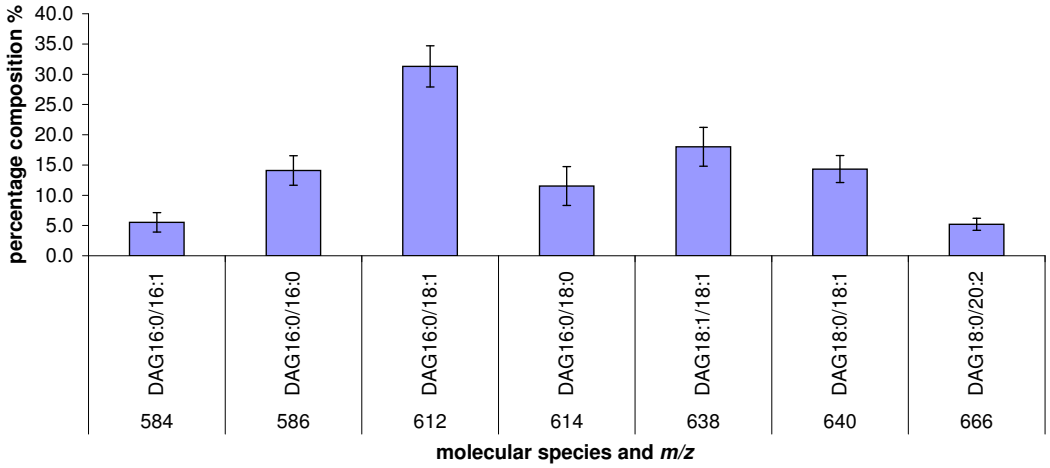

Figure 3.3: Molecular species percentage composition of DAG for asynchronous whole cells (average of 6 triplicate measurements of phospholipid composition). The error bars represent the first standard deviation of this data and include errors arising from biological variability and instrument instability.

The whole cell PI contains molecular species with both monounsaturated and polyunsaturated chains. The molecular species with monounsaturated chains contribute to $> 63\%$ of the total whereas the species with polyunsaturated chains contribute approximately half that value. The most abundant species are 18:0/18:1 (m/z 863), 16:0/18:1 (m/z 835), 18:1/18:1 (m/z 861) and 18:0/20:2 (m/z 889), comprising 24.8%, 17.5%, 14.2% and 12.3% of the total respectively.

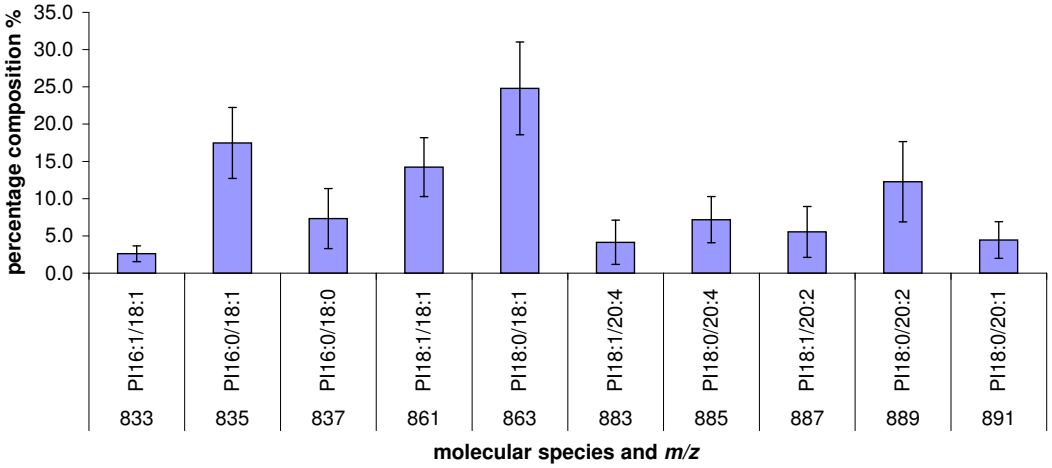

Figure 3.4: Molecular species percentage composition of PI for asynchronous whole cells (average of 6 triplicate measurements of phospholipid composition). The error bars represent the first standard deviation of this data and include errors arising from biological variability and instrument instability.

As described for PE and PI, whole cell PS contains molecular species with both monounsaturated and polyunsaturated fatty acid chains. The most abundant species are 18:0/18:1 (m/z 788) at 36.2%, 18:1/18:1 (m/z 786) at 12.9% and 16:0/18:1 (m/z 760) at 9.8% of the total. Molecular species containing monounsaturated chains contribute to 78% of the total whereas those containing polyunsaturated chains contribute 22%.

PS can be synthesised from either PC or PE by two different phosphatidylserine synthases [4] which may account for the mixture of monounsaturated and polyunsaturated molecular species. A potential reason for the apparent similarity to PI is however less clear.

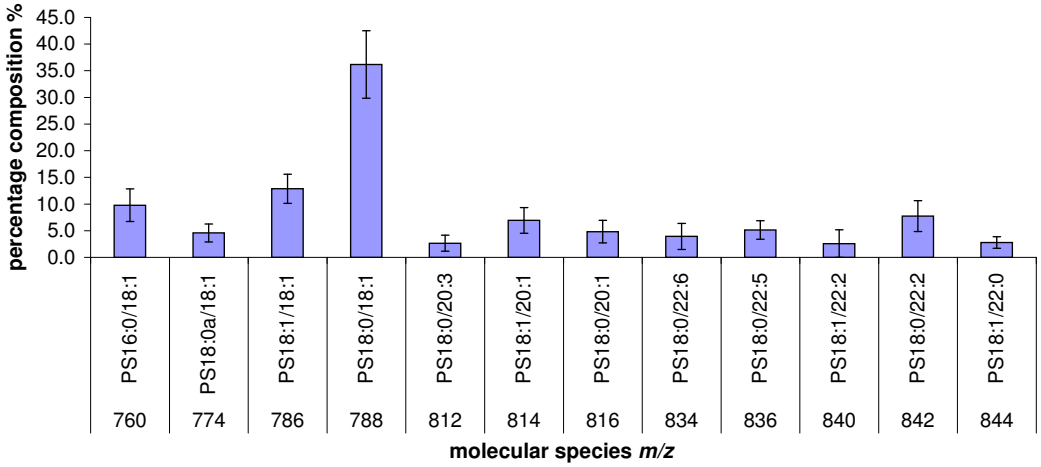

Figure 3.5: Molecular species percentage composition of PS for asynchronous whole cells (average of 6 triplicate measurements of phospholipid composition). The error bars represent the first standard deviation of this data and include errors arising from biological variability and instrument instability.

PG is visible on a P153 scan in addition to PA (table 7.2) and is therefore shown in Figure 3.6. The most abundant PA species is 18:0/18:1 (m/z 701) at 17% of the total and the most abundant PG molecular species is 16:0/18:1 (m/z 747) at 32.8% of the total. PA isolated from IMR-32 cells was also found to be composed mainly of monounsaturated molecular species [1].

In addition to the synthetic route from glycerol-3-phosphate, PA can also be generated from PC through the action of the enzyme phospholipase-D or from DAG by the action of diacylglycerol kinase. Conversely, DAG can also be generated from PA by the enzyme phosphatidate phosphatase. Both PG and PI are synthesised from PA via the precursor CDP-diacylglycerol [5]. The interconversion between these phospholipid classes may account for some similarities in the most abundant molecular species in each case.

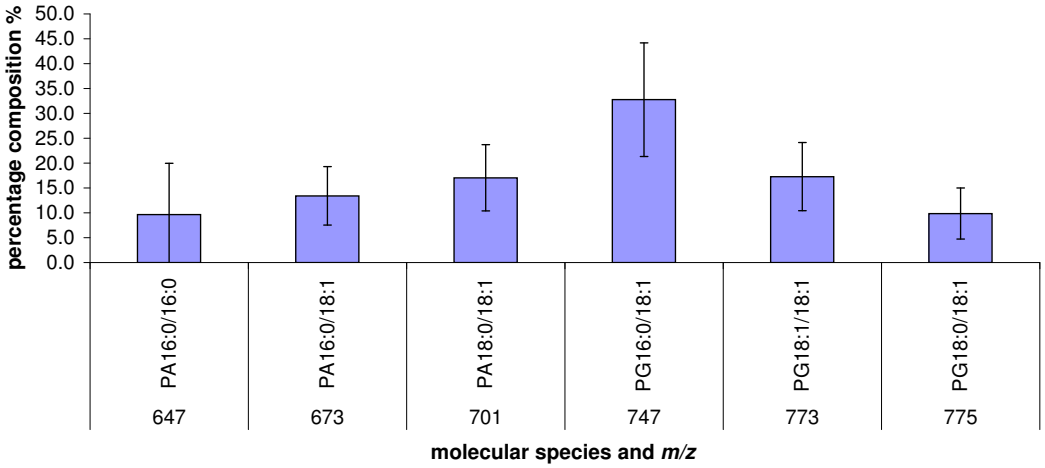

Figure 3.6: Molecular species percentage composition of PA and PG for asynchronous whole cells (average of 6 triplicate measurements of phospholipid composition). The error bars represent the first standard deviation of this data and include errors arising from biological variability and instrument instability.

It is clear that similarities exist between the molecular species composition of the HeLa, IMR-32 and HL-60 cell lines. Several differences were however noted and these are probably indicative of the different functions of each cell type. There also appears to be some consistency between the most abundant molecular species in each headgroup class. As discussed above this is possibly due to the interconversion of different phospholipid classes as shown in Figure A.9.

3.2.2 Quantified data

The absolute amount per cell of each phospholipid was determined by the inclusion of internal standards as described in section 7.4.4. The results of this analysis are shown in Figure 3.7. This data provides a control for the comparison of quantified data from synchronised whole cells and nuclei.

Addition of the amounts of each phospholipid class (Figure 3.7) gives a total phospholipid content per cell of $1.17 \times 10^{-4} \pm 7.72 \times 10^{-5}$ nmoles. Newly synthesised PC is shown as this is included in the total however further discussion regarding this species can be found in Chapter 5.

The values presented in Figure 3.7 are an average of measurements taken on four separate days. On each of these days the phospholipid from three different flasks

of cells was analysed giving 12 samples in total. The error bars in Figure 3.7 represent the first standard deviation of this data. As described in section 3.2.1 this standard deviation includes instrument instability (see also section 2.3.5) and biological variability. As this is quantified data, the standard deviation also includes errors arising from cell counting and internal standard addition.

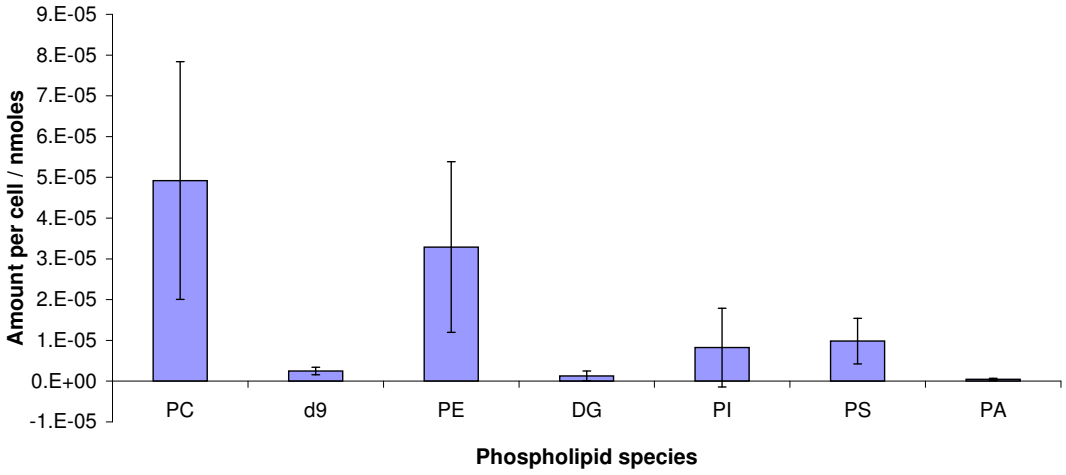

Figure 3.7: Absolute amount per cell of each phospholipid class determined from an average of 12 samples. Newly synthesised PC (d9) is also displayed as this is included in the total. The error includes biological variability, instrument instability and errors arising from cell counting and internal standard addition.

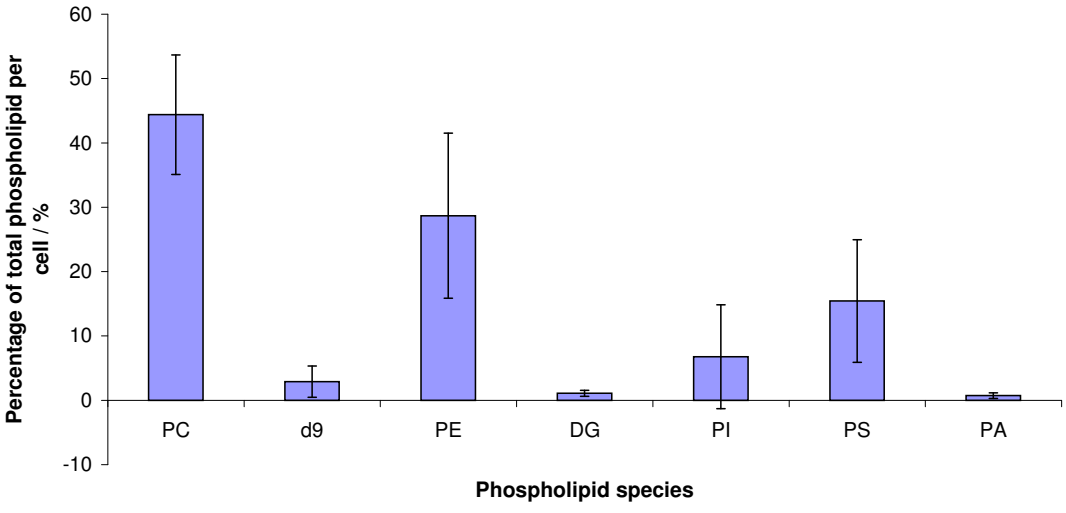

Figure 3.8: Each phospholipid class as a percentage of total phospholipid content per cell. The error includes biological variability, instrument instability and errors arising from cell counting and internal standard addition.

PC and PE are the most abundant classes of phospholipid in the cell forming 44% and 29% of the total respectively (Figure 3.8) with the other species accounting for the remaining 27%. PI and PS are the most abundant of the remaining species totaling 22%, with DAG and PA accounting for less than 2% of the total.
The exact proportions of each phospholipid class vary depending on the cell type however the high proportion of PC and PE is typical of a eukaryotic cell [6, 7]. The Human erythrocyte membrane for example contains choline phospholipids (including PC, lyso-PC and sphingomyelin) at 55.8%, PE at 27.6% and acidic phospholipids (PS, PI and PA) at 16.6% of the total [8, 9].

3.3 The phospholipid composition of synchronised whole cells

Membrane phospholipid synthesis is required for cell division and is thought to be coordinated with the cell cycle as described in section 1.3.1. It has also been suggested that phospholipids might in turn be an important element in the regulation of the cell cycle [10]. Indeed, it has been found that a PC deficiency can arrest C3H/10T1/2 fibroblasts before the S phase [11].
Within a normal cell culture the cells are distributed between the phases of the cell cycle. To study a particular phase, it is therefore necessary to synchronise the population so that the majority of cells are within the same phase of the cycle. Several methods exist to synchronise cell populations and are introduced in section 1.3.2. In this study a cell cycle blocking agent, L-mimosine, is used. This is a plant amino acid derived from *Mimosa* and blocks cell cycle progression near the G1/S boundary. It is thought to prevent replicative chain elongation by inhibiting the enzyme ribonucleotide reductase, thereby arresting cell cycle progression [12]. The exact point at which mimosine arrests the cell cycle, either before or after the onset of the S phase, is still a topic of debate [13, 14, 15]. A large proportion of the cell population reach the arrest point and on release from the block progress through the cell cycle with a greater synchronicity than prior to the block.

3.3.1 Cell cycle determination by FACS

As introduced in section 1.4, flow cytometry enables the DNA content of a cell to be determined by measuring the fluorescence of a dye that has been allowed to bind to the DNA. Cells containing more DNA will take up more of the dye and therefore fluoresce brighter than those with less DNA.

For a cell to undergo mitosis its DNA content must be double that of cells in the G1 phase of the cell cycle. DNA synthesis occurs during the S phase leading to a doubling of DNA content in the G2 and M phases. Cells in the S phase of the cell cycle therefore contain a variable amount of DNA depending on their stage of DNA synthesis. Flow cytometry can be used to assess the cell cycle phase by determining the DNA content of a cell although it is not possible to distinguish between the G2 and M phase and between the G1 and G0 phase as these contain the same amount of DNA [16].

The cell cycle of the HeLa-GFP cells was analysed by flow cytometry following staining with propidium iodide [17]. Figure 3.9 shows a typical result for an asynchronous population of HeLa cells. The x-axis indicates the DNA content (fluorescence intensity) and the y-axis the number of cells.

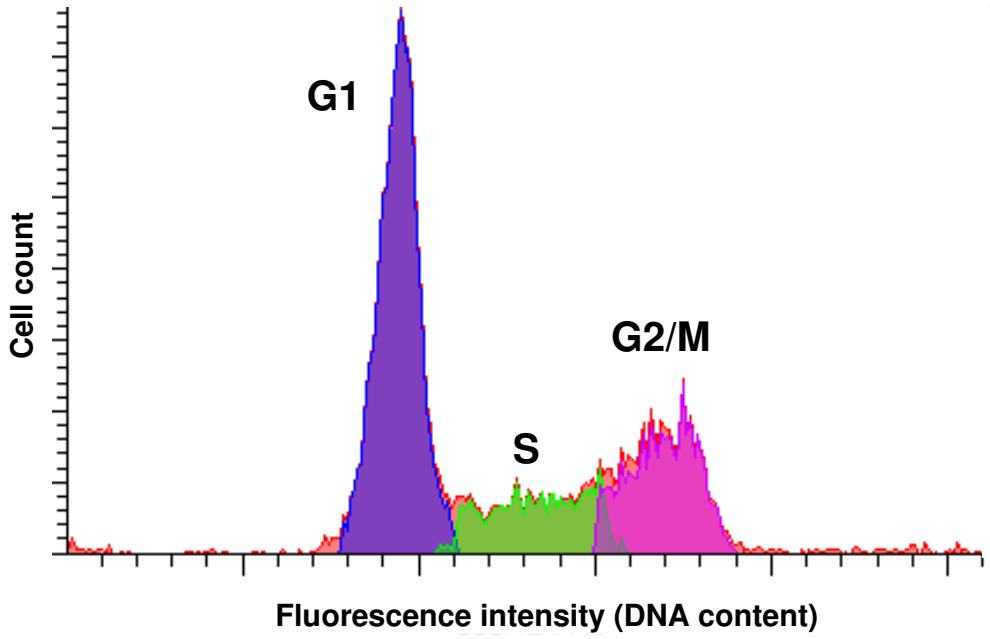

Figure 3.9: A typical FACS plot for asynchronous HeLa cells. The phases of the cell cycle represented by each peak are labelled

Flow cytometry was used to assess the DNA content of HeLa cells following treatment with mimosine (synchronised cells). The cells were synchronised and prepared for analysis by flow cytometry following the protocol described in sections 7.2 and 7.8. The proportion of the cell population within each phase following release from the cell cycle block was estimated using BD FACS Diva software (Figure A.10).

Figure 3.10 shows the percentage of the cell population in each phase following release of the cell cycle block. At 12 hours post removal of the mimosine block 4 samples were measured and at 15 hours 6 samples were measured. At all other time points, 3 samples were measured. The values presented are the average of these samples and the error bars represent the first order standard deviation of this data. With the exception of 12 hours and 15 hours, the three samples per data point were prepared from the same flask of cells. The standard deviation on these data points therefore represents the error in the measurement and subsequent analysis. As described in section 7.8 the percentage of cells in each phase of the cell cycle is determined by estimating the area of each peak (see Figure 3.9). The standard deviation of this data will therefore include error from this analysis process. The results for 12 hours and 15 hours include samples from two different flasks of cells. The standard deviation for these data points therefore also includes any biological variation between flasks. The standard deviation of the 12 hour data point is the largest. This is most likely due to variation in DNA content of cells in a population undergoing cell division.

The data presented in Figure 3.10 is summarised in Table 3.1. On release of the cell cycle block (0 hours) the majority of the cell population is in the G1 phase and this is also true 3 hours post removal of the block. This indicates that the cell cycle is arrested prior to the onset of DNA replication. After 21 hours the phase distribution of the cell population resembles that at 0 hours and 3 hours, indicating that the cell cycle length is approximately 21hrs. This value is similar to previously reported estimates of HeLa cell cycle length which range from 18 hours to 23 hours [18, 19, 20]. The proportion of cells in the G1 phase at 21 hours is however more than 10% less than at 0 hours and 4% less than at 3 hours post block removal which may be indicative of cell cycle synchronicity being lost.

At 0 hours, 3 hours, 15 hours, 18 hours and 21 hours post removal of the mimosine block, the majority of the cell population is in the G1 phase. At 6 hours

the S phase becomes predominant although it is possible that this change occurs between the 3 hour and 6 hour time points. The S phase remains the predominant phase until 12 hours post block removal. Assuming that the majority of the cell population enter the S phase at approximately 4 hours following release of the mimosine block then the G1 phase is approximately 10 hours and the S phase approximately 8 hours. The highest proportion of cells in the G2/M phases occurs between 12 hours and 15 hours post block removal, indicating that these phases last approximately 3 hours. The comparatively short length of the G2/M phases and the lack of 100% synchronicity (see discussion below) may account for them not appearing as the predominant phases at any of the measured time points. These cell cycle phase lengths are similar to those reported for HeLa cells following a thymidine-nocodazole block (arrest at mitosis) [18].

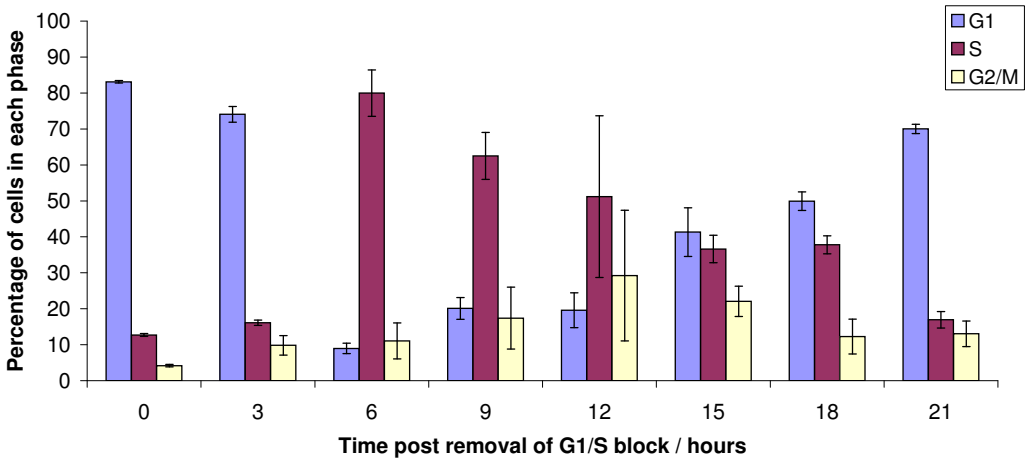

Figure 3.10: The proportion of the cell population in each phase following release from the mimosine block. The standard deviation on these data points represents the error in the measurement and subsequent analysis.

		Percentage of cell population in each phase / %		
Time following release of mimosine block (hours)	**Predominant phase of cell cycle**	**G1**	**S**	**G2/M**
0	G1	83	13	4
3	G1	74	16	10
6	S	9	80	11
9	S	20	62	17
12	S and G2/M	20	51	29
15	G1	41	37	22
18	G1	50	38	12
21	G1	70	17	13

Table 3.1: The cell cycle phase occupied by the largest proportion of the cell population following release from the mimosine block

The proportion of cells in each phase of an asynchronous and a blocked population is shown in Figure 3.11. On release from the cell cycle block approximately 80% of the cell population is in the G1 phase. This indicates that blocking the cells with mimosine results in an enrichment of over 20% in the proportion of cells in the G1 phase relative to the distribution of the asynchronous population. The consecutive use of mimosine over two cell cycles (double block), as shown in Figure 3.11, did not appear to increase the degree of synchronicity instead resulting in only a 10% enrichment in the proportion of cells in the G1 phase.

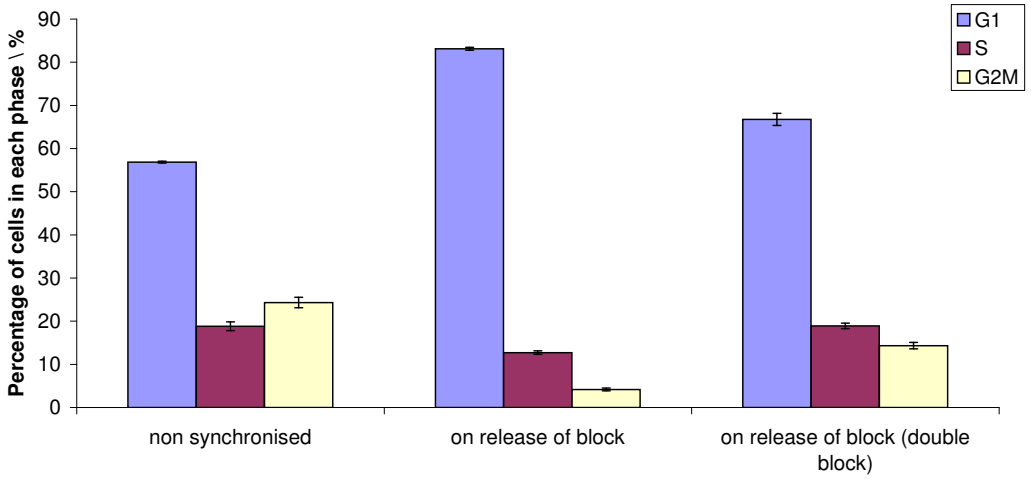

Figure 3.11: The proportion of the cell population in each phase of an asynchronous population and immediately following release from the cell cycle block. The double block represents the proportion of cells in each phase following the consecutive use of mimosine over two cell cycles.

3.3.2 Molecular species percentage composition

The data acquired from ESI-MS analysis of synchronous HeLa cell populations is summarised in this section. The fatty acid molecular species are expressed as a percentage of the total for each head group class. The molecular species composition of each head group is measured at time intervals following release from the cell cycle block, allowing the phospholipid composition to be monitored throughout the cell cycle. Throughout this section, hour has been abbreviated to 'hr'. As described in section 2.3.5 variation can occur between measurements obtained on separate occasions therefore a second independent measurement of each species is presented in the Appendix (Section B, Figures B.1 to B.7). These two independent measurements are referred to as set 1 and set 2 so that it is possible to distinguish between them in subsequent analysis.

The molecular species composition of PC at three hourly intervals following release from the cell cycle block is shown in Figures 3.12 (data set 2) and B.1 (data set 1). As found for asynchronous whole cells, species 16:0/18:1 (m/z 760) and 18:1/18:1 (m/z 786) are the most abundant. The data presented for each time point is an average of the results from three phospholipid samples. The error bars on this data represent the first standard deviation of the three measurements. Each sample was

obtained from separate flasks of cells, therefore, the reported standard deviation includes biological variability in addition to systematic errors.

The data for asynchronous cells was used as a control to allow direct comparison of the two data-sets and a detailed analysis of the compositional variation. As the asynchronous data represents an average of the phospholipid composition over the cell cycle it is possible to assess which species have changed relative to this. Figure 3.13 shows the result of subtracting the asynchronous PC data from the synchronised. The error bars represent the combined standard deviation of the synchronised and asynchronous results. This combined standard deviation is determined by calculating the square root of the sum of the squared standard deviations for each equivalent data point. This combined standard deviation therefore includes the error of instrument instability from the asynchronous data (see section 3.2.1) and the biological variability and systematic errors from both data sets. Species which show a significant change relative to the asynchronous control are defined as those which show a difference which is greater that the combined standard deviation. This method provides a good indication of likely changes. The use of more thorough statistical measures of this significance (such as a t-test) was investigated however a much larger number of measurements would be required for an accurate assessment.

Several of the PC molecular species show a significant (change greater than the combined standard deviation) increase or decrease relative to the control. It appears that this change, relative to the control, may depend on the degree of saturation of the species. Figures 3.14 to 3.17 therefore show this data with the molecular species grouped according to their level of saturation.

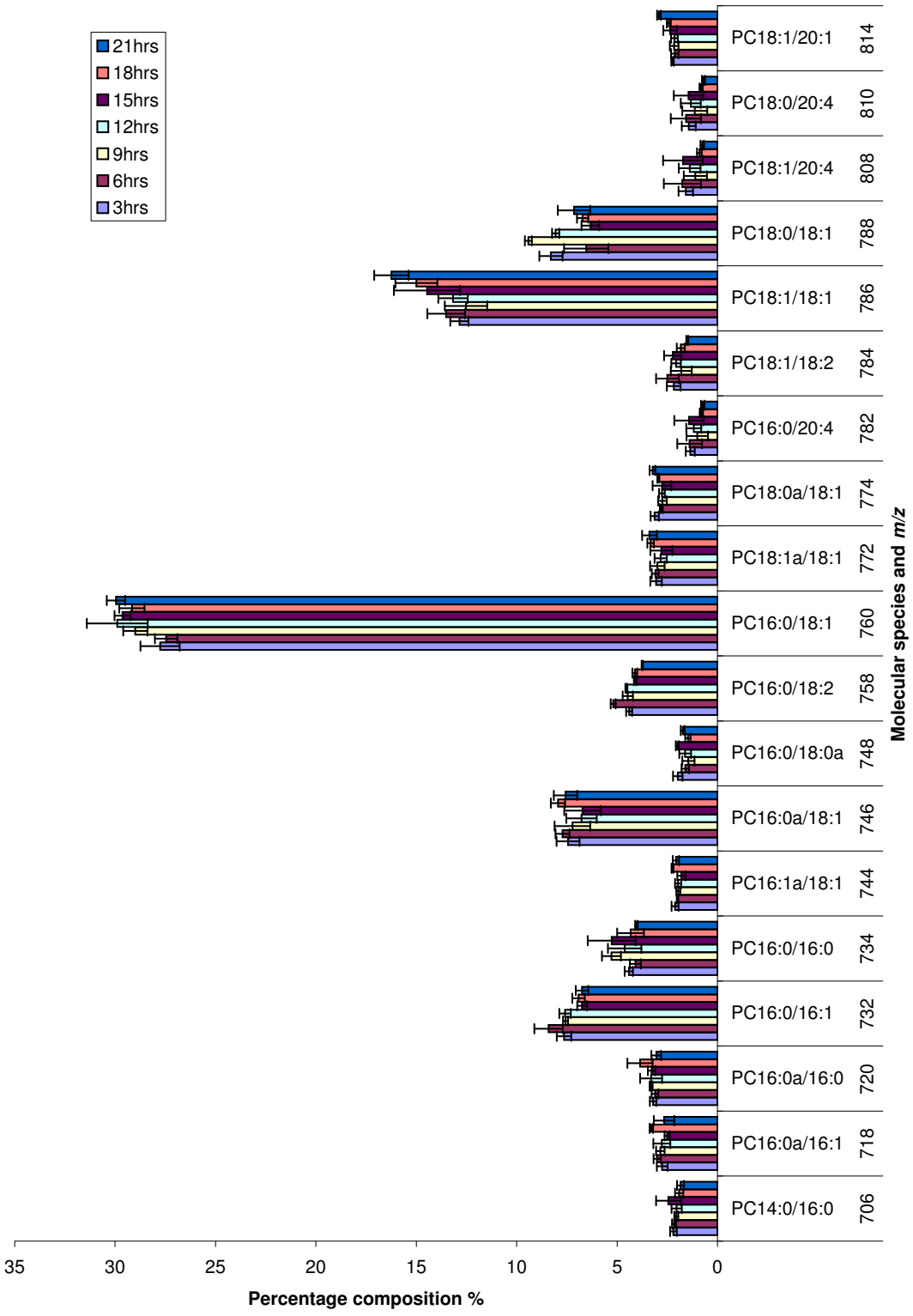

Figure 3.12: Molecular species percentage composition of PC for synchronised whole cells (data set 2). This data is an average of three separate samples. The error bars represent the first standard deviation of these measurements and include systematic errors and biological variability.

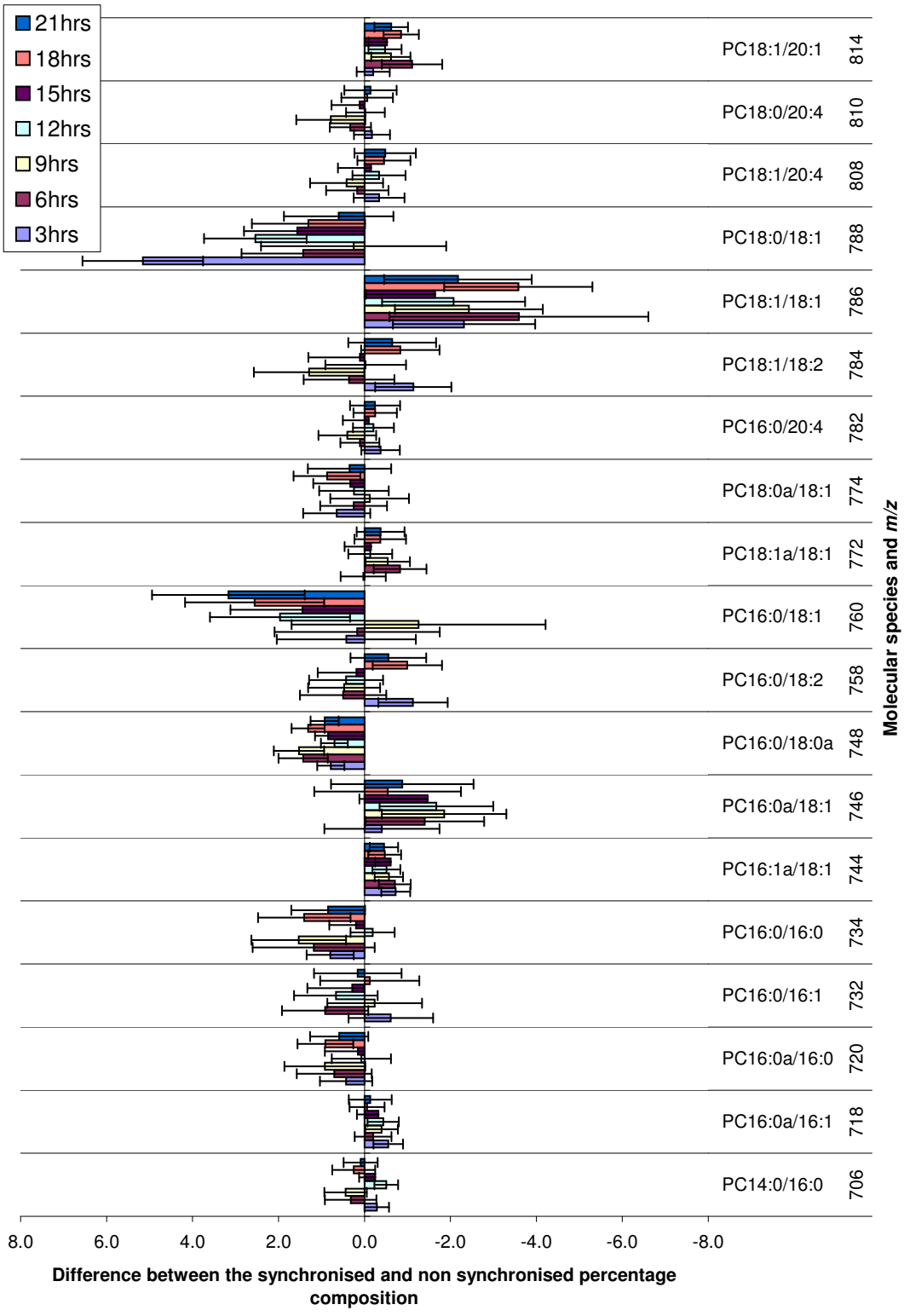

Figure 3.13: Difference between the synchronised and non-synchronised PC molecular species percentage composition (The asynchronous data subtracted from set 1 of the synchronised data). The error bars represent the combined standard deviation of the synchronised and asynchronous data. This standard deviation includes systematic errors and biological variability from both data sets. It aslo includes instrument instability from the asynchronous data set.

The saturated species (Figure 3.14) generally show no change or a small increase relative to the asynchronous data. The increase is most obvious in set 1 for species 16:0/18:0a (m/z 748), however, only two of the time points show an increase in set 2. Interestingly, the time points which show some increase in set 2 (3hrs and 15hrs) are not the ones which show the greatest increase in set 1 (6, 9 and 18hrs). Some significant changes are also seen for species 16:0/16:0 (m/z 734) at the 3hr, 9hr and 18hr time points in set 1. The 9hr time point in set 2 also shows an increase, however, this is not the case for the other time points. At the 9hr time point, the majority of the cell population is in the S phase (Table 3.1) during which the cell normally doubles its phospholipid mass ready for division [21].
Set one shows a wave-like pattern over the time points for every species. A rise in the value until 9hrs accompanies the S phase of the cell cycle. A sudden decrease in the value occurs at 12hrs followed by a second gradual increase until 18hrs. These time points coincide with the G2/M phase where cell division occurs followed by the G1 phase during which cell growth resumes (section 1.3 and 3.3). A small decrease in the value is seen for the 21hr time point where the cells have completed the cell cycle. Figure 3.10 shows that a significant proportion of the cell population is still in the S phase at 18hrs which is not the case at 21hrs. This occurs as a result of the cell population not being 100% synchronised and may lead to the difference between the two time points. The obvious discrepancies between the two data-sets make it impossible to determine with any certainty whether the observed variations over the time points are linked to cell cycle position.

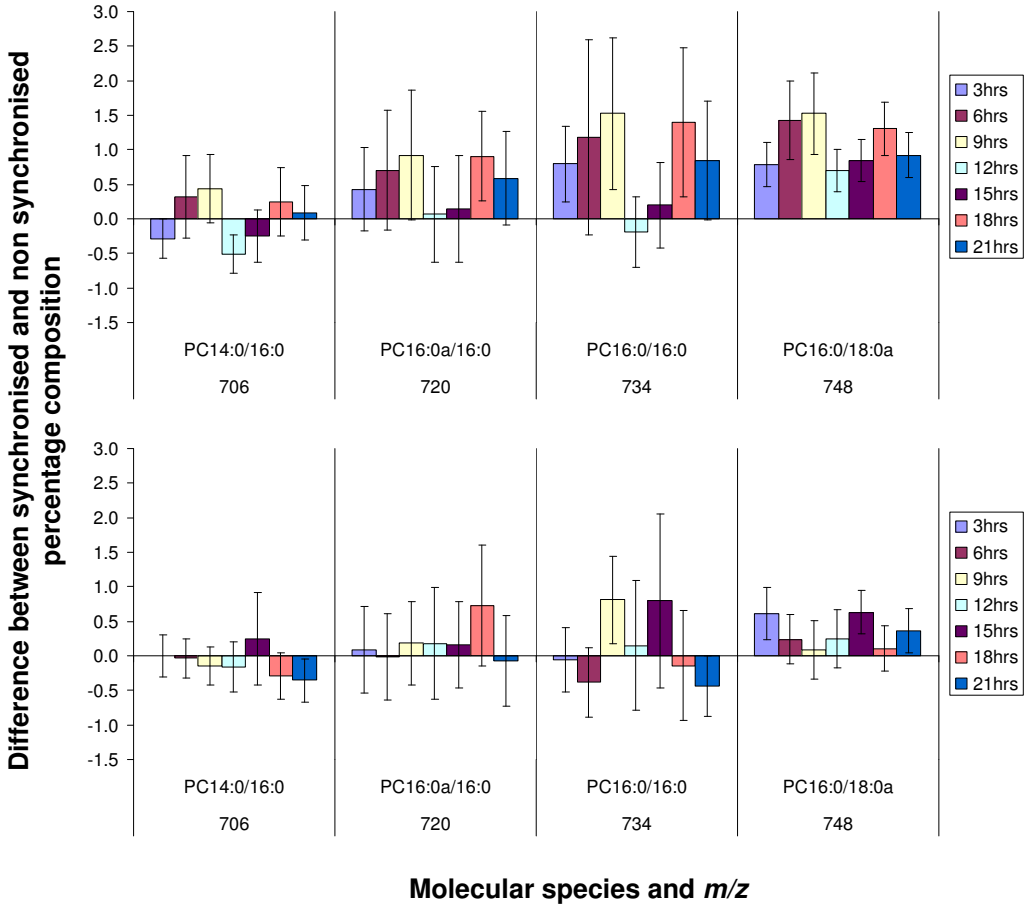

Figure 3.14: Difference between synchronised and non-synchronised percentage composition for saturated PC species. Set 1 is shown at the top followed by set 2. The error bars represent the combined standard deviation of the synchronised and asynchronous data.

The monounsaturated species (Figure 3.15) also show a similar trend to the saturated species with most molecular species remaining unchanged or increasing relative to the asynchronous control. Species 16:0/18:1 (m/z 760) and 18:0/18:1 (m/z 788) show the most significant increases relative to the asynchronous control. For species 18:0/18:1 the 3hr and 12hr time points show a consistent increase over both data sets. The 9hr time point shows a significant increase in set 2 but not in set one. For species 16:0/18:1 there appears to be an increase particularly of the later time points (12hrs onwards) in both data sets.

As for the saturated data, the cell cycle phase of the population may affect the magnitude of variation relative to the non synchronised control but the differences between the data sets preclude an accurate assessment. Contrary to the general

trend there is one species, 16:0a/18:1 (m/z 746), which shows a small decrease relative to the asynchronous data. This indicates that the saturation level of the species may not be the only factor which determines whether the species is increased or decreased relative to the control.

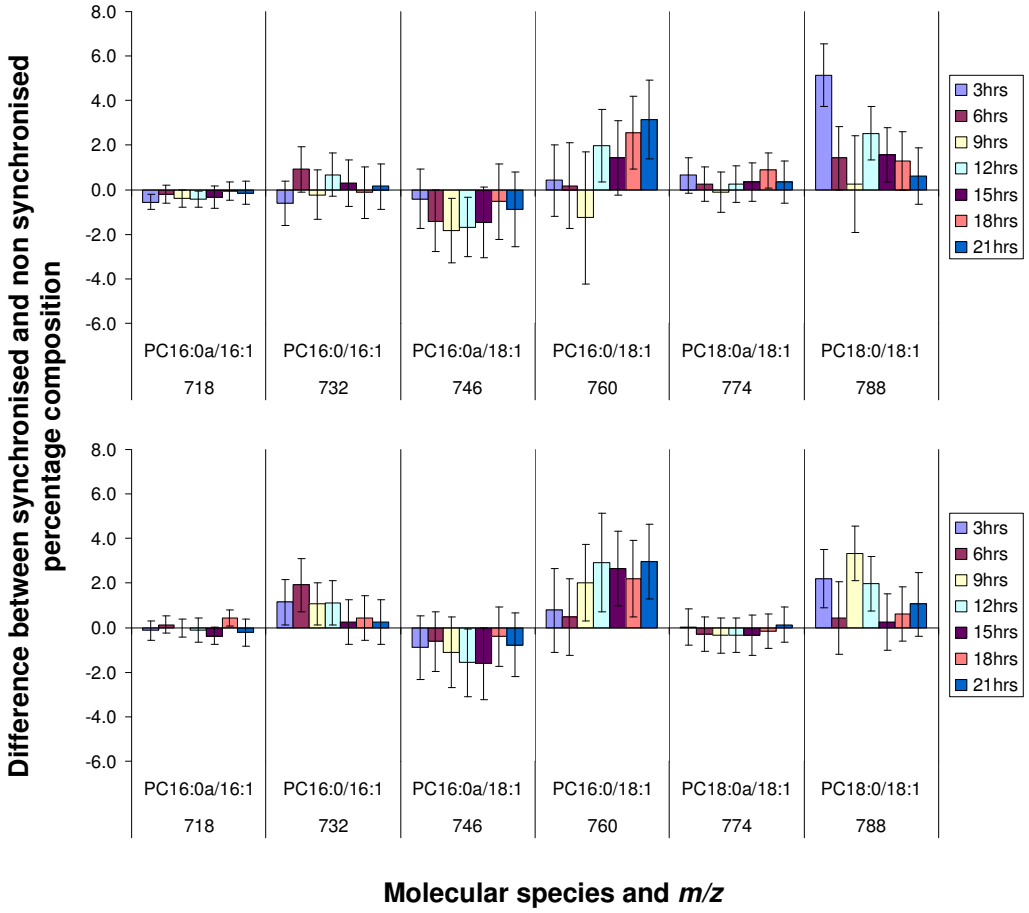

Figure 3.15: Difference between synchronised and non-synchronised percentage composition for monounsaturated PC molecular species. Set 1 is shown at the top followed by set 2

The di-monounsaturated species (Figure 3.16) all show a reduction when compared to the asynchronous data except species 18:1a/18:1 (m/z 772) which remains unchanged apart from a decrease in the 6hr time point of set 1. Species 18:1/18:1 (m/z 786) shows the largest decrease in both data sets. The 15hr, 18hr and 21hr time points of data set 2 however, remain unchanged within error.

The highly unsaturated species (Figure 3.17) generally remain very similar to the non-synchronised control. There is a small decrease at 3hrs and 18hrs of species

16:0/18:2 (m/z 758) and at 3hrs of species 18:1/18:2 (m/z 784) in set 1 but this is not observed in set 2.

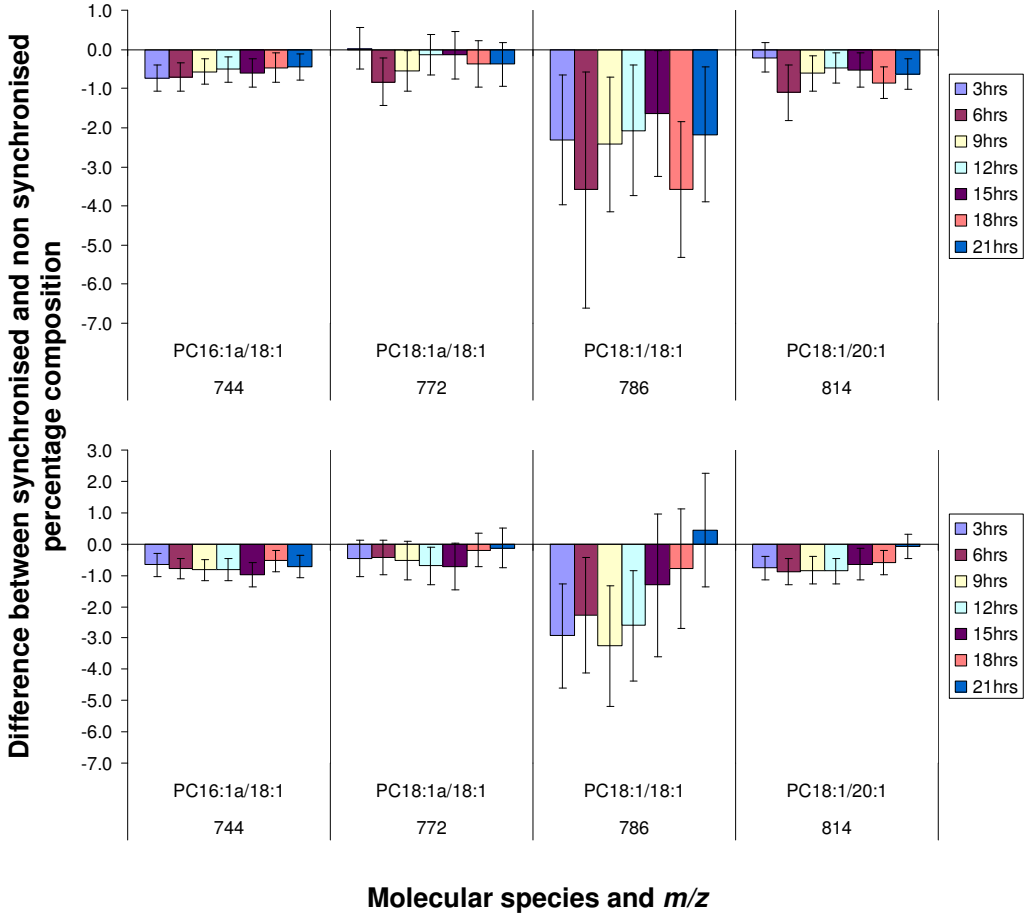

Figure 3.16: Difference between synchronised and non-synchronised percentage composition for di-monounsaturated PC molecular species. Set 1 is shown at the top followed by set 2

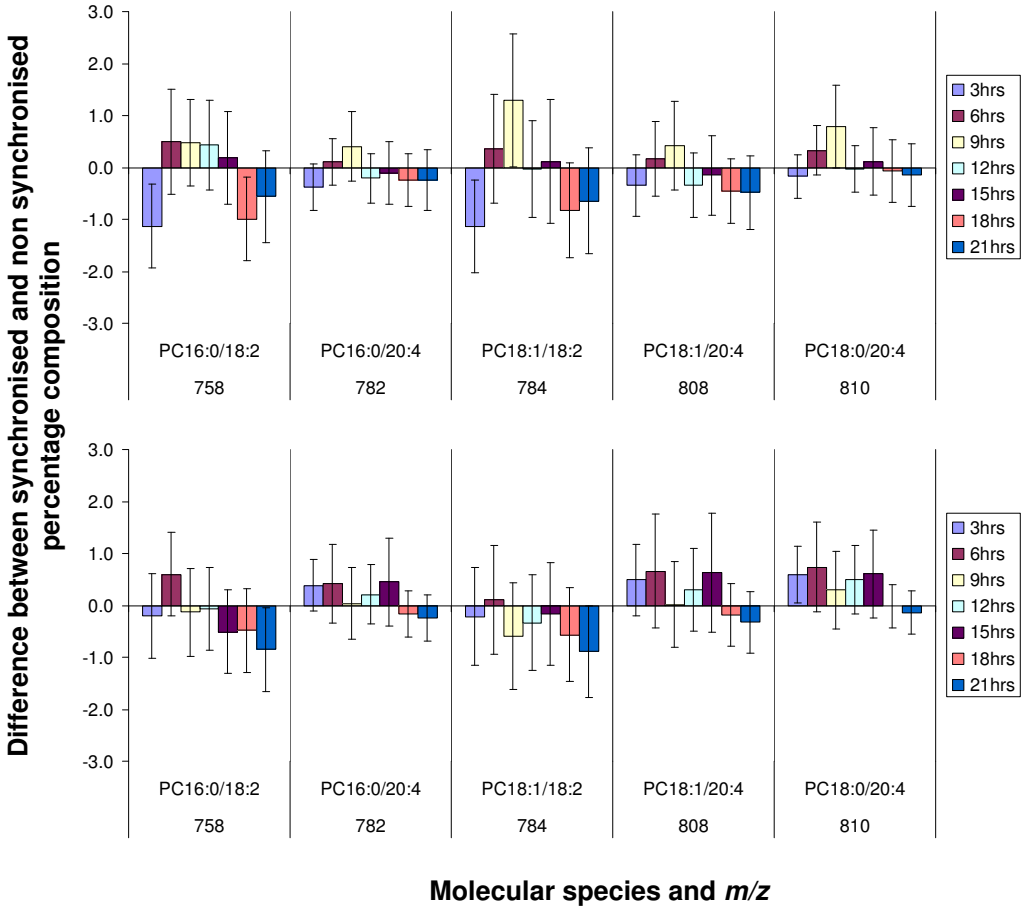

Figure 3.17: Difference between synchronised and non-synchronised percentage composition for highly unsaturated PC molecular species. Set 1 is shown at the top followed by set 2

The changes in molecular species composition for PC, relative to the asynchronous control, appear to be related mainly to the saturation level of the species. Discrepancies between the two data sets make it very difficult to determine any trends over the cell cycle although cell cycle position may influence the magnitude of this change. The discrepancies between the two data sets however, may also indicate that the cell cycle phase is not linked to any observed changes and that an alternative explanation such as measurement error may account for variation over the time points. Whatever the role of cell cycle position, these results indicate that the synchronisation procedure itself leads to a change in PC molecular species composition. The resulting change in saturation level may therefore be an artefact of mimosine addition.

Certain species, such as 18:1/18:1 (m/z 786) (Figure 3.16), appear to show a

greater change relative to the non synchronised control than other species of the same saturation level. It is possible that these species are preferentially altered during the remodelling of the molecular species composition which occurs at some point during or after synchronisation. The molecular species which show the largest changes, at one or more time points in both data sets, are 16:0/18:1 (m/z 760), 18:0/18:1 (m/z 788), and 18:1/18:1 (m/z 786). These molecular species are also the most abundant in the cell (Figure 3.12).

Figures 3.18 and B.2 show the molecular species composition of the PE headgroup. The composition is very similar to that of the asynchronous whole cells (Figure 3.2) with species 18:1/18:1 (m/z 744), 18:0/18:1 (m/z 746) and 16:0/18:1 (m/z 718) the most abundant. In both data sets however, species 18:1/20:4 (m/z 766) is less than species 18:0/20:4 (m/z 768) although they are almost identical in the non synchronised data. Species 16:0/20:4 (m/z 740) and 20:4/22:5 (m/z 814) are also not visible on the synchronised data.

Figure 3.19 shows the result of subtracting the non synchronised data from the synchronised data. Unlike the PC molecular species, PE species remain the same, within error, as the non synchronised control. It is important to note however that the error is very large and may mask changes and patterns. Species 18:0/18:1 (m/z 746), for instance, shows a small increase relative to the control in set 1 however this is not mirrored in set 2 (Figure B.8). It should also be noted that PE is composed of several highly unsaturated molecular species and it was found that highly unsaturated PC species remain very similar to the asynchronous control.

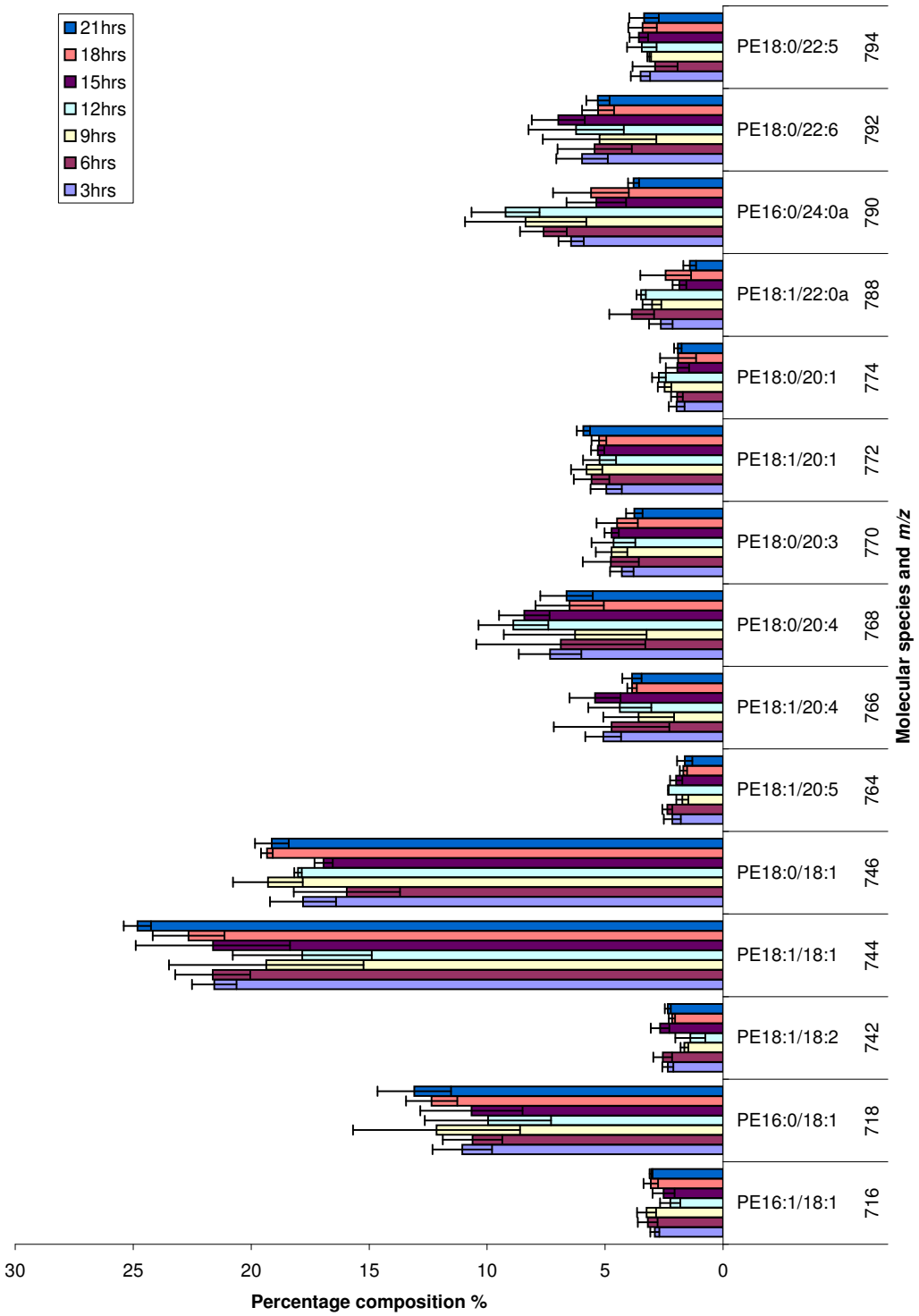

Figure 3.18: Molecular species percentage composition of PE for synchronised whole cells (data set 2)

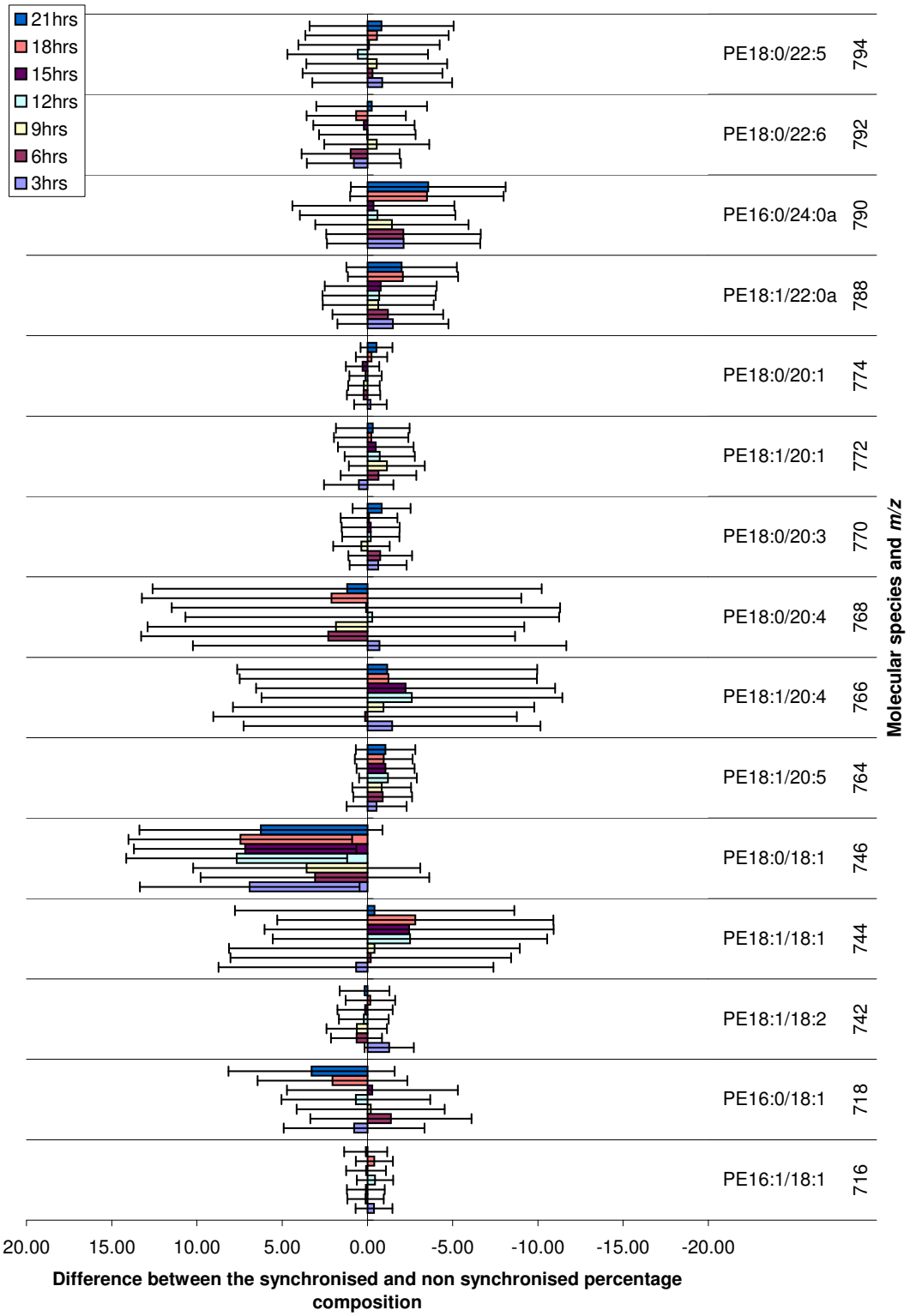

Figure 3.19: Difference between synchronised and non-synchronised percentage composition of PE molecular species (data set 1)

Figures 3.20 (data set 2) and B.3 (data set 1) show the molecular species composition of DAG in whole cells at three hourly intervals following removal of the mimosine block. Like the asynchronous whole cells (Figure 3.3) species 16:0/18:1 (m/z 612) is the most abundant, however, there are also some noticable differences. Species 16:0a/16:0 (m/z 572), 16:0a/18:1 (m/z 598) and 16:0a/18:0 (m/z 600), which each comprise approximately 10% in the synchronised data, are below the selection threshold (section 2.3.3) in the asynchronous data. Conversely species 16:0/16:1 (m/z 584) and 18:0/20:2 (m/z 666) are present in the asynchronous data but not in the synchronised.

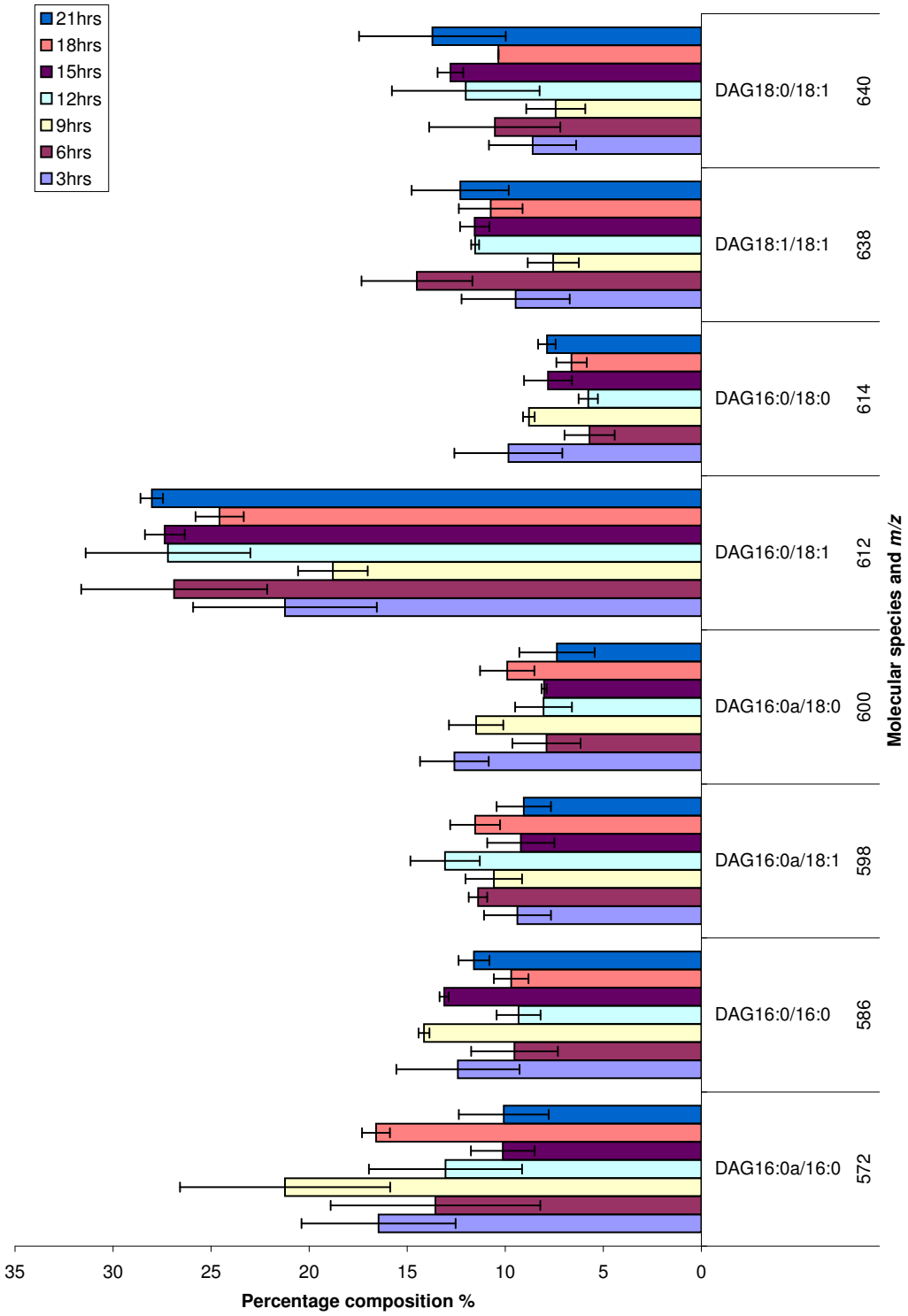

Figure 3.20: Molecular species percentage composition of DAG for synchronised whole cells (data set 2)

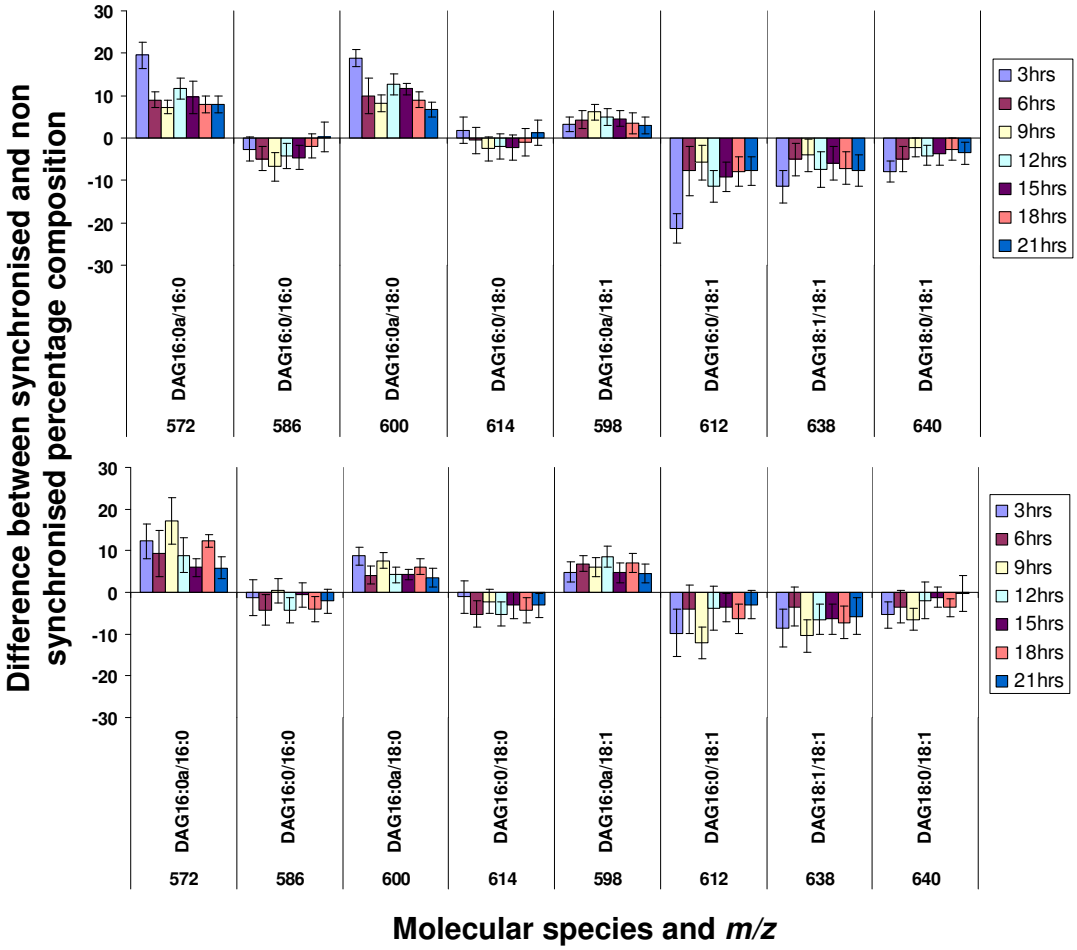

Figure 3.21: Difference between synchronised and non-synchronised percentage composition of DAG molecular species. Set 1 is shown at the top followed by set 2

When compared to the asynchronous control, DAG species show a general increase in saturated molecular species and a decrease in unsaturated species in both data sets. This is similar to the findings for PC although there is also a decrease in the monounsaturated species 16:0/18:1 (m/z 612) and 18:0/18:1 (m/z 640) which is different to the trend for PC. As described above, all species with an alkyl link (see section 1.2) are increased relative to the control, including one species which is monounsaturated (16:0a/18:1). The saturated species 16:0/16:0 (m/z 586) shows a small decrease in set 1 between time points 6hrs and 15hrs. Species 16:0/18:0 (m/z 614) also shows a small decrease relative to the asynchronous control at the 6hr, 12hr and 18hr time points of set 2. This decrease in saturated species which do not have an alkyl link may indicate that this characteristic has a greater influence than saturation level on the change relative to the asynchronous control for DAG

molecular species. It is possible that DAG species containing an alkyl link may be involved in signalling through the regulation of Protein Kinase C (PKC) [22, 23]. In set 1 the 3hr time points of species 16:0a/16:0 (m/z 572) and 16:0a/18:0 (m/z 600) are increased, relative to the asynchronous control, by approximately twice that of the other time points. This pattern is mirrored by species 16:0/18:1 (m/z 612) and 18:0/18:1 (m/z 640) which show a larger decrease at 3hrs. A similar trend occurs in set 2 where the 3hr and 9hr time points show a greater change relative to the asynchronous data. This indicates that the increase in species 16:0a/16:0 and 16:0a/18:0 may be achieved from the remodelling of species 16:0/18:1 and 18:0/18:1. It is not however clear from this data where the fatty acid 16:0a is obtained from. Species 18:1/18:1 (m/z 638) also shows this greater decrease at 3hrs in set 1 and at 3hrs and 9hrs in set 2. The increase in species 16:0a/18:1 (m/z 598) does not however follow this pattern.

Figures 3.22 (data set 2) and B.4 (data set 1) show the molecular species composition of PI in whole cells at three hourly intervals following removal of the mimosine block. As for asynchronous cells, species 18:0/18:1 (m/z 863) is the most abundant and species 18:1/20:4 (m/z 883), 18:1/20:2 (m/z 887) and 18:0/20:1 (m/z 891) are the least abundant at most time points. Species 16:1/18:1 (m/z 833) is visible in the asynchronous data but is below the selection threshold in the synchronised data.

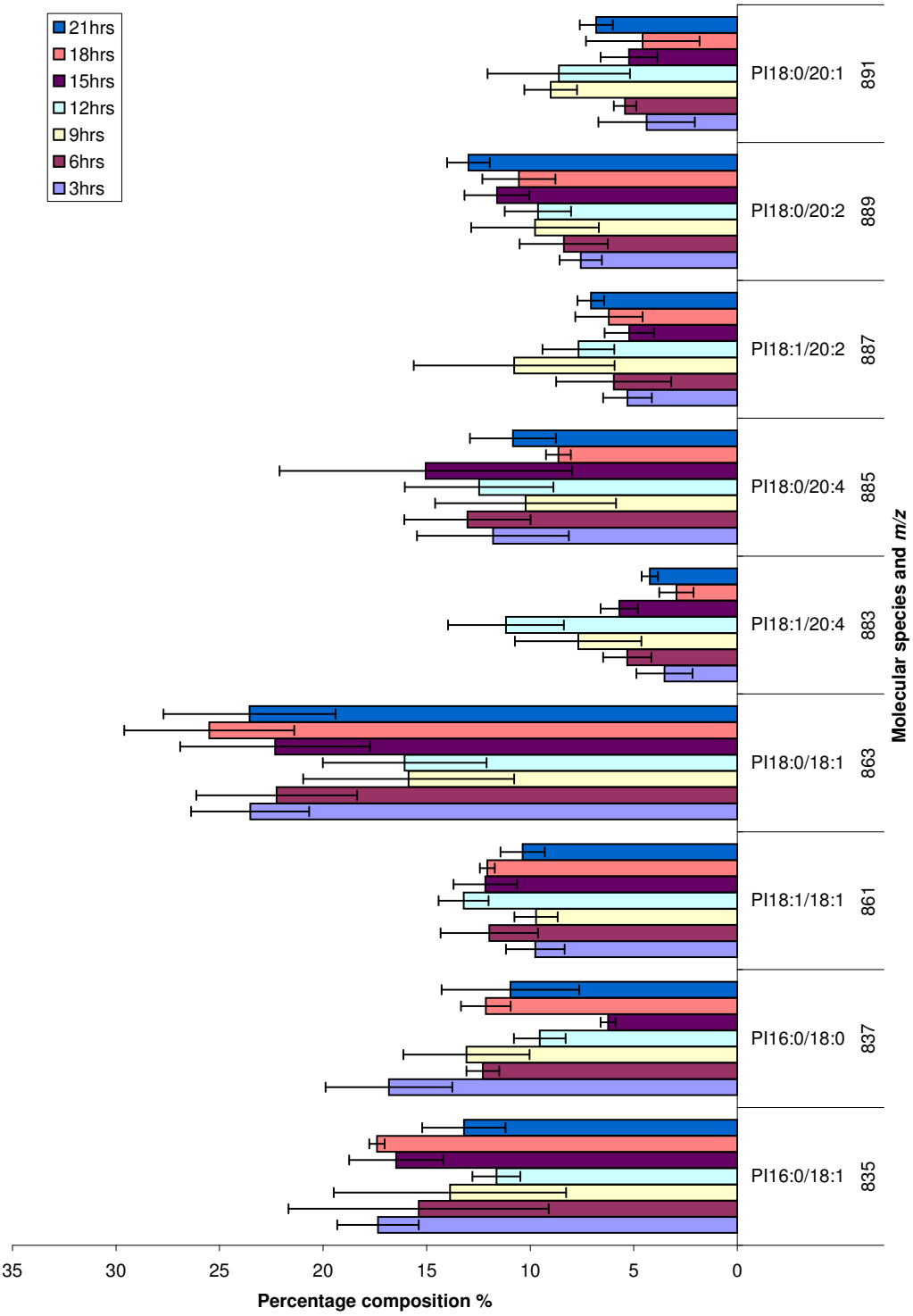

Figure 3.22: Molecular species percentage composition of PI for synchronised whole cells (data set 2)

PI species broadly remain very similar to the asynchronous control although the large error makes a detailed assessment of trends difficult. The three hour time point for species 16:0/18:0 (m/z 837), however, shows a significant increase relative to the control in both data sets (Figures 3.23 and 3.24). There is also a consistent decrease over both data sets in the 3hr time point of species 18:1/18:1 (m/z 861). In set 1 a change relative to the asynchronous control occurs for species 16:0/18:0 (m/z 837), 18:1/18:1 (m/z 861) and and 18:0/20:4 (m/z 885) at 12hrs, 12hrs and 9hrs respectively. The same species in set 2 also show a change but at time points 9hrs, 9hrs and 6hrs respectively.

The shift in time points at which changes occur may arise due to variations in the cell cycle position of the cell population. As discussed in section 3.3.1, cell populations are not 100% synchronised following treatment with mimosine. It is possible that variations in the level of synchronisation could occur between different cell populations. Even if the cell populations are in the same phase, there could also be variations in what stage of that phase the majority cells have reached.

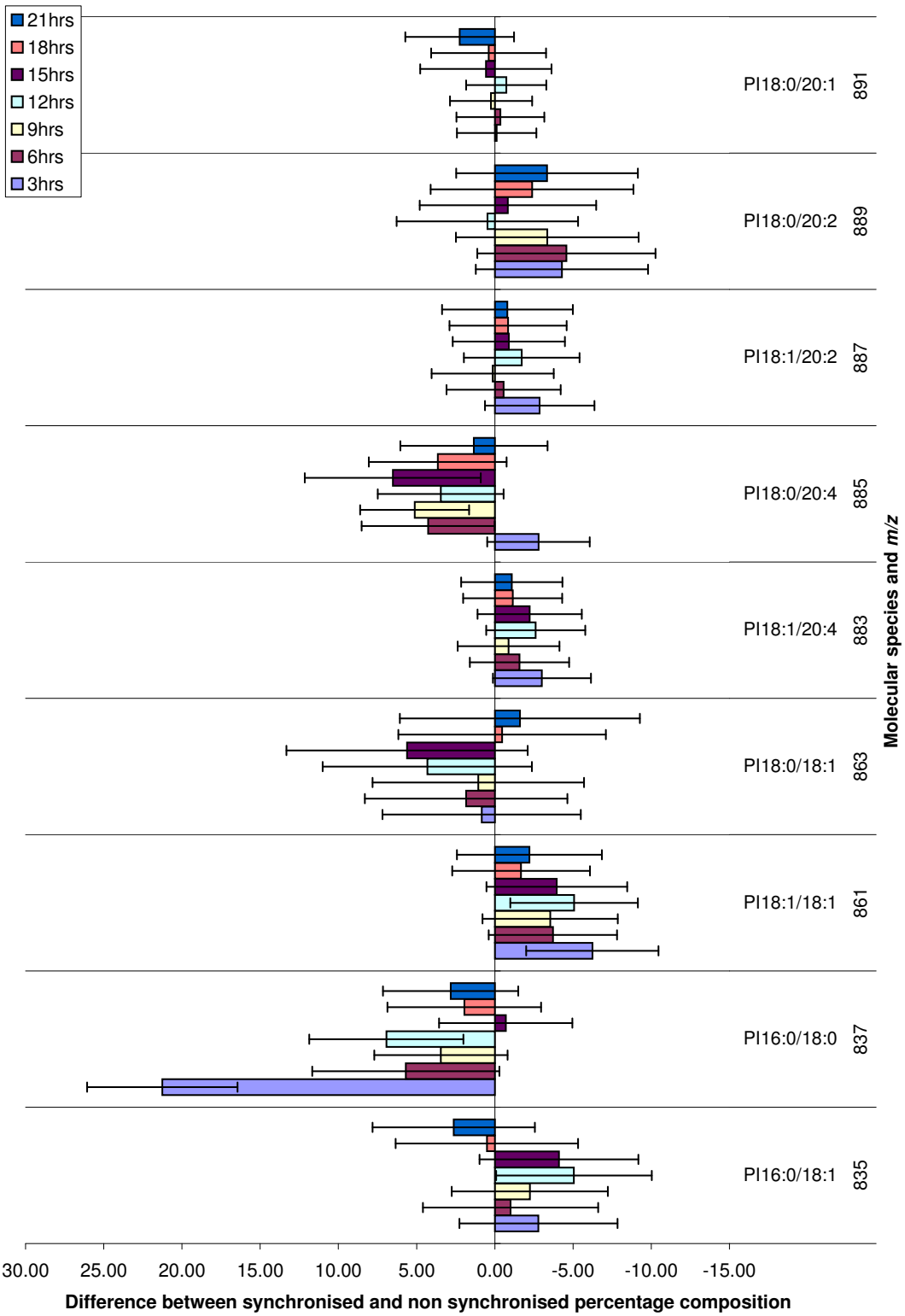

Figure 3.23: Difference between synchronised and non-synchronised percentage composition of PI molecular species (data set 1)

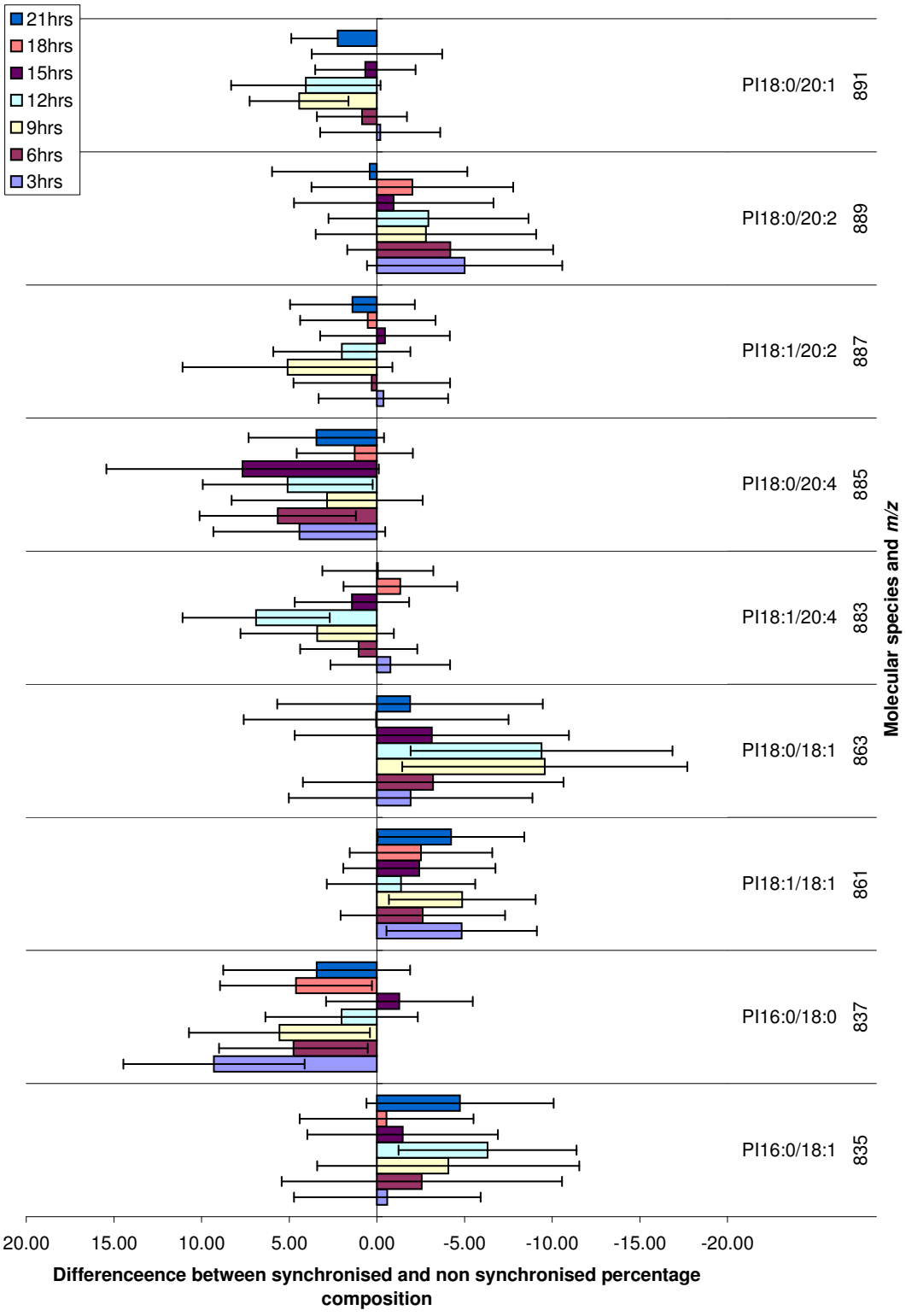

Figure 3.24: Difference between synchronised and non-synchronised percentage composition of PI molecular species (data set 2)

The PS molecular species composition of synchronised whole cells is shown in Figures 3.25 and B.5. The composition is very similar to that of asynchronous whole cells (Figure 3.5) with species 18:0/18:1 (m/z 788), 18:1/18:1 (m/z 786) and 16:0/18:1 (m/z 760) the most abundant. Species 18:0/18:0 (m/z 790), 18:0/20:1a (m/z 802) and 18:0/20:4 (m/z 810) are visible in both data sets of the synchronised whole cell results but below the selection threshold of the asynchronous data.

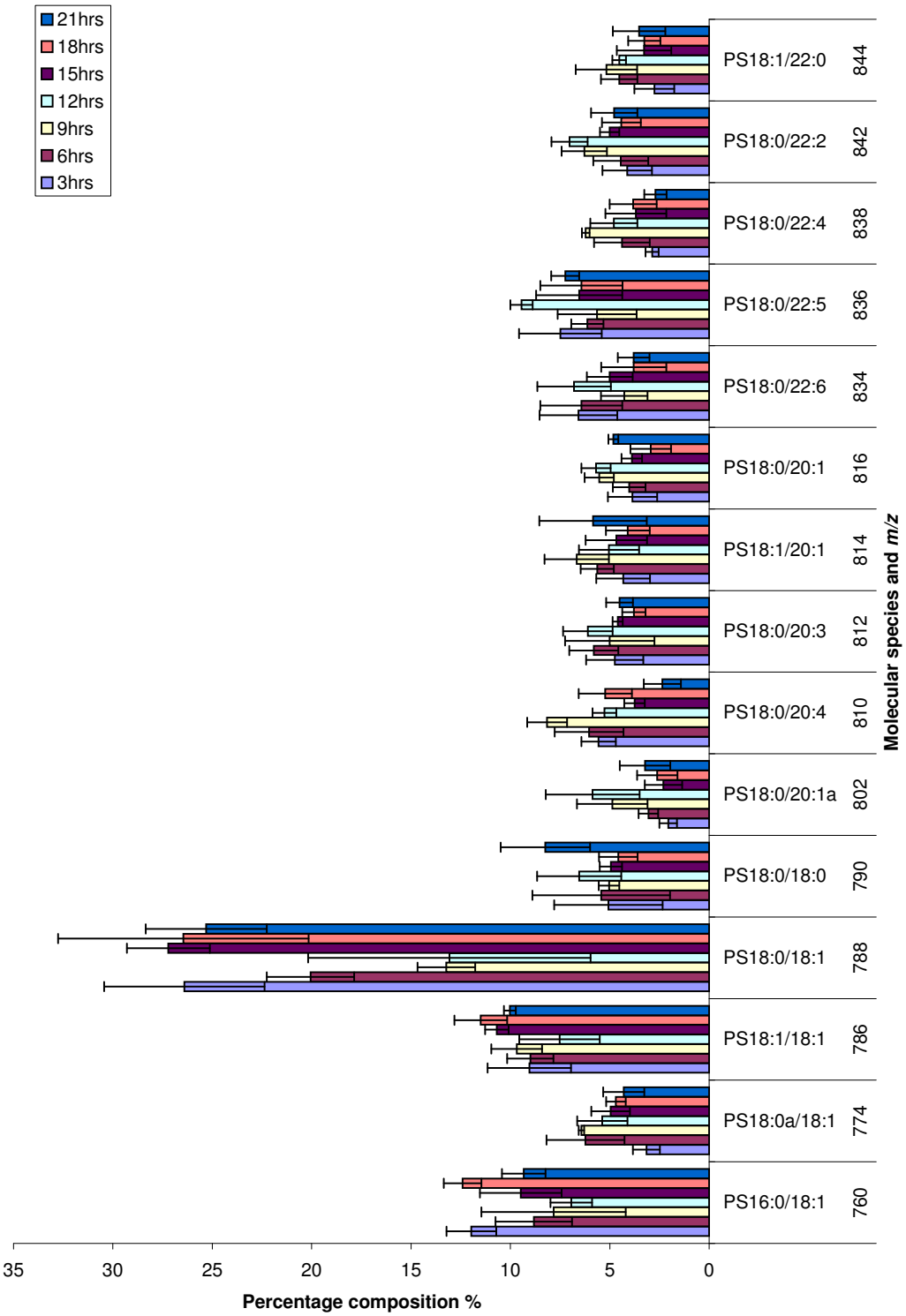

Figure 3.25: Molecular species percentage composition of PS for synchronised whole cells (data set 2)

Figures 3.26 and 3.27 show the percentage composition of PS relative to the asynchronous control for set 1 and 2 respectively. There does not appear to be a consistent trend between these two data sets. Set 1 shows a decrease in species 18:1/20:1 (m/z 814) whereas set 2 shows no change. Similarly set 2 shows an increase across all time points in species 18:0/18:0 (m/z 790) and a decrease in all but the 18hr time point of species 18:0/18:1 (m/z 788) which is not apparent in set 1. All except the 15hr and 21hr time points of species 18:0/20:4 (m/z 810) show an increase relative to the non synchronised control, as do the 6hr and 12hr time points of species 18:0/20:3 (m/z 812) in set 2. Only the 9hr time point of species 18:0/20:3 shows a small increase in set 1. Species 18:0/20:1a (m/z 802) shows an increase relative to the non synchronised at most time points in both data sets, with the exception of 3hrs and 9hrs in set 1 and 3hrs and 15hrs in set 2.

The large error on the data should be taken into account as this may lead to some of the discrepancies between the two data sets. As described above, species 18:0/18:0 (m/z 790), 18:0/20:1a (m/z 802) and 18:0/20:4 (m/z 810) are visible on both sets of the synchronised data but not in the asynchronous data. Despite this, only data set 2 (Figure 3.27) shows a significant increase in all these species due to the error.

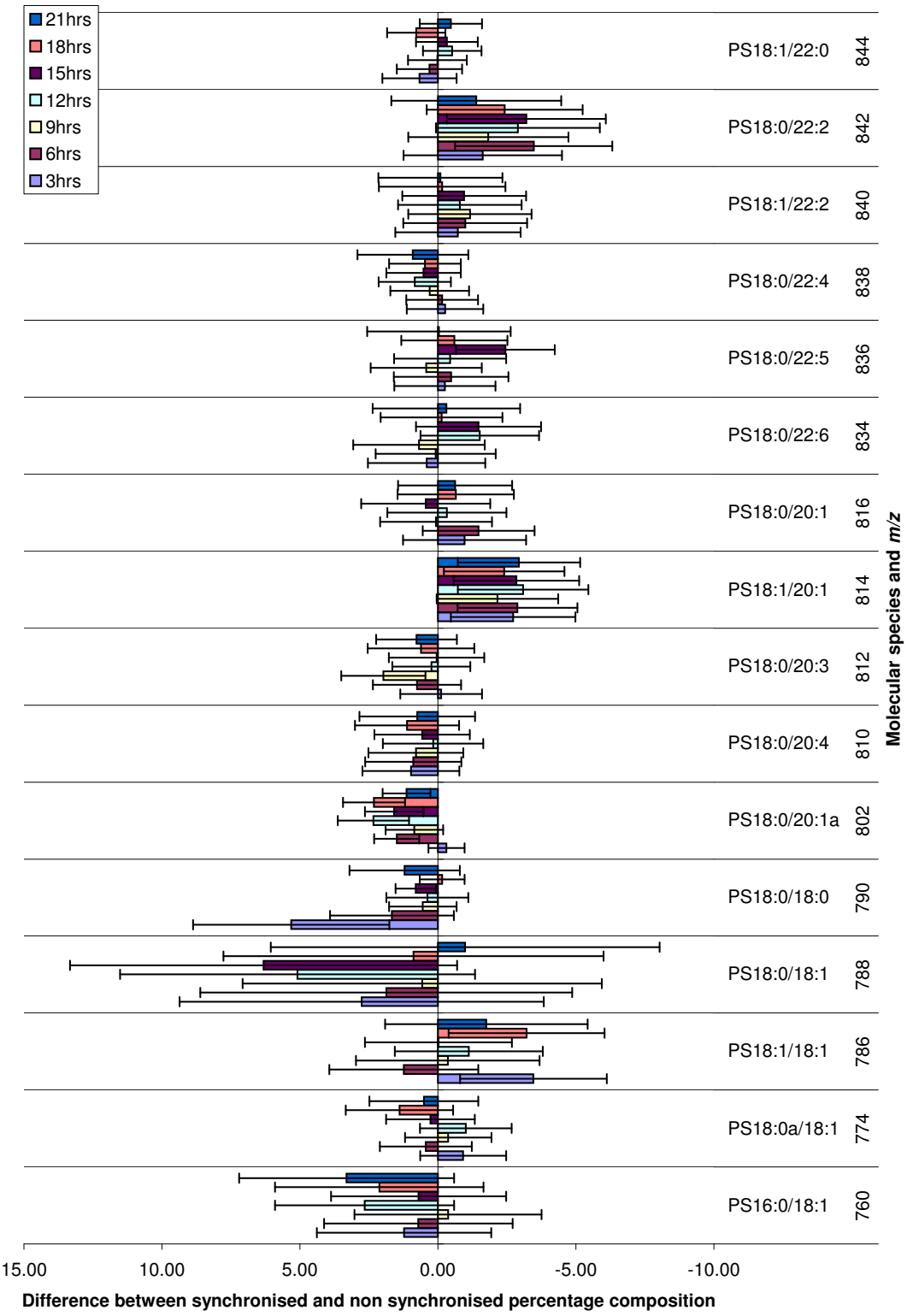

Figure 3.26: Difference between synchronised and non-synchronised percentage composition of PS molecular species. (data set 1)

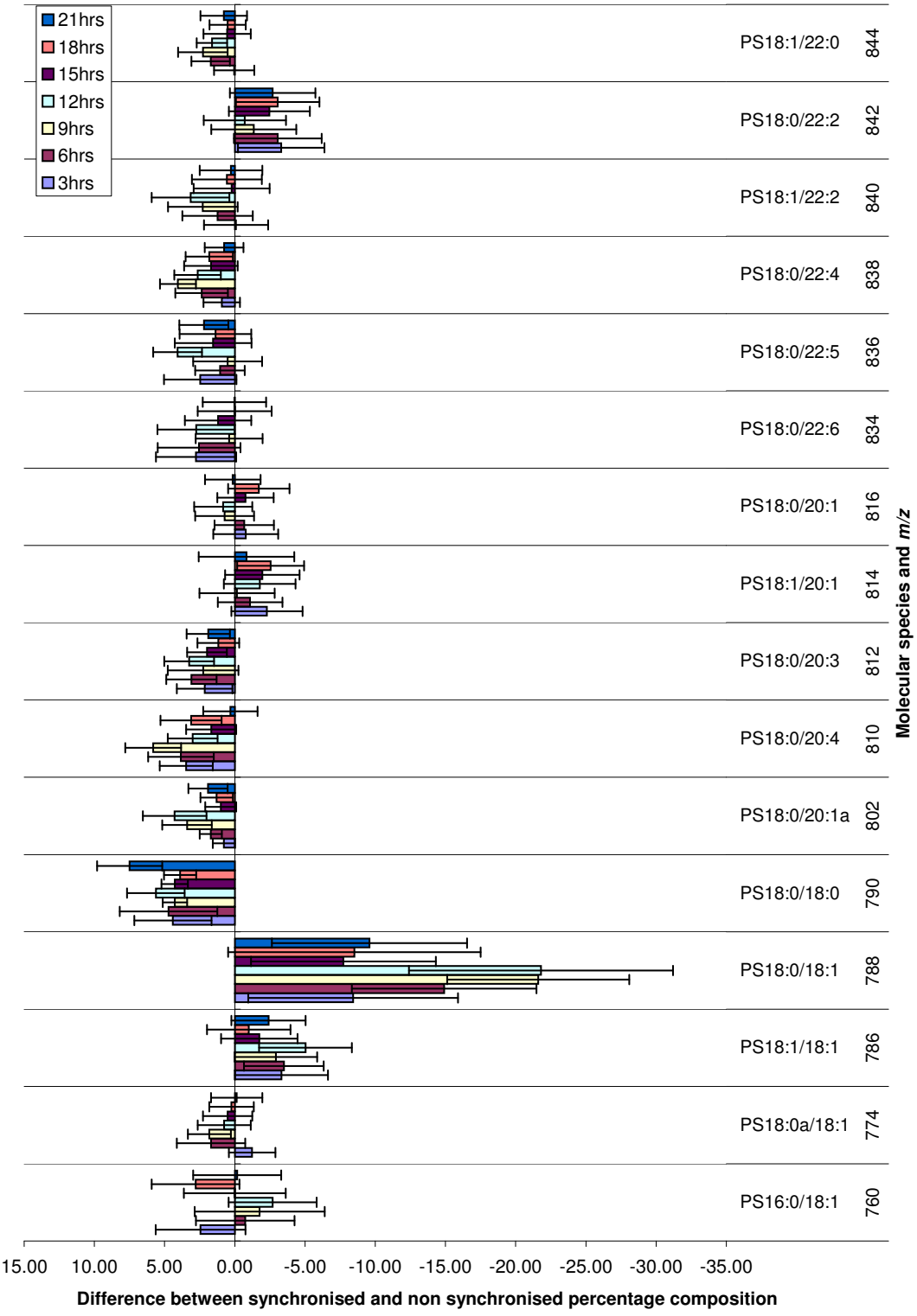

Figure 3.27: Difference between synchronised and non-synchronised percentage composition of PS molecular species (data set 2)

In addition to PA species, PG is also visible on the P153 scan and is therefore shown in Figures 3.28 and B.6. Unlike the asynchronous whole cells (Figure 3.6) the most abundant species in both sets of the synchronised data is PA16:0/18:1 (m/z 673) rather than PG 16:0/18:1 (m/z 747). Species 18:1/18:1 (m/z 773) which is present at almost 20% in the asynchronous data is below the selection threshold in both sets of the synchronised data.

The difference between synchronised and asynchronous PA molecular species is shown in Figure 3.29. As described above, the PG species (PG16:0/18:1) is decreased relative to the non-synchronised data in both data sets. This is in contrast to the PA16:0/18:1 (m/z 673) species which shows a slight increase. The saturated species PA16:0/18:0 (m/z 675) is also increased relative to the non-synchronised control in both data sets.

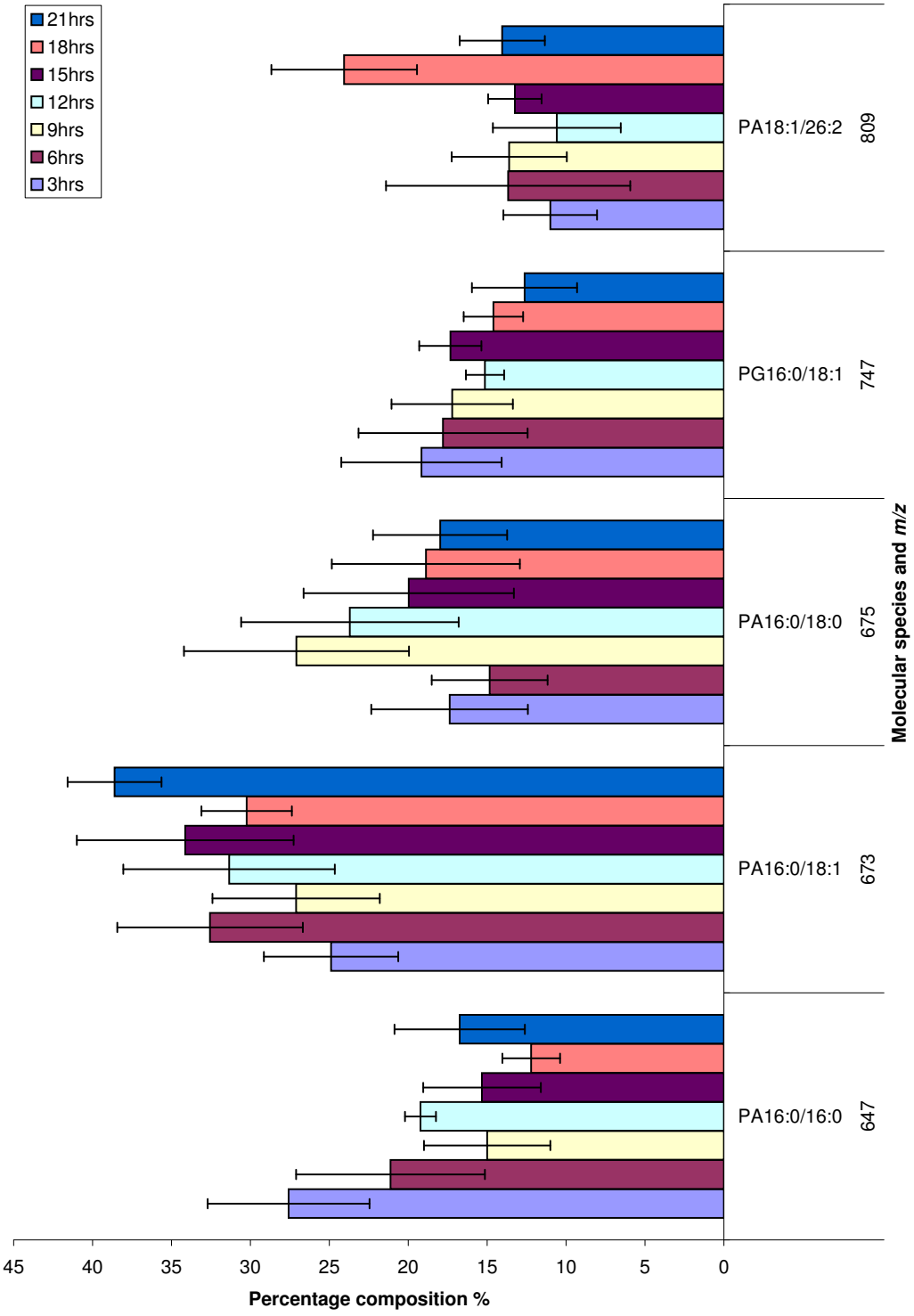

Figure 3.28: Molecular species percentage composition of PA for synchronised whole cells (data set 2)

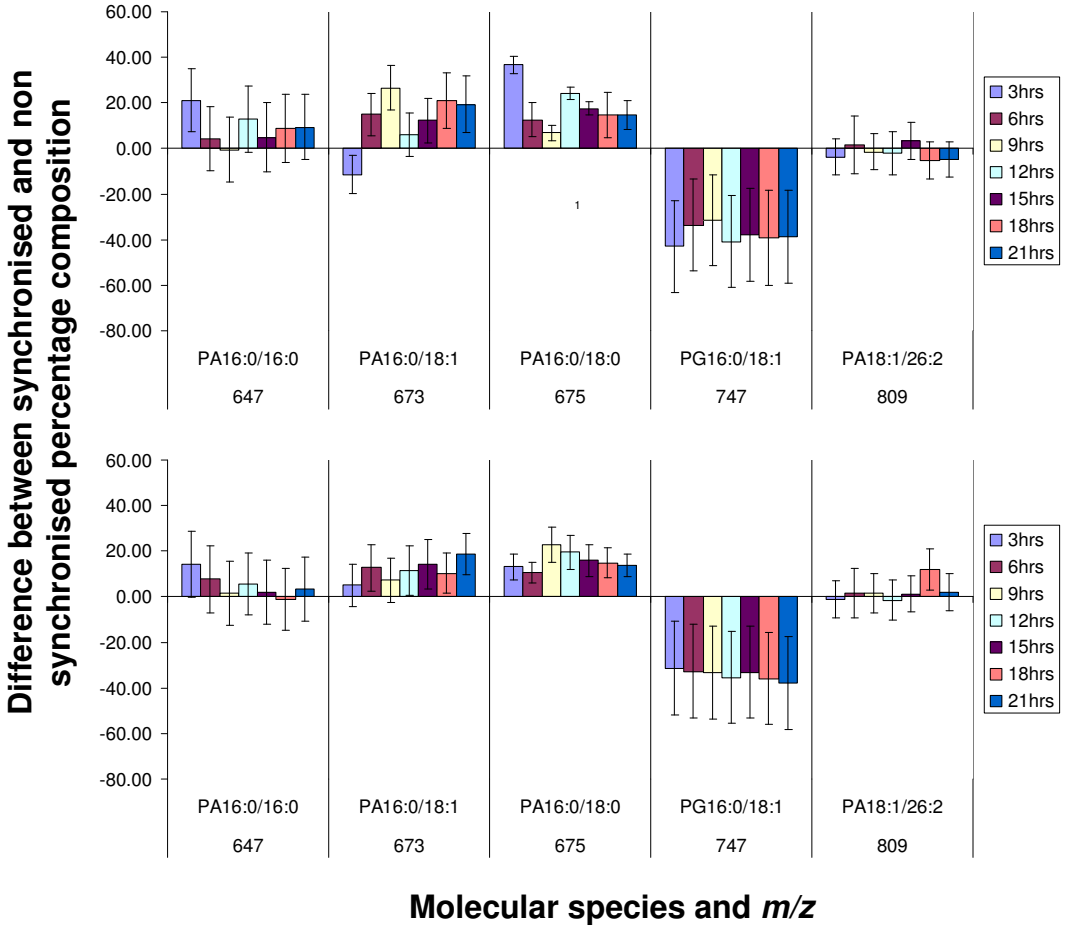

Figure 3.29: Difference between synchronised and non-synchronised PA molecular species percentage composition. Set 1 is shown at the top followed by set 2

The results presented in this section indicate that the phospholipid composition of synchronised HeLa cells differs to that of asynchronous populations, usually in a saturation level dependent fashion. It was not possible to determine many changes that were consistently linked to particular time points over both data-sets. These two observations strongly suggest that these differences between the synchronised and non-synchronised populations are mainly artefacts of the synchronisation with mimosine rather than simply the effect of cell cycle phase. This does not, however, preclude the possibility of changes that are related to the cell cycle phase of the population as these may have been masked by the error of the technique or indeed the effect of cell cycle synchronisation. Some evidence, however, was presented which suggests a possible link between the cell cycle position and the magnitude of the change relative to the asynchronous control.

Mimosine and other chemicals that lead to cell cycle inhibition, such as hydrox-

yurea, have been shown to cause DNA damage and in the HL-60 cell line mimosine is known to cause apoptosis [24, 25, 26, 27]. It is possible that the use of mimosine causes cellular changes that may correlate with the apoptotic process. Iron depletion by chelation with mimosine has been shown to activate the hypoxia response pathway and hypoxia can lead to apoptosis [24, 28]. A study of the neuronal cell line HN2-5 found an increase in saturated fatty acid containing phospholipids associated with apoptosis. This increase in saturated species was attributed to the changes in membrane morphology such as shrinkage and fluidity that occur during apoptosis [29, 30]. The changes observed in certain species could therefore be linked to alterations in the membrane structure as a result of treatment with mimosine.

Synchronisation methods are widely used to study the cell cycle and are presumed to represent the events occuring during an unperturbed cycle. Although these cells may have certain properties in common, it has been proposed that that they are not truely synchronised. The inhibition of DNA synthesis for example may not inhibit protein synthesis or mass increase. Cell cycle studies using whole-culture methods of synchronisation, such as cell cycle arrest with mimosine, may therefore not completely reflect the normal cell cycle [31, 32, 33, 34]. If the phospholipid is not truely synchronised with the DNA synthesis following treatment with mimosine, this may account for the discrepancies between data sets.

3.3.3 Quantified data

Inclusion of internal standards during phospholipid extraction also allowed the absolute amount per cell of each phospholipid class to be determined by ESI-MS. The data sets 1 and 2 referred to in this section correspond to those in section 3.3.2. Figures 3.30 to 3.35 show the total amount per cell of each phospholipid class over the cell cycle and also the value for non-synchronised cells. As described in section 3.3.2, the data presented for each time point is an average of the results from three phospholipid samples. The error bars on this data represent the first standard deviation of the three measurements. Each sample was obtained from separate flasks of cells, therefore, the reported standard deviation includes biological variability

in addition to systematic errors. This is quantified data and therefore includes any error resulting from cell counting and internal standard addition. For a discussion of the errors on the non-synchronised data see section 3.2.2.

There is a significant difference between the two PC data-sets (Figure 3.30) with the set 2 values up to nine times greater than those of set 1. The set 1 3hr value is however larger than the other time points and thus very similar to the set 2 value. The set 1 values remain quite stable over the cell cycle, with the exception of the 3hr time point, and are also very similar to the result for non-synchronised cells. Set 2 however follows a wave-like pattern across the time points and is consistently higher than the non-synchronised result.

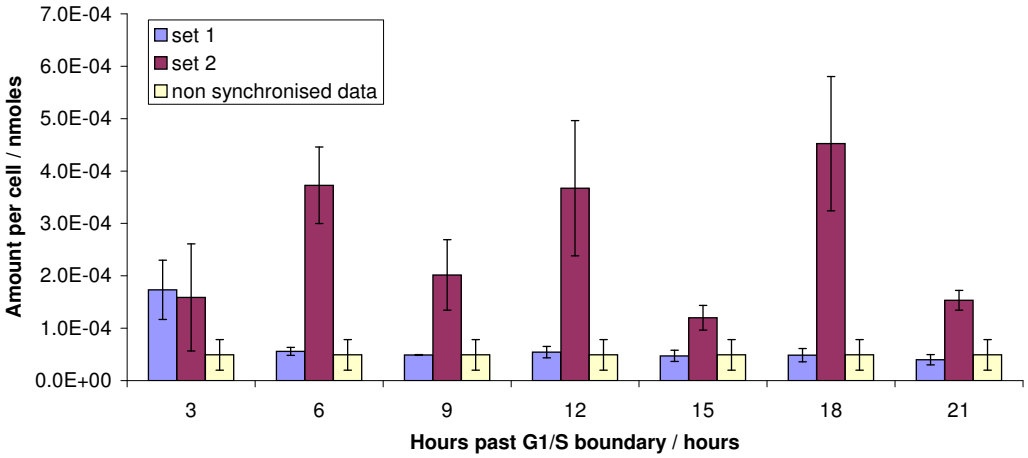

Figure 3.30: Absolute amount per cell of PC for synchronised whole cells. The error bars represent the first standard deviation of this data and includes error arising from biological variability and systematic errors.

Over the 6hr-15hr time points the amount per cell of PE in each data sets remains very similar. The value of data set 1 is almost twice that of data set 2 in each case. At the 3hr, 18hr and 21hr time points, however, the values are, within error, the same for each data set. Although the non-synchronised value is larger than either data set, the standard deviation is very large and therefore encompasses the values of both data sets at all time points.

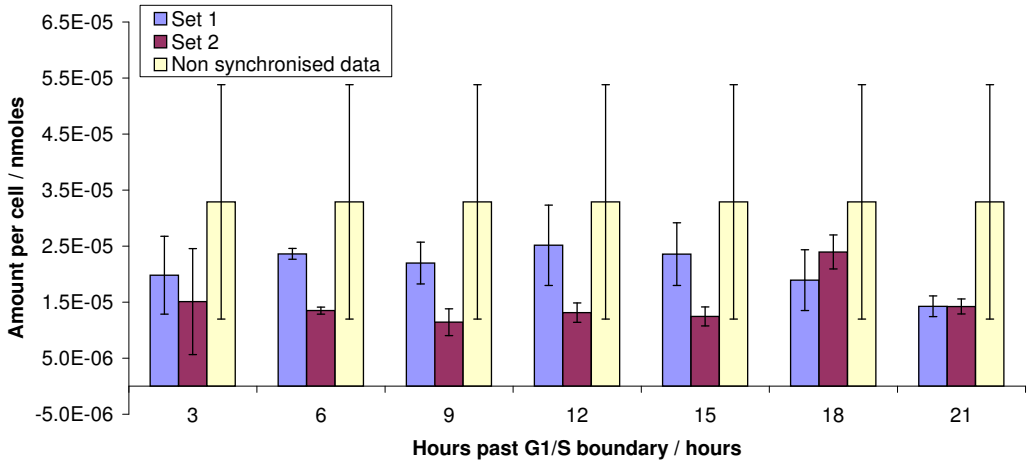

Figure 3.31: Absolute amount per cell of PE for synchronised whole cells. The error bars represent the first standard deviation of this data and includes error arising from biological variability and systematic errors.

The set 1 data for DAG (Figure 3.32) shows a similar trend to that of set 1 PC with a high 3hr time point and smaller consistent values from 6hrs to 21hrs. There is a wave-like pattern in the 6-21hr time points but this is less pronounced than that of PC data-set 2. Unlike the PC results, the DAG set 2 values are generally less than those of set 1. At the 18hr and 21hr time point though, the values are the same within error. In all cases the amount of DAG per cell is higher for the synchronised populations than the non-synchronised.

Within error the values for set 1 and 2 of PI (Figure 3.33) are the same for the 3hr, 6hr, 9hr and 21hr time points. At 15hrs the set 1 value is almost three times larger than the set 2 value however this pattern is reversed at the 18hr time point with the set 2 value more than four times larger. At 3hrs and 21hrs both data sets are similar to the non-synchronised result. From 6hrs to 15hrs the set 2 results are within error similar to the non-synchronised value although the standard deviation is large therefore precluding a more detailed assessment. At 15hrs the set 2 time point is similar to the non-synchronised value whereas it is the set 1 result which is most similar at the 18hr time point.

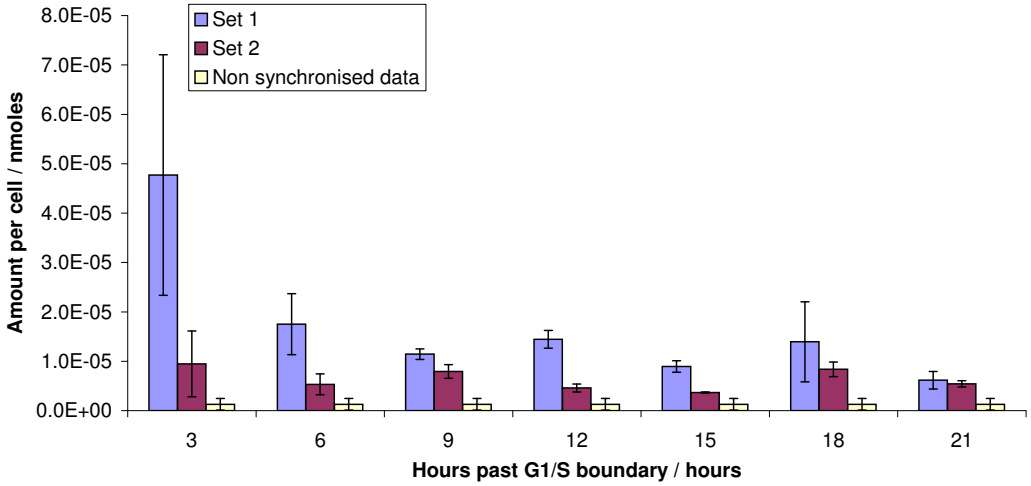

Figure 3.32: Absolute amount per cell of DAG for synchronised whole cells. The error bars represent the first standard deviation of this data and includes error arising from biological variability and systematic errors.

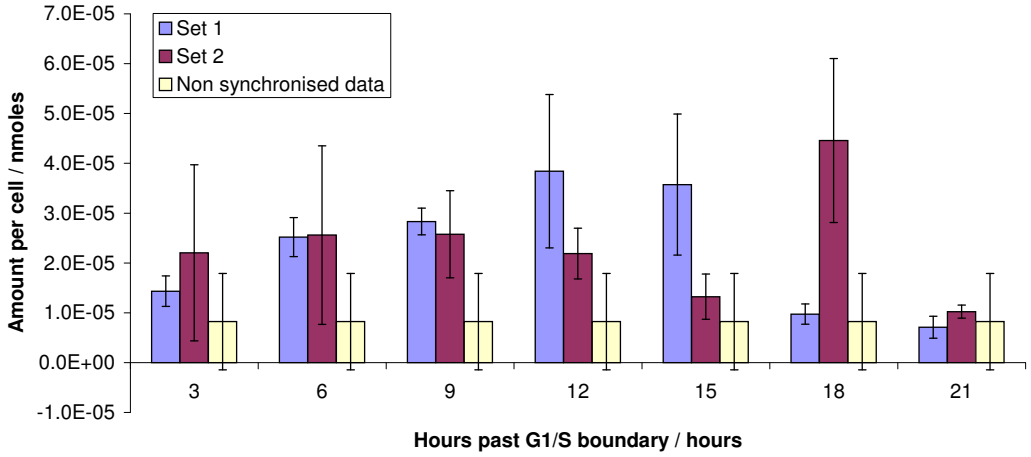

Figure 3.33: Absolute amount per cell of PI for synchronised whole cells. The error bars represent the first standard deviation of this data and includes error arising from biological variability and systematic errors.

The values of both PS data sets and the non synchronised result are very similar at the 3hr, 6hr and 15hr time points (Figure 3.34). At 12hrs the set 1 value is similar to the non-synchronised but the set 2 value is four times larger than the non-synchronised value. At 18hrs the set 1 value is again similar to that of the non-synchronised but the set 2 value is almost three times as large. At 9hrs the pattern is very similar to that at 12hrs and 18hrs, however, within error the set 2 value is not significantly different to either the non-synchronised or set 1 value. At

21hrs the set 2 value is very similar to the non-synchronised but the set 1 value is less than half that of set 2.

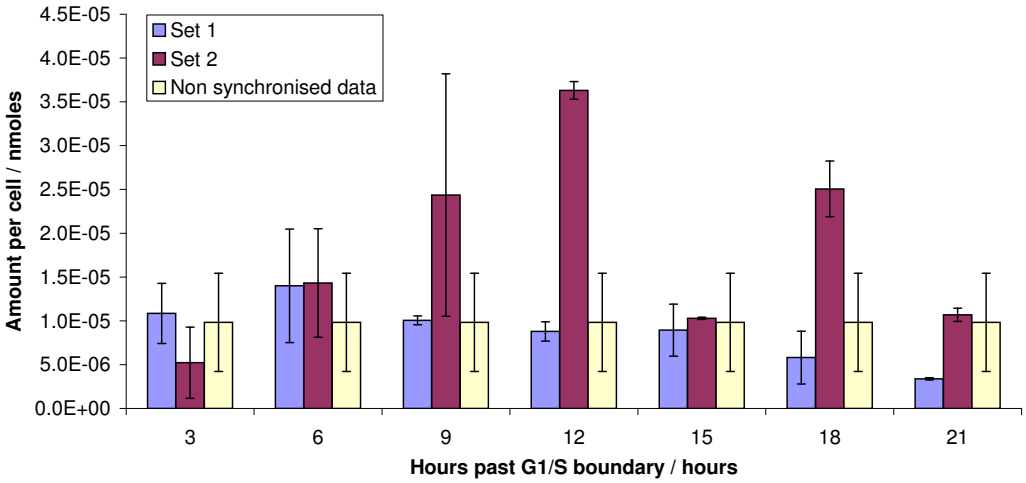

Figure 3.34: Absolute amount per cell of PS for synchronised whole cells. The error bars represent the first standard deviation of this data and includes error arising from biological variability and systematic errors.

As for PC and DAG the PA/PG 3hr time point is the largest in set 1 and is, within error, the same as the set 2 value. The set 2 value is more than twice that of the set 1 value at the 6hr, 9hr and 21hr time points and more than four times larger at the 18hr time point. At 12hrs and 15hrs the values are very similar for both data sets. In all cases the non-synchronised result is smaller than that of the synchronised.

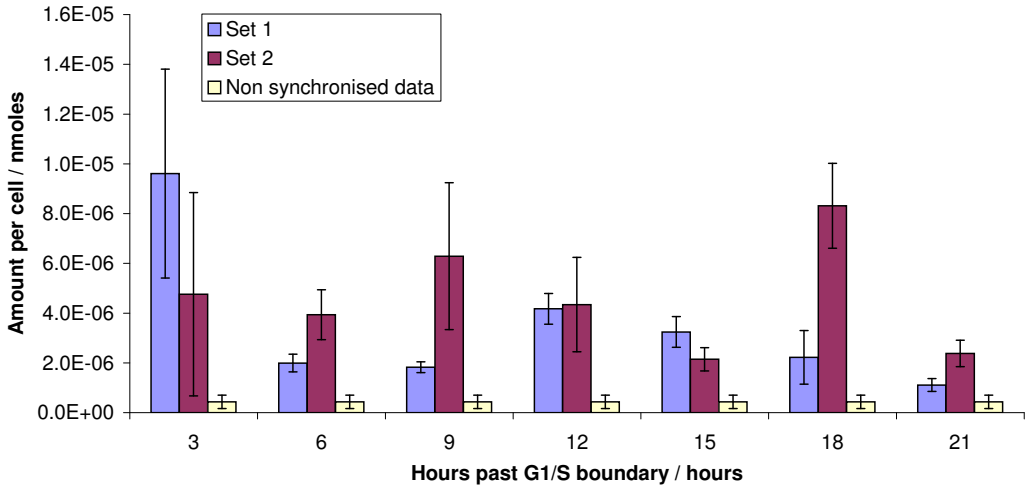

Figure 3.35: Absolute amount per cell of PA and PG for synchronised whole cells.The error bars represent the first standard deviation of this data and includes error arising from biological variability and systematic errors.

The total amount of phospholipid per cell is shown in Figure 3.36. The pattern is very similar to that of the total PC per cell, however this is unsurprising as PC forms the greatest proportion of cellular phospholipid content. There does not appear to be a doubling of phospholipid before mitosis as would be expected for the formation of two daughter cells [10]. There are several possible explanations for this observation. It was suggested in section 3.3.2 that some alterations in the phospholipid composition of synchronised populations relative to asynchronous populations was an artefact of treatment with mimosine. It is therefore possible that artefacts in total lipid content may arise from mimosine treatment thereby masking any contribution from the cell cycle position. It is also possible that the phospholipids are not fully synchronised with DNA synthesis following the cell cycle block. The flow cytometry analysis presented in section 3.3.1 indicated that the cell population was not 100% synchronised. A proportion of the cell population may therefore be halving their mass whilst others are doubling leading to only a small net increase in the total phospholipid that is not visible by this technique.

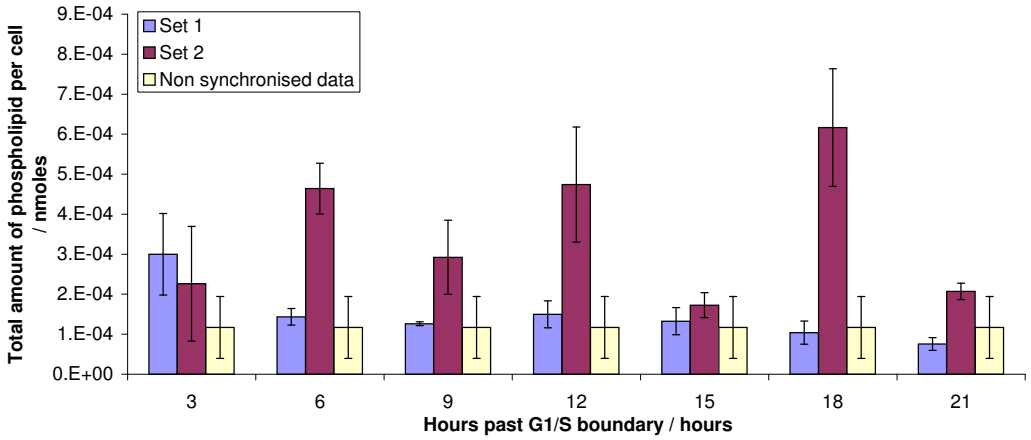

Figure 3.36: Total amount of phospholipid per cell

The composition of each phospholipid class as a percentage of the total content is shown in Figure 3.37. The proportion of PC in set 1 is similar to the non synchronised data (Figure 3.8) except for the 3hr, 18hr and 21hr time points which are at least 10% greater. Set 2 however shows a higher proportion of PC than the non synchronised data over all time points, ranging from more than 20% greater at the 3hr, 9hr and 15hr time points to more than 30% greater at the 6hr time point.

In both data sets the percentage of PE per cell is less than the 27% of non synchronised cells, comprising less than 20% of the total in set 1 and less than 10% of the total in set 2. As described in section 3.3.2, there seems to be an increase in saturated phospholipid molecular species and a decrease in unsaturated species which accompanies synchronisation of the cell population with mimosine. The PE phospholipid class has a higher proportion of unsaturated molecular species than PC which contains mainly saturated or monounsaturated molecular species. It is possible that the larger proportion of PC and lower proportion of PE in synchronised cells relates to this apparent alteration in the saturation level.

The percentage of DAG in set 1 of the synchronised data ranges between 7% and 15.5% of the total in contrast to only 1% in non-synchronised data. The percentage of DAG in set 2 of the synchronised data, however, is very similar to that of the non-synchronised data. The percentage of PI in set 1 ranges from 17.6% to 26.4% over the 6hr-15hr time points compared to only 6.8% in the non-synchronised data. The 3hr, 18hr and 21hr PI time points however range between 5% and 9.6%, probably corresponding to the increase in PC at those times. DAG and PI act as

lipid second messengers which control many aspects of cellular function such as proliferation and apoptosis [35, 36]. It is therefore possible that these species are increased in synchronised cell populations as a response to the effect of mimosine. Unlike set 1, however, the proportion of DAG and PI in set 2 is very similar to that of non-synchronsied whole cells.

The proportion of PA/PG in set 1 of the synchronised data is approximately twice that of the non-synchronised. The set 2 value is however very similar to that of the non-synchronised data. The deuterated PC will be discussed in Chapter 5.

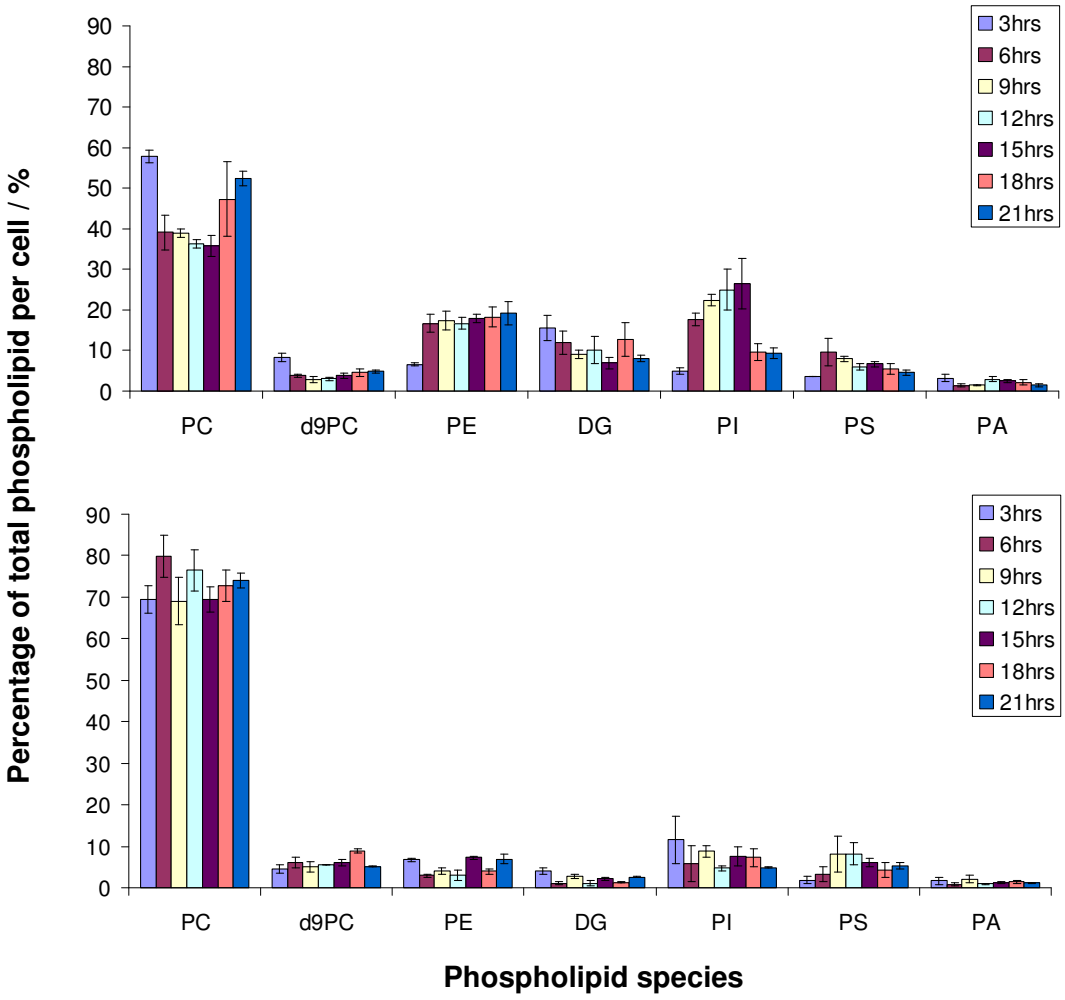

Figure 3.37: Each phospholipid species as a percentage of total phospholipid content per cell. Set 1 and 2 respectively from top. (In this case DAG is labelled as DG)

The results presented in this section indicate that the amount per cell of each phospholipid species is variable over different data-sets. This might be expected due to natural variations in cell size however the changes in the absolute amounts also translate into a different overall composition of phospholipid classes. It is possible that variations could arise from incorrect internal standard addition, however, this seems improbable as such a mistake is unlikely to affect the whole set. Although further investigation would be required for a more detailed assessment, these results indicate that the overall phospholipid content can vary. It has previously been suggested that membrane torque tension is under homeostatic control as this parameter is intrinsically linked to properties such as membrane fluidity and permiability which are in turn linked to the functional properties of the membrane [37]. It is possible that several different membrane compositions may achieve a similar value of membrane torque tension. The variations between data sets described in this chapter may therefore reflect different phospholipid compositions which maintain a similar value of membrane torque tension.

3.4 Summary

This chapter described the use of ESI-MS to determine the phospholipid composition of whole HeLa cells. Section 3.2 detailed the analysis of non-synchronised whole cells. These asynchronous cell populations were found to contain a large proportion of PC and PE (44% and 29% respectively) which is typical of eukaryotic cells. The total phospholipid content per cell was found to be $1.17 \times 10^{-4} \pm 7.72 \times 10^{-5}$ nmoles.

The molecular species composition of each phospholipid class was also determined. PC was found to be comprised mainly of monounsaturated molecular species, the most abundant of which is 16:0/18:1 at 28.2% of the total. This composition is similar to that previously reported for HL-60 and IMR-32 cells although molecular species containing polyunsaturated chains were also found in IMR-32 cells. PE comprised a mixture of monounsaturated molecular species (63% of the total) and polyunsaturated molecular species (37% of the total). The most abundant species was 18:1/18:1 at 23.8% of the total. The molecular species composition of DAG was very similar to that of PC. Interconversion of PC and DAG was discussed

as a possible explanation for this similarity. As found for PE, PI and PS were composed of both monounsaturated and polyunsaturated molecular species with monounsaturated species comprising over 60% of the total in each case. As found for PC and DAG, PA/PG was composed mainly of monounsaturated molecular species. The biosynthetic pathways between PC, PA, PG and DAG were discussed as this could account for some of the similarities in the composition of the phospholipid classes.

Flow cytometry was used to assess the DNA content of HeLa cells at regular intervals following treatment with mimosine (section 3.3.1). Mimosine was found to arrest the cell cycle prior to the onset of DNA replication. An enrichment of over 20% in the proportion of cells in the G1 phase relative to an asynchronous population was found on removal of the mimosine cell cycle block. The G1 phase was estimated to last for approximately 10 hours, the S phase for 8 hours and the G2/M phases for 3 hours giving a total cell cycle length of 21 hours. These times are similar to previously reported results for HeLa cells.

Section 3.3.2 detailed the molecular species composition of synchronised HeLa cell populations at three hour intervals following removal of the cell cycle block. The non-synchronised data was used as a control to allow direct comparison of the two synchronised data sets and a detailed analysis of the compositional variation between time points. Saturated and monounsaturated PC molecular species were found to show no change or increase relative to the non-synchronised data. Dimonounsaturated species showed the opposite trend with a significant reduction compared to the non-synchronised data. Highly unsaturated PC molecular species, however, showed little change relative to the control. It was noted that certain PC molecular species showed a greater change relative to the non-synchronised control. These species were also the most abundant molecular species in the cell. PE molecular species, within error, remained the same as the non-synchronised control and it was suggested that this may be due to the high proportion of highly unsaturated molecular species in this phospholipid class. DAG molecular species containing an alkyl link were found to be increased relative to the control. There

were some indications that the increase in certain DAG molecular species may be achieved by the remodelling of other DAG molecular species, however further investigation would be required to determine this with any certainty. PI molecular species remained very similar to the non-synchronised data however the large error precluded a detailed assessment. The PS molecular species did not show any consistent trend across both data sets although again the large error precluded a detailed assessment. In the synchronised data, species PA16:0/18:1 became the most dominant instead of PG16:0/18:1.

The molecular species composition of synchronised cells was found to differ to that of non-synchronised cells usually in a saturation dependant manner. It was suggested that this arose as a consequence of the synchronisation technique. A possible link between the synchronisation procedure and cell apoptosis was proposed to account for this change in composition. Two independent measurements were presented for each result, however, differences between these measurements made an accurate assessment of the effect of cell cycle position very difficult. There were however some indications that the cell cycle position may alter the magnitude of changes relative to the non-synchronised control.

The total amount of each phospholipid class per cell was determined (section 3.3.3). A doubling of phospholipid prior to mitosis, as would be expected for the formation of two daughter cells, was not observed. It was suggested that the phospholipids were not synchronised with DNA synthesis following treatment with mimosine. It was also noted that the population was not 100% synchronised and this could lead to no net increase in phospholipid content as some cells would be dividing whilst others are doubling their mass.

The proportion of each phospholipid class was also found to change relative to the non-synchronised. The proportion of PC was found to be greater in the synchonised data at three time points in set 1 and over all time points in set 2. The proportion of PE was less than in the non-synchronised data at all time points in both data sets. The proportion of DAG and PI was higher in set 2 than in the non-synchronised data. It was suggested that DAG and PI might be involved in signalling which controls cellular functions such as apoptosis. The amount per cell of each phospholipid class was found to be variable over the two data sets.

It was suggested that membrane torque tension was under homeostatic control but that different phospholipid compositions may maintain a similar value of this parameter.

References

[1] A. Hunt, G. T. Clark, G. S. Attard, and A. D. Postle. Highly saturated endonuclear phosphatidylcholine is synthesized in situ and colocated with CDP-choline pathway enzymes. *The Journal of Biological Chemistry*, 276(11):8492–8499, 2001.

[2] M.K. Dymond. *An investigation into the mechanism of action of amphiphiles with antineoplastic properties*. PhD thesis, 2001.

[3] C. Kent. Eukaryotic phospholipid biosynthesis. *Annual Reviews*, 64:315–343, 1995.

[4] J.E. Vance and R. Steenbergen. Metabolism and functions of phosphatidylserine. *Progress in Lipid Research*, 44:207–234, 2005.

[5] J.E. Bleasedale, N.E. Tyler, F.N. Busch, and J.G. Quirk. The influence of myo-inositol on phosphatidylglycerol synthesis by rat type II pneumonocytes. *Journal of Biochemistry*, 212:811–818, 1983.

[6] X. Han and R. Gross. Shotgun lipodomics: Electrospray ionisation mass spectrometric analysis and quantitation of cellular lipodomes directly from crude extracts of biological samples. *Mass Spectrometry Reviews*, 24:367–412, 2005.

[7] P. R. Cullis, D. B. Fenske, and M. J. Hope. *Physical Properties and Functional Roles of Lipids in Membranes*. Elsevier, 1996.

[8] J. T. Dodge and G. B. Phillips. Composition of phospholipids and of phospholipid fatty acids and aldehydes in Human red cells. *Journal of Lipid Research*, 8:667–675, 1967.

[9] J. A. Virtanen, K. H. Cheng, and P. Somerharju. Phospholipid composition of the mammalian red cell membrane can be rationalised by a superlattice model. *Proc Natl Acad Sci*, 95:4964–4969, 1998.

[10] S. Jackowski. Cell cycle regulation of membrane phospholipid metabolism. *The Journal of Biological Chemistry*, 271:20219–20222, 1996.

[11] F. Terce, H. Brun, and D. Vance. Requirement of phosphatidylcholine for normal progression through the cell cycle in C3H/10T1/2 fibroblasts. *Journal of Lipid Research*, 35:2130–2142, 1994.

[12] S. Tate and P. Ko Ferringo. Cell cycle: Synchronization at various stages. *Encyclopedia of Life Sciences*, 2005.

[13] T. Krude. Mimosine arrests proliferating human cells before onset of DNA replication in a dose-dependant manner. *Experimental Cell Research*, 247:148–159, 1999.

[14] T. A. Hughes and P. R. Cook. Mimosine arrests the cell cycle after cells enter S-phase. *Experimental Cell Research*, 222:275–280, 1996.

[15] P. Watson, H. Hanauske-Abel, A. Flint, and M. Lalande. Mimosine reversibly arrests cell cycle progession at the G1-S phase border. *Cytometry*, 12:242–246, 1991.

[16] J. W. Gray, F. Dolbeare, M. G. Pallavicini, W. Beisker, and F. Waldman. Cell cycle analysis using flow cytometry. *Int. J. Radiat. Biol*, 49(2):237–255, 1986.

[17] A. Longobardi Givan. *Flow cytometry first principles.* Wiley-Liss, second edition, 2001.

[18] M. L. Whitfield, G. Sherlock, A. J. Saldanha, J. I. Murray, C. A. Ball, K. E. Alexander, J. C. Matese, C. M. Perou, M. M. Hurt, P. O. Brown, and D. Botstein. Identification of genes periodically expressed in the Human cell cycle and their expression in tumors. *Molecular Biology of the Cell*, 13:1977–2000, 2002.

[19] S. M. Janicki and M. J. Monteiro. Presenilin overexpression arrests cells in the G1 phase of the cell cycle. *American Journal of Pathology*, 155(1):135–144, 1999.

[20] M. J. Monteiro and T. I. Mical. Resolution of kinase activities during the HeLa cell cycle: Identification of kinases with cyclic activities. *Experimental Cell Research*, 223:443–451, 1996.

[21] S. Jackowski. Coordination of membrane phospholipid synthesis with the cell cycle. *The Journal of Biological Chemistry*, 269:3858–3867, 1994.

[22] D.A. Ford, R. Miyake, P.E. Glaser, and R.W. Gross. Activation of protein kinase C by naturally occuring ether-linked diglycerides. *Journal of Biological Chemistry*, 264(23):13818–13824, 1989.

[23] A. Musial, A. Mandal, E. Coroneos, and M. Kester. Interleukin-1 and endothelin stimulate distinct species of diglycerides that dfferentially regulate protein kinase C in Mesangial cells. *Journal of Biological Chemistry*, 270(37):21632–21638, 1995.

[24] D. Szuts and T. Krude. Cell cycle arrest at the initiation step of human chromosomal DNA replication causes DNA damage. *Journal of Cell Science*, 117:4897–4908, 2004.

[25] A. Kurose, T. Tanaka, X. Huang, F. Traganos, and Z. Darzynkiewicz. Synchronization in the cell cycle by inhibitors of DNA replication induces histone H2AX phosphorylation: an indication of DNA damage. *Cell Prolif.*, 39:231–240, 2006.

[26] F. Reno, A. Tontini, S. Burattini, S. Papa, E. Falcieri, and G. Tarzia. Mimosine induces apoptosis in HL60 Human tumor cell line. *Apoptosis*, 4:469–477, 1999.

[27] F. Quignon, L. Rozier, A.M. Lachages, A. Bieth, M. Simili, and M. Debatisse. Sustained mitotic block elicits DNA breaks: one-step alteration of ploidy and chromosome integrity in mammalian cells. *Oncogene*, 26:165–172, 2007.

[28] A. E. Greijer and E. van der Wall. The role of hypoxia inducible factor 1 (HIF-1) in hypoxia induced apoptosis. *J. Clin. Pathol.*, 57:1009–1014, 2004.

[29] J. K. Singha, A. Dasguptab, T. Adayeva, S. A. Shahmehdia, D. Hammondc, and P. Banerjee. Apoptosis is associated with an increase in saturated fatty acid containing phospholipids in the neuronal cell line, HN2-5. *Biochimica et Biophysica Acta (BBA) - Lipids and Lipid Metabolism*, 1304:171–178, 1996.

[30] S. Franz, K. Herrmann, B. Fuhrnrohr, A. Sheriff, B. Frey, U.S. Gaipl, R.E. Voll, J.R. Kalden, H-M. Jack, and M. Herrmann. After shrinkage apoptotic cells expose internal membrane-derived epitopes on their plasma membranes. *Cell Death and Differentiation*, 14:733–742, 2007.

[31] L. Urbani, S. Sherwood, and R. Schimke. Dissociation of nulcear and cytoplasmic cell cycle progression by drugs employed in cell synchronization. *Experimental Cell Research*, 219:159–168, 1995.

[32] S. Cooper. Rethinking synchronisation of mammalian cells for cell cycle analysis. *Cell. Mol. Life Sci*, 60:1099–1106, 2003.

[33] S. Cooper, G. Lyer, M. Taruini, and P. Bissett. Nocodazole does not synchronize cells: implications for cell-cycle control and whole-culture synchronization. *Cell Tissue Res*, 324:237–242, 2006.

[34] S. Cooper, K. Z. Chen, and S. Ravi. Thymidine block does not synchronize L1210 mouse leukemic cells: implications for cell cycle control, cell cycle analysis and whole-culture synchronization. *Cell prolif.*, 41:155–167, 2008.

[35] S. Spiegel, D. Foster, and R. Kolesnick. Signal transduction through lipid second messengers. *Currents Opinion in Cell Biology*, 8:159–167, 1996.

[36] M. Wright and C. McMaster. Phospholipid synthesis, diacylglycerol compartmentation and apoptosis. *Biol Res*, 35:223–229, 2002.

[37] J. Beard, G. S. Attard, and M. J. Cheetham. Integrative feedback and robustness in a lipid biosynthetic network. *Journal of the Royal Society Interface*, 5:533–543, 2008.

Chapter 4

Endonuclear phospholipid composition

4.1 Introduction

As introduced in section 1.2.1 phospholipids, distinct from those in the nuclear envelope are found within the endonuclear compartment. Following nuclear isolation and nuclear envelope removal (see sections 7.3 and 2.2.1), ESI-MS was used to probe the endonuclear phospholipid content of HeLa cells. The results of this analysis are detailed in this chapter. For simplicity the detergent n-Decyl β-D-Maltopyranoside is referred to as maltopyranoside during this chapter.

4.2 The phospholipid composition of non-synchronised naked nuclei

The results presented in this section are from cells which have not been treated with a cell cycle inhibitor. They therefore represent the phospholipid composition of a population of cells that is distributed throughout the cell cycle (an asynchronous population).

4.2.1 Molecular species percentage composition

The molecular species composition of endonuclear phospholipid is compared to that of whole cells in Figures 4.1 to 4.6. Additionally the molecular species composition of nuclei extracted with Triton-X-100 is compared to that of nuclei extracted with maltopyranoside. The molecular species composition of the nuclei extracted with Triton-X-100 is an average of measurements obtained over four different days. For nuclei extracted with matopyranoside, the result presented is an average of measurements taken over three different days. On each day the composition of phospholipid extracted from three separate flasks of cells was measured. The error bars on the data represent the first standard deviation of all these measurements (12 samples in total for Triton-X-100 and 9 for maltopyranoside). The reported standard deviation therefore includes error resulting from both biological variability and instrument instability. The reader is referred to section 3.2.1 for a discussion of the errors associated with the whole cell data.

For all phospholipid classes, the molecular species composition is essentially the same for nuclei extracted with either detergent. This observation gives further evidence to that presented in section 2.2.1 that maltopyranoside is a suitable alternative to Triton-X-100. In addition, this finding also suggests that the molecular species composition observed is not simply an artefact of the detergent used.

Analysis of the PC fraction (Figure 4.1) shows that endonuclear PC is enriched, with respect to whole cell PC, in species where both fatty acid chains are saturated. Disaturated PC molecular species total 34.4% in nuclei extracted with Triton-X-100 and 22% in nuclei extracted with maltopyranoside. This is in contrast to a total of 12.3% in whole cells. Species where both fatty acid chains are unsaturated are found in a higher proportion in the whole cell. Diunsaturated PC molecular species total 32.7% in the whole cell. In nuclei extracted with maltopyranoside this value is 14.1% and in nuclei extracted with Triton-X-100 it is 21.6%. Monounsaturated species, however, remain at a very similar value between the whole cell and nucleus.

The finding that endonuclear PC is enriched in saturated molecular species agrees with previous study of IMR-32 cells [1] and gives further evidence that this is a generalised phenomenon across a variety of Human cell lines [2]. The precise role

of this saturated endonuclear PC is currently unknown although several ideas have been put forward including structural, signalling and antioxidant [2].
Unlike PC, the molecular species compositions of PE (Figure 4.2), PS (Figure 4.5) and PA/PG (Figure 4.6) remain the same between the whole cell and endonuclear compartments. This also agrees with the previous analysis of PA and PE composition for IMR-32 cells [1].

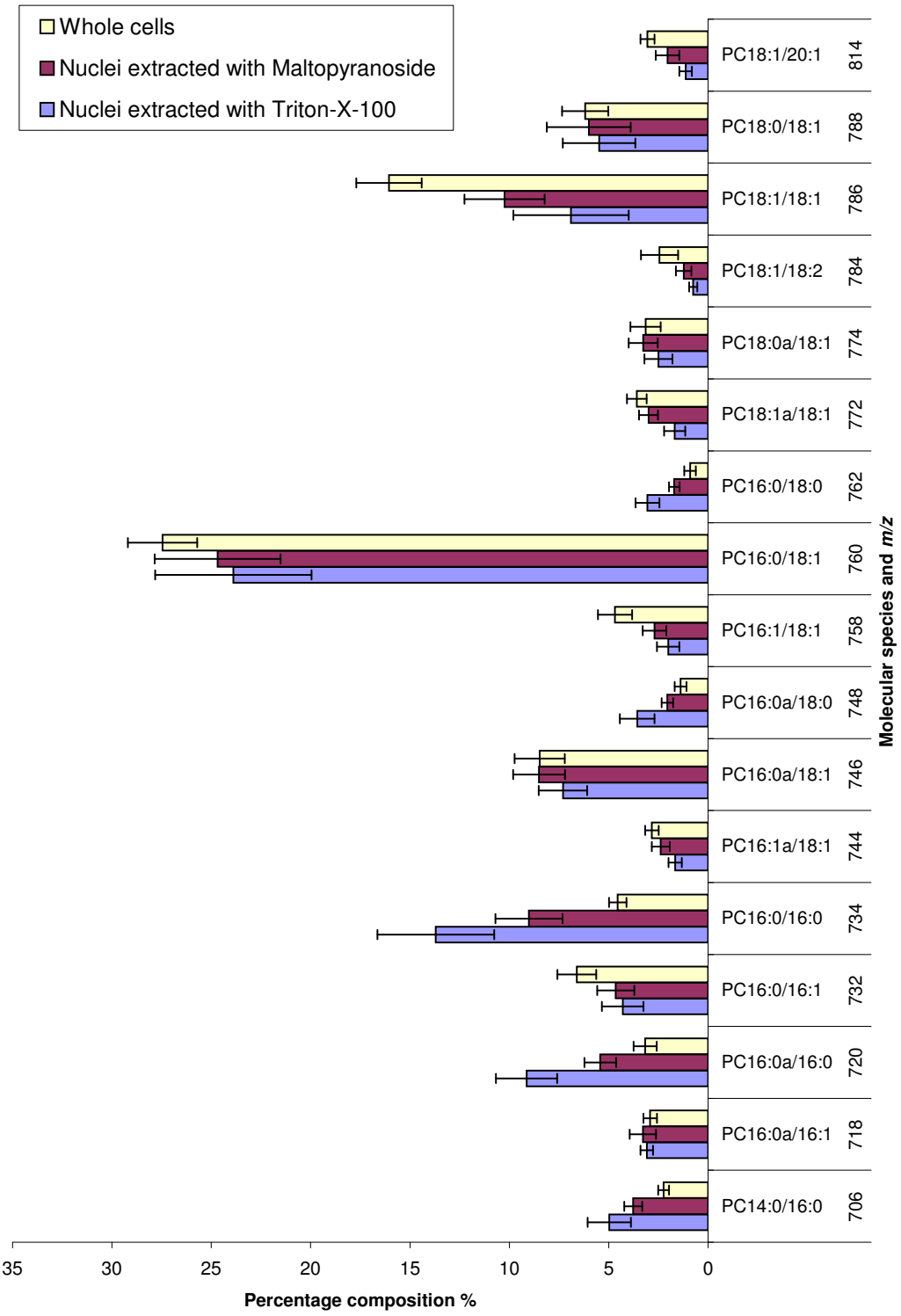

Figure 4.1: Molecular species percentage composition of PC in nuclei. Endonuclear PC is enriched in molecular species where both fatty acid chains are saturated. The error bars represent the first standard deviation of this data and include errors arising from biological variability and instrument instability.

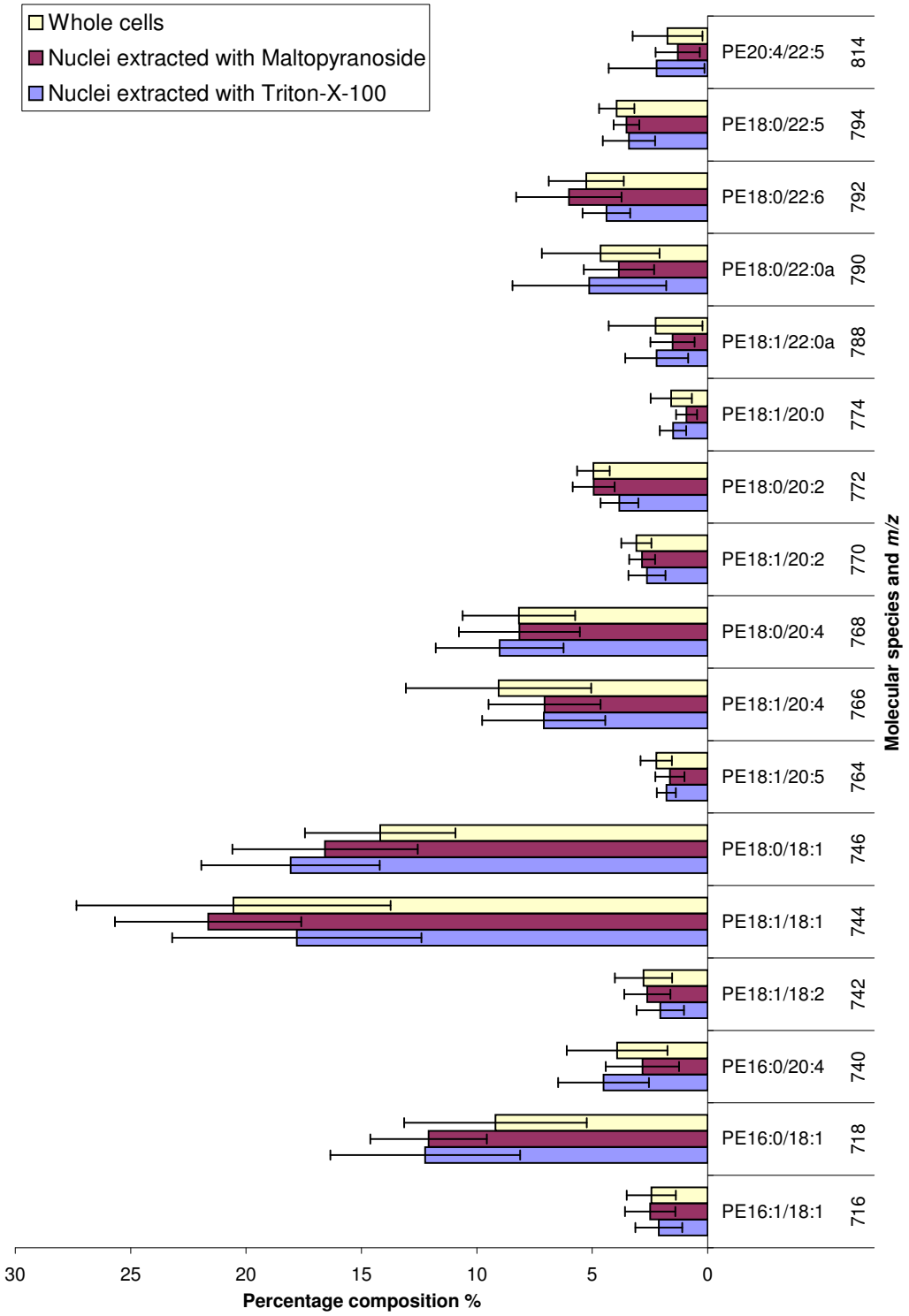

Figure 4.2: Molecular species percentage composition of PE in nuclei. The composition of endonuclear PE remains the same as whole cell PE. The error bars represent the first standard deviation of this data and include errors arising from biological variability and instrument instability.

Assessment of DAG and PI indicates that the difference between whole cell and nuclear molecular species composition is not restricted to PC. The most abundant molecular species of DAG in the whole cells is 16:0/18:1 (m/z 612) but this is replaced by 16:0/18:0 (m/z 614) in the nucleus. There also appears to be an increase relative to the whole cells in the other saturated species, 16:0/16:0 (m/z 586) and 18:0/18:0 (m/z 642), although the large standard deviation precludes an accurate assessment. Similarly there is a greater proportion of PI16:0/18:0 (m/z 837) in the nucleus to that in the whole cell. Although the endonuclear PI is enriched in 16:0/18:0 when compared to the whole cell, it is important to note that PI isolated from both fractions is mainly unsaturated with a high proportion of species containing polyunsaturated chains.

Nuclear DAG can be generated by the hydrolysis of PC or by the hydrolysis of PI. It has been shown that DAG derived from PI is mainly unsaturated whereas that derived from PC is predominantly disaturated and monounsaturated [3]. It was suggested that nuclei contain two independently regulated pools of DAG, one that is highly polyunsaturated (derived from PI) and one that is mainly disaturated and monounsaturated (derived from PC). Analysis of the PA composition showed that this was highly polyunsaturated indicating that it was generated from polyunsaturated DAG [4].

Our ESI-MS study indicates that the endonuclear DAG present in HeLa cells is most likely derived from PC as it is composed mainly of disaturated and monounsaturated species (Figure 4.3). Endonuclear PA however is composed mainly of polyunsaturated molecular species (Figure 4.6) although the standard deviation of this data prevents a detailed analysis. This would indicate that PA is being generated from a pool of polyunsaturated DAG which forms a smaller fraction of the endonuclear DAG content.

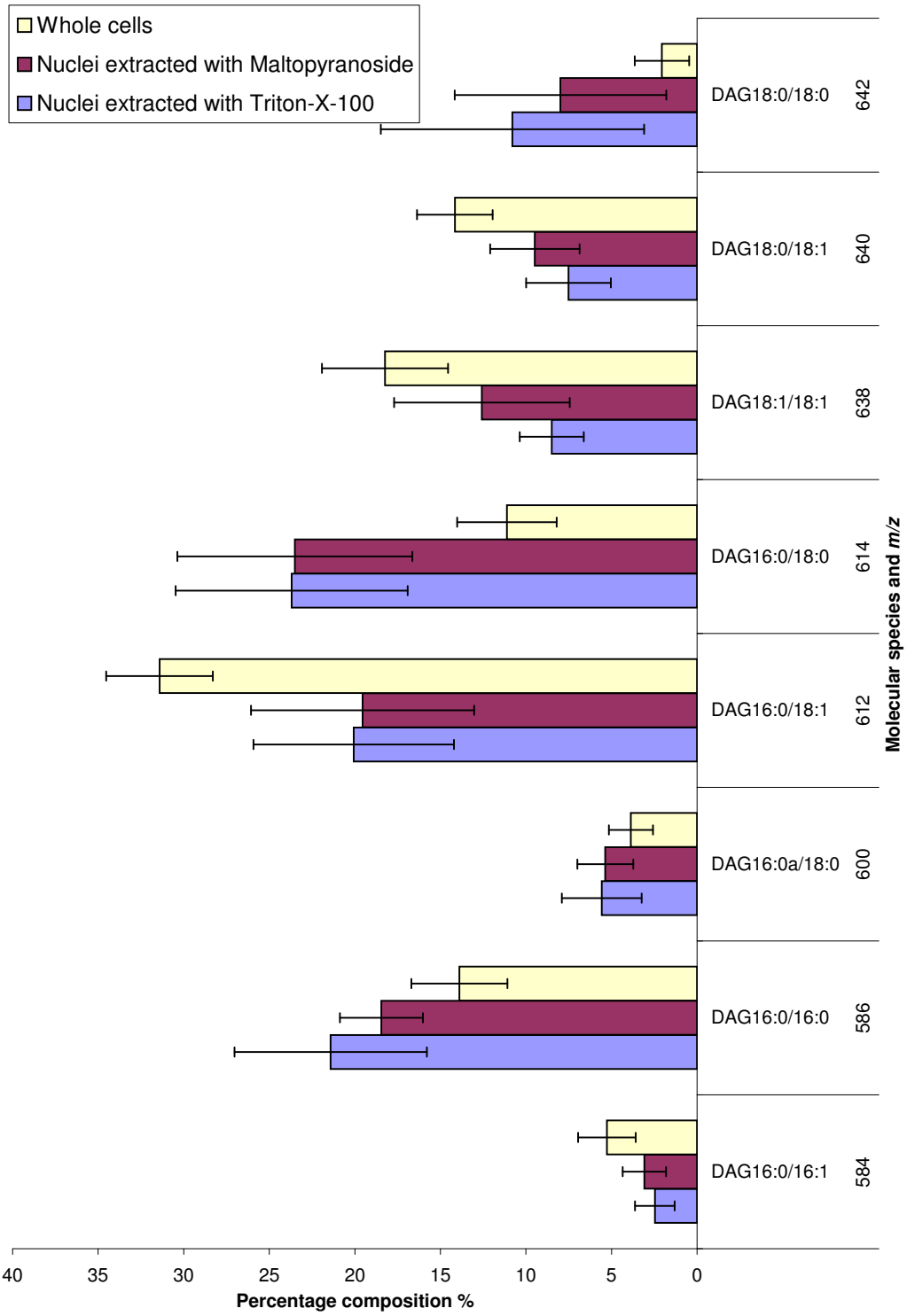

Figure 4.3: Molecular species percentage composition of DAG in nuclei. Endonuclear DAG is enriched in molecular species where both fatty acid chains are saturated. The error bars represent the first standard deviation of this data and include errors arising from biological variability and instrument instability.

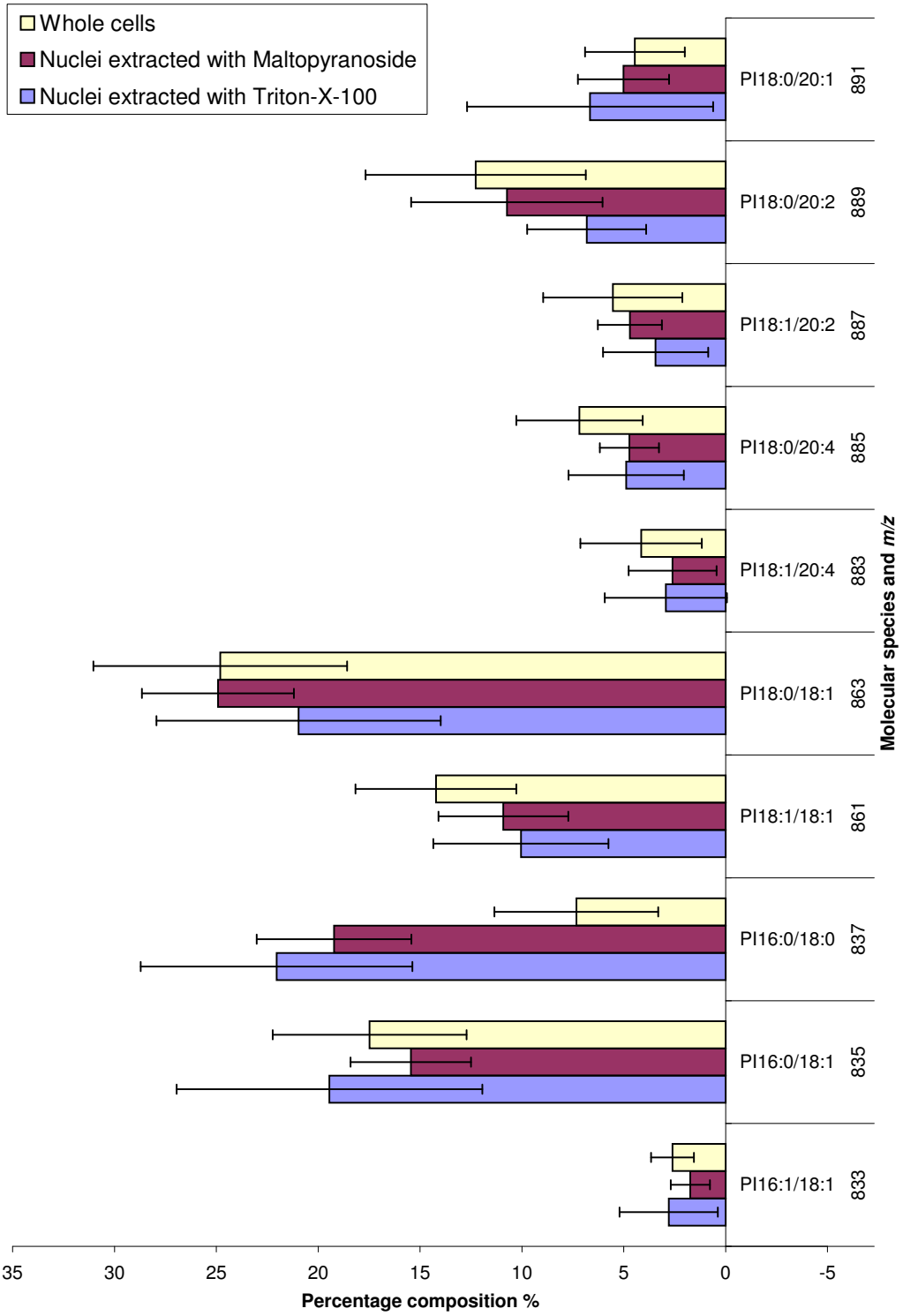

Figure 4.4: Molecular species percentage composition of PI in nuclei. Endonuclear PI is enriched in molecular species where both fatty acid chains are saturated although both whole cell and nuclear fractions contain a high proportion of unsaturated species. The error bars represent the first standard deviation of this data and include errors arising from biological variability and instrument instability.

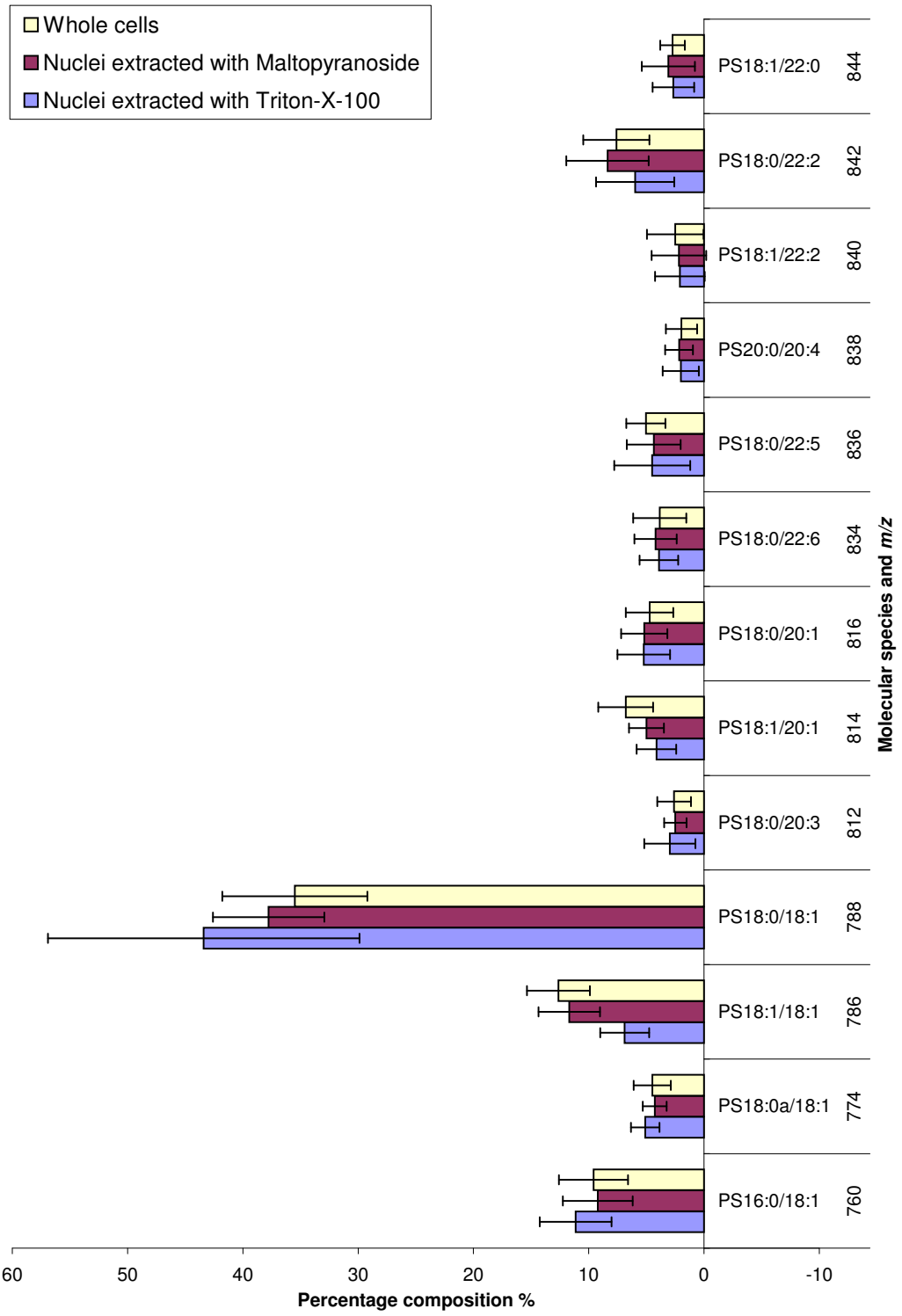

Figure 4.5: Molecular species percentage composition of PS in nuclei. The composition of endonuclear PS remains the same as whole cell PS. The error bars represent the first standard deviation of this data and include errors arising from biological variability and instrument instability.

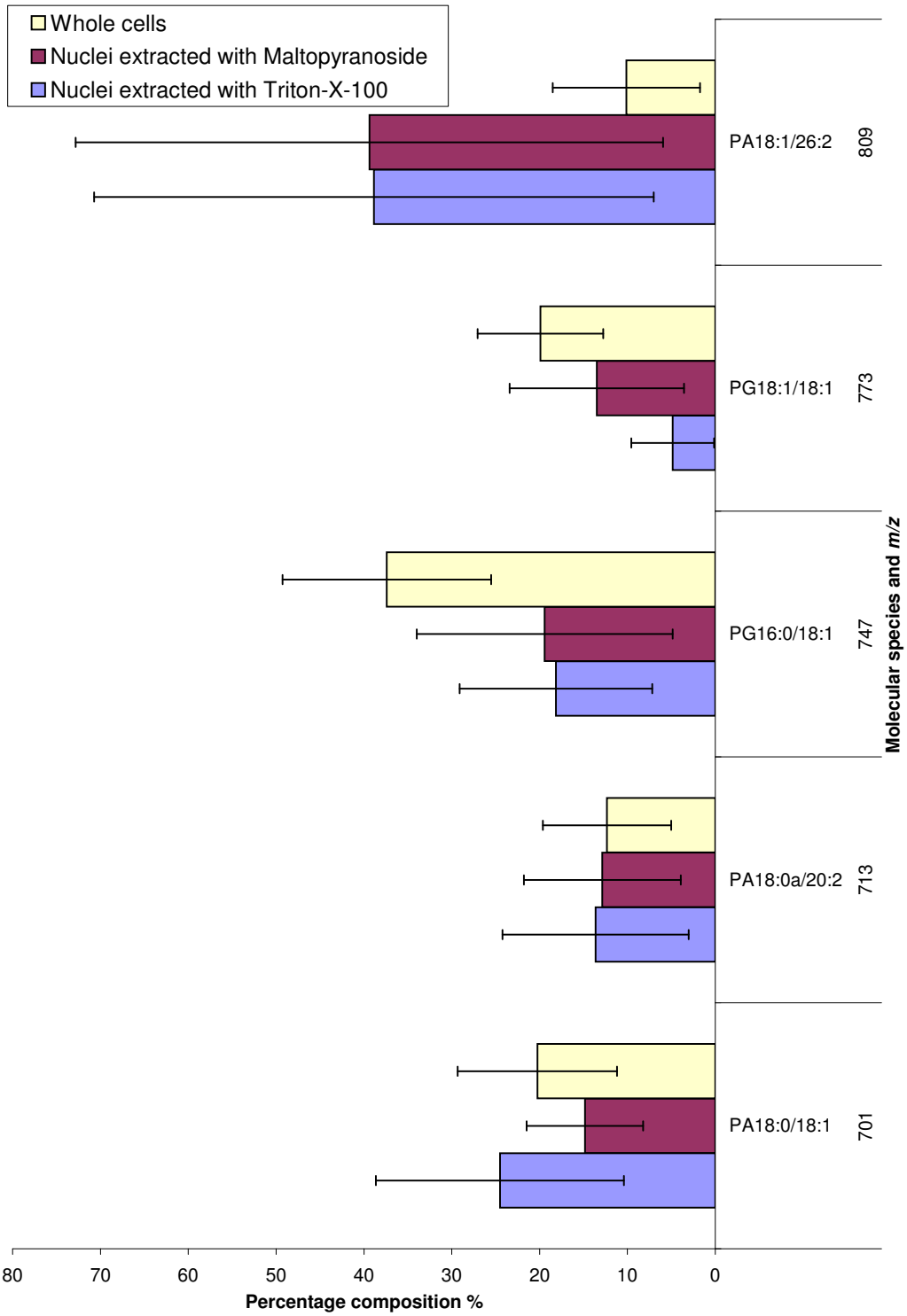

Figure 4.6: Molecular species percentage composition of PA and PG in nuclei. The composition of endonuclear PA/PG remains the same as whole cell PA/PG. The error bars represent the first standard deviation of this data and include errors arising from biological variability and instrument instability.

4.2.2 Quantified data

Inclusion of internal standards enabled the concentration of endonuclear phospholipids to be determined. The total amount of endonuclear phospholipid for nuclei extracted with maltopyranoside is $1.39 \times 10^{-5} \pm 1.3 \times 10^{-5}$ nmoles which is approximately 12% of that in the whole cell. For nuclei extracted with Triton-X-100 the total amount of phospholipid per cell is $1.59 \times 10^{-5} \pm 2.41 \times 10^{-5}$ nmoles which is approximately 14% that in the whole cell.

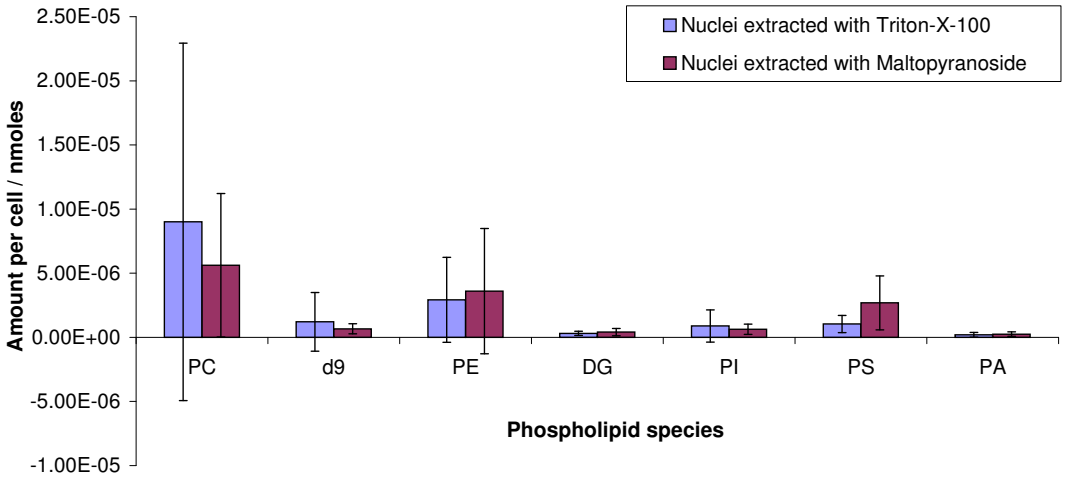

Figure 4.7: Absolute amount per nucleus of each phospholipid class. The error includes biological variability, instrument instability and errors arising from cell counting and internal standard addition.

Figure 4.7 shows the amount in nmoles of each phospholipid class per nucleus. The values presented are an average of measurements taken over different days as detailed in section 4.2.1. In addition to instrument instability and biological variability, the reported first standard deviation also inlcudes errors arising from cell counting and internal standard addition. The error on this measurement is very large, probably due to the problems in counting nuclei as described in section 2.2.2. The proportion of phospholipid classes in the nucleus is within error the same as that in the whole cell (Figure 4.8). This suggests that although the molecular species composition (section 4.2.1) of PC, DAG and PI is found to vary between the whole cell and nucleus, the overall amount of each phospholipid class is maintained. The values, within error, are comparable for nuclei extracted with

either Triton-X-100 or maltopyranoside giving further evidence that the results are not an artefact of the detergent.

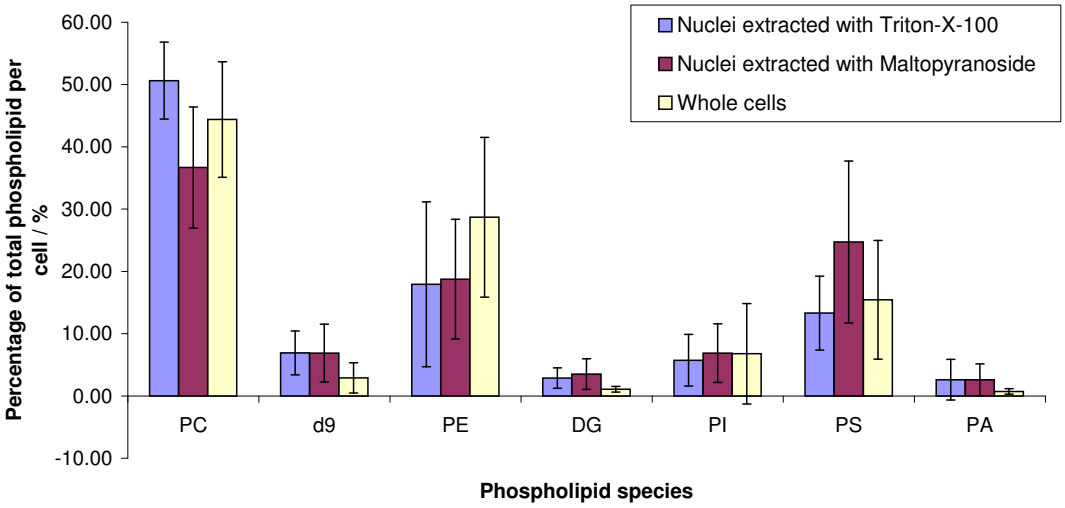

Figure 4.8: Each phospholipid class as a percentage of total phospholipid content per cell or nucleus

4.3 Endonuclear phospholipid composition of synchronised cells

As described in section 3.3, L-mimosine was used to synchronise cell populations. After removal of the cell cycle block, the cells were allowed to progress through the cell cycle to an appropriate point before isolation of the naked nuclei. The phospholipid content of these nuclei was then assessed by ESI-MS. Throughout this section, hour has been abbreviated to 'hr'.

4.3.1 Molecular species percentage composition

The phospholipid molecular species composition of naked nuclei, extracted from synchronised populations of HeLa cells, was determined by ESI-MS and is summarised in this section. The molecular species are expressed as a percentage of the total for each head group class. The molecular species composition was monitored at time intervals throughout the cell cycle as described for whole cells in section

3.3.2. For each class of phospholipid, the molecular species composition of nuclei extracted both with Triton-X-100 and maltopyranoside is shown. A second independent measurement from nuclei extracted with maltopyranoside is also shown. Figures 4.9 to 4.11 show the molecular species composition of PC in HeLa cell nuclei at three hourly intervals following removal of the cell cycle block. The data presented for each time point is an average of the results from three phospholipid samples. The error bars on this data represent the first standard deviation of the three measurements. Each sample was obtained from separate flasks of cells, therefore, the reported standard deviation includes biological variability in addition to systematic errors.

As described for non-synchronised cells (section 4.2), endonuclear PC is enriched in saturated PC molecular species with respect to the whole cell. In the whole cells (section 3.3.2) the most abundant PC molecular species were found to be 16:0/18:1 (m/z 760) and 18:1/18:1 (m/z 786), however, in the nuclei species 18:1/18:1 (m/z 786) is below 10% of the total in all three data sets. The most abundant species in the nuclei are 16:0/18:1 (m/z 760) and 16:0/16:0 (m/z 734). Species 16:0/16:0 is, however, at or below 5% of the total in whole cells. The saturated molecular species 16:0/18:0(m/z 762) is present in all three synchronised nuclei data sets but below the selection threshold (section 2.3.3) for whole cells. Conversely, species 16:1a/18:1 (m/z 744), 16:0/20:4 (m/z 782), 18:1/18:2 (m/z 784), 18:1/20:4 (m/z 808), 18:0/20:4 (m/z 810) and 18:1/20:1 (m/z 814) are above the selection threshold in the whole cells but not in the nuclei.

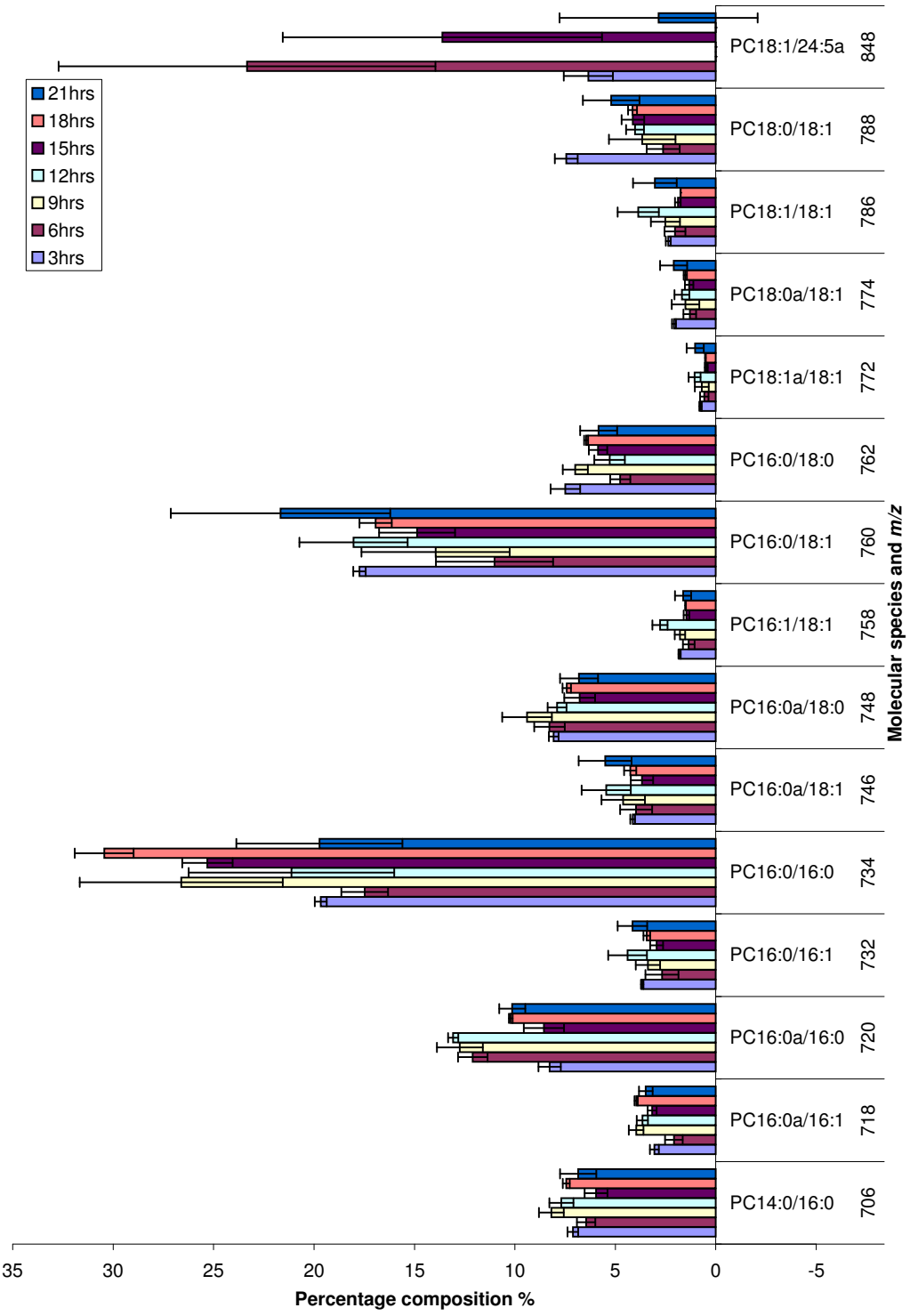

Figure 4.9: Molecular species percentage composition of PC for synchronised nuclei extracted with Triton-X-100. The error bars represent the first standard deviation of these measuremtns and include systematic errors and biological variability.

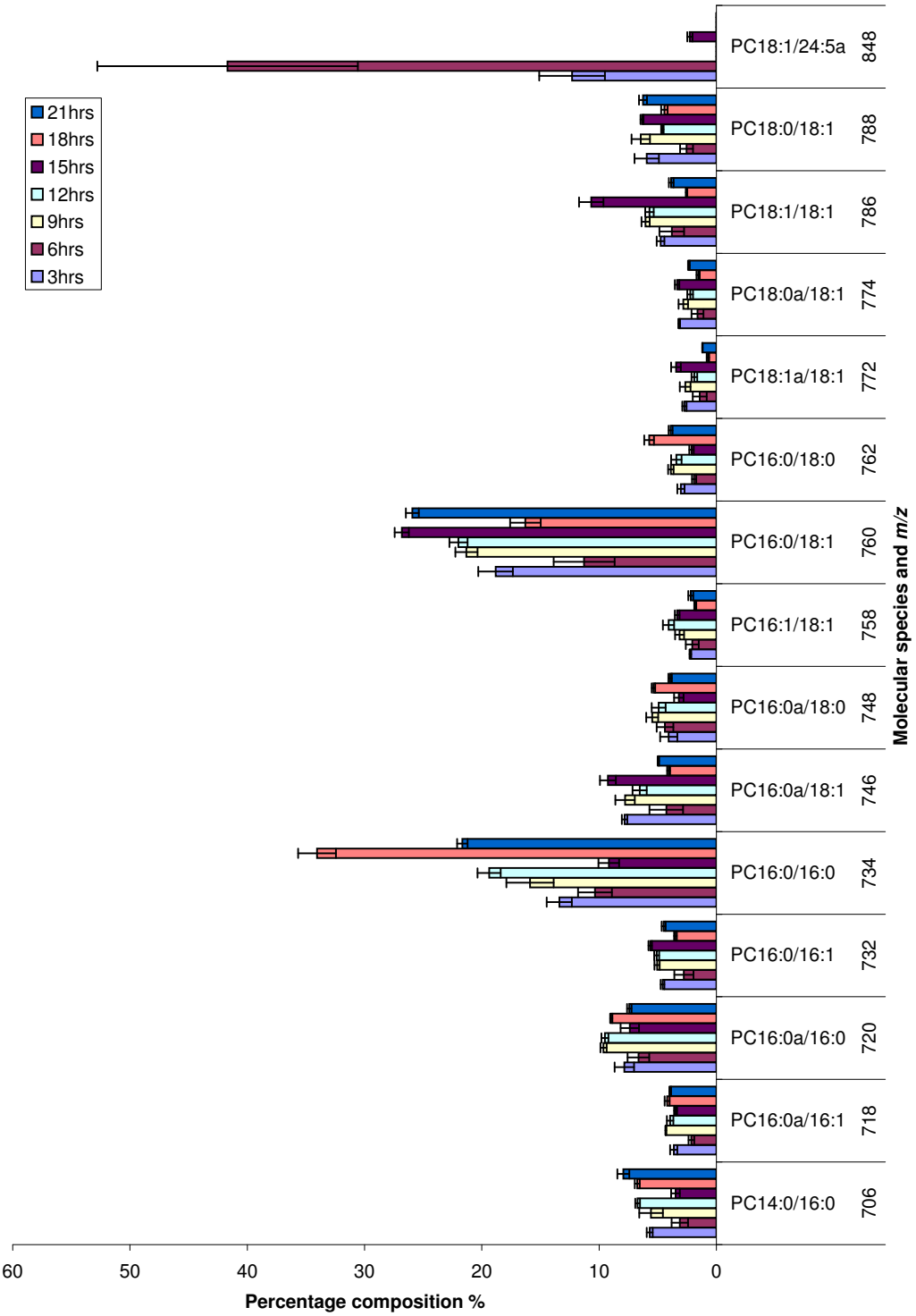

Figure 4.10: Molecular species percentage composition of PC for synchronised nuclei extracted with maltopyranoside. The error bars represent the first standard deviation of these measuremtns and include systematic errors and biological variability.

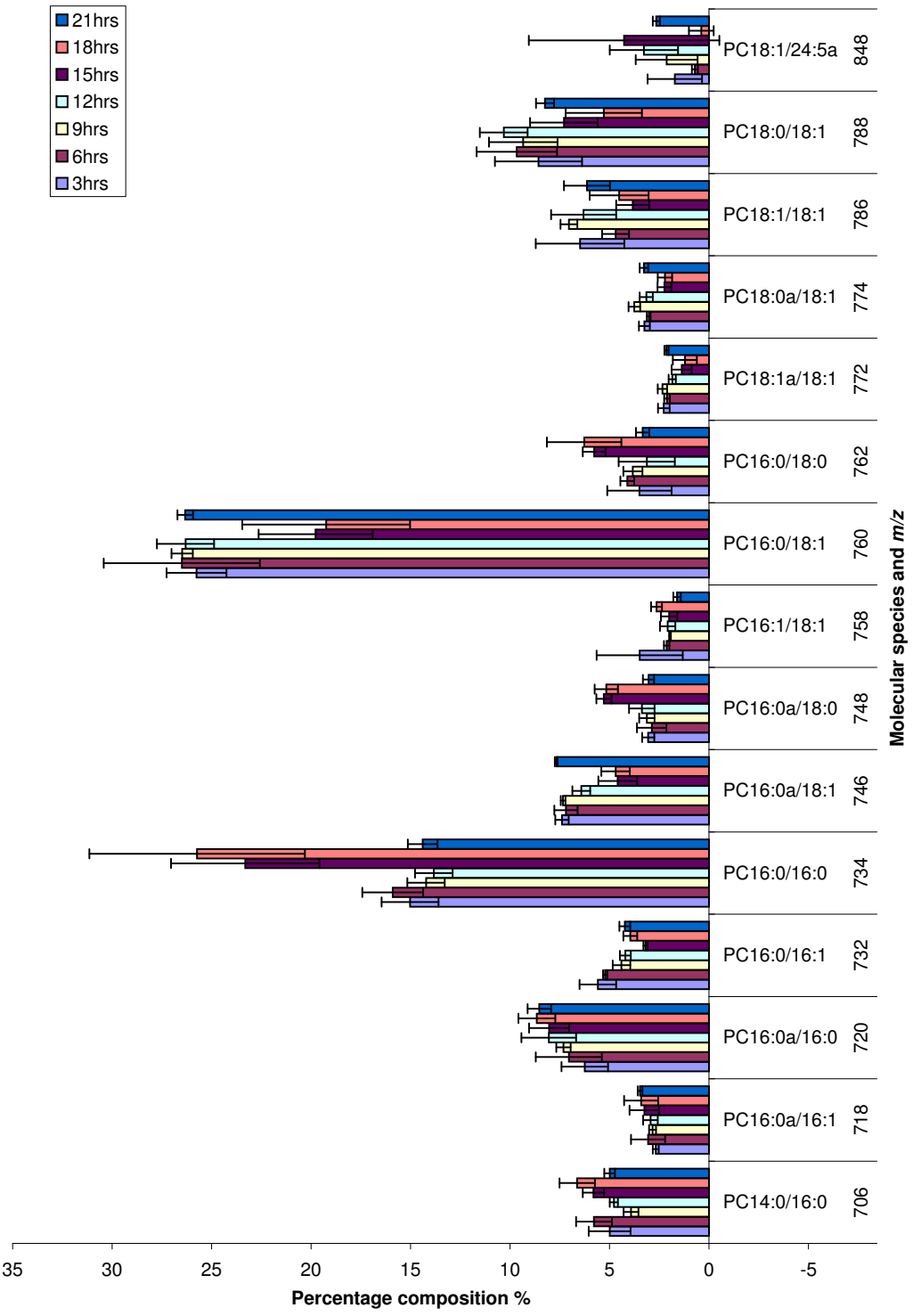

Figure 4.11: Molecular species percentage composition of PC for synchronised nuclei extracted with maltopyranoside repeat. The error bars represent the first standard deviation of these measuremtns and include systematic errors and biological variability.

For whole cells (section 3.3.2), the non-synchronised data was used as a control to allow detailed analysis of compositional variation. This same method was also applied to the nuclei. The species which show a significant change relative to the non-synchronised control are again defined as those which show a difference greater than the combined standard deviation of the synchronised and asynchronous results.

Figures 4.12 to 4.14 show the result of subtracting the asynchronous PC data from the synchronised. Set 1 corresponds to the nuclei extracted with Triton-X-100, set 2 to the nuclei extracted with maltopyranoside and set 3 to the second independent measurement of nuclei extracted with maltopyranoside. The error bars represent the combined standard deviation of the synchronised and asynchronous results. This combined standard deviation is determined by calculating the square root of the sum of the squared standard deviations for each equivalent data point. This combined standard deviation therefore includes the error of instrument instability from the asynchronous data (see section 4.2.1) and the biological variability and systematic errors from both data sets.

The saturated PC species (Figure 4.12) show a general increase relative to the non synchronised control with the 18hr time point of species 16:0/16:0 (m/z 734) consistently showing the greatest increase over all three data-sets. At the 18 hour time point a large proportion of the cell population is in the G1 phase of the cell cycle (Table 3.1). During the G1 phase cells are thought to 'commit' to undergo mitosis and it is possible that a change in nuclear phospholipid composition may be linked to this [5].

Although whole cells (Figure 3.14) also showed a general increase in saturated molecular species relative to the non-synchronised control, the trend was less consistent between data sets. In the whole cells, species 16:0/18:0a (m/z 748) shows an increase relative to the non-synchronised over all time points in set 1 but only the 3hr and 15hr time points are increased in set 2. This contrasts with the nuclei data in which there is an increase over all time points in all data sets, with the exception of 6hrs in set 3. Species 14:0/16:0 (m/z 706) and 16:0a/16:0 (m/z 720) show an increase at most time points in all data sets in the nuclei data. These species only show an increase at 12hrs and 18hrs respectively in set 1 of the whole cell data. The magnitude of changes in the whole cell data are also less than that

of nuclei with a maximum difference of approximatly 1.5% compared to almost 25% for species 16:0/16:0 (m/z 734) in set 2 of the nuclei data.

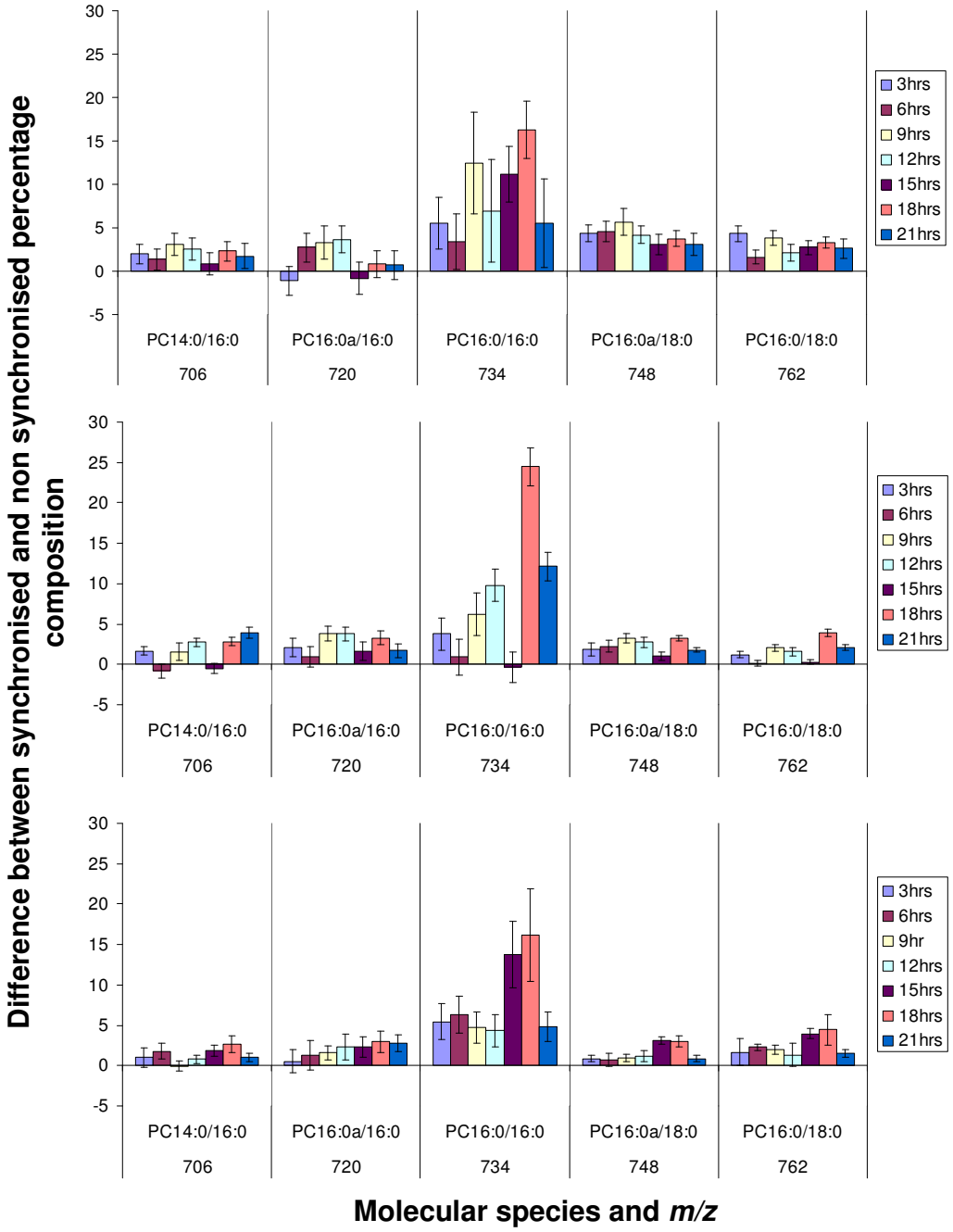

Figure 4.12: Difference between synchronised and non-synchronised percentage composition for saturated PC molecular species. Set 1 (nuclei extracted with Triton-X-100) is shown at the top followed by set 2 (nuclei extracted with maltopyranoside) and set 3 (independent repeat of nuclei extracted with maltopyranoside). The error bars represent the combined first standard deviation of the synchronised and asynchronous data.

The monounsaturated PC molecular species (Figure 4.13) generally show no change or a decrease relative to the non-synchronised control although a slight increase of species 18:0/18:1 (m/z 788) is seen at 12hrs in set 3. The 6hr time point of species 16:0/18:1 (m/z 760) shows the most significant decrease in set 1 and 2 however no change is seen at this time point in set 3. The 15hr and 18hr time points also show a significant decrease in sets 1 and 3 for species 16:0a/18:1 (m/z 746) and 16:0/18:1 (m/z 760) although the 15hr time point shows no change in set 2 for either species.

This decrease in monounsaturated PC molecular species contrasts with the findings for whole cells (Figure 3.15) which show no change or an increase relative to the non-synchronised control. The small increase of species 18:0/18:1 (m/z 788) at 12hrs in data set 3 agrees with the whole cell results but this is not consistent with the other two data sets.

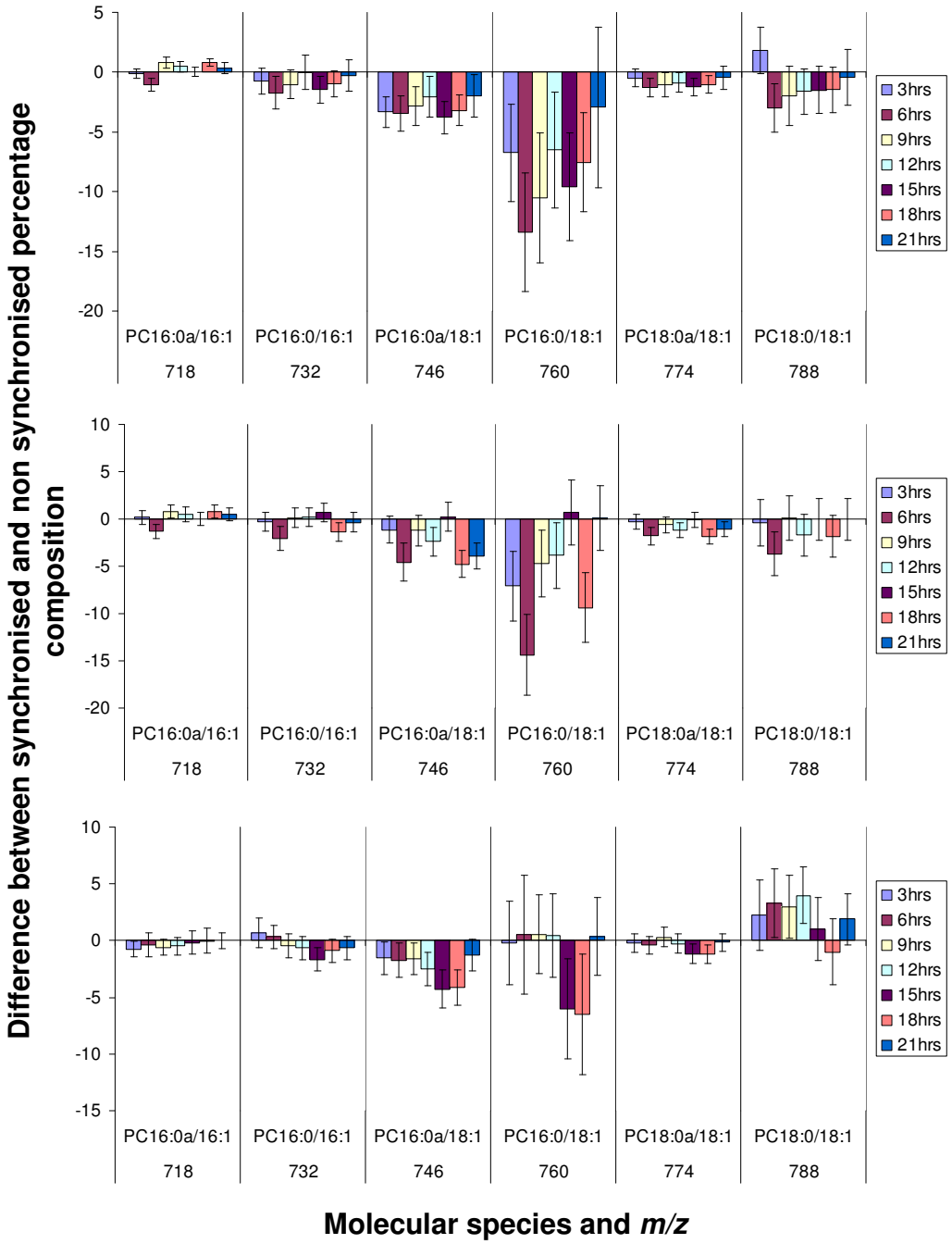

Figure 4.13: Difference between synchronised and non-synchronised percentage composition for monounsaturated PC molecular species. Set 1 (nuclei extracted with Triton-X-100) is shown at the top followed by set 2 (nuclei extracted with maltopyranoside) and set 3 (independent repeat of nuclei extracted with maltopyranoside)

The di-monounsaturated species (Figure 4.14) generally show no change or a decrease relative to the non-synchronised control with species 18:1/18:1 (m/z 786) showing the most significant change. The highly unsaturated 18:1/24:5a (m/z 848) species shows no change over most time points, however, in both set 1 and 2 the 6hr time point shows a significant increase relative to the non-synchronised data. At 6hrs, the majority of the cell population have entered the S phase of the cell cycle (section 3.3.1) It is possible that this molecular species is involved in the regulation of progression into this phase.

The di-monounsaturated and highly unsaturated PC species of the whole cells (Figures 3.16 and 3.17) also showed similar results except for the increase at 6hrs. As mentioned earlier, however, the highly unsaturated species such as 16:0/20:4 (m/z 782) which are present in the whole cell data are below the selection threshold in the nuclei data.

As described for whole cells (section 3.3.2) certain molecular species show more change relative to the non-synchronised control than others. The largest changes, at one or more time points, are in species 16:0/16:0 (m/z 734) and 16:0/18:1 (m/z 760). This again correlates with the most abundant endonuclear PC molecular species (Figures 4.9 to 4.11).

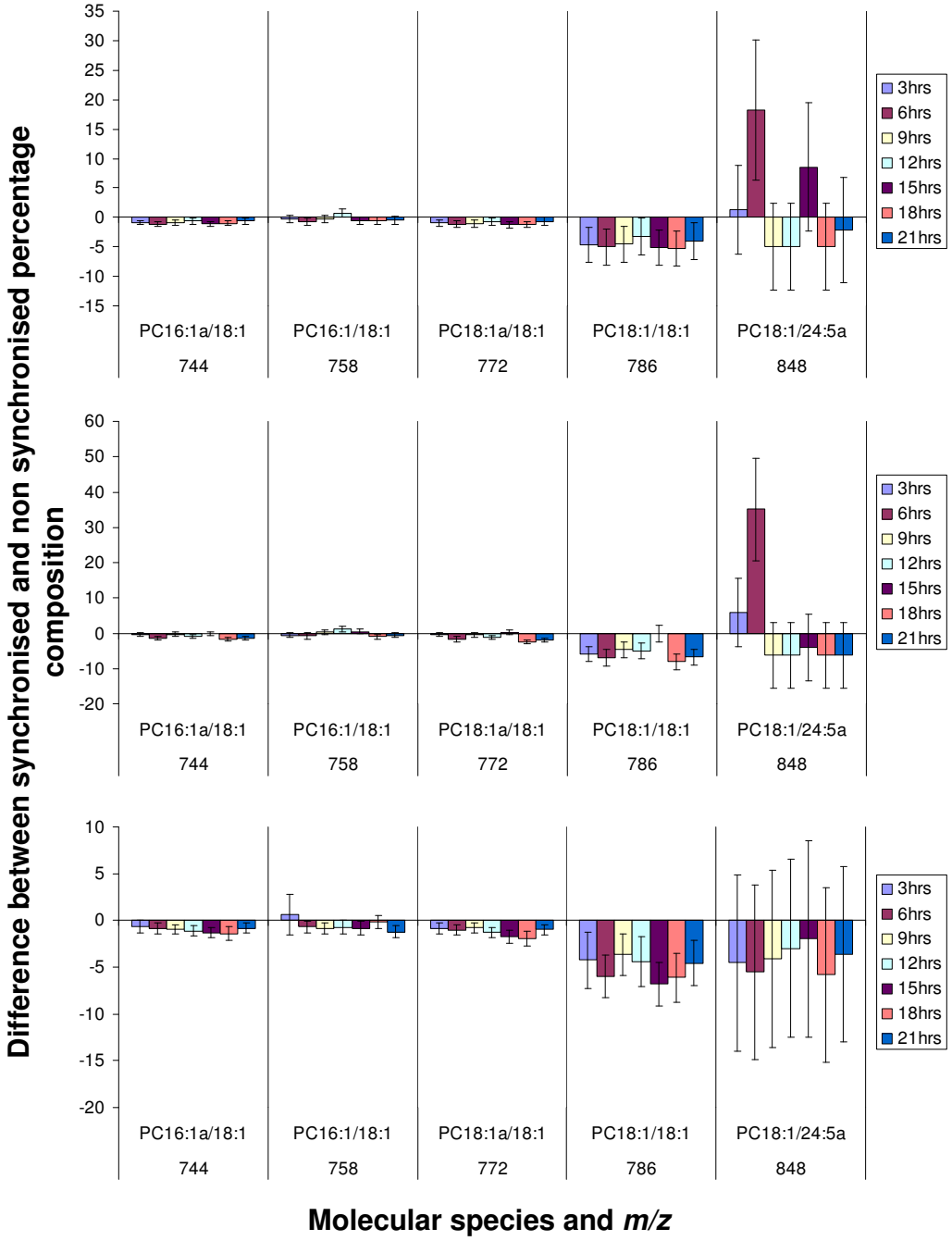

Figure 4.14: Difference between synchronised and non-synchronised percentage composition for unsaturated PC molecular species. Set 1 (nuclei extracted with Triton-X-100) is shown at the top followed by set 2 (nuclei extracted with maltopyranoside) and set 3 (independent repeat of nuclei extracted with maltopyranoside)

Figures 4.15 to 4.17 show the molecular species composition of PE in HeLa cell nuclei at three hourly intervals following removal of the cell cycle block. As described for whole cells and nuclei from non-synchronised cells, the most abundant species are 18:0/18:1 (m/z 746) and 18:1/18:1 (m/z 744). Species 14:0/16:0 (m/z 664), 16:0/16:0 (m/z 692), 16:0/18:0 (m/z 720), 18:0a/18:1 (m/z 732), 18:0/18:0 (m/z 748), 18:0/22:0 (m/z 804) and 20:3/22:0 (m/z 826) are shown in the synchronised nuclei data but are below the selection threshold in the whole cell data and non-synchronised nuclei data. It should be noted, however, that the standard deviation on these species is very large. A more detailed comparison to the non-synchronised data is shown below (Figures 4.18 to 4.21).

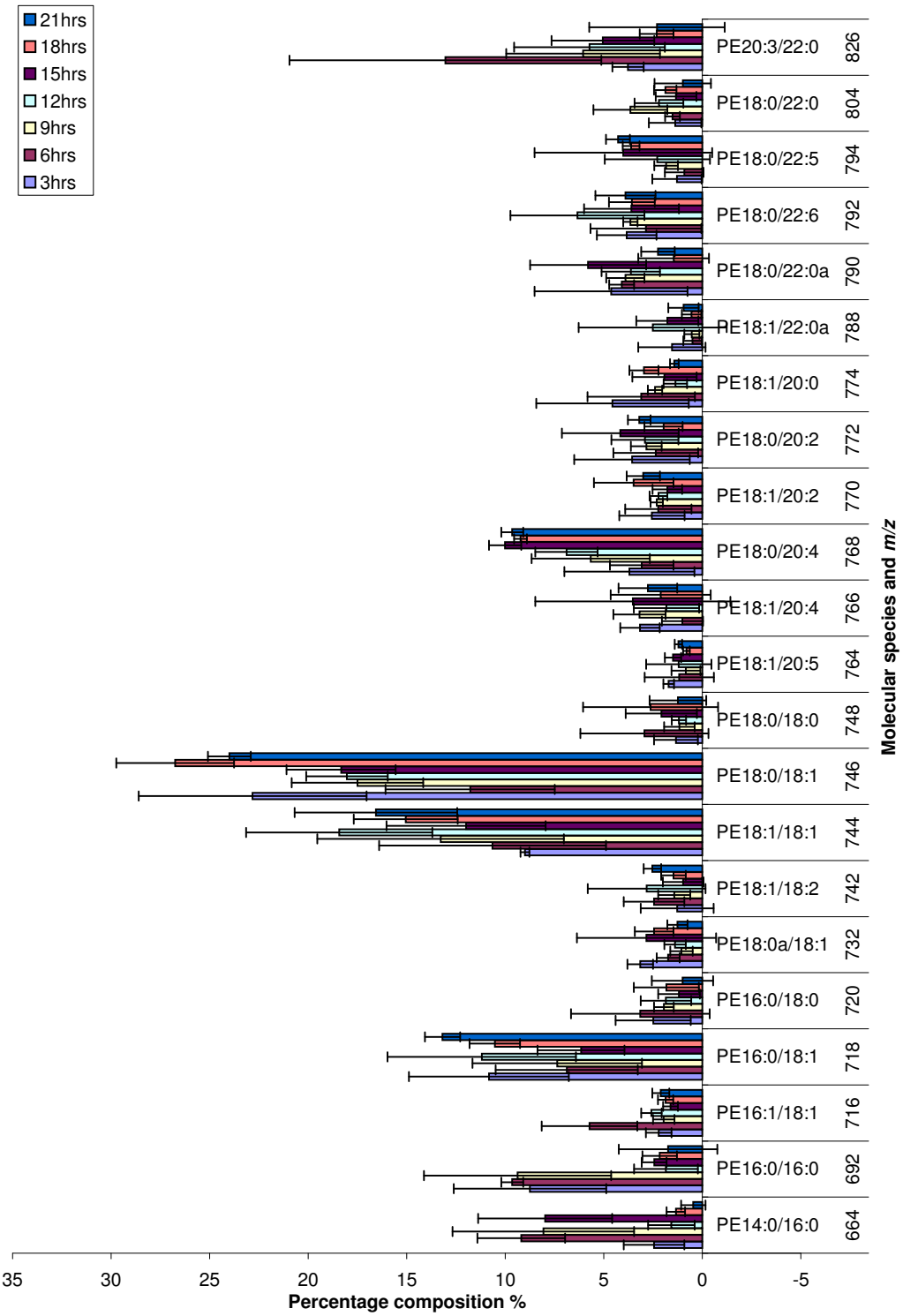

Figure 4.15: Molecular species percentage composition of PE for synchronised nuclei extracted with Triton-X-100

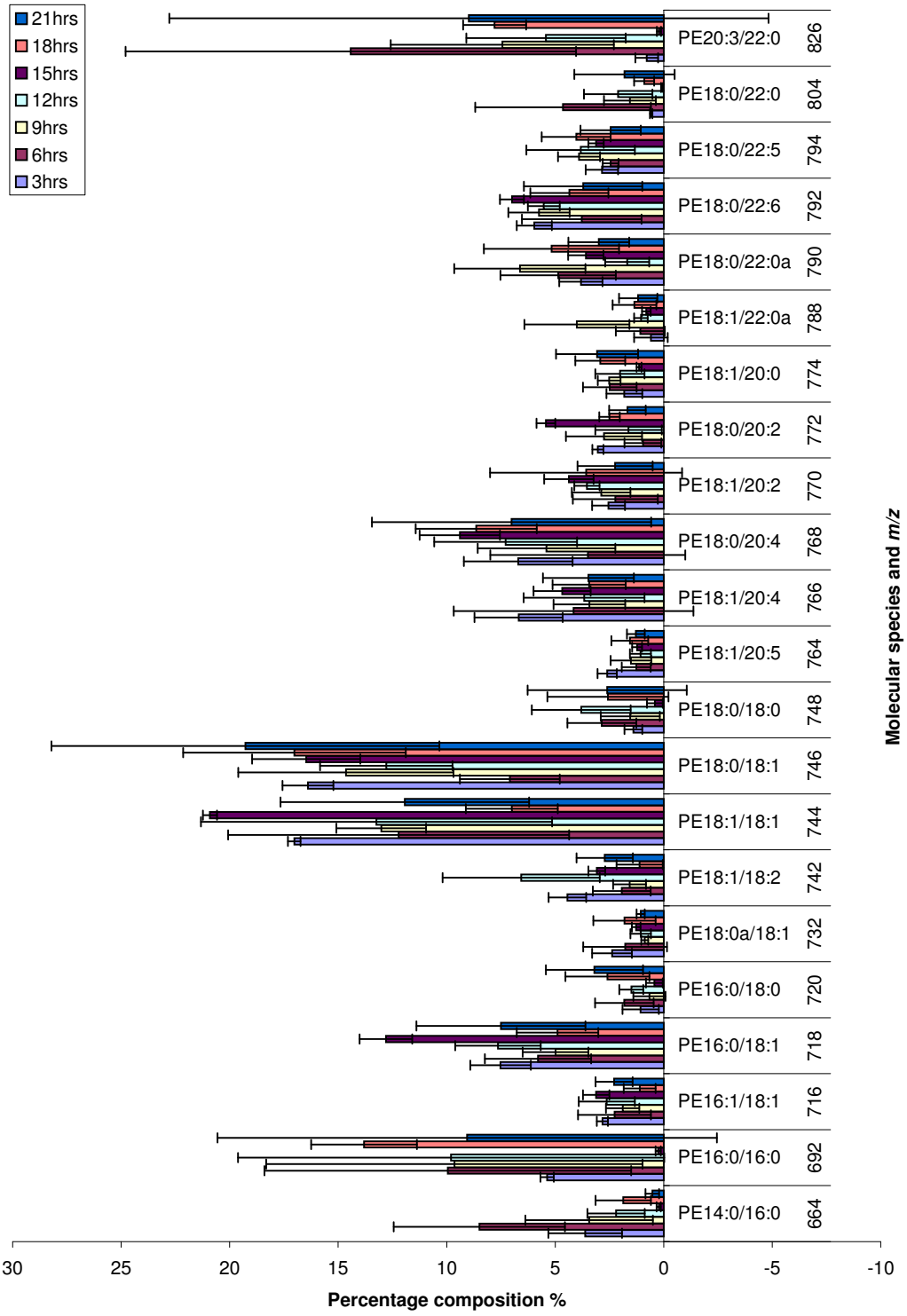

Figure 4.16: Molecular species percentage composition of PE for synchronised nuclei extracted with Maltopyranoside

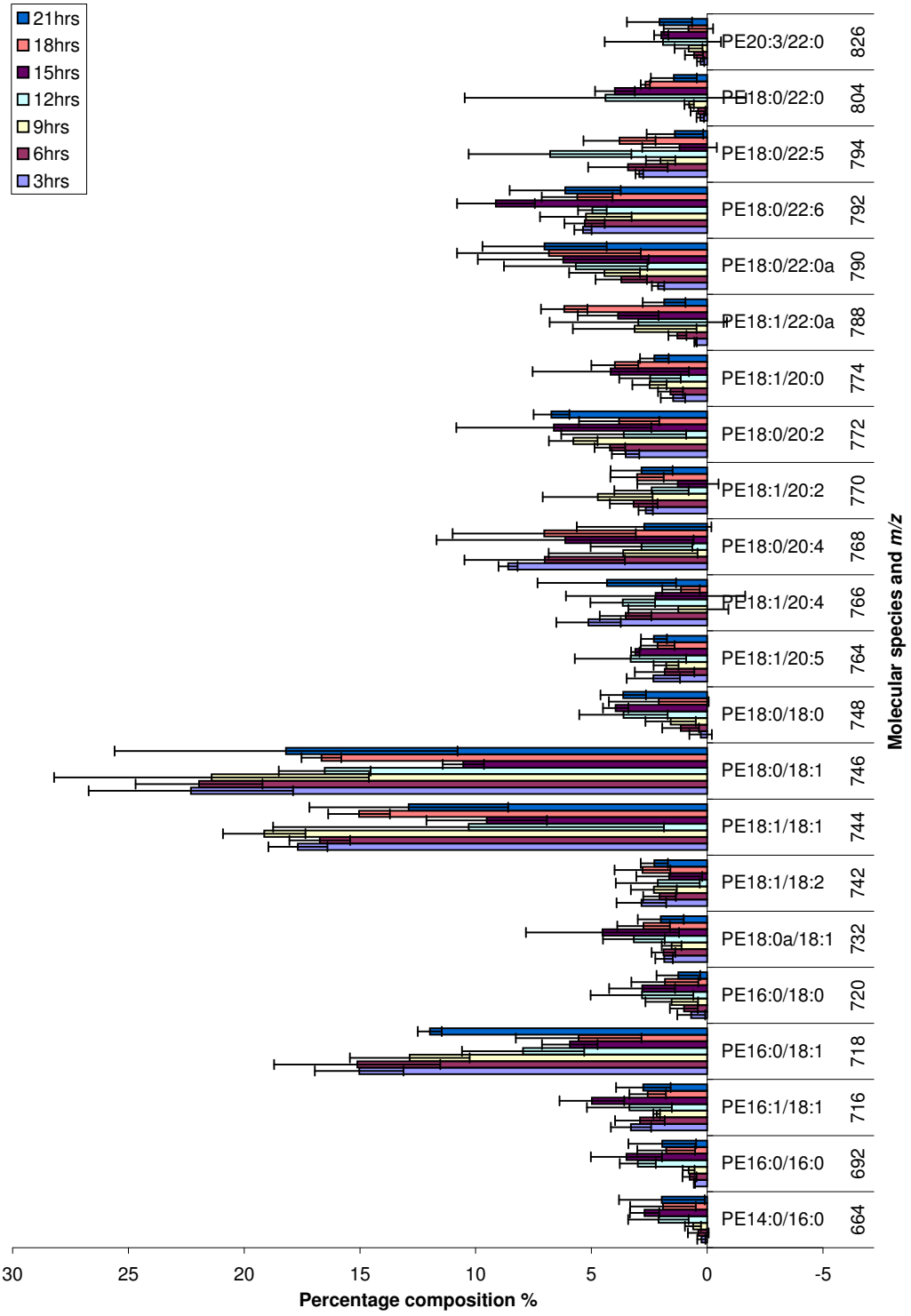

Figure 4.17: Molecular species percentage composition of PE for synchronised nuclei extracted with Maltopyranoside repeat

The saturated PE species (Figure 4.18) show very little consistent change relative to the asynchronous control. There is an increase in species 14:0/16:0 (m/z 664) at 6hrs in set 2 however this does not occur in set 1 or 3. Species 16:0/16:0 (m/z 692) also shows an increase at the 3hr, 6hr and 9hr time points in set 1 and the 3hr and 18hr time points in set 2. There is a small increase at 12hrs, 15hrs and 18hrs in set 3 for species 18:0/18:0 (m/z 748), however, only the 12hr time point in set 2 shows a similar increase. The 15hr and 18hr time points of species 18:0/22:0 (m/z 804) show a small increase in data set 3 but this is not seen in data set 1 or 2. These findings agree well with those for whole cells (Figure 3.19) which also showed very little change, within error, relative to the asynchronous control.

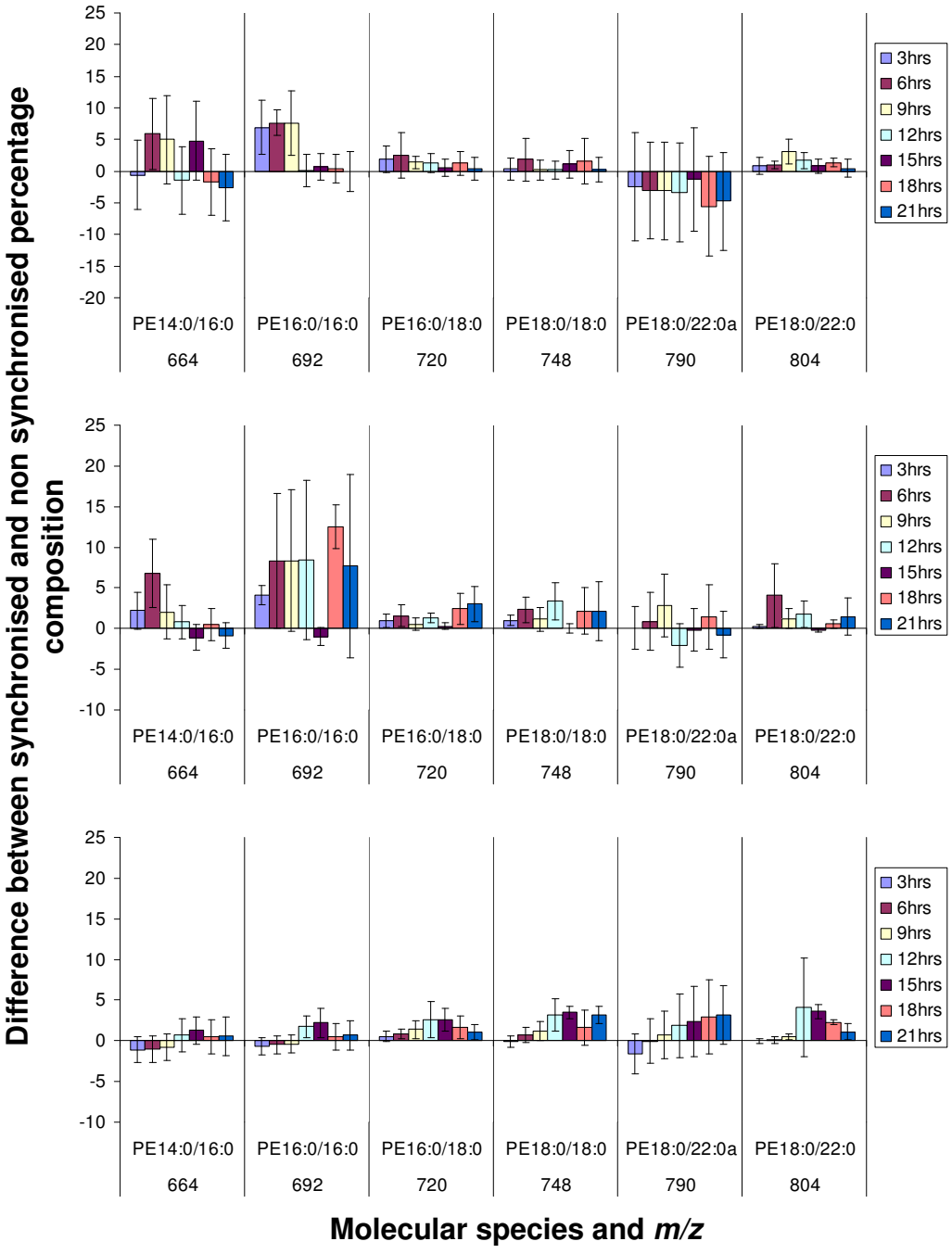

Figure 4.18: Difference between synchronised and non-synchronised percentage composition for saturated PE molecular species. Set 1 (nuclei extracted with Triton-X-100) is shown at the top followed by set 2 (nuclei extracted with maltopyranoside) and set 3 (independent repeat of nuclei extracted with maltopyranoside)

The monounsaturated species tend to show a decrease or very little change relative to the asynchronous control. Species 16:0/18:1 (m/z 718) shows a significant decrease in set 1 at 6hrs, 9hrs and 15hrs. In set 2 all time points show a significant decrease except 15hrs which remains the same as the asynchronous control. In set 3 it is the 12hr, 15hr and 18hr time points which show a decrease. No such decrease in this species was found in the whole cell data (Figure 3.19).
Species 18:0/18:1 (m/z 746) shows a decrease at the 6hr time point in set 1 and 2 and a decrease in the 15hr time point in set 3. This contrasts with the small increase seen in this species in set 1 of the whole cell data (Figure 3.19). There are some indications of small increases relative to the asynchronous control for species 18:0a/18:1 (m/z 732), 18:1/20:0 (m/z 774) and 18:1/22:0a (m/z 788) but these changes are not consistent over all three data sets.

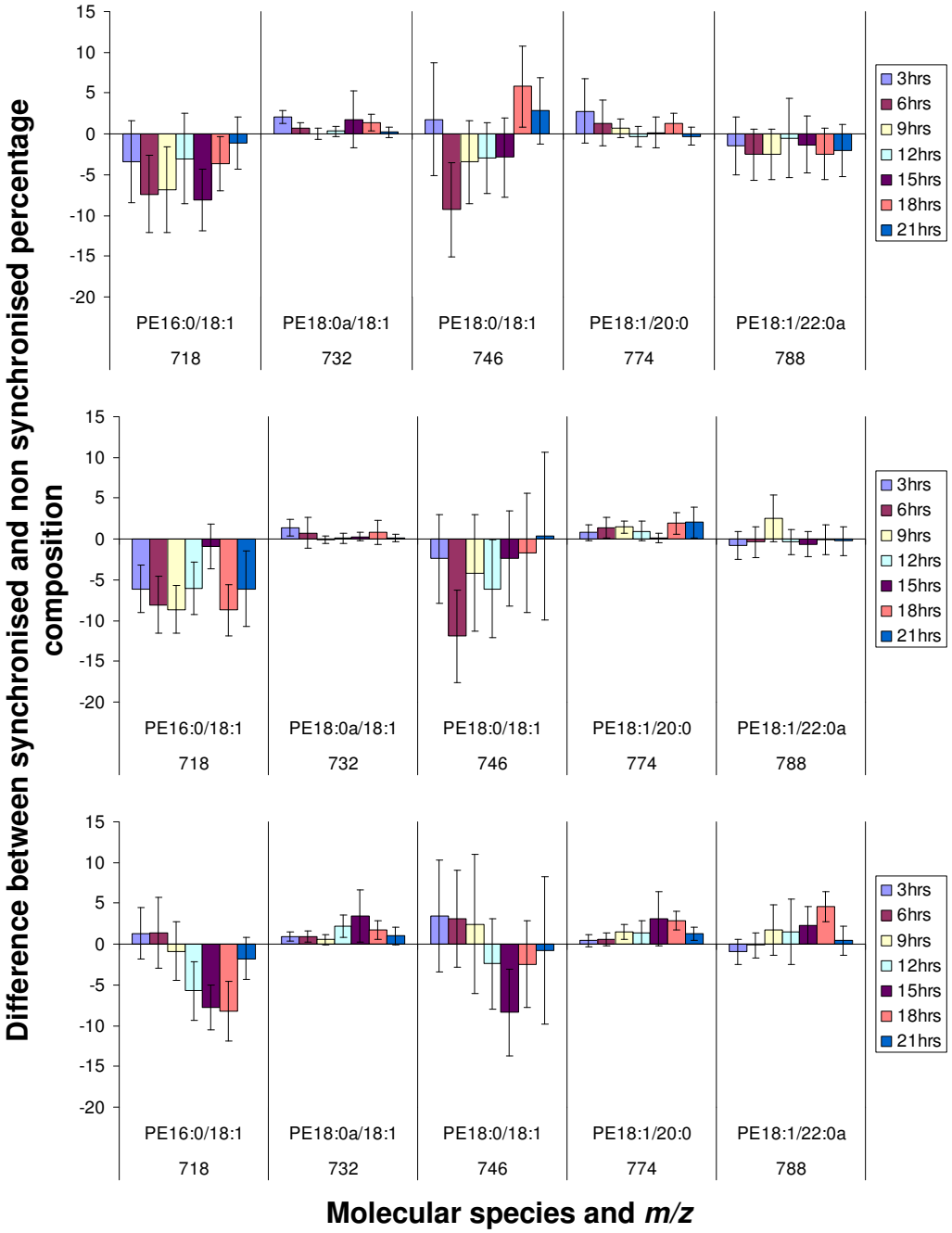

Figure 4.19: Difference between synchronised and non-synchronised percentage composition for monounsaturated PE molecular species. Set 1 (nuclei extracted with Triton-X-100) is shown at the top followed by set 2 (nuclei extracted with maltopyranoside) and set 3 (independent repeat of nuclei extracted with maltopyranoside)

The di-monounsaturated species 16:1/18:1 (m/z 716) and 18:1/22:1 (m/z 800) show no change relative to the asynchronous control, however, species 18:1/18:1 (m/z 744) shows a significant decrease (Figure 4.20). Although a decrease of this species is seen in all three data-sets the pattern over the time points is not the same in each case. In set 1 the 3hr time point shows the largest decrease whereas this occurs at 18hrs in set 2 and 15hrs in set 3. In set 3 all time points are decreased relative to the asynchronous control however at 15hrs there is no change in set 2 and at 9hrs, 12hrs and 21hrs there is no significant change in set 1. No significant change in this species, relative to the non-synchronised control, is seen in the whole cell data (Figure 3.19).

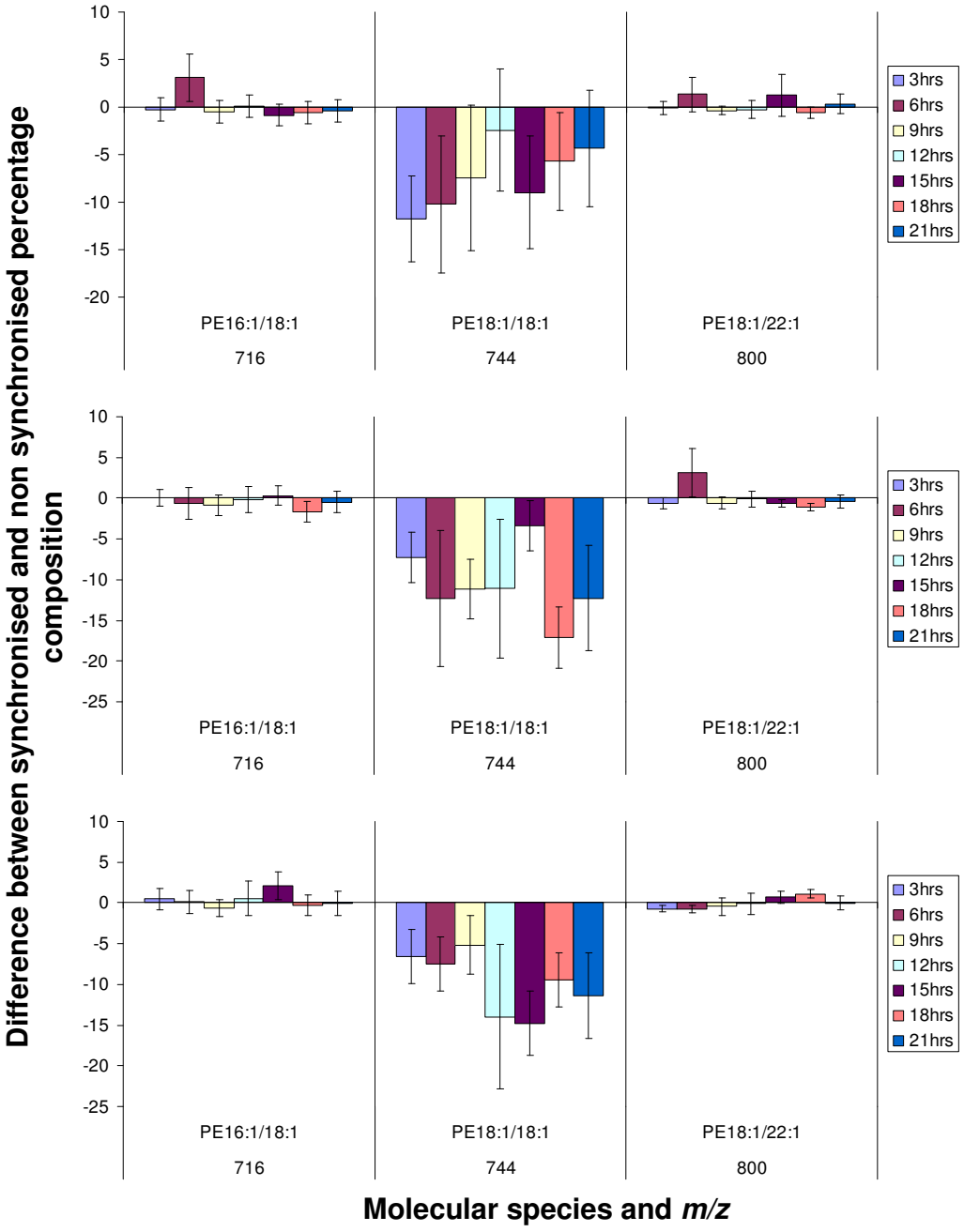

Figure 4.20: Difference between synchronised and non-synchronised percentage composition for di-monounsaturated PE molecular species. Set 1 (nuclei extracted with Triton-X-100) is shown at the top followed by set 2 (nuclei extracted with maltopyranoside) and set 3 (independent repeat of nuclei extracted with maltopyranoside)

Very little consistent change relative to the asynchronous data is seen for the highly unsaturated species (Figure 4.21). Species 20:3/22:0 (m/z 826) is increased at the 3hr, 6hr, 9hr and 12hr time points in set 1 and the 6hr, 9hr, 12hr and 18hr time points in set 2 however no change is seen in set 3. An increase is also apparent at the 12hr-21hr time points for species 18:0/20:4 (m/z 768) but only in set 1. There is some indication of a decrease in species 18:0/20:2 (m/z 772) in set 2 however this is not the case for set 1 and 3. The whole cell data (Figure 3.19) also showed very little change, relative to the non-synchronised control, for highly unsaturated molecular species.

As described for PC (Figures 4.12 to 4.14), the molecular species which show the greatest change relative to the asynchronous control are those which are most abundant (16:0/18:1, 18:0/18:1 and 18:1/18:1).

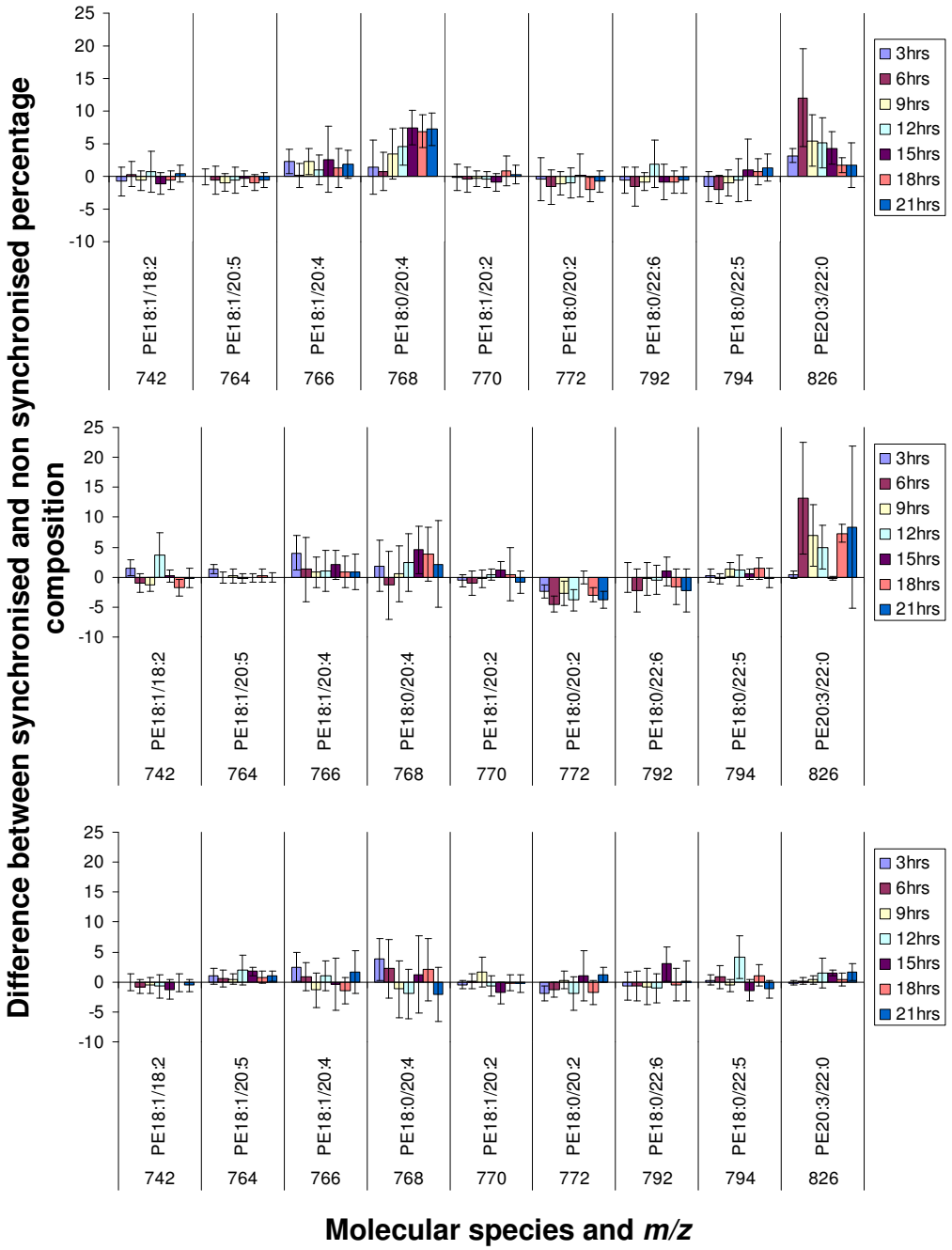

Figure 4.21: Difference between synchronised and non-synchronised percentage composition for unsaturated PE molecular species. Set 1 (nuclei extracted with Triton-X-100) is shown at the top followed by set 2 (nuclei extracted with maltopyranoside) and set 3 (independent repeat of nuclei extracted with maltopyranoside)

The molecular species composition of DAG in HeLa cell nuclei at three hourly intervals following removal of the cell cycle block is shown in Figures 4.22 to 4.24. In data set 1 (Triton-X-100 extracted nuclei) and 2 (maltopyranoside extracted nuclei), species 16:0/18:0 (m/z 614) is the most abundant. In set 3 (maltopyranoside extracted nuclei repeat), however, all species are approximately equal, within error, except 16:0/18:1 (m/z 612) and 18:0/18:0 (m/z 642) which are less. This contrasts with the findings from whole cells which indicated that species 16:0/18:1 (m/z 612) was the most abundant over the majority of time points (figure 3.20).
At most time points in the synchronised nuclei data, species 18:0/18:0 (m/z 642) comprises more than 10% of the total, however, this species is below the selection threshold in the whole cell data. Conversely, species 18:1/18:1 (m/z 638) and 18:0/18:1 (m/z 640) are present at more than 5% in the whole cell data but below the selection threshold in the synchronised nuclei data. This data also suggests that, as described for nuclei from asynchronous cells (section 4.2.1), endonuclear DAG is enriched in saturated molecular species.

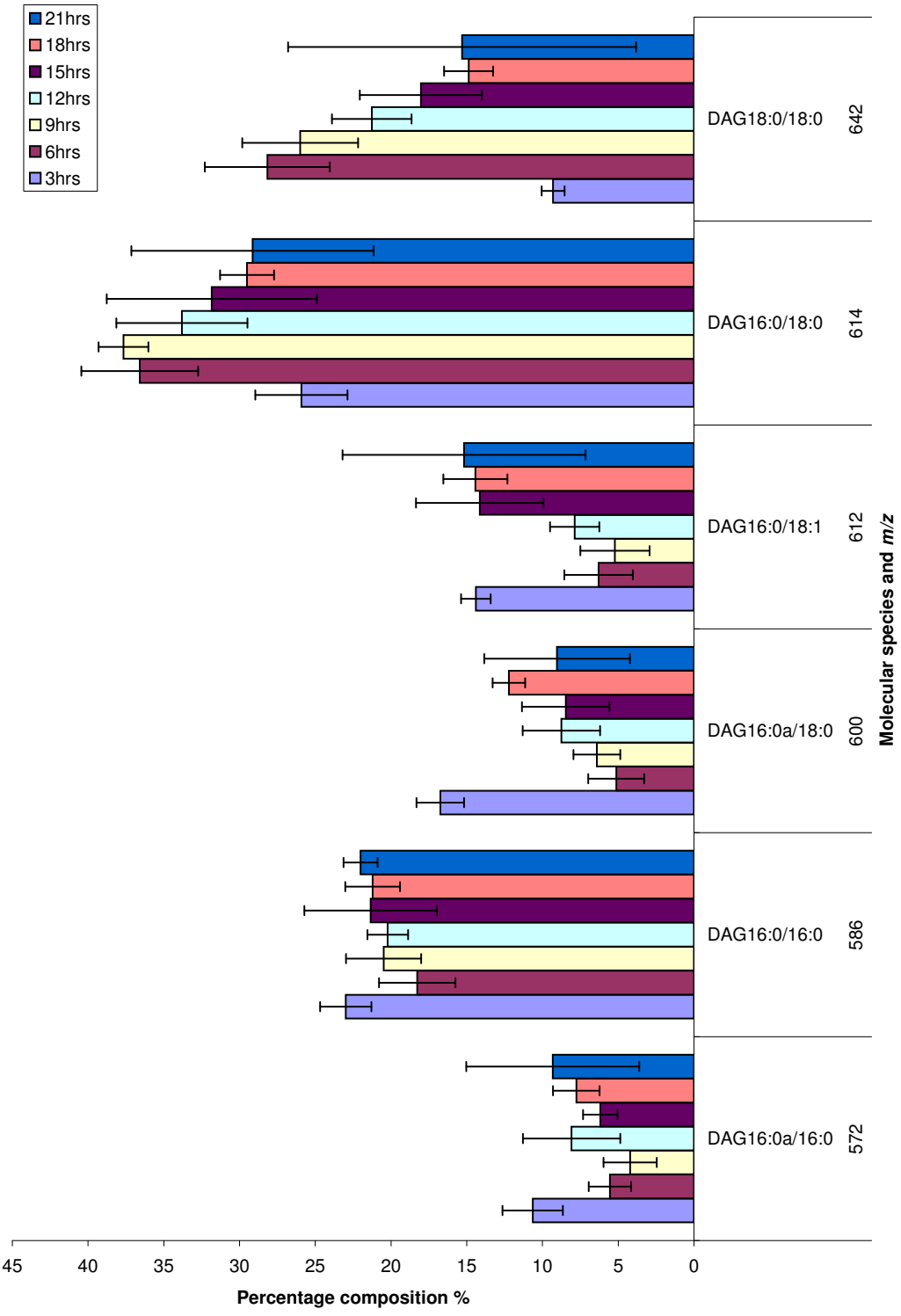

Figure 4.22: Molecular species percentage composition of DAG for synchronised nuclei extracted with Triton-X-100

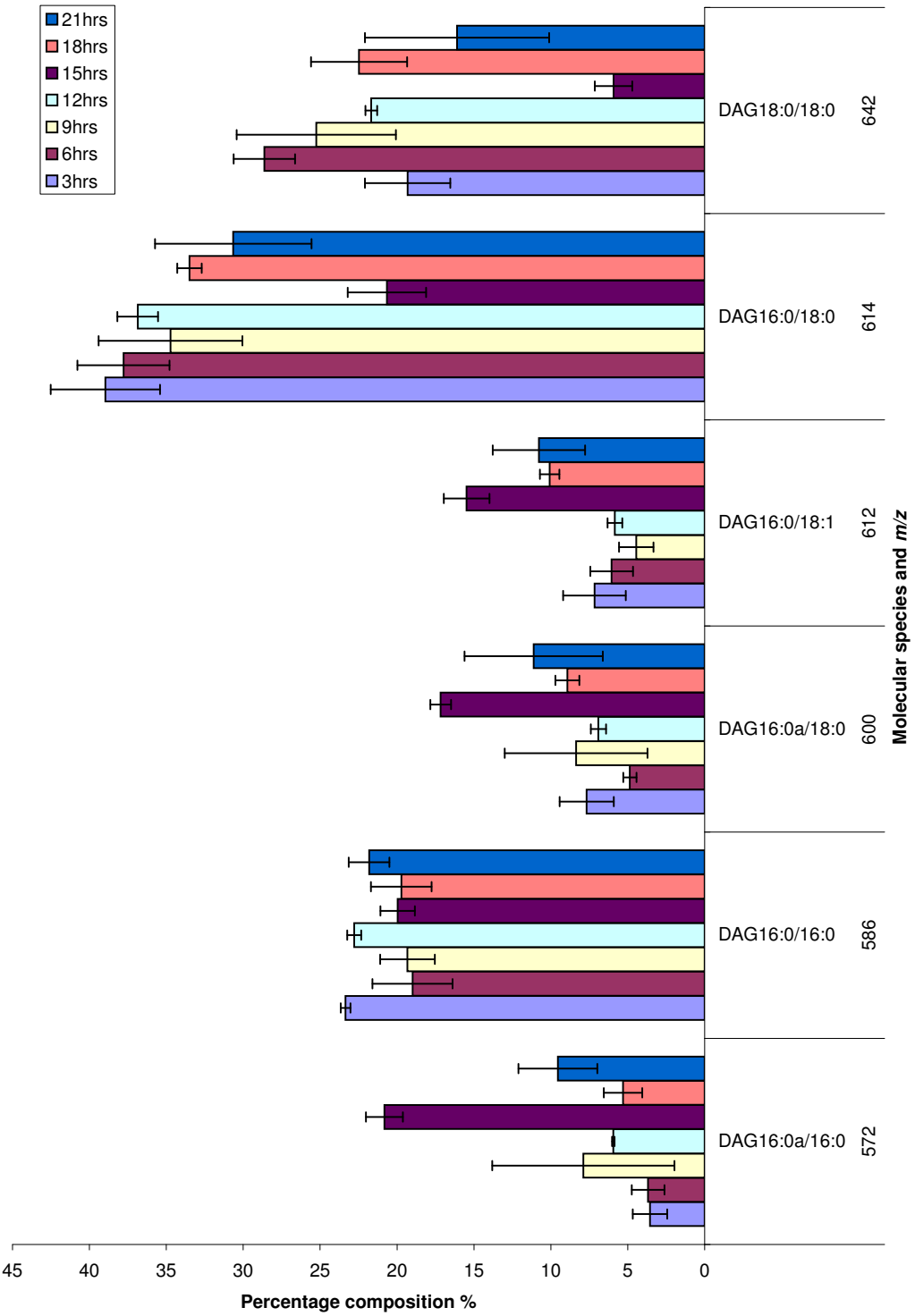

Figure 4.23: Molecular species percentage composition of DAG for synchronised nuclei extracted with maltopyranoside

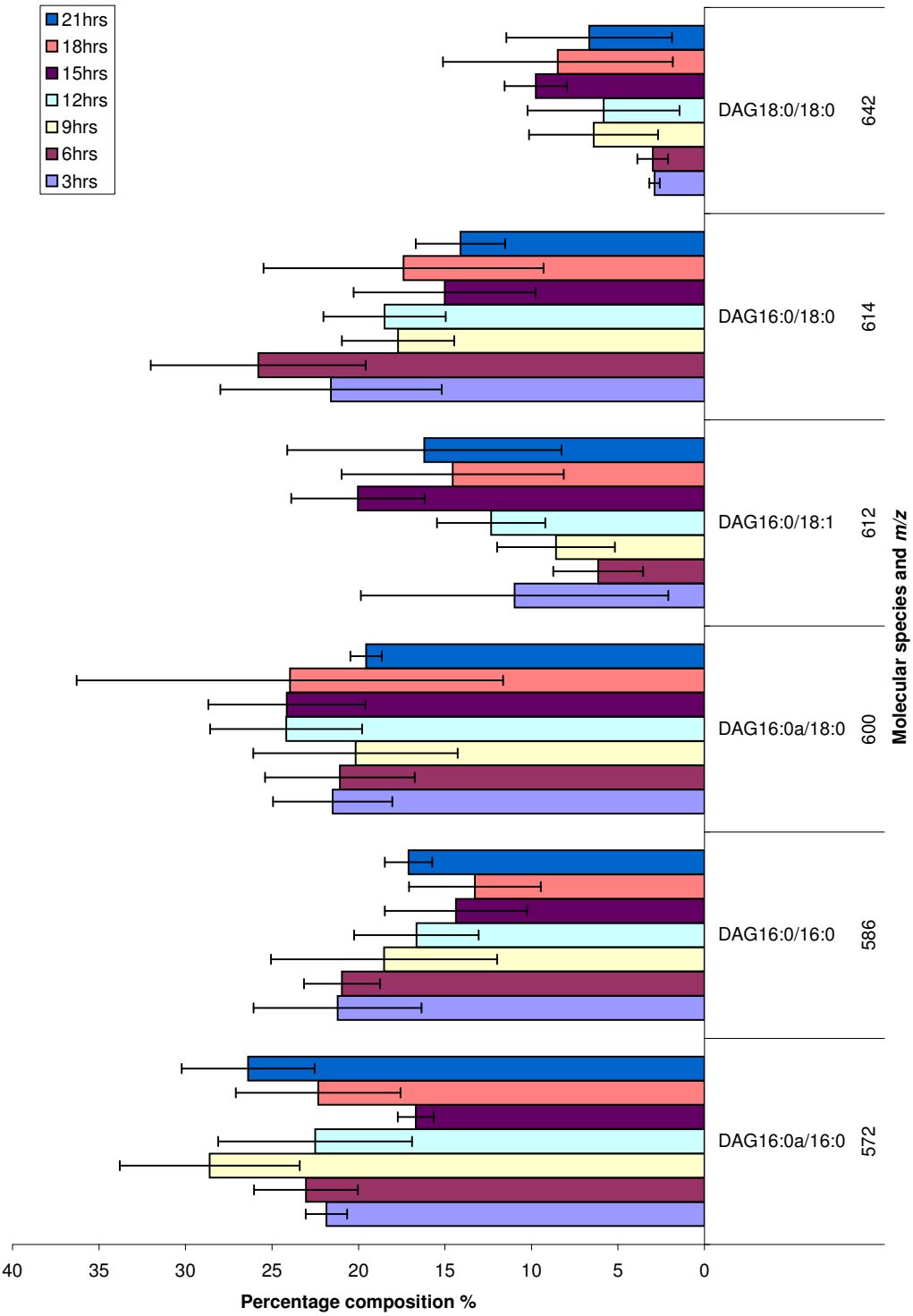

Figure 4.24: Molecular species percentage composition of DAG for synchronised nuclei extracted with maltopyranoside repeat

Data sets 1 and 2 show an increase in most saturated DAG species and a decrease in unsaturated DAG species relative to the asynchronous control (Figure 4.25), which is a very similar trend to that of PC. Set 3, however, only shows an increase in species containing an alkyl link (16:0a/16:0 and 16:0a/18:0) and either no change or a decrease in the remaining species. This is similar to that found for DAG species in the whole cell data (Figure 3.21). Species 16:0a/16:0 (m/z 572) shows very little change in set 1 except for a very small increase at the 3hr time point. In set 2 there is also very little change in this species except for the 15hr time point which shows an increase of over 10%. In set 3 however, all time points are significantly increased relative to the asynchronous control. Species 16:0a/18:0 (m/z 600) again shows a similar increase in set 3 but little change except for the 3hr and 18hr time points in set 1 and the 15hr time point in set 2.

In set 1 there is an increase in species 16:0/18:0 (m/z 614) at 6hrs, 9hrs, and 12hrs but no significant change in the remaining time points. In set 2 there is an increase in all time points except 15hrs and 21hrs. In set 3 however, there is a decrease at 15hrs and 21hrs and no change at the other time points. Species 18:0/18:0 (m/z 642) shows little change relative to the asynchronous control in set 3. In set 2 however there is an increase at all time points except 15hrs and 21hrs and in set 1 the 6hr, 9hr and 12hr time points are increased. For set 1 and 2, the time points which show a change or no change are the same for species 16:0/18:0 (m/z 614) and 18:0/18:0 (m/z 642) possibly indicating a link to the cell cycle position.

A previous study of intact nuclei from U937 promonocytic cells found an increase in tetraunsaturated DAG species during G2/M associated with the activation of PKC-βII [6]. No such tetraunsaturated species were detected in the endonuclear compartment, most likely reflecting the requirement of membrane association for enzyme activation.

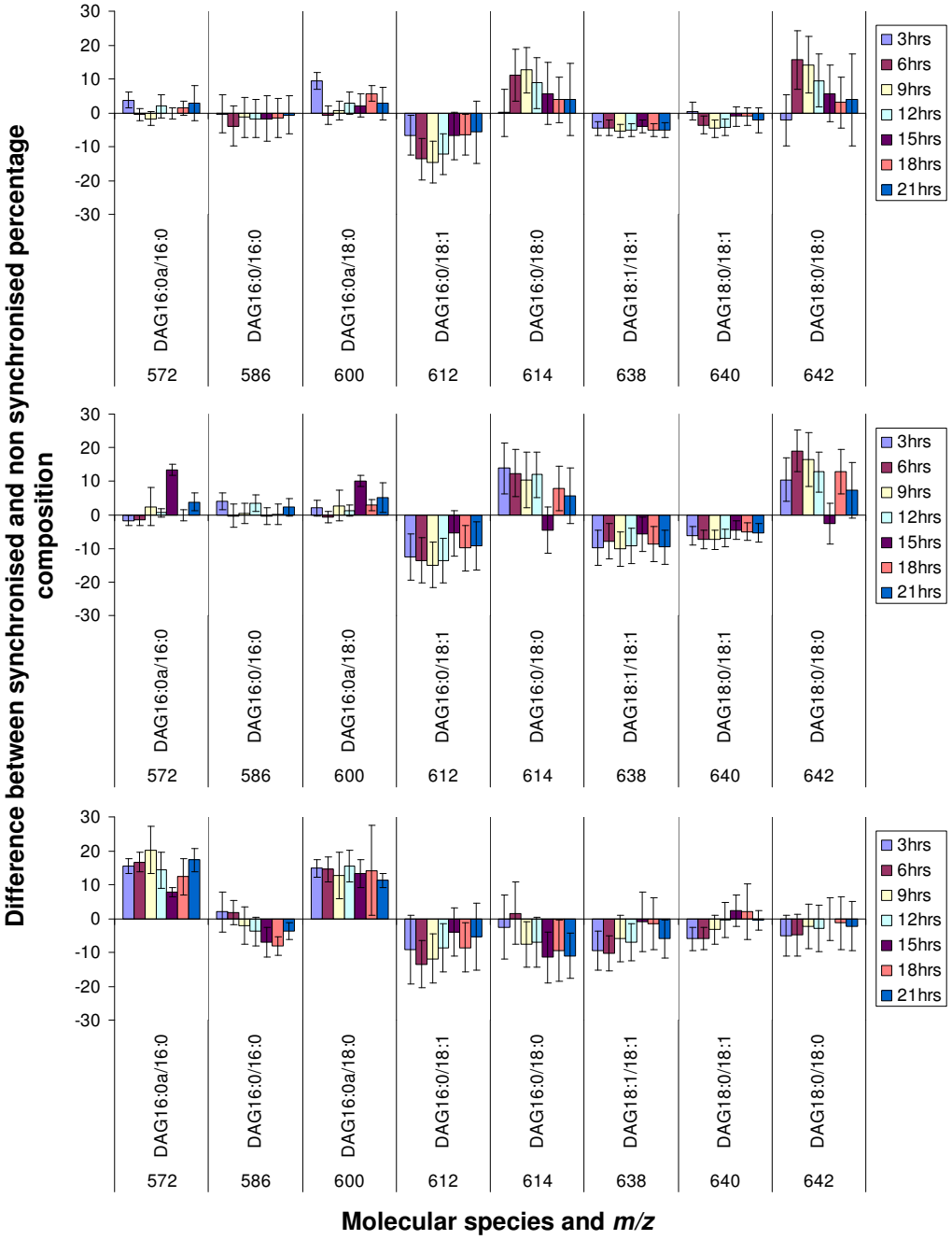

Figure 4.25: Difference between synchronised and non-synchronised DAG molecular species percentage composition. Set 1 (nuclei extracted with Triton-X-100) is shown at the top followed by set 2 (nuclei extracted with maltopyranoside) and set 3 (independent repeat of nuclei extracted with maltopyranoside)

For the whole cell data (section 3.3.2) it was suggested that the increase in certain DAG molecular species, relative to the asynchronous control, may be achieved by the remodeling of other DAG molecular species. It is possible that the increase in set 1 of species 16:0/18:0 (m/z 614) at the 6hr, 9hr and 12hr time points corresponds to the decrease of species 16:0/18:1 (m/z 612) at those time points. Similarly the changes in these species in set 2 may also correlate. In both set 1 and 2 the decrease in species 18:0/18:1 (m/z 640) may be linked to the increase in species 18:0/18:0 (m/z 642) although the magnitude of the decrease is approximately half that of the increase in species 18:0/18:0 (m/z 642). In set 2 there is an increase of approximately 10% in species 16:0a/16:0 (m/z 572) and 16:0a/18:0 (m/z 600) at 15hrs and a very small increase at 21hrs but very little change at the other time points. At the 15hrs and 21hrs there is no change, relative to the asynchronous control, in species 16:0/18:0 (m/z 614) and 18:0/18:0 (m/z 642) which contrasts with the increase at all other time points. In set 3 there is an increase of species 16:0a/18:0 (m/z 600) over all time points but only a decrease at 15hrs, 18hrs and 21hrs in species 16:0/18:0 (m/z 614). Similarly there is an increase of species 16:0a/16:0 (m/z 572) over all time points, however, species 16:0/16:0 (m/z 586) is only decreased at the 15hr and 18hr time points and species 16:0/18:1 (m/z 612) at the 6hr and 9hr time points. As for whole cells, the origin of the increase in species containing the 16:0a fatty acid is unclear from this data.

The molecular species composition of PI in nuclei following synchronisation with mimosine is shown in Figures 4.26 to 4.28. The most abundant species are 16:0/18:0 (m/z 837) and 18:0/18:1 (m/z 863). Species 18:1/20:4 (m/z 883) is present in the whole cell (figure 3.22) data but below the selection threshold in the nuclei data. Conversely, species 16:0a/18:0 (m/z 823), 14:0a/22:6 (m/z 839), 18:0/18:0 (m/z 865), 16:0a/22:6 (m/z 867) and 18:1a/20:4 (m/z 869) are present in the nuclei data but below the selection threshold in the whole cell data.

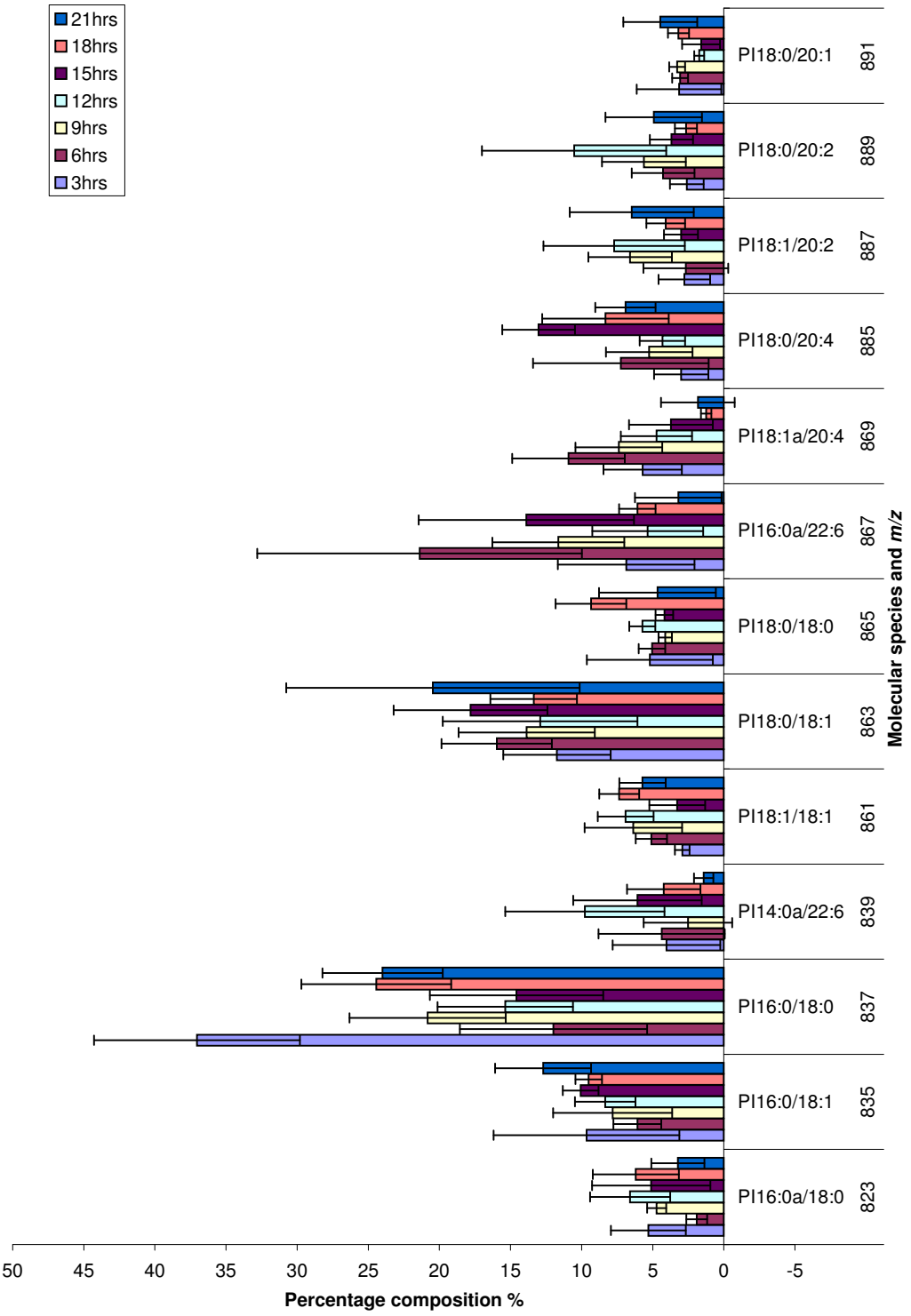

Figure 4.26: Molecular species percentage composition of PI for synchronised nuclei extracted with Triton-X-100

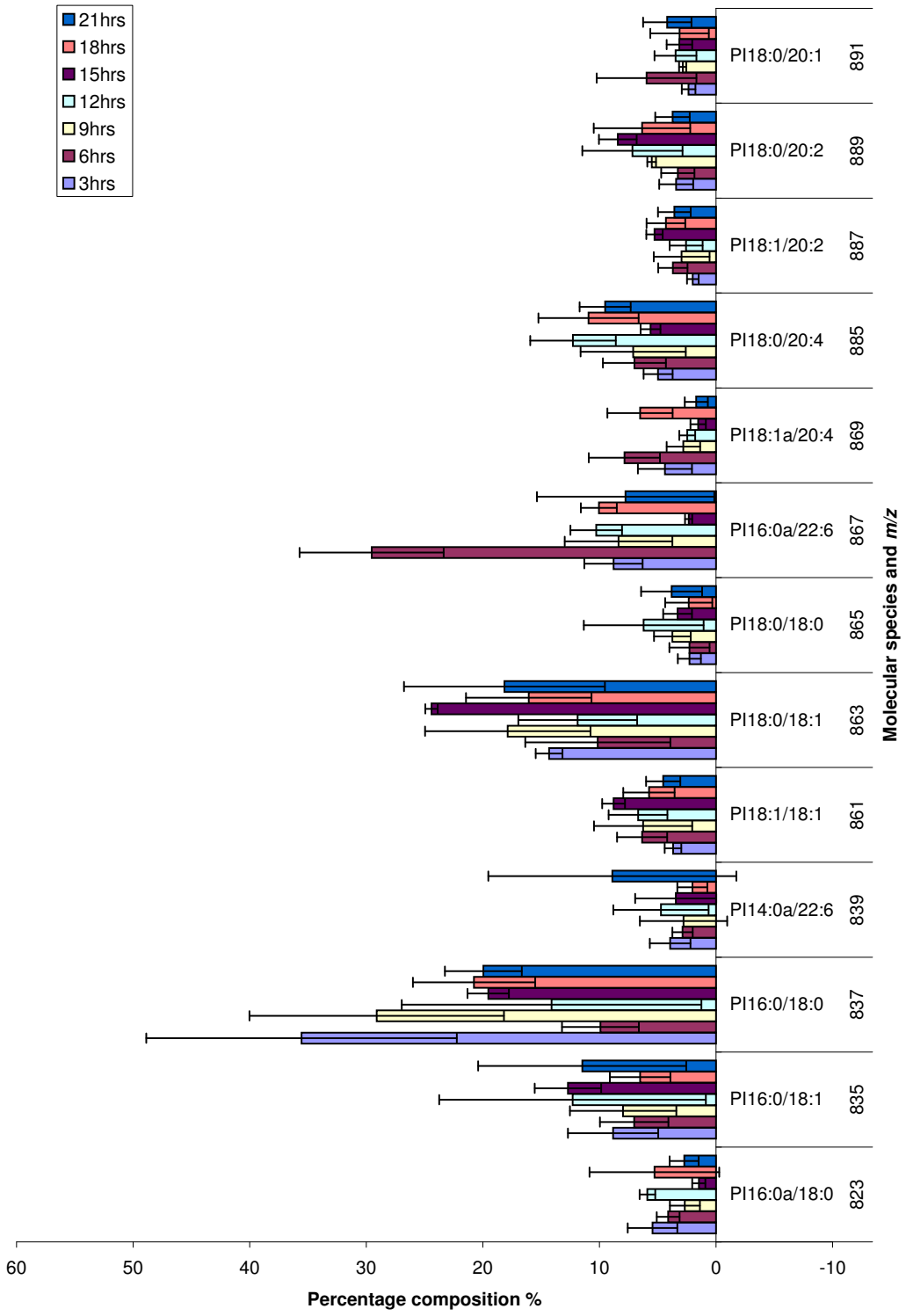

Figure 4.27: Molecular species percentage composition of PI for synchronised nuclei extracted with maltopyranoside

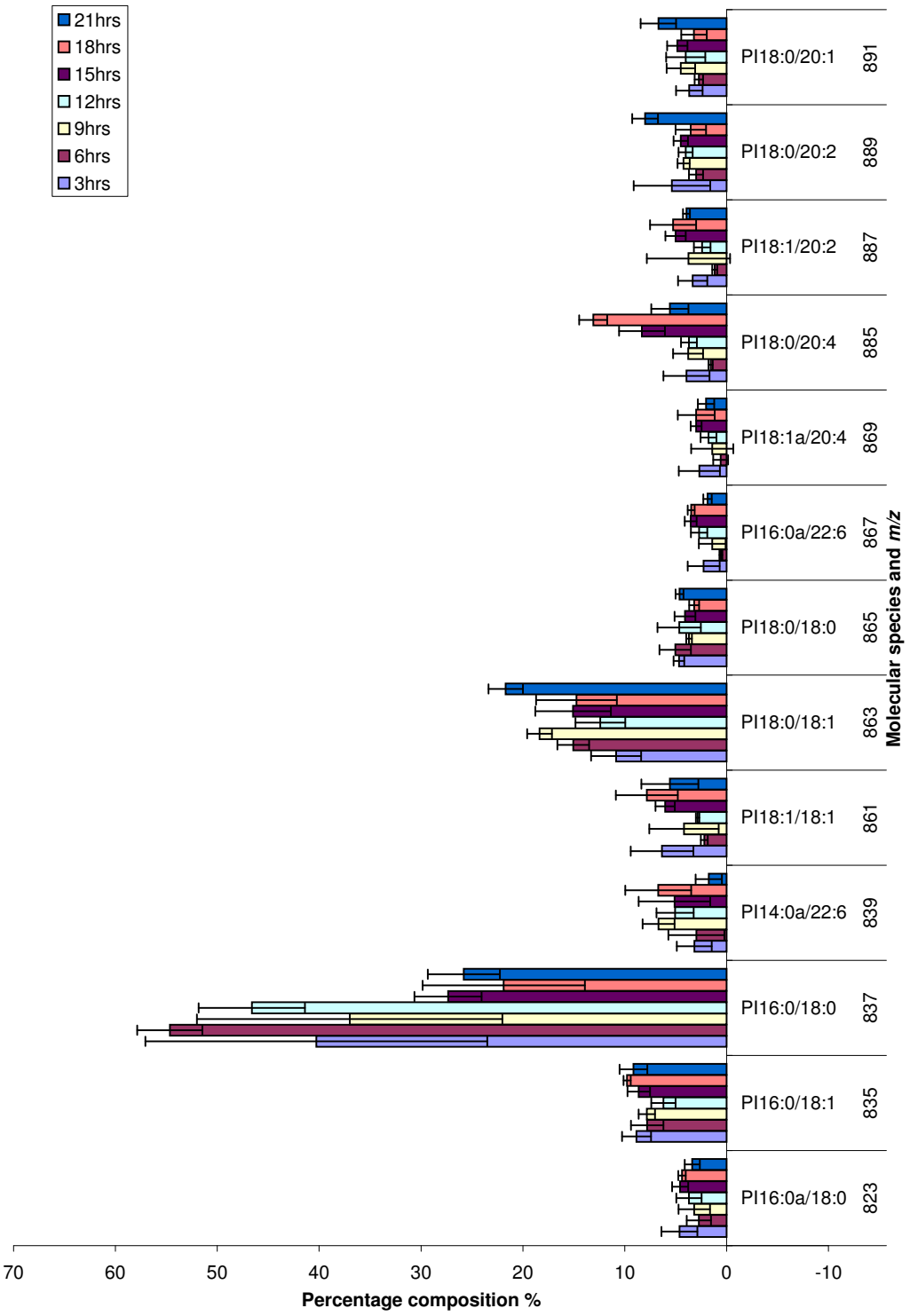

Figure 4.28: Molecular species percentage composition of PI for synchronised nuclei extracted with maltopyranoside repeat

As found for the whole cells (Figure 3.23), the PI molecular species generally show little change relative to the asynchronous data. The most significant change in the saturated species (Figure 4.29) is seen in set 3 for species 16:0/18:0 (m/z 837) in which all time points are increased except 18hrs which shows no change. In set 1 and 2, however, only the 3hr time point is increased and there is also a small decrease in the 6hr time point of set 2.

Species 16:0/18:1 (m/z 835) (Figure 4.30) shows a significant decrease over all time points in set 3. In set 2 it is decreased at all time points except 12hrs, 15hrs and 21hrs and in set 1 it is decreased at all time points except 3hrs and 21hrs. Species 18:1.18:1 (m/z 861) shows a small decrease at 3hrs and 15hrs in set 1 and a decrease at 3hrs, 6hrs, 18hrs and 21hrs in set 2. In set 3, there is a decrease for every time point except 3hrs and 18hrs. In set 3, species 18:0/18:1 (m/z 863) is decreased at all time points except 21hrs and in set 2 it is decreased at the 3hr, 6hr, 12hrs and 18hr time points. In set 1, however, this species shows no significant change relative to the asynchronous control. Species 18:0/20:2 (m/z 889) is decreased at all time points except 3hrs and 21hrs in set 3 and decreased at the 3hr, 6hr and 21hr time points in set 2. In set 1 most time points show no change and there is only a small decrease at the 3hr and 18hr time points.

Species 14:0a/22:6 (m/z 839) shows a small increase in the 12hr time point in set 1 and an increase at the 9hr, 12hr and 18hr time points of set 3 but no change in set 2. In set 1, species 16:0a/22:6 (m/z 867) is increased relative to the asynchronous control at the 6hr, 9hr and 15hr time points and in set 2 at the 3hr, 6hr, 12hr and 18hr time points. In both cases the most significant change occurs at 6hrs. This species shows no change relative to the asynchronous control in set 3. Species 18:1a/20:4 (m/z 869) again shows no change in set 3 but an increase in the 6hr and 18hr time points of set 2 and an increase in the 6hr time point of set 1. Species 18:0/20:4 (m/z 885) is increased at the 15hr time point in set 1, at 12hrs, 18hrs and 21hrs in set 2 and at the 15hr and 18hr time points of set 3.

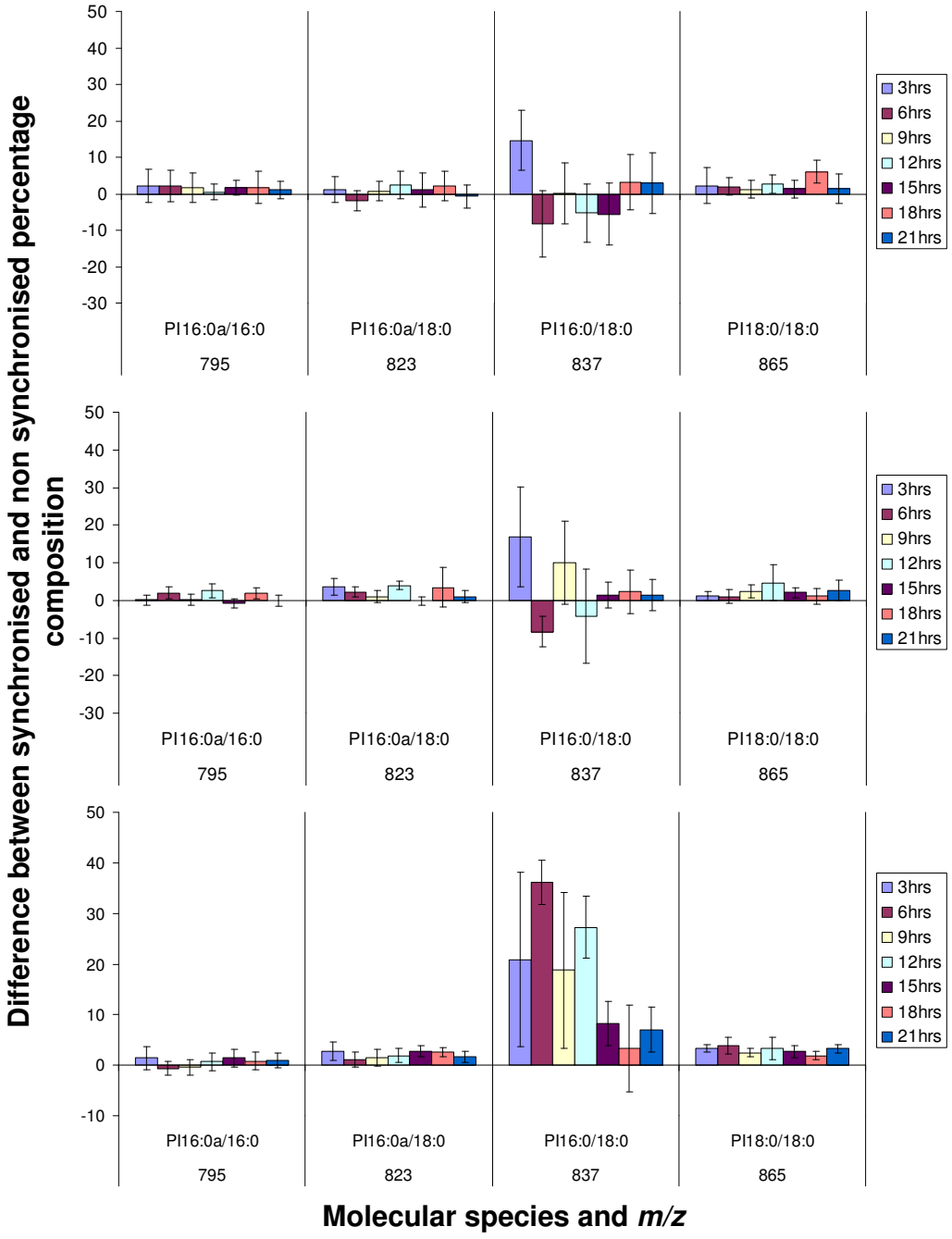

Figure 4.29: Difference between synchronised and non-synchronised percentage composition for saturated PI molecular species. Set 1 (nuclei extracted with Triton-X-100) is shown at the top followed by set 2 (nuclei extracted with maltopyranoside) and set 3 (independent repeat of nuclei extracted with maltopyranoside)

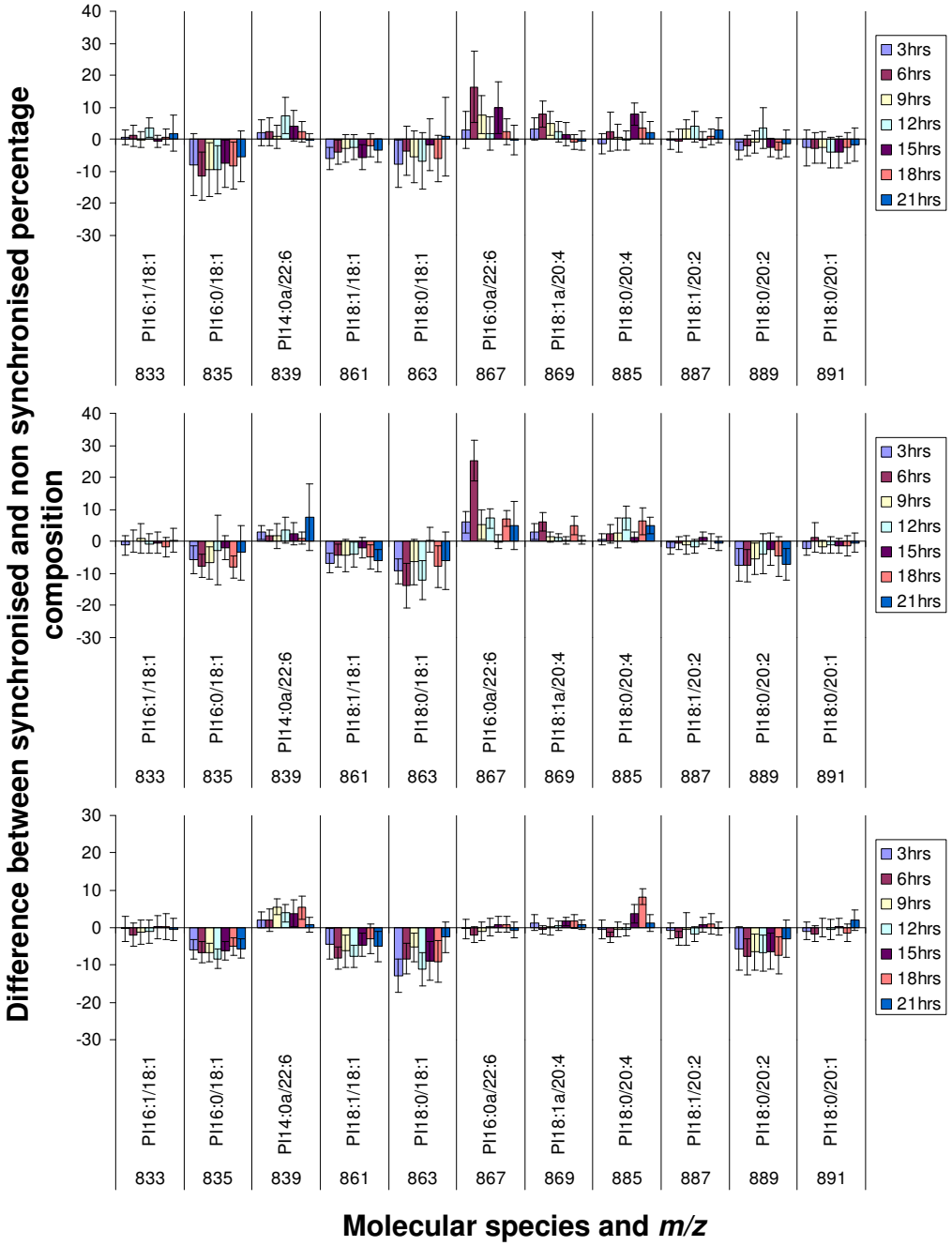

Figure 4.30: Difference between synchronised and non-synchronised percentage composition for saturated PI molecular species. Set 1 (nuclei extracted with Triton-X-100) is shown at the top followed by set 2 (nuclei extracted with maltopyranoside) and set 3 (independent repeat of nuclei extracted with maltopyranoside)

The molecular species composition of PS in nuclei extracted from a population of synchronised cells is shown in Figures 4.31 to 4.33. As found for whole cells (Figure 3.25), species 18:0/18:1 (m/z 788) is the most abundant. The majority of the other species are at or below 10% of the total. Species 18:1a/18:2 (m/z 770) and 18:0/20:0 (m/z 818) are shown in the nuclei data but are below the selection threshold in the whole cell data (Figure 3.25). Species 18:0/20:1a (m/z 802) and 18:1/22:0 (m/z 844) are shown in the whole cell data but not in the nuclei data.

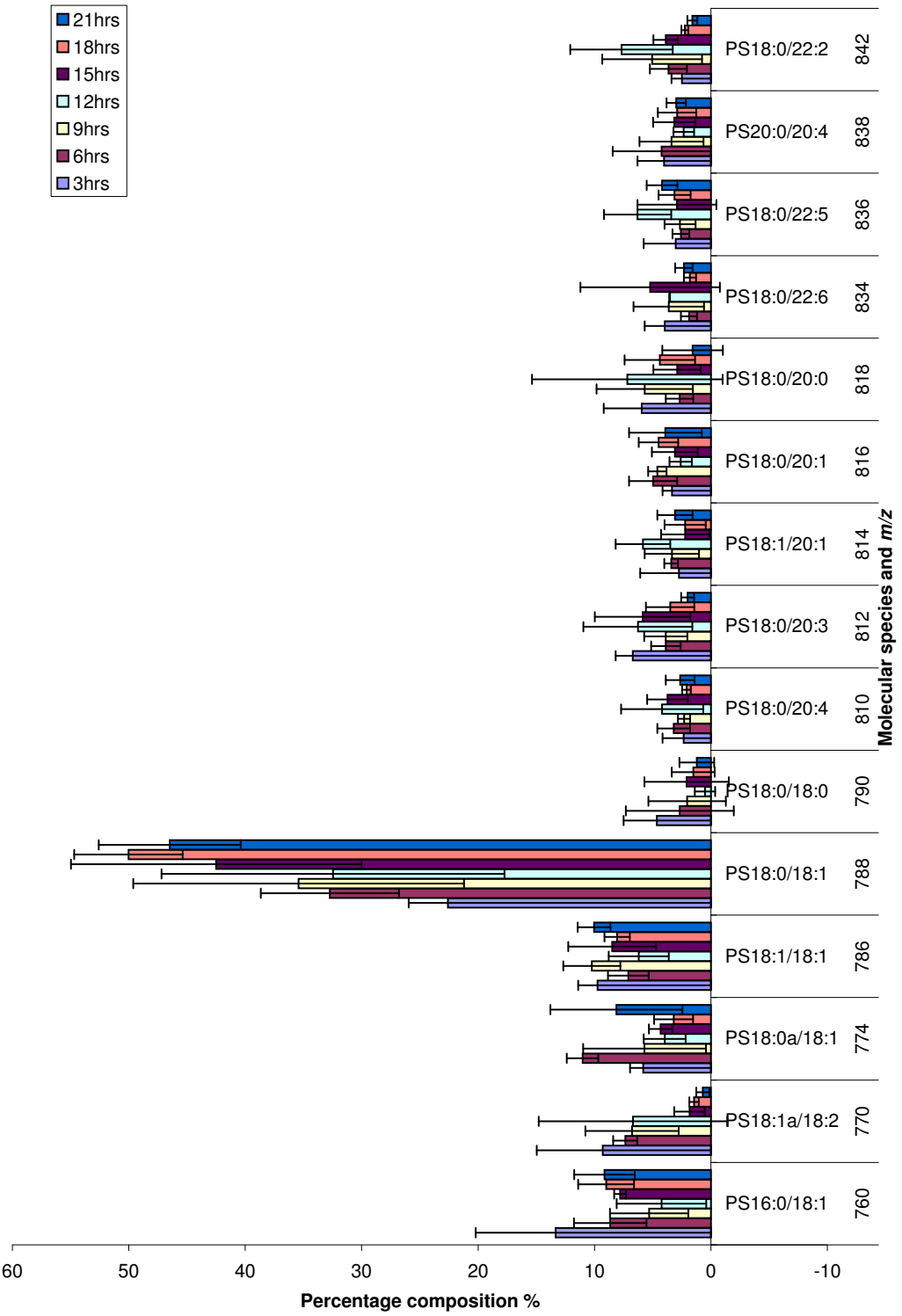

Figure 4.31: Molecular species percentage composition of PS for synchronised nuclei extracted with Triton-X-100

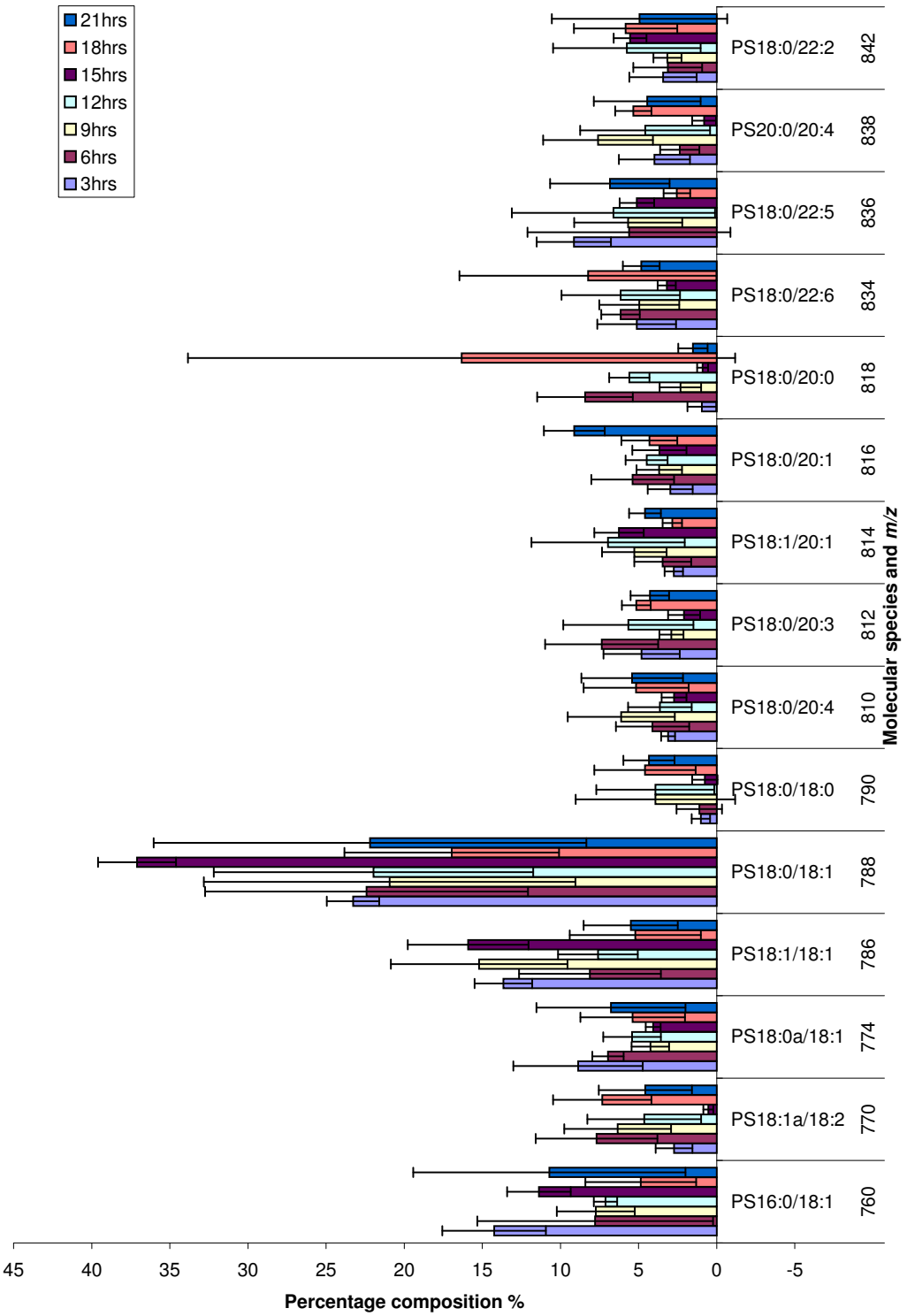

Figure 4.32: Molecular species percentage composition of PS for synchronised nuclei extracted with maltopyranoside

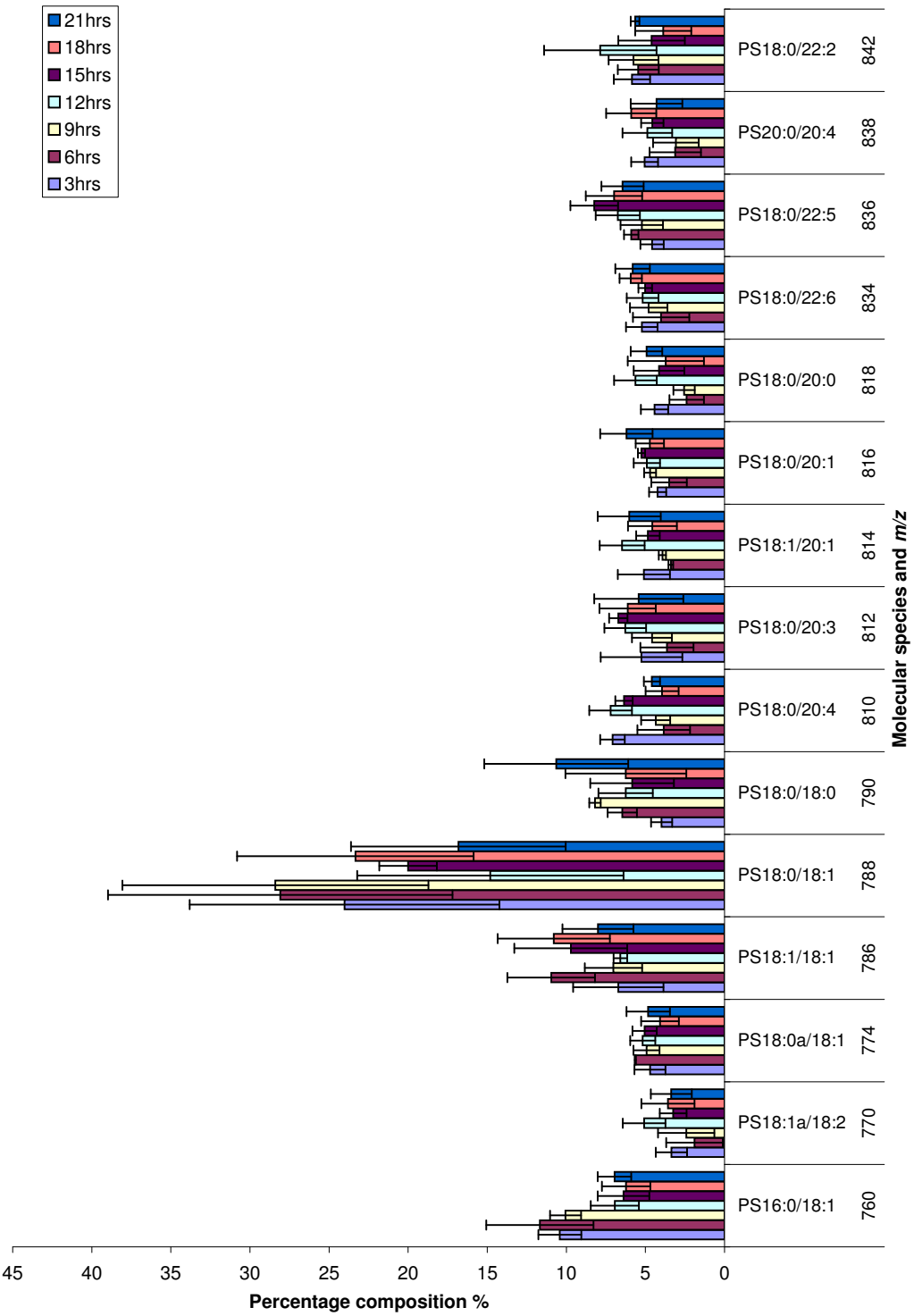

Figure 4.33: Molecular species percentage composition of PS for synchronised nuclei extracted with maltopyranoside repeat

Most PS molecular species (Figure 4.34) show very little difference to the non synchronised data, however, there are indications of some changes. Species 18:1a/18:2 (m/z 770) is increased at the 3hr and 6hr time points in set 1, at the 6hr, 9hr and 18hr time points in set 2 and at 12hrs in set 3. In set 1 and 2 there is an increase at the 6hr time point for species 18:0a/18:1 (m/z 774) but no change in set 3. There is a significant decrease for species 18:0/18:1 (m/z 788) at the 3hr time point in set 1, at 3hrs, 9hrs, 12hrs and 18hrs in set 2 and 12-21hrs inclusive in set 3. A decrease of this species was also observed in set 2 of the whole cell results (Figure 3.27). All time points of species 18:0/18:0 (m/z 790) are increased relative to the asynchronous control in set 3. This is again similar to set 2 of the whole cell results. In set 2, however, it is only increased at 18hrs and 21hrs and no change is seen in set 1. The 12hr, 15hr and 18hr time points of species 18:0/20:3 (m/z 812) are increased relative to the asynchronous control in set 3. In set 2 the 6hr and 18hr time points are increased but in set 1 the only increase is at 3hrs.

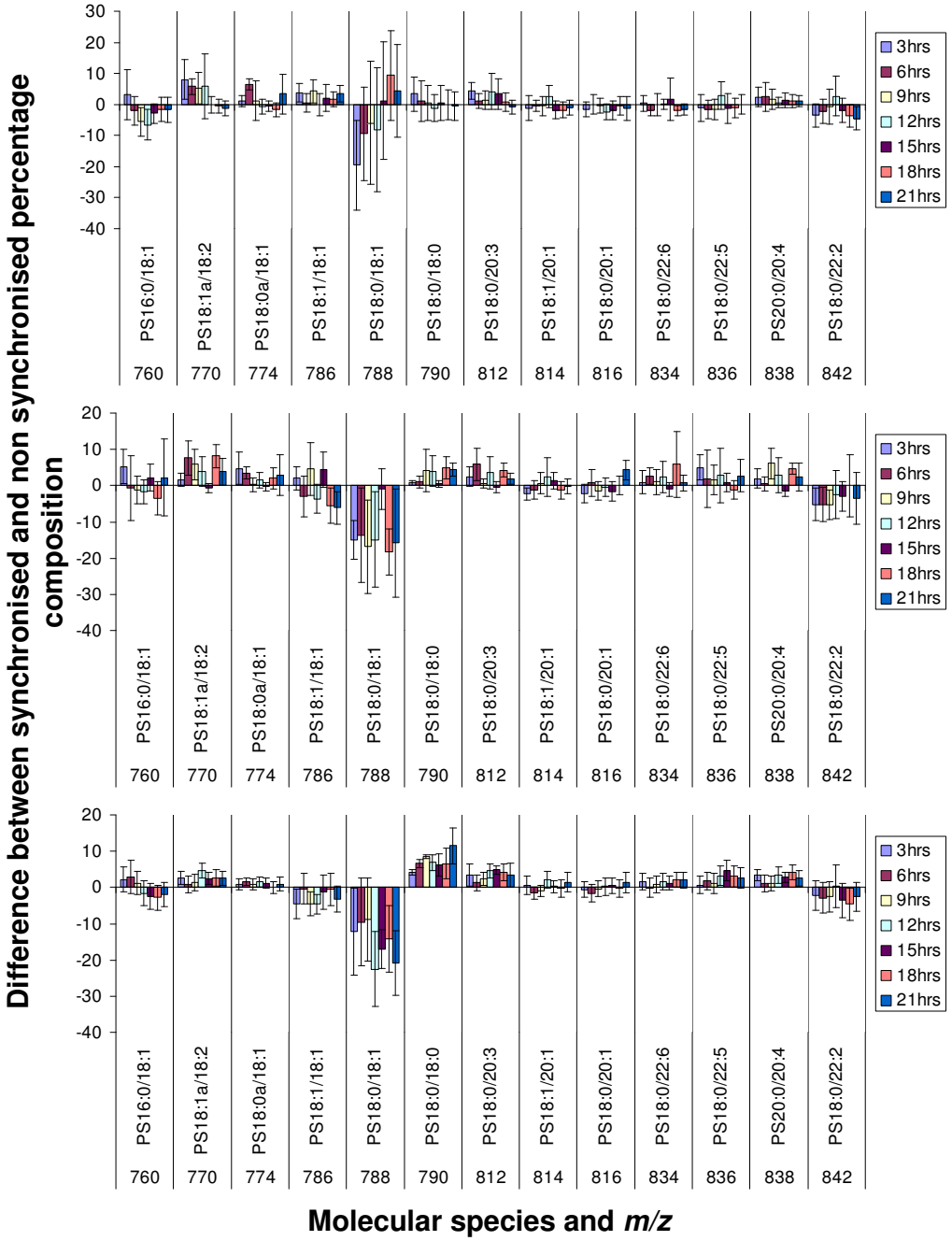

Figure 4.34: Difference between synchronised and non-synchronised percentage composition. Set 1 (nuclei extracted with Triton-X-100) is shown at the top followed by set 2 (nuclei extracted with maltopyranoside) and set 3 (independent repeat of nuclei extracted with maltopyranoside)

The molecular species composition of PA in nuclei extracted from a synchronised cell population is shown in Figures 4.35 to 4.37. At most time points, species 16:0/18:1 (m/z 673) is the most abundant species in the whole cell data (Figure 3.28), however, this species is below the selection threshold in the nuclei data. Species PG16:0/18:1 (m/z 747) which comprises more than 10% of the total in whole cell PA is also below the selection threshold in the nuclei data.

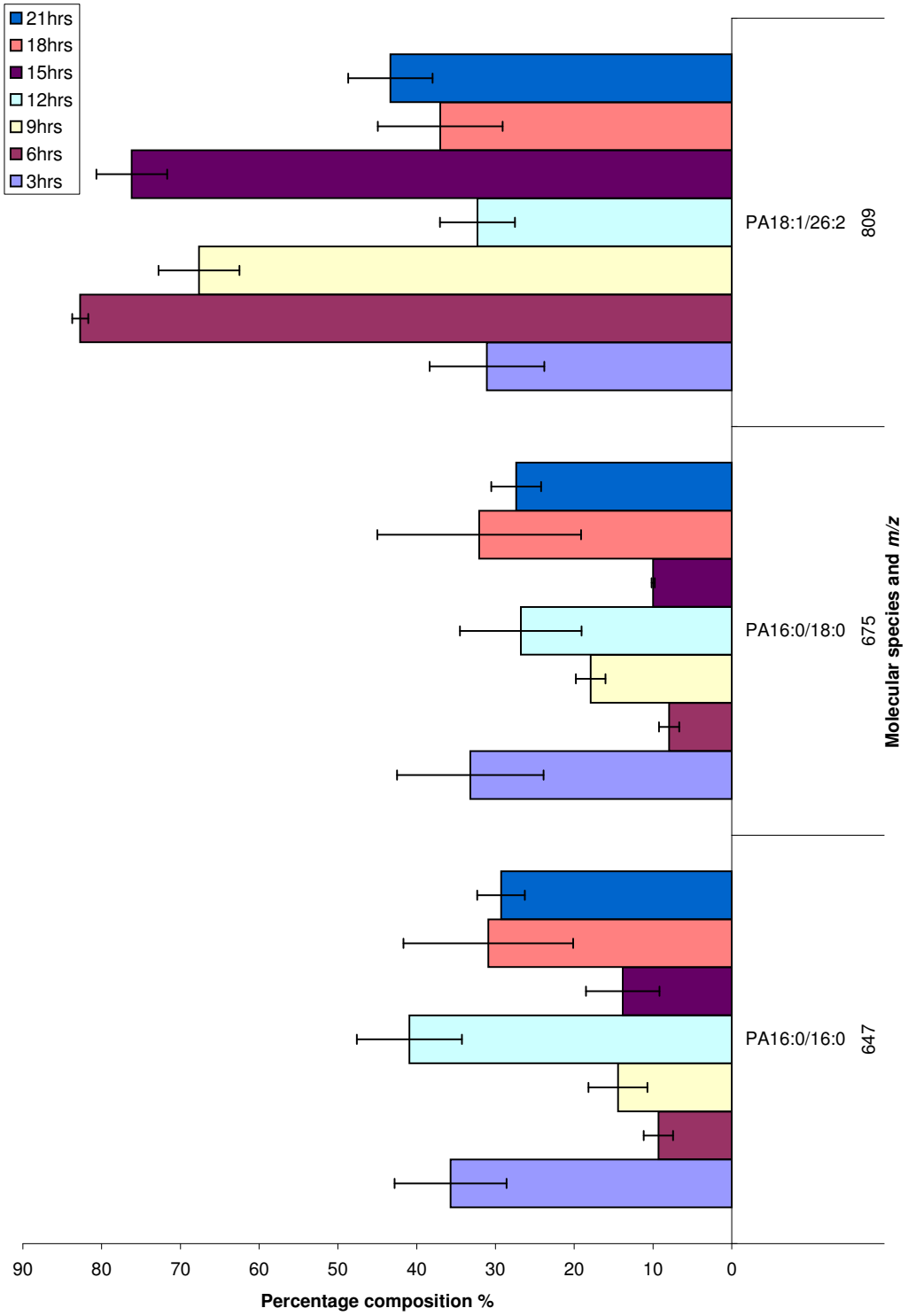

Figure 4.35: Molecular species percentage composition of PA for synchronised nuclei extracted with Triton-X-100

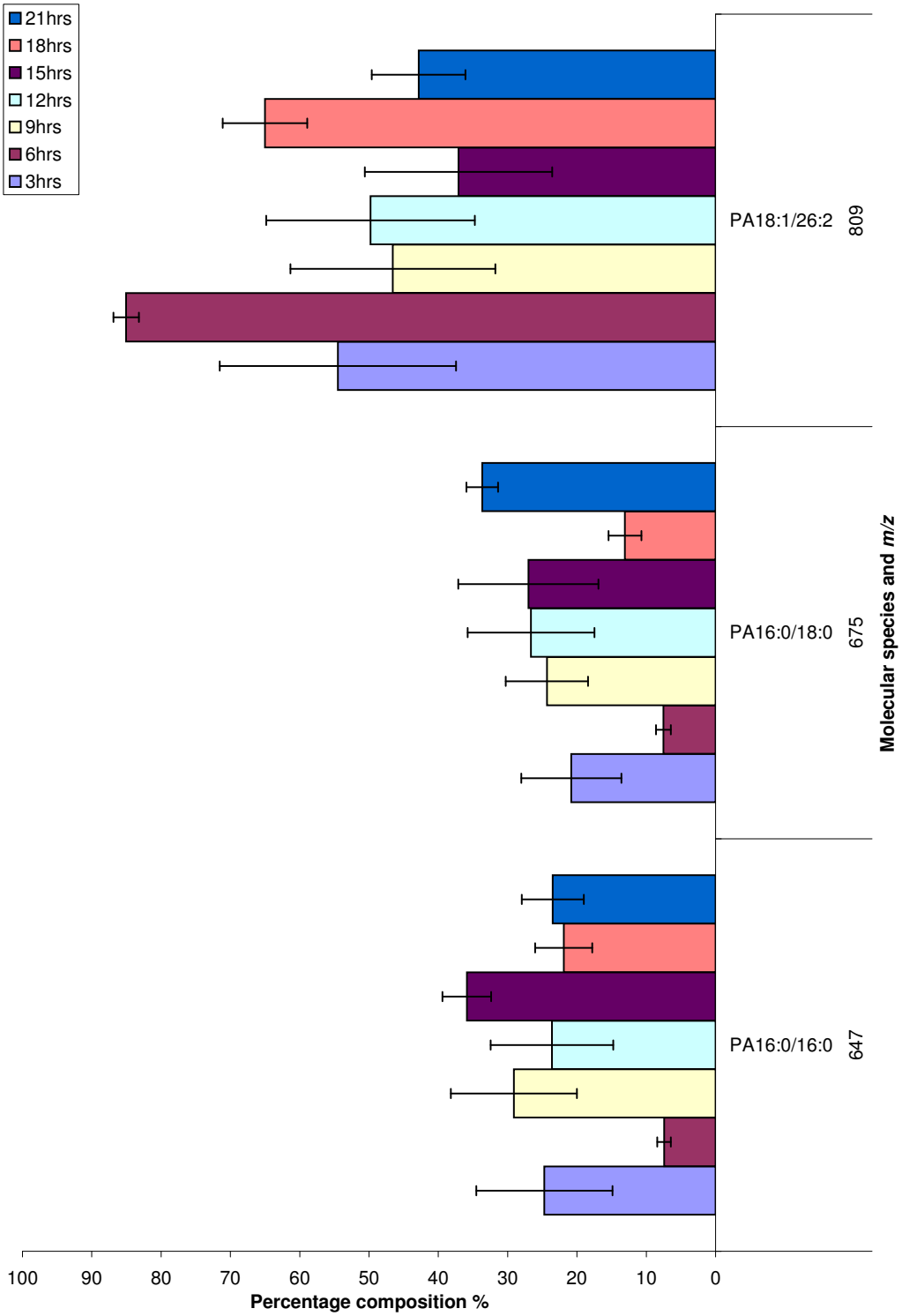

Figure 4.36: Molecular species percentage composition of PA for synchronised nuclei extracted with Maltopyranoside

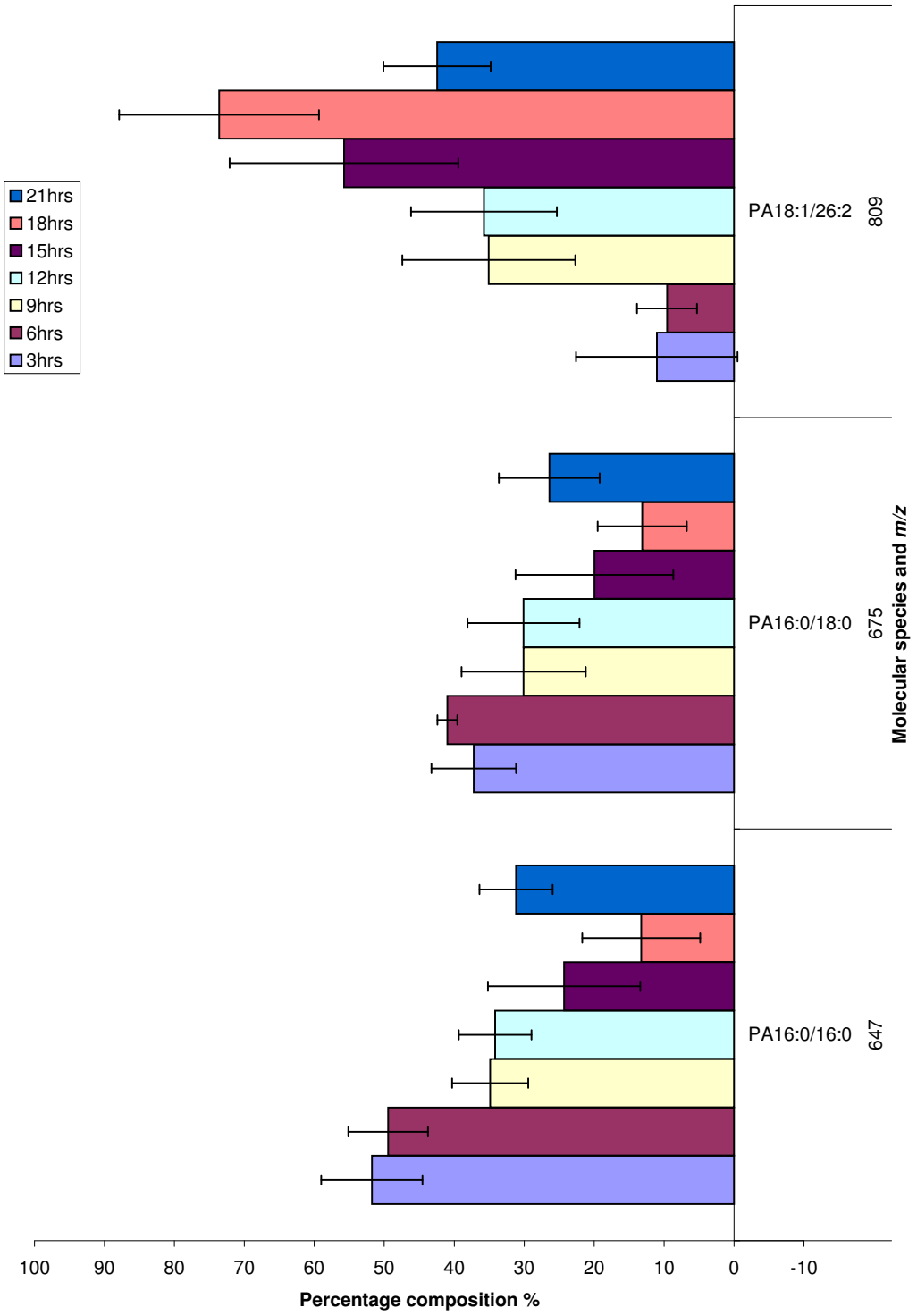

Figure 4.37: Molecular species percentage composition of PA for synchronised nuclei extracted with Maltopyranoside repeat

Figure 4.38 shows the difference between the PA molecular species composition of nuclei from synchronised and non-synchronised cells. In set 1 there is an increase in the 3hr and 12hr time points of species 16:0/16:0 (m/z 647) relative to the asynchronous control. In set 3 there is an increase at 3hrs and 6hrs, however, there is no significant change in set 2. Species 16:0/18:0 (m/z 675) is increased at all time points except 6hrs and 15hrs in set 1, at the 21hrs time point in set 2 and at the 3hr-12hr time points of set 3. This agrees with the result for whole cells which also showed an increase of this species (Figure 3.29).

A small decrease is seen at the 3hr time point of species 18:0/18:1 (m/z 701) in set 2 and the 6hr time point of both set 1 and 3. In set 3 there is a decrease in the 3hr and 6hr time points of species 18:1/26:2 (m/z 809), however, there is no significant change in either set 1 or 2.

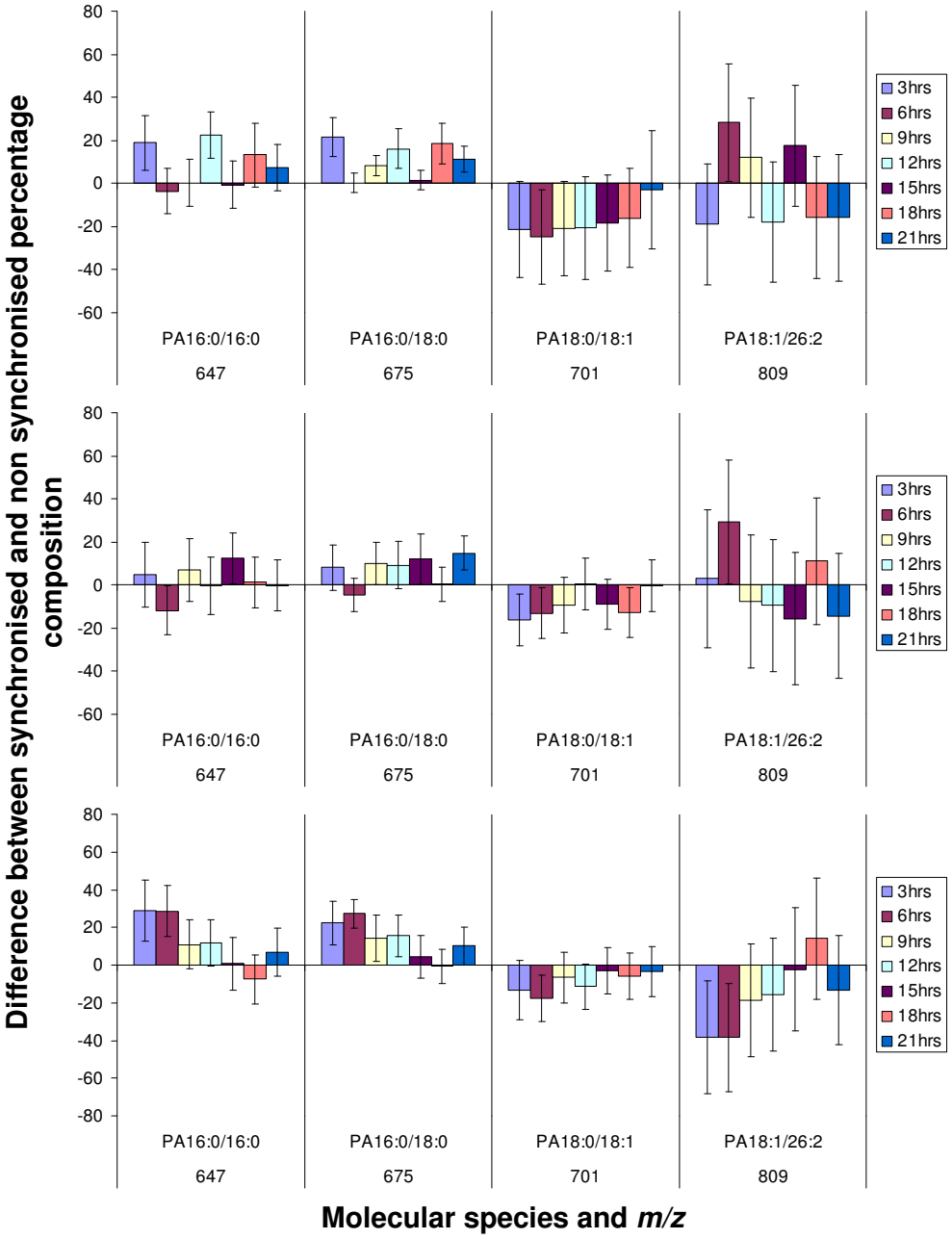

Figure 4.38: Difference between synchronised and non-synchronised PA molecular species percentage composition. Set 1 (nuclei extracted with Triton-X-100) is shown at the top followed by set 2 (nuclei extracted with maltopyranoside) and set 3 (independent repeat of nuclei extracted with maltopyranoside)

As described for whole cells, the endonuclear phospholipid composition of synchronised HeLa cells differs to that of non-synchronised cells in a saturation dependent fashion. There is, however, a distinction between the compositional changes of certain molecular species in whole cells and nuclei following synchronisation. The saturated endonuclear PC molecular species showed a larger and more consistent change, relative to the asynchronous control, than the whole cell saturated PC. The endonuclear monounsaturated PC molecular species showed a decrease which contrasts with the increase or no change of the whole cell monounsaturated PC molecular species. The decreases in certain monounsaturated and di-monounsaturated endonuclear PE species is also not seen in the whole cell data. It was suggested in section 3.3.2 that the use of mimosine may cause cellular changes that correlate with the apoptotic process. It is possible that endonuclear lipid may be effected in a different way to whole cell phospholipid during apoptosis, leading to the discrepancies noted above. Previous studies have indicated that endonuclear phospholipids may interact with DNA and be involved with DNA synthesis [7, 8]. The process of synchronisation with mimosine may interfere with this lipid-DNA interaction and thus lead to alterations in endonuclear phospholipid composition that are different to the whole cell.

Three data sets were presented for each phospholipid class in this section. Although the general trend is very similar across all three data sets for most phospholipid molecular species, some variations were observed. The differences do not, however, seem to be linked to the detergent as no greater variation was observed between the results for Triton-X-100 and maltopyranoside than between the two maltopyranoside data sets. It is perhaps more likely that these differences are attributable to variations between the cell populations such as their exact position in the cell cycle.

4.3.2 Quantified data

Internal standards were included during phospholipid extraction to allow quantification of the phospholipid species. Figures 4.40 to 4.45 show the amount of each species per nucleus over the cell cycle. The results for non-synchronised cells are

also included again here for easy reference (Figure 4.39). As described in section 4.3.1, the data presented for each time point is an average of the results from three phospholipid samples. The error bars on this data represent the first standard deviation of the three measurements. Each sample was obtained from separate flasks of cells, therefore, the reported standard deviation includes biological variability in addition to systematic errors. This is quantified data and therefore also includes any error resulting from cell counting and internal standard addition. For a discussion of the errors on the non-synchronised data see section 4.2.1.

The amount of PC per nucleus is very similar for all three data sets except at the 12hr and 15hr time points (Figure 4.40). At 12hrs the value of data set 3 ('maltopyranoside repeat' data) is more than four times larger than the other two data sets and at 15hrs it is less than half the value. The amount of PC per nucleus decreases in all three data sets from the 3hr time point to the 9hr time point. This coincides with the S-phase of the cell cycle (Table 3.1) during which a reduction in nuclear phospholipid has been reported for rat liver cells [9]. The value at 12hrs is approximately the same as at 9hrs with the exception of data set 3. At 15hrs the amount per nucleus reaches a value slightly greater than at 3hrs, again with the exception of data set 3. At 18hrs data set 3 appears to be almost twice the value of set 1 and 2, however, within the reported error they are the same. The non-synchronised value is very similar to that of the 3hr time point, however, the standard deviation on the non-synchronised results is very large and encompasses all the synchronised results.

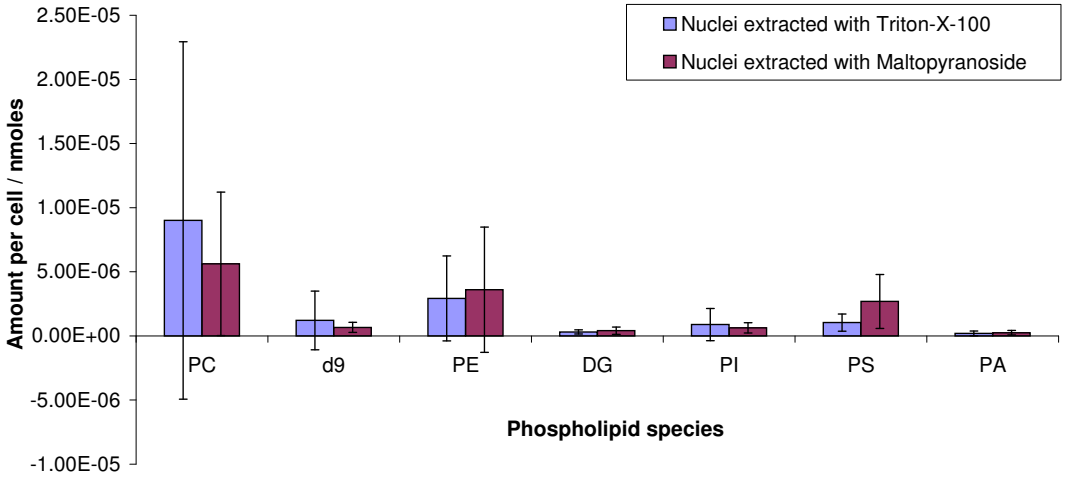

Figure 4.39: Absolute amount per nucleus of each phospholipid species for nuclei extracted from an asynchronous cell population

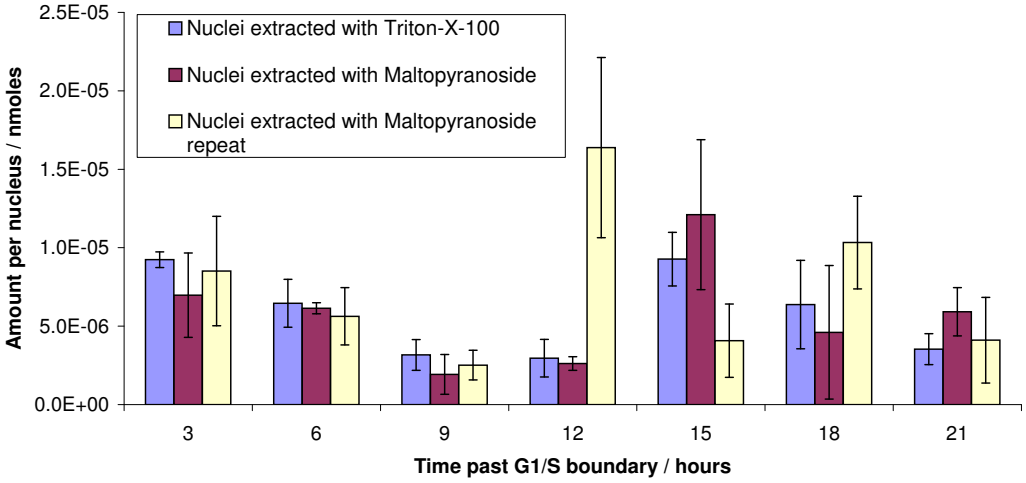

Figure 4.40: Absolute amount per cell of endonuclear PC for synchronised cells. Data is shown for nuclei extracted with Triton-X-100 (data set 1), nuclei extracted with n-Decyl β-D-Maltopyranoside (data set 2) and a second independent measurement of nuclei extracted with n-Decyl β-D-Maltopyranoside (data set 3). The error bars represent the first standard deviation of this data and include error arising from biological variability and systematic errors.

The total amount of PE per nucleus is mainly consistent across the three data sets and across the time points (Figure 4.41). This pattern is very similar to that described for whole cells in section 3.3.3. At the 15hr time point, however, the set 2 value is more than twice that of either set 1 or 3. There is also some indication that the set 3, 12hr time point may be larger than set 1 and 2 but the standard

deviation on this result is very large. Although the non-synchronised value is generally larger than either data set, the standard deviation is very large and therefore encompasses the values of both data sets at all time points.

The 3hr, 6hr and 15hr time points of the set 1 DAG data (Figure 4.42) are all approximately twice the value of the 9hr, 12hr, 18hr and 21hr time points. From 6hrs to 18hrs, the set 2 values are, within error, consistent with those of data set 1. At both 3hrs and 21hrs however, the set 2 value is more than twice that of the set 1. Data set 3 appears to be consistently larger than set 1 or 2 however its standard deviation is very large and encompasses the set 1 and 2 values at 3hrs, 9hrs and 21hrs. This data set also shows a wave-like pattern similar to that of the whole cell, set 1 data for DAG. The minimum amount of DAG per nucleus from synchronised cells is 1.25×10^{-6} nmoles which is larger than the 4.09×10^{-7} nmoles in non-synchronised cells.

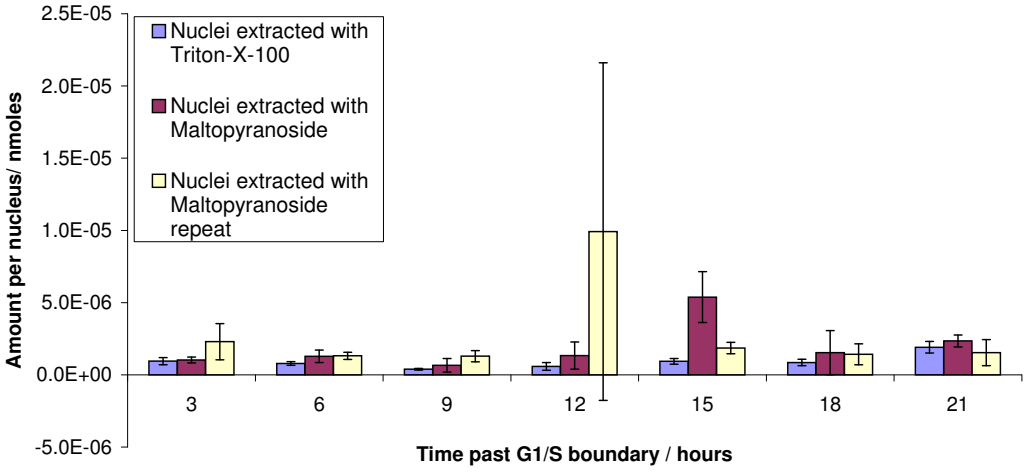

Figure 4.41: Absolute amount per cell of endonuclear PE for synchronised cells. Data is shown for nuclei extracted with Triton-X-100 (data set 1), nuclei extracted with n-Decyl β-D-Maltopyranoside (data set 2) and a second independent measurement of nuclei extracted with n-Decyl β-D-Maltopyranoside (data set 3). The error bars represent the first standard deviation of this data and include error arising from biological variability and systematic errors.

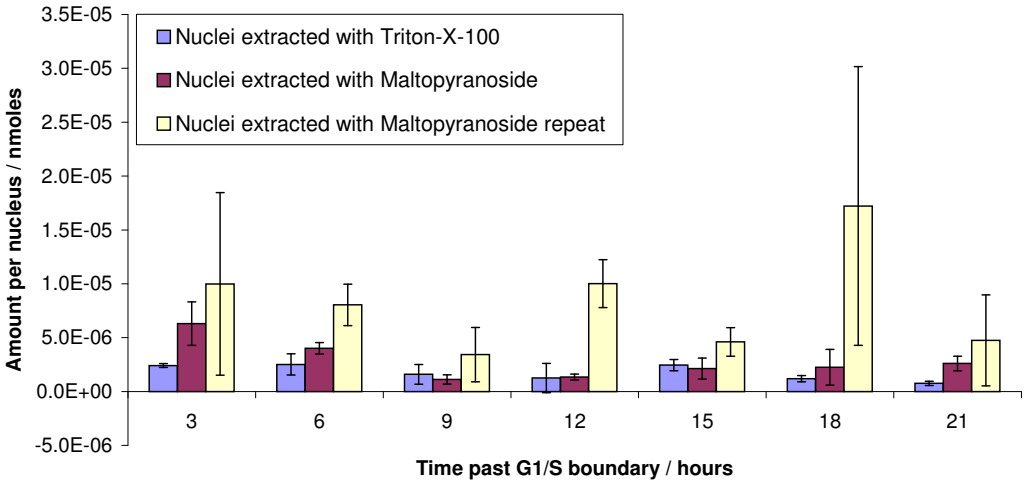

Figure 4.42: Absolute amount per cell of endonuclear DAG for synchronised cells. Data is shown for nuclei extracted with Triton-X-100 (data set 1), nuclei extracted with n-Decyl β-D-Maltopyranoside (data set 2) and a second independent measurement of nuclei extracted with n-Decyl β-D-Maltopyranoside (data set 3). The error bars represent the first standard deviation of this data and include error arising from biological variability and systematic errors.

The amount of PI per nucleus (Figure 4.43) is very similar, within error, over most time points. When compared to the asynchronous PI data (Figure 4.39), the values are also similar to this at most time points. Data set 1 and 2 closely resemble the non-synchronised results at 12hrs, however, as also found for PC (Figure 4.40), the value of data set 3 is more than five times larger. At 3hrs, data sets 1 and 3 are approximately twice and four times as large as the asynchronous data respectively. Data set 3 of the 18hr time point is more than twice the asynchronous value, as is data set 2 of the 21hr time point. At 18hrs and 21hrs, data sets 2 and 3 respectively are also larger than the asynchronous data, however, the error on these data points are large and encompass the asynchronous values.

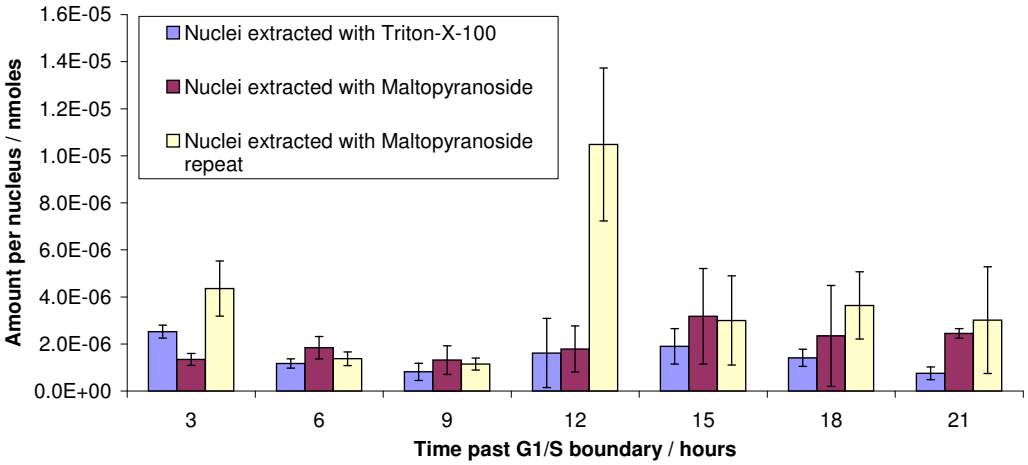

Figure 4.43: Absolute amount per cell of endonuclear PI for synchronised cells. Data is shown for nuclei extracted with Triton-X-100 (data set 1), nuclei extracted with n-Decyl β-D-Maltopyranoside (data set 2) and a second independent measurement of nuclei extracted with n-Decyl β-D-Maltopyranoside (data set 3). The error bars represent the first standard deviation of this data and include error arising from biological variability and systematic errors.

With the exception of 12hrs, the amount per nucleus of PS (Figure 4.44) is, within error, very similar in both data sets 1 and 2. The value of data set 3 is, however, consistently less than set 1 or 2 at all time points except 12hrs. The large standard deviation on the asynchronous data (Figure 4.39) precludes a detailed analysis, however, the values of data set 1 and 2 are similar to that of nuclei extracted from an asynchronous population with maltopyranoside. The value of data set 3 is very similar to that of nuclei extracted from an asynchronous population by Triton-X-100.

At 9hrs, 18hrs and 21hrs the amount per nucleus of PA (Figure 4.45) is very similar between data set 3 and the non-synchronised results. Set 1 and 2, however, are at least twice as large at these time points. The value for all three data sets is very similar at the 6hr and 12hr time points but more than three times that of the non-synchronised data. At 3hrs and 15hrs all data sets are, within error, the same as the non-synchronised results although the standard deviation of data set 3 at 3hrs is very large.

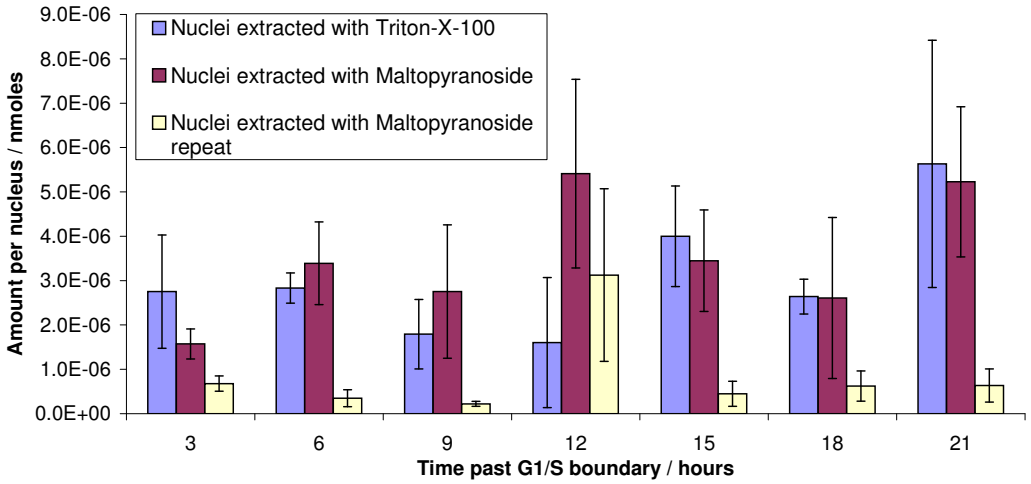

Figure 4.44: Absolute amount per cell of endonuclear PS for synchronised cells. Data is shown for nuclei extracted with Triton-X-100 (data set 1), nuclei extracted with n-Decyl β-D-Maltopyranoside (data set 2) and a second independent measurement of nuclei extracted with n-Decyl β-D-Maltopyranoside (data set 3). The error bars represent the first standard deviation of this data and include error arising from biological variability and systematic errors.

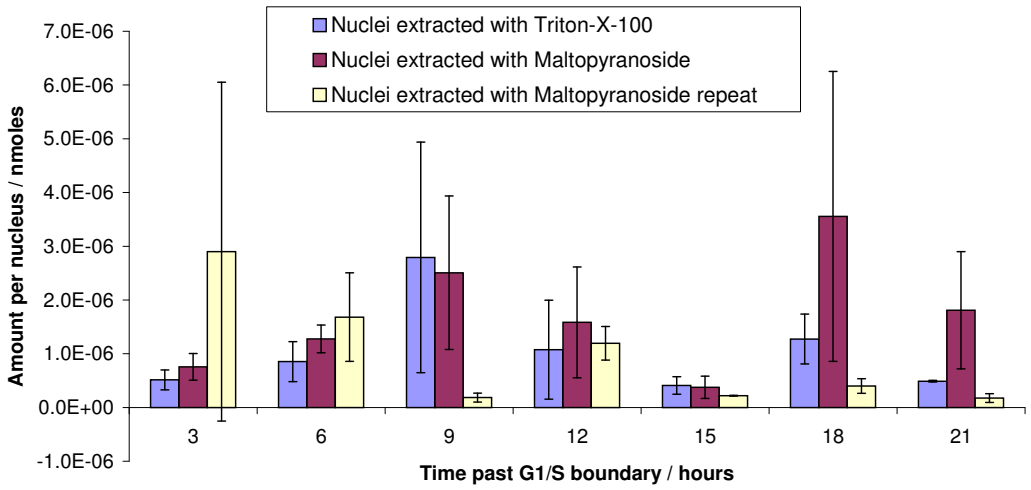

Figure 4.45: Absolute amount per cell of endonuclear PA for synchronised cells. Data is shown for nuclei extracted with Triton-X-100 (data set 1), nuclei extracted with n-Decyl β-D-Maltopyranoside (data set 2) and a second independent measurement of nuclei extracted with n-Decyl β-D-Maltopyranoside (data set 3). The error bars represent the first standard deviation of this data and include error arising from biological variability and systematic errors.

The total amount of phospholipid per nucleus is shown in Figure 4.46. As found for whole cells (section 3.3.3) there does not appear to be a doubling of the phospholipid content as would be expected prior to mitosis in either set 1 or set 2. Instead, the value remains, within error, constant across the time points. There is an increase in set 3 at 12hrs which gives a value approximately twice that of the 6hr, 15hrs and 21hrs time points. Within error, however, the 12hr time point is not significantly different to set 3 of the 18hr or 3hr time points or set 2 of the 15hrs time point.

The large value of total phospholipid at 12hrs in set 3 is mainly due to the large amount of PC at this time point. It is possible that this is an artefact due to incorrect internal standard addition or error within the cell count however this seems unlikely. If the PC internal standard was added incorrectly this would not effect the quantitation of other species, however, the 12hr time point of PI in set 3 is also very high. An incorrect cell count would lead to a comparably high value at the 12hr time point in all species but this is not the case.

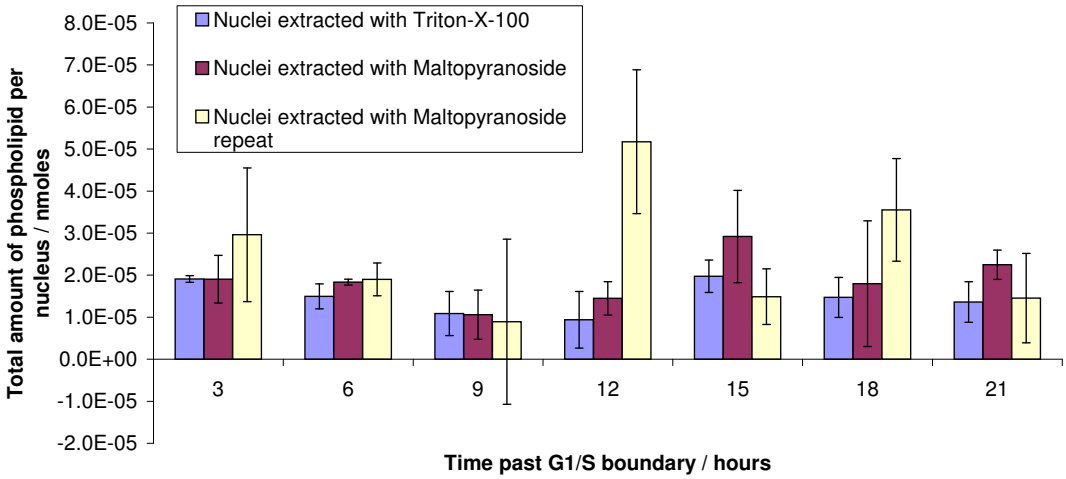

Figure 4.46: Total amount of phospholipid per nucleus

Figure 4.47 shows each phospholipid species as a percentage of the total phospholipid content per nucleus. When compared to the same analysis for nuclei of an asynchronous cell population (Figure 4.8) it is obvious that DAG comprises a larger proportion of the total. In an asynchronous cell population, DAG was found to comprise less than 5% of the total endonuclear phospholipid content. The proportion of total endonuclear DAG was, however, more than 5% and at most time

points greater that 10% for nuclei extracted from synchronised populations (Figure 4.47). It has been suggested that accumulation of endonuclear DAG may be a pro-apoptotic signal [10, 11]. This observation is consistent with the idea discussed in sections 3.3.2 and 4.3.1 that some differences between the phospholipid composition of synchronous and asynchronous cell populations may be an artefact attributable to synchronisation with mimosine. Set 1 of the synchronised whole cell data (Figure 3.37) shows a comparable proportion of DAG to set 1 and 2 of the nuclei data. The percentage of DAG per whole cell in data set 2 is, however, more similar to the results for nuclei from asynchronous populations than synchronised. At most time points, within error, there is no significant difference between the endonuclear proportion of PC, d9PC and PE in nuclei of synchronised cell populations (Figure 4.47) with respect to those of asynchronous populations (Figure 4.8). The 9hr and 15hr time points of data set 2 PC are however approximately half the value of maltopyranoside extracted nuclei from asynchronous cells and less than half that of Triton-X-100 extracted nuclei from asynchronous cells. The proportion of PC in set 2 of synchronised whole cell data (Figure 3.37) is at least 20% higher than endonuclear PC and in set 1 at least 10% larger than most time points of the nuclei data.

The proportion of PI is at most time points, within error, not significantly different to the data for nuclei of asynchronous populations. The 12hr, 15hr and 21hr time points of set 3 are, however, more than twice the value of the asynchronous data. The proportion of PS in data set 1 and 2 is also, within error, similar to the asynchronous data, however, in set 3 all time points are less than half the value of either asynchronous data set. With the exception of the 9hr, 12hr and 15hr time points in set 1 and the 9hr and 18hr time points in set 2, the proportion of PA in nuclei of synchronised cells is not significantly different to that of nuclei from asynchronous populations.

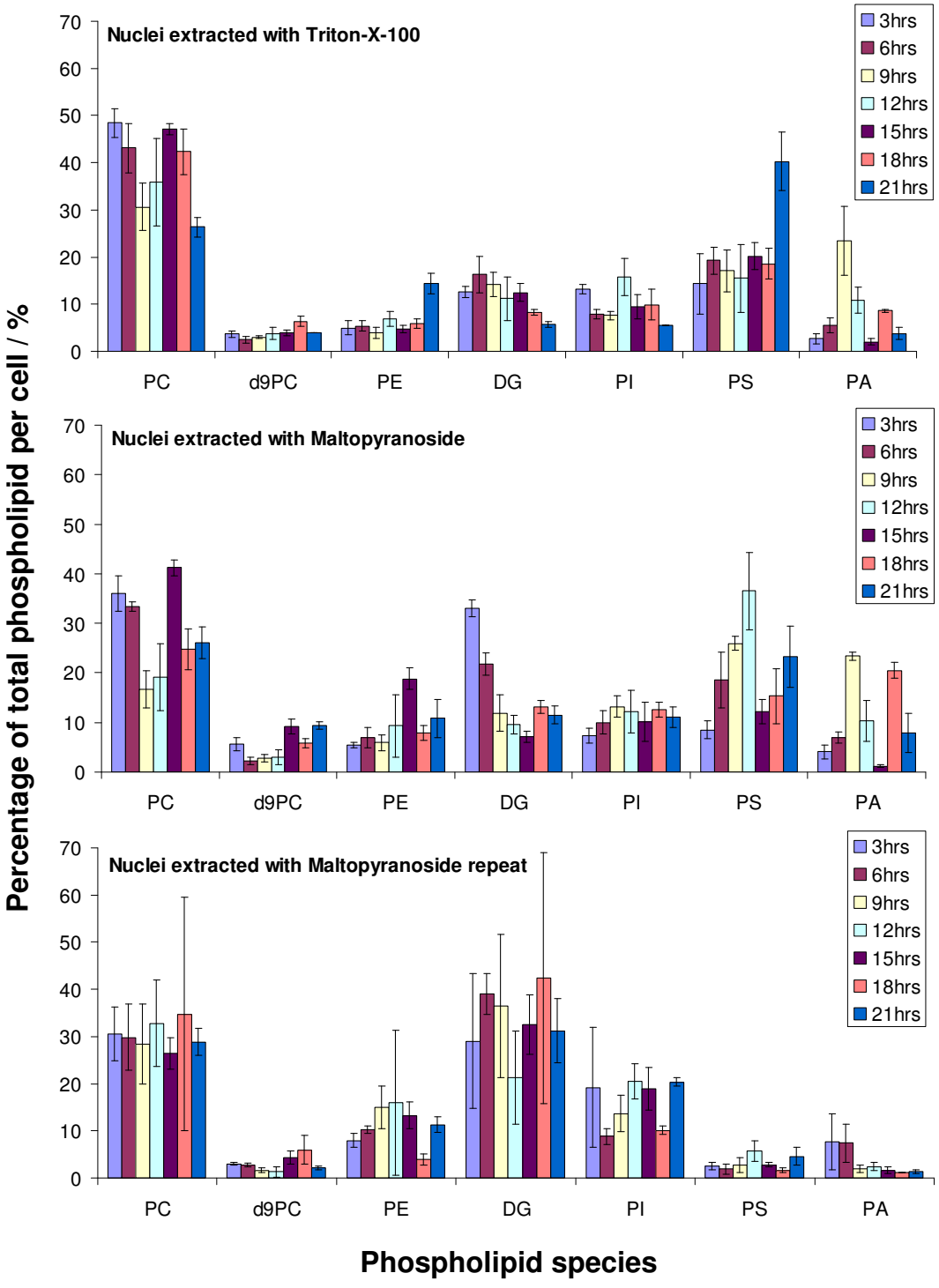

Figure 4.47: Each phospholipid class as a percentage of total phospholipid content per nucleus. Set 1 (Triton-X-100) is shown at the top followed by set 2 (maltopyranoside) and set 3 (maltopyranoside repeat)

The amount per nucleus of each phospholipid class and the resulting overall composition are found to vary between data sets. As described for whole cells it is plausible that these variations may relate to different phospholipid compositions which maintain the same value of membrane torque tension. As discussed in section 1.2.1 though, endonuclear membrane structures have not yet been found. These variations may also be linked to population differences due to lack of 100% synchronicity.

4.4 Summary

This chapter described the use of ESI-MS to determine the endonuclear phospholipid composition of HeLa cells. Section 4.2 described the analysis of nuclei extracted from asynchronous cell populations. The molecular species composition of nuclei extracted with both Triton-X-100 and maltopyranoside was found to be, within error, the same. This indicated that maltopyranoside is a suitable alternative to Triton-X-100 and that the phospholipid composition is not an artefact of the detergent used. Endonuclear PC, DAG and PI was found to be enriched in saturated molecular species with respect to the whole cell composition. Disaturated PC molecular species were found to total 34.4% in nuclei extracted with Triton-X-100 and 22% in nuclei extracted with maltopyranoside. This contrasts with only 12.3% in whole cells. The molecular species composition of PE, PS and PA/PG, however, was found to remain the same between the whole cell and endonuclear compartment. It was noted that endonuclear DAG was most likely to be derived from PC as it is composed mainly of disaturated and monounsaturated molecular species. Endonuclear PA was however, found to be composed mainly of polyunsaturated molecular species indicating that it was generated from a pool of polyunsaturated DAG.

The total amount of endonuclear phospholipid was approximately 12% and 14% of that in the whole cell for nuclei extracted with maltopyranoside and Triton-X-100 respectively. The amount per nucleus of each phospholipid class was very similar for nuclei extracted with each detergent, giving further evidence that the results are not an artefact of the detergent used. The proportion of each phospholipid

class within the nucleus was found to be the same as that within the whole cell.

Section 4.3 described the analysis of nuclei extracted from cell populations which had been treated with mimosine to increase cell cycle synchronicity. As descibed for non-synchronised cells, endonuclear PC is enriched in saturated PC molecular species. Saturated molecular PC species were also found to increase relative to the non-synchronised control. The consistency and magnitude of these changes were greater in the nuclei than the whole cell. The monounsaturated PC molecular species showed either no change or a decrease relative to the non-synchronised control. This contrasted with the whole cell results which showed an increase in some species. The unsaturated PC molecular species showed either no change or a decrease relative to the control which agrees with the whole cell results. As described for whole cells, certain molecular species show more change relative to the non-synchronised control. The largest changes are in species which are also the most abundant.

Saturated and highly unsaturated PE molecular species showed little consistent change relative to the non-synchronised control which agrees with the whole cell findings. Monounsaturated and di-monounsaturated PE species showed either no change or a decrease. As found for PC, most saturated DAG molecular species were increased relative to the non-synchronised control and most unsaturated DAG molecular species were decreased. Set 3, however, showed an increase in molecular species containing an alkyl link but no change in the other species. This result is similar to the findings for whole cell DAG molecular species. As described for whole cells, it was suggested that the increase in certain molecular species may be achieved by the remodelling of other DAG molecular species. The saturated and highly unsaturated PI molecular species showed either no change or an increase relative to the non-synchronised control. The monounsaturated species, however, tend to show a decrease. The PS molecular species show very little consistent change relative to the non-synchronised control. The most significant changes were in species 18:0/18:1 which was decreased and species 18:0/18:0 which was increased. The PA molecular species also showed very little consistent change over the three data sets. Species 16:0/18:0 and 16:0/16:0, however, showed an increase at some time points and species 18:0/18:1 showed a decrease.

The compositional changes of certain molecular species, following synchronisation, differ between the whole cell and nucleus. It was suggested that this may be caused by differences in the way that mimosine interacts with phospholipid of the whole cell and nucleus.

The total amount of each phospholipid class per nucleus was determined (section 4.3.2). As found for whole cells there did not appear to be a doubling of the phospholipid content as would be expected prior to mitosis. There was an increase of the 12 hour time point in set 3, however, within error this was not significantly different to the 3 hour or 15 hour values. DAG was found to comprise a larger proportion of the total phospholipid content in nuclei from synchronised cell compared to nuclei from non-synchronised cells. It was suggested that this increase in endonuclear DAG may be acting as a pro-apoptotic signal.

As described for whole cells, the variations between data sets may reflect different molecular species compositions that maintain the same value of membrane torque tension. The variation may also be due to population differences arising from a lack of 100% synchronicity.

References

[1] A. Hunt, G. T. Clark, G. S. Attard, and A. D. Postle. Highly saturated endonuclear phosphatidylcholine is synthesized in situ and colocated with CDP-choline pathway enzymes. *The Journal of Biological Chemistry*, 276(11):8492–8499, 2001.

[2] A. Hunt. *Nuclear Matrix phosphatidylcholine biosynthesis: Why is it essential, why is there so much and why is it so saturated?*, pages 47–61. Research Signpost, 2003.

[3] C.S D'Santos, J.H. Clarke, and N. Divecha. Phospholipid signalling in the nucleus. *Biochemica et Biophysica Acta*, 1436:201–232, 1998.

[4] C.S D'Santos, J.H Clarke, R. I. Irvine, and N. Divecha. Nuclei contain two differentially regulated pools of diacylglycerol. *Current Biology*, 9:437–440, 1999.

[5] K.Vermeulen, D.R.Van Bockstaele, and Z.N.Berneman. The cell cycle: a review of regulation, deregulation and therapeutic targets in cancer. *Cell Prolif.*, 36:131–149, 2003.

[6] E. M. Deacon, T. R. Pettitt, P. Webb, T. Cross, H. Chahal, M. J. O. Wakelam, and J. M. Lord. Generation of diacyglycerol molecular species through the cell cycle: a role for 1-stearoyl,2-arachidonyl glycerol in the activation of nuclear protein kinase C-βII at G2/M. *Journal of Cell Science*, 115(5):983–989, 2001.

[7] E. Albi, M. Micheli, and M.P. Viola Magni. Phospholipids and nuclear RNA. *Cell Biology International*, 20(6):407–412, 1996.

[8] V.V. Kuvichkin. DNA-lipid interactions in vitro and in vivo. *Bioelectrochemistry*, 58:3–12, 2002.

[9] N. M. Maraldi, S. Santi, N. Zini, A. Ognibene, R. Rizzoli, G. Mazzotti, R. Di Primio, R. Bareggi, V. Bertagnolo, and C. Pagliarini. Decrease in nuclear phospholipids associated with DNA replication. *Journal of Cell Science*, 104:853–859, 1993.

[10] A. Hunt. Dynamic lipidomics of the nucleus. *Journal of Cellular Biochemistry*, 97:244–251, 2006.

[11] T. A. Lagace, J. R. Miller, and N. D. Ridgway. Caspase processing and nuclear export of CTP:Phosphocholine cytidyltransferase α during farnesol-induced apoptosis. *Molecular and Cellular Biology*, 22:4851–4862, 2002.

Chapter 5

Phosphatidylcholine biosynthetic dynamics

5.1 Introduction

Phosphatidylcholine (PC) accounts for a large proportion of both whole cell and endonuclear lipids (Chapters 3 and 4). Biosynthesis of PC is thought to regulate the accumulation of diacylglycerol (DAG) which is involved in cell signalling [1, 2, 3]. In eukaryotic cells, synthesis of PC proceeds principally via the Kennedy pathway in which choline is converted to phosphatidylcholine following a three step process (Figure 5.1).

Several isoforms of the Kennedy pathway enzymes exist and are distributed within spatially distinct areas of the cell [4]. A study of IMR-32 cells indicated that these enzymes retained activity in isolated nuclei and may therefore represent an intact pathway for the synthesis of endonuclear PC, separate to that of the whole cell [2].

Deuterium enriched choline-d9 can be used as a substrate to allow PC biosynthesis to be analysed by ESI-MS. The deuterated label is added to the culture medium in excess as described in section 7.4.1. Newly synthesised PC incorporates the choline-d9 and can be identified by ESI-MS by scanning for the parents of m/z 193 [5]. This method was used to determine the relationship between cell cycle progression and PC biosynthesis within the whole cell and endonuclear compartment.

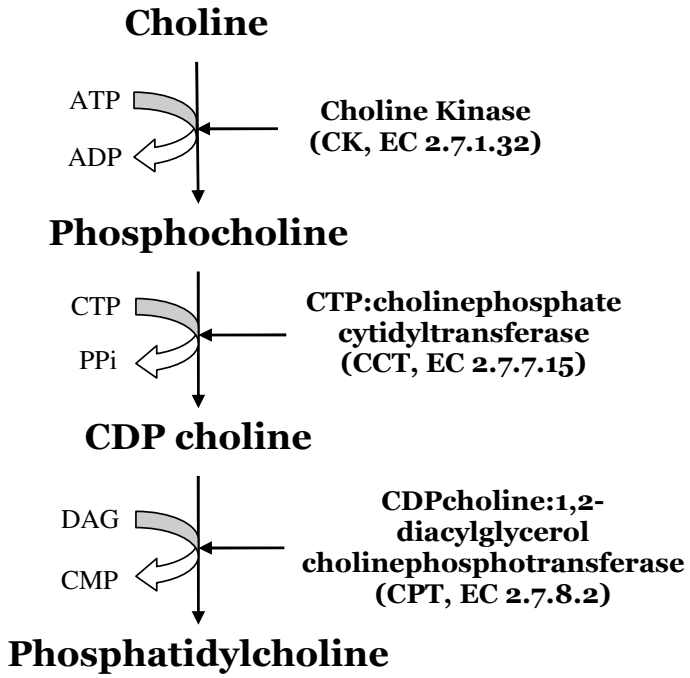

Figure 5.1: Phosphatidylcholine synthesis by the Kennedy pathway. This is the principal pathway for phosphatidylcholine synthesis in eukaryotic cells.

5.2 Whole cell PC synthesis

The molecular species composition of newly synthesised PC in non-synchronised whole cells is shown in Figure 5.2. As described in section 3.2.1, the molecular species composition presented is an average of measurements obtained over six different days. On each day the composition of phospholipid extracted from three separate flasks of cells was measured. The error bars shown on the data represent the first standard deviation of all these measurements (18 samples in total). The reported stardard deviation therefore includes error resulting from both biological variability and instrument instability.

The composition is very similar to that of the endogeonous PC shown in Figure 3.1, with species 16:0/18:1 and 18:1/18:1 the most abundant. This observation agrees well with a previous study of IMR-32 cells [2]. As described for endogenous PC (section 3.2.1), the molecular species composition is similar to that of DAG (Figure 3.3). Figures 5.1 and A.9 show that DAG is required for the synthesis of PC via the Kennedy pathway and this may explain the similarity in composition to newly synthesised PC.

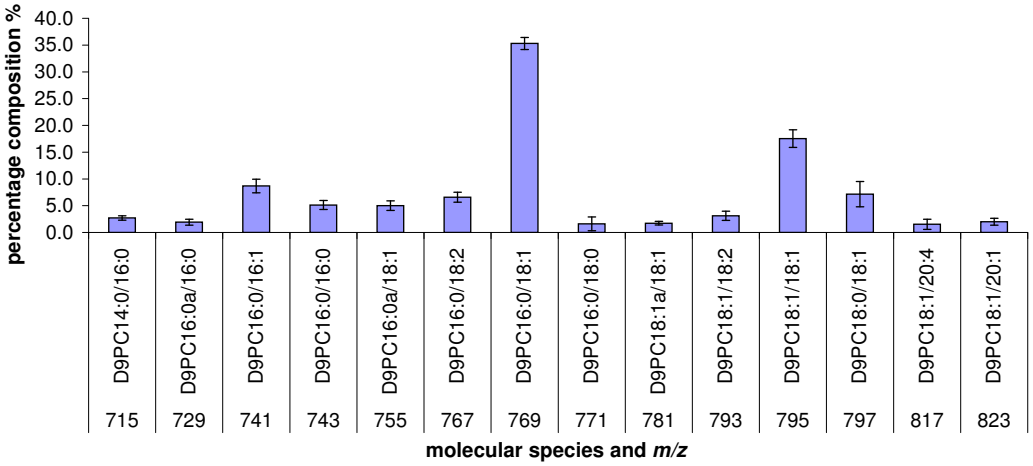

Figure 5.2: Molecular species percentage composition of d9PC for whole cells. The error bars represent the first standard deviation of this data and inlclude errors arising from biological variability and instrument instability.

Table 5.1 summarises the total amount of endogenous and newly synthesised PC per cell. As described in section 3.2.2, the values presented are an average of measurements taken on four separate days. The reported first standard deviation therefore includes instrument instability, biological variability and errors arising from cell counting and internal standard addition. The newly synthesised PC is found to account for approximately 5.7% of the total PC in the cell. When the error on the measurement is taken into account, this value is quite similar to the 8.6% newly synthesised PC found for IMR-32 cells [2].

Total amount of PC per cell /nmoles			
Type of PC	**Average**	**Standard deviation**	**Coefficient of Variation (%)**
Endogenous	4.9×10^{-5}	2.9×10^{-5}	59.3
Newly synthesised	2.5×10^{-6}	9.2×10^{-7}	36.8
Total	5.2×10^{-5}	2.9×10^{-5}	57.6
Newly synthesised PC as percentage of total PC	5.7	2.8	50.2

Table 5.1: Total amount of endogenous and newly synthesised PC per non-synchronised whole cell following a three hour incubation with d9-choline. The reported first standard deviation includes instrument instability, biological variability and errors arising from cell counting and internal standard addition.

The molecular species composition of newly synthesised PC over the cell cycle is shown in Figures 5.3 and B.7. Data set 1 and 2 refer to those described in section 3.3.2. The data presented for each time point is an average of the results from three phospholipid samples. The error bars on this data represent the first standard deviation of the three measurements. Each sample was obtained from separate flasks of cells, therefore, the reported standard deviation includes biological variability in addition to systematic errors.

The composition is very similar to that of endogenous PC (Figure 3.12) and newly synthesised PC in non-synchronised cells (Figure 5.2), with species 16:0/18:1 and 18:1/18:1 the most abundant. Species 16:0a/16:1, 16:1a/18:1 and 16:0/18:0a are present in the endogenous PC data (Figure 3.12) but not in the newly synthesised data. Species 16:0/18:0, 18:1a/20:4 and 16:0/22:6 are however present in the newly synthesised data but below the selection threshold in the endogenous PC data.

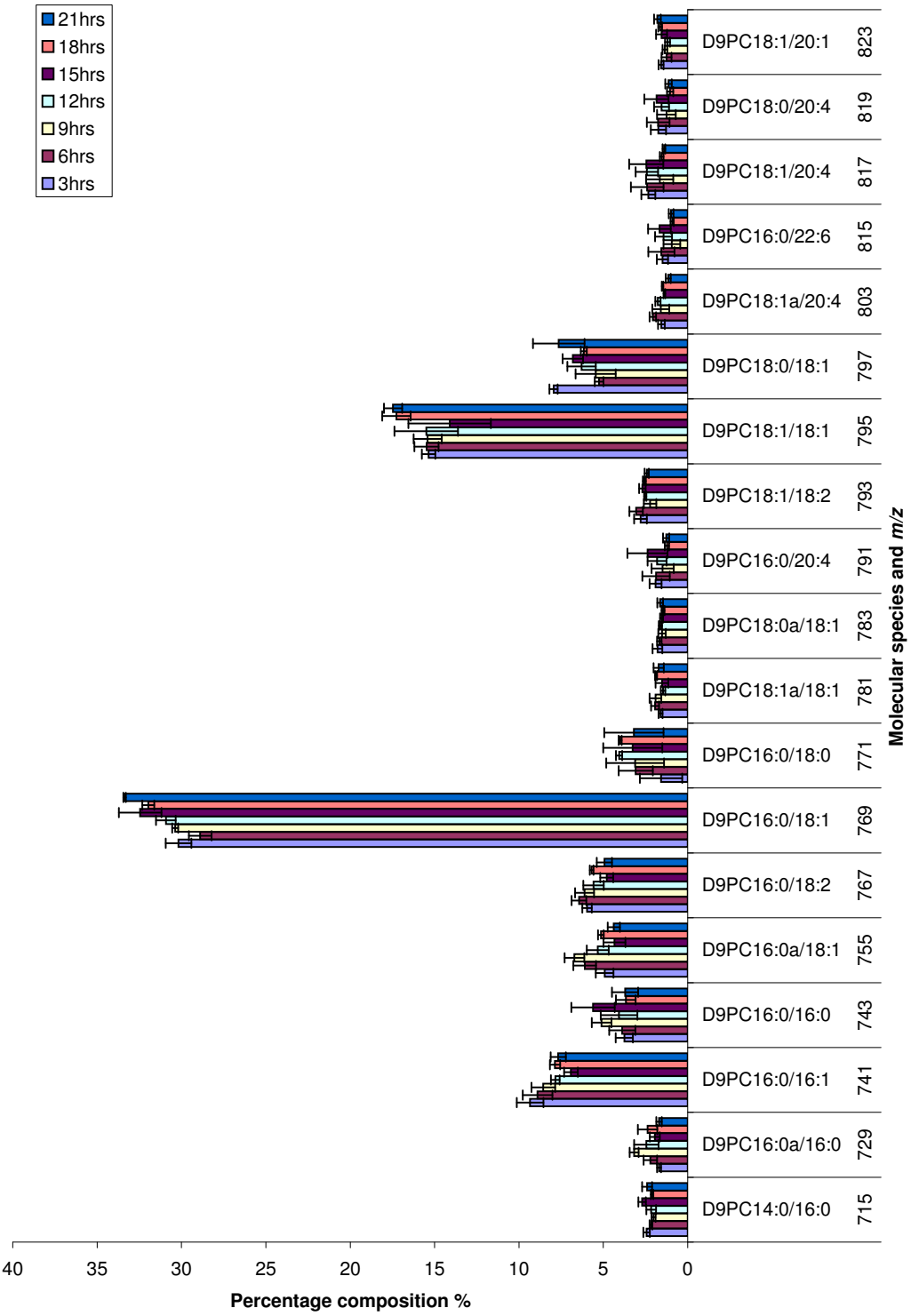

Figure 5.3: Molecular species percentage composition of d9PC for synchronised whole cells. Data set 2. The error bars on this data represent the first standard deviation over three measurements and include biological variability in addition to systematic errors.

The synchronised data was compared to that obtained for non-synchronised cells as described in section 3.3.2. The results of this analysis are presented in Figures 5.4 to 5.7. As previously described, the error bars represent the combined standard deviation of the synchronised and non-synchronised results. This combined standard deviation therefore includes the error of instrument instability from the asynchronous data (see section 3.2.1) and the biological variability and systematic errors from both data sets.

The saturated molecular species (Figure 5.4) generally show very little change relative to the non-synchronised control. The largest change is seen for the 12hr and 18hr time points of species 16:0/18:0 (m/z 771) in set 2 which are increased by more than 2%. The other time points, within error, remain unchanged relative to the control. The changes seen for this species in set 2 are not apparent in set 1 with all time points showing no significant variation to the control.

Species 16:0/16:0 (m/z 743) shows an increase at the 9hr and 18hr time points in set 1. This is not however repeated in set 2, rather a small reduction in the 3hr and 18hr points occurs. When compared to the equivalent endogenous PC species (Figure 3.14, m/z 734) it is clear that the results for set 1 are quite similar with both showing the increase at 9hrs and 18hrs.

The 9hr time point of species 16:0a/16:0 (m/z 729) shows an increase relative to the non-synchronised data in set 2 but this is not apparent in set 1. There is also no increase at 9hrs in either data set of the equivalent endogenous PC species (Figure 3.14, m/z 720). The very small increase in the 18hr time point of set 1 is, however, consistent with set 1 of the endogenous PC. The 14:0/16:0 (m/z 715) species remains very similar to the control although the 3hr time point in set 1 and the 9hr and 18hr time points of set 2 show a very small decrease.

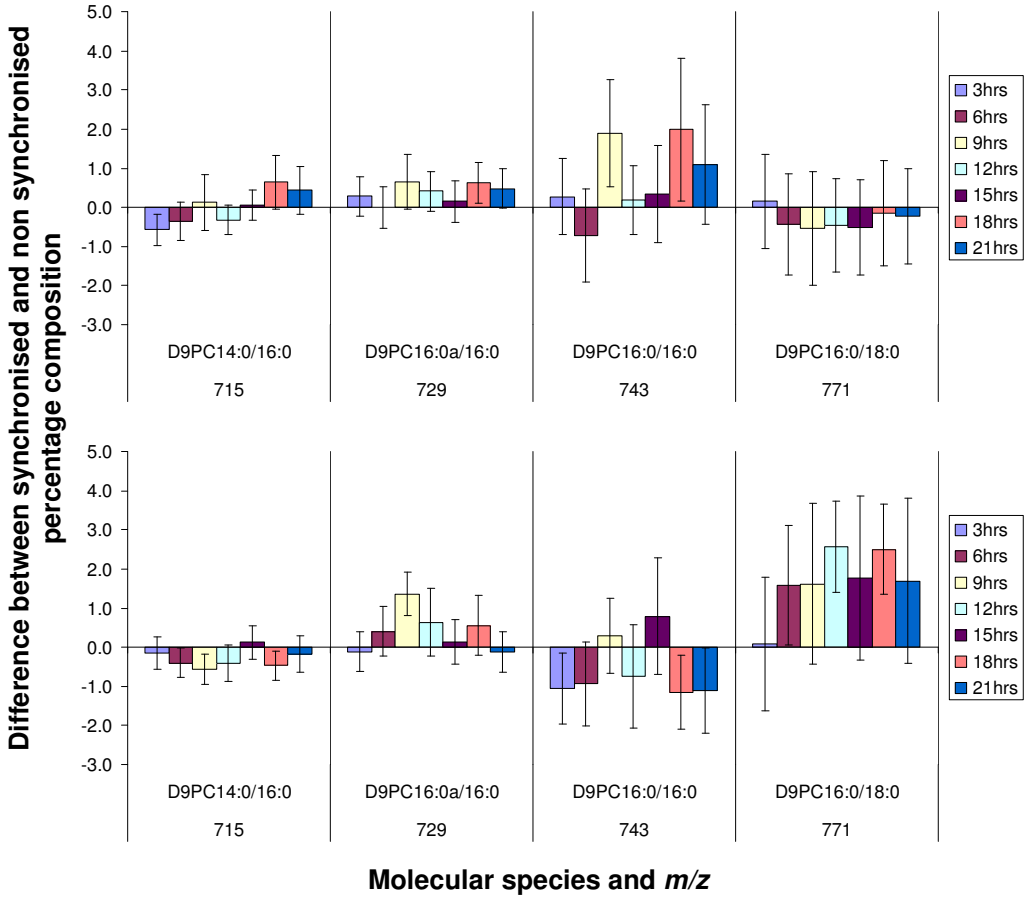

Figure 5.4: Difference between synchronised and non synchronised percentage composition for saturated d9PC species. Set 1 is shown at the top followed by set 2. The error bars represent the combined standard deviation of sysnchronised and non-synchronised data. This includes instrument instability from the asynchronous data and the biological variability and systematic errors from both data sets.

Figure 5.5 shows the difference between the monounsaturated molecular species of synchronised cells and non-synchronised cells. The most significant change occurs for species 16:0/18:1 (m/z 769). Unlike the equivalent endogenous PC species (Figure 3.15, m/z 760) the newly synthesised PC species shows a reduction, relative to the asynchronous data, over most time points and in both data sets. There is however a small increase for the 18hr time point of set 1 but this is not mirrored in set 2.

The 3hr time point of set 1 species 18:0/18:1 (m/z 797) shows an increase which is also seen in both data sets of the endogenous PC (Figure 3.15, m/z 788). This is not however seen in set 2 and, unlike the endogenous PC, the other time points

remain unchanged relative to the asynchronous control.

Species 16:0a/18:1 (m/z 755) shows an increase at the 9hr time point in set 2 but none of the time points show any change in set 1. This is in contrast to the endogenous PC (Figure 3.15, m/z 746) which shows no change in set 2 but a small decrease in the 9hr and 12hr time points of set 1. The increase in set 1 species 18:0a/18:1 (m/z 783), over all time points, is not apparent in set 2 or in the endogenous PC.

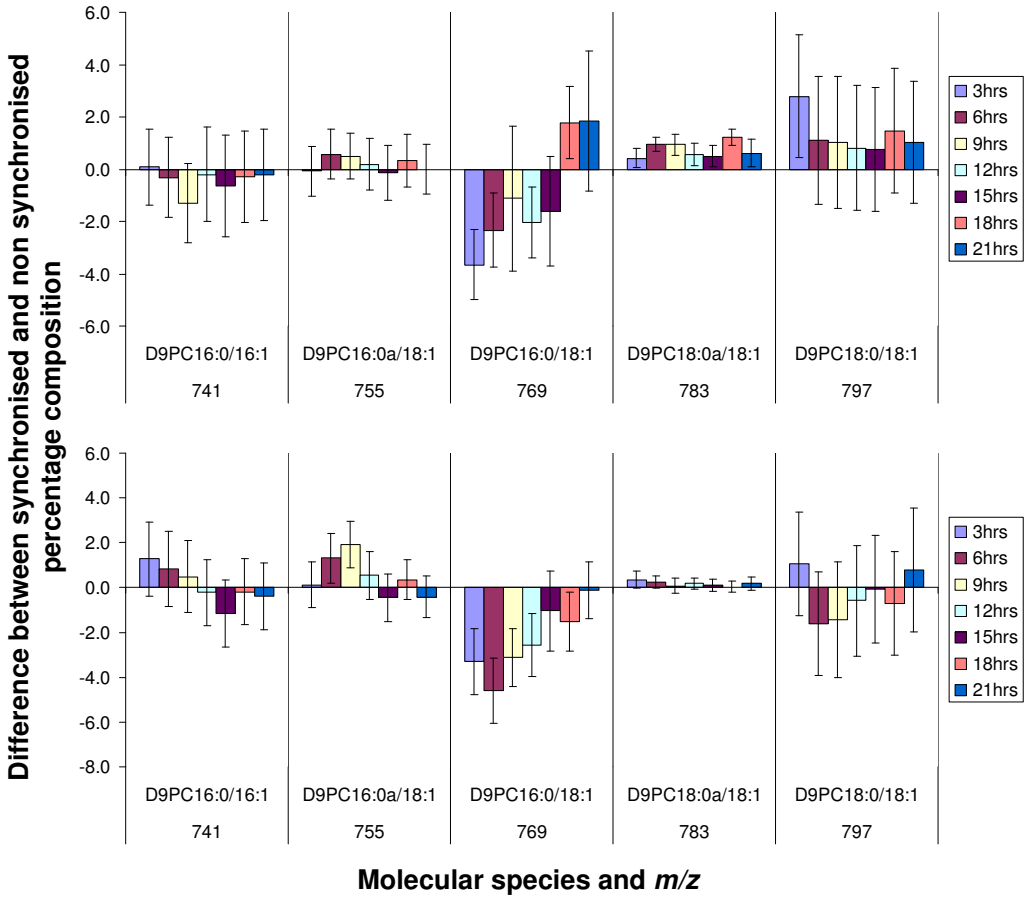

Figure 5.5: Difference between synchronised and non synchronised percentage composition for monounsaturated d9PC species. Set 1 is shown at the top followed by set 2

The di-monounsaturated species (Figure 5.6) show very little change relative to the non-synchronised data. The most significant change is observed in set 1 for species 18:1/18:1 (m/z 795) in which the 9hr, 18hr and 21hr time points are reduced. No other changes are apparent which is quite different to the finding for the

endogenous PC which indicated a decrease in all di-monounsaturated molecular species relative to the non-synchronised.

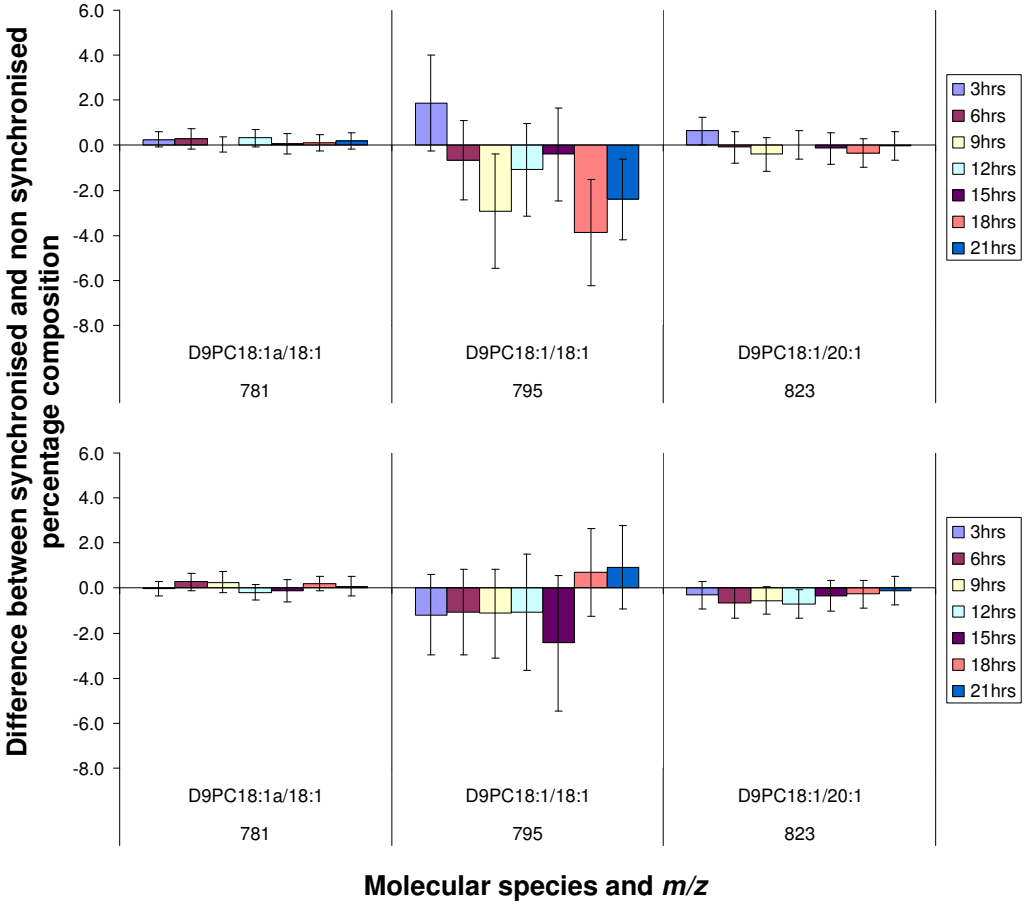

Figure 5.6: Difference between synchronised and non synchronised percentage composition for di-monounsaturated d9PC species. Set 1 is shown at the top followed by set 2

The polyunsaturated species (Figure 5.7) generally remain very similar to the asynchronous control, an observation that was also made for the endogenous PC. There is however an increase of species 18:1a/20:4 (m/z 803) in set 2 over all time points. It is interesting to note that this species contains an alkyl link, a property which appeared to be linked to increases in DAG molecular species relative to the non-synchronised (Figure 3.21). A decrease, relative to the non synchronised, of species 16:0/18:2 (m/z 767) occurs at the 18hr time point in set 1 and the 15hr and 21hrs time points of set 2. The decrease at 18hrs in set 1 is also seen for the equivalent endogenous species.

As mentioned in section 5.2, DAG is involved in the synthesis of PC. There does not, however, appear to be an obvious correlation between the changes, relative to the non-synchronised control, in DAG and newly synthesised PC. The species which shows the greatest change, at one or more time points, in both data sets is 16:0/18:1 (m/z 769). As described for endogenous PC, this species is also the most abundant newly synthesised PC molecular species in the cell (Figure 5.3).

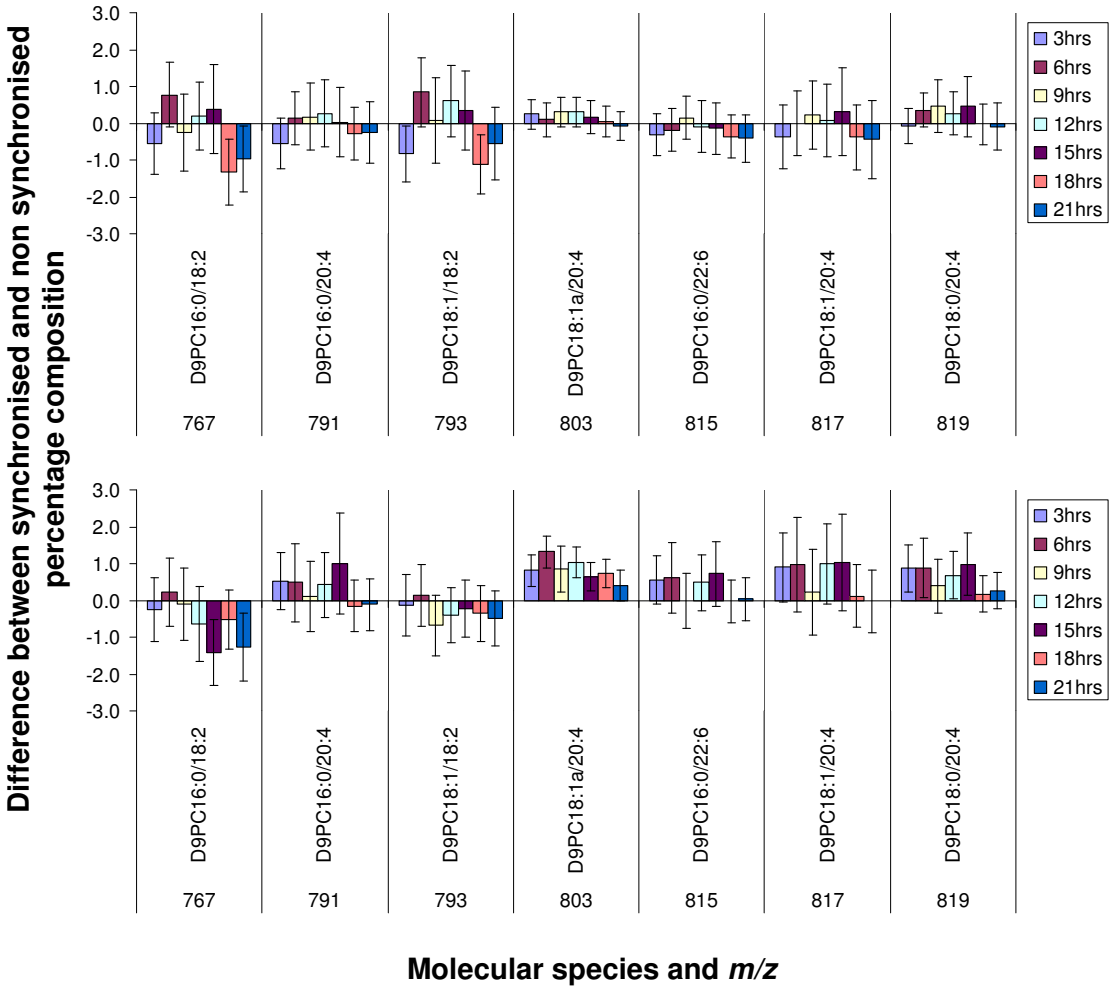

Figure 5.7: Difference between synchronised and non synchronised percentage composition for highly unsaturated d9PC species. Set 1 is shown at the top followed by set 2

Figure 5.8 shows the total amount of newly synthesised PC per cell over the cell cycle. As described above, the data presented for each time point is an average of the results from three phospholipid samples. The error bars on this data represent

the first standard deviation of the three measurements. Each sample was obtained from separate flasks of cells, therefore, the reported standard deviation includes biological variability in addition to systematic errors. As this is quantified data it includes any error resulting from cell counting and internal standard addition.
In set 1 the amount per cell remains very stable at all time points except 3hrs which is more than two times greater than the others. This is not however reflected in set 2 which shows the greatest amount per cell at the 18hr time point. The pattern of results is almost identical to that of the endogenous PC shown in Figure 3.30. The amount per cell of newly synthesised PC in cells from an asynchronous population (Table 5.1) is, within error, very similar to the values of set 1 except at 3hrs.

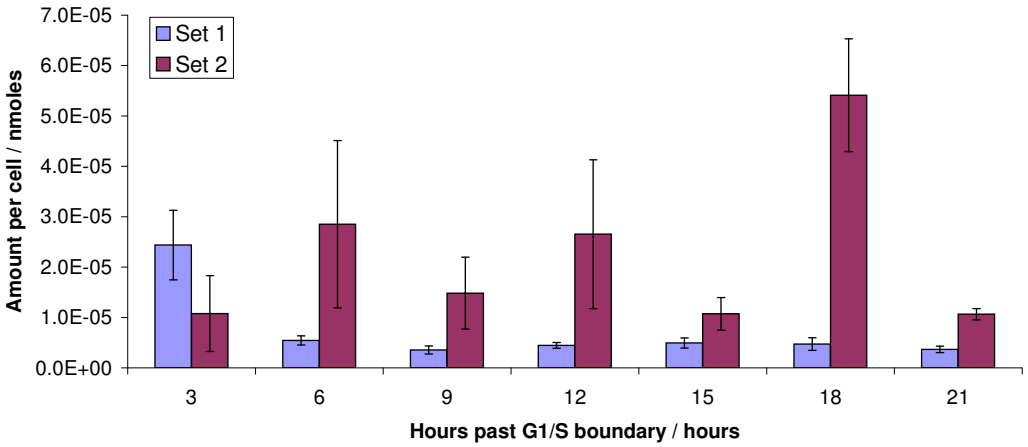

Figure 5.8: Absolute amount per cell of d9PC for synchronised whole cells

Newly synthesised PC as a percentage of the total PC per cell over the cell cycle is shown in Figure 5.9. At most time points the value is very similar for both data-sets and also, within error, very similar to the value found for non-synchronised cells. The 3hr and 15hr time points of set 1 and the 18hr time point of set 2 show the greatest difference to the non-synchronised value. A previous study of HeLa cells suggested an increase in net PC synthesis, particularly of saturated molecular species, associated with the M and early G1 phase of the cell cycle [6]. Although there is no evidence of an increase in saturated species (Figure 5.4), the small increase in the percentage of newly synthesised PC at 15hrs and 18hrs may indicate such an increase in synthesis during the early G1 phase (see Table 3.1).

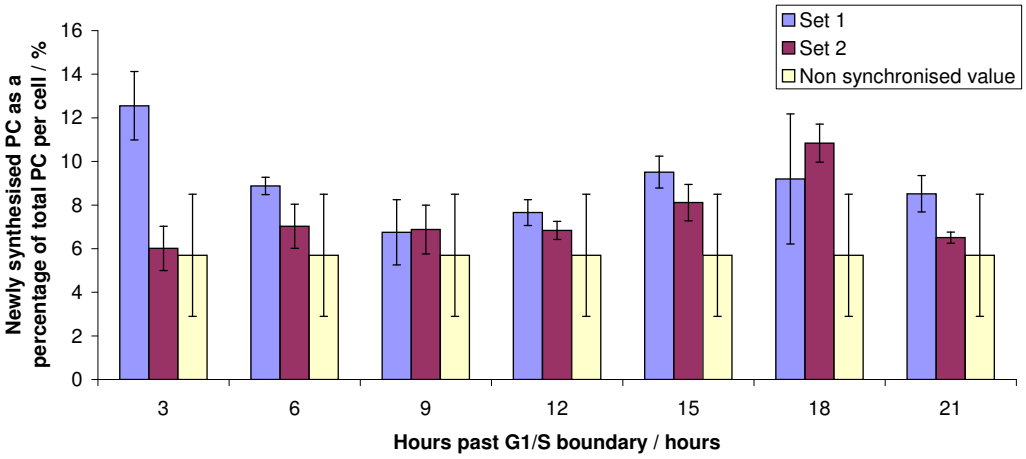

Figure 5.9: Newly synthesised PC as a percentage of the total PC per cell.

5.3 Endonuclear PC synthesis

CTP cholinephosphate cytidyltransferase (CCT) is the regulatory enzyme for PC biosynthesis via the Kennedy pathway and exists in three isoforms [7, 8]. The CCTα isoform is located in the nucleus throughout the cell cycle and forms part of an intact pathway for endonuclear PC synthesis, separate to that of the whole cell [9, 2].

Previous studies have indicated that changes in nuclear PC synthesis can accompany progression through the cell cycle [10, 6]. These studies were not conducted on nuclear envelope free nuclei but they do suggest a variation in PC synthesis which is specific to the nucleus. This section describes the extent to which endonuclear HeLa cell PC synthesis is cell cycle dependent and how it differs from that in the whole cell.

Figure 5.10 shows the molecular species composition of newly synthesised endonuclear PC. The molecular species composition of the nuclei extracted with Triton-X-100 is an average of measurements obtained over four different days. For nuclei extracted with matopyranoside, the result presented is an average of measurements taken over three different days. On each day the composition of phospholipid extracted from three separate flasks of cells was measured. The error bars on the data represent the first standard deviation of all these measurements (12 samples in total for Triton-X-100 and 9 for maltopyranoside). The reported standard deviation therefore includes error resulting from both biological variabil-

ity and instrument instability.

As described for endogenous PC (section 4.2.1), the newly synthesised endonuclear PC has a higher proportion of saturated species than the whole cell newly synthesised PC. Disaturated molecular species total 37.7% in nuclei extracted with Triton-X-100 and 32.5% in nuclei extracted with maltopyranoside. This contrasts with a total of 11.7% in the whole cell. Species where both fatty acid chains are unsaturated are, as also described for endogenous PC, found in a higher proportion in the whole cell. Diunsaturated newly synthesised PC molecular species total 30.1% in the whole cell. In nuclei extracted with Triton-X-100 this value is 12.6% and in nuclei extracted with maltopyranoside it is 17%. These values are very similar to those for endogenous PC (section 4.2.1). Such similarity was not found for a previous study on IMR-32 cells [2] which instead suggested a continuation of endonuclear newly synthesised PC remodelling after the 3 hour d9-choline incubation time.

As seen for the whole cells (section 5.2), the composition of newly synthesied endonuclear PC is similar to that of the endogenous endonuclear PC shown in Figure 4.1. In both cases, species 16:0/18:1 is the most abundant and species 16:0/16:0, 18:1/18:1 and 18:0/18:1 are present at more than 5%. Species 16:0a/18:1, however, is above 5% of the endogenous PC but below 5% of the newly synthesised PC. There is also a marked reduction in the number of molecular species containing an alkyl link in the newly synthesised PC data with respect to the endogenous PC. Species 16:0a/16:1, 16:1a/18:1, 16:0a/18:0, 18:1a/18:1 and 18:0a/18:1 are below the selection threshold in the newly synthesised PC data (Figure 5.10) but not in the endogenous PC data (Figure 4.1). Although the proportion of disaturated and diunsaturated molecular species is similar to endogenous PC, this reduction in the number of species containing an alkyl link may suggest that further remodelling takes place after 3 hours.

Within error the results obtained with each detergent are the same. This suggests that the type of detergent used is not effecting the molecular species composition of the newly synthesised PC.

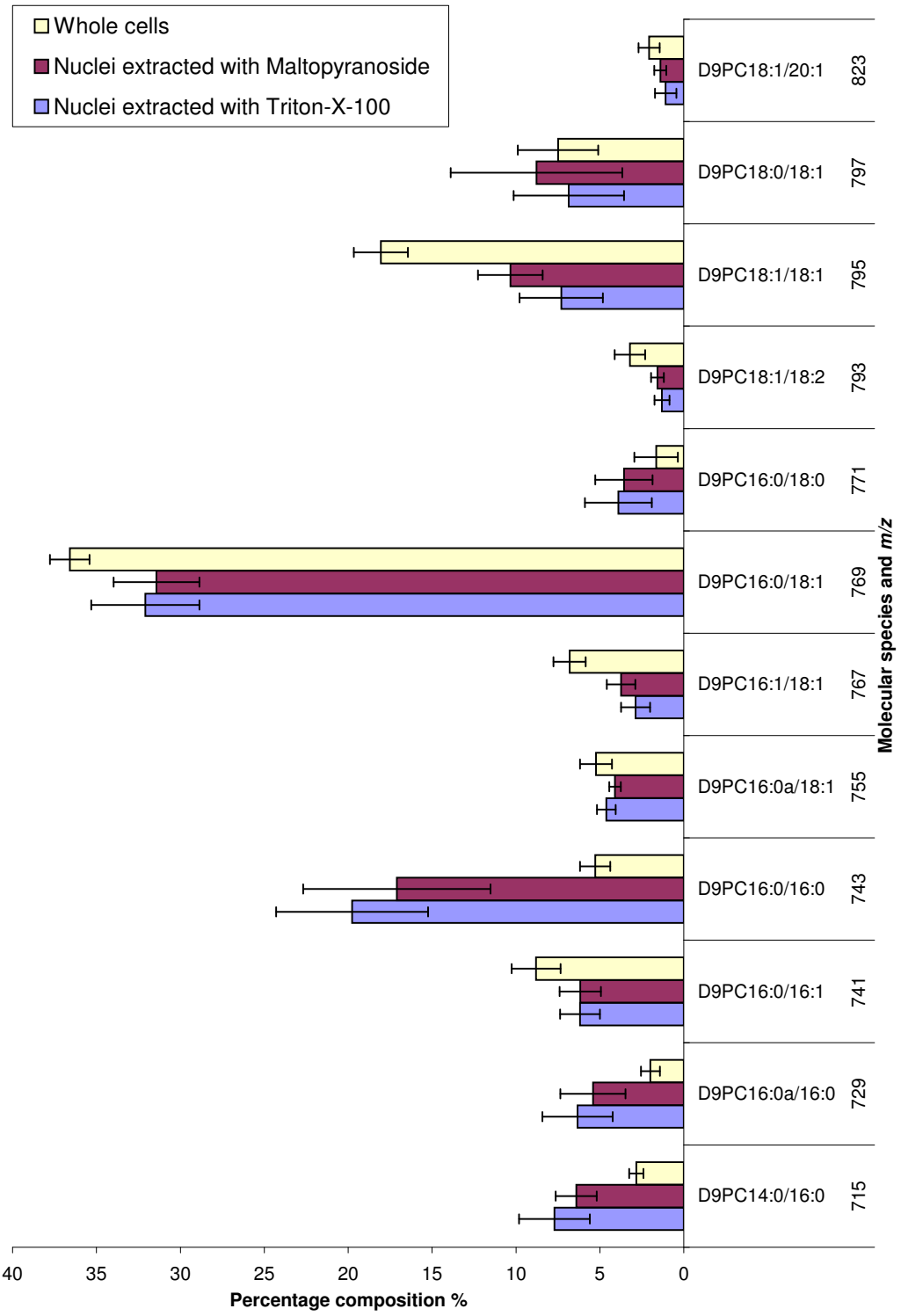

Figure 5.10: Molecular species percentage composition of d9PC in nuclei. The reported standard deviation includes error resulting from both biological variability and instrument instability.

The total amount of endogenous and newly synthesised PC per nucleus is shown in Table 5.2. The reported standard deviation includes error arising from instrument instability, biological variability, internal standard addition and cell counting. The newly synthesised PC as a percentage of the total PC per nucleus (also shown in Table 5.2) is higher than the 5.7% in the whole cell (Table 5.1). The error on this data is, however, very large. Newly synthesised PC as a percentage of the total PC is, within error, the same for nuclei extracted with each detergent. This suggests that the type of detergent used for nuclei extraction does not influence the rate of PC synthesis.

Total amount of PC per nucleus /nmoles				
Detergent used for nuclei extraction	**Type of PC**	**Average**	**Standard deviation**	**Coefficient of Variation (%)**
Maltopyranoside	Endogenous	5.6×10^{-6}	5.6×10^{-6}	99.5
	Newly synthesised	6.7×10^{-7}	3.9×10^{-7}	58.8
	Total	6.3×10^{-6}	5.8×10^{-6}	92.5
Triton-X-100	Endogenous	9.0×10^{-6}	1.4×10^{-5}	154.7
	Newly synthesised	1.2×10^{-6}	2.3×10^{-6}	189.0
	Total	1.0×10^{-5}	1.6×10^{-5}	158.3
Newly synthesised PC as percentage of total PC per nucleus				
Maltopyranoside nuclei		15.3	±7.74	
Triton-X-100 nuclei		11.7	±5.32	

Table 5.2: Amount of endogenous and newly synthesised PC per nucleus and newly synthesised PC as a percentage of the total PC per nucleus

The molecular species composition of newly synthesised endonuclear PC over the cell cycle is shown in Figures 5.11, 5.12 and 5.13. The data presented for each time point is an average of the results from three phospholipid samples. The error bars on this data represent the first standard deviation of the three measurements.

Each sample was obtained from separate flasks of cells, therefore, the reported standard deviation includes biological variability in addition to systematic errors. As found for endogenous endonuclear PC (Figures 4.9 to 4.11), species 16:0/16:0 and 16:0/18:1 are the most abundant.

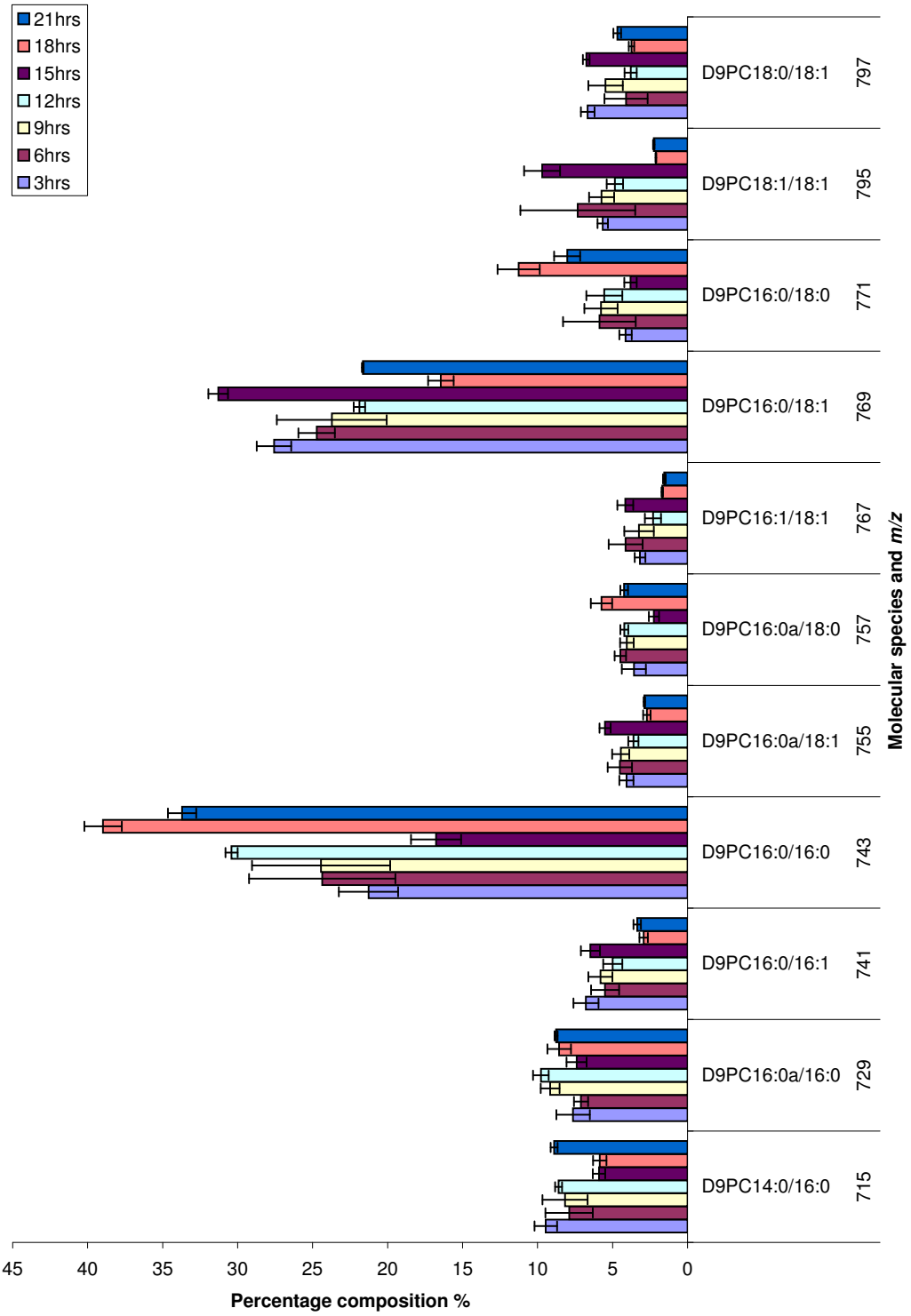

Figure 5.11: Molecular species percentage composition of newly synthesised PC for synchronised nuclei extracted with Triton-X-100

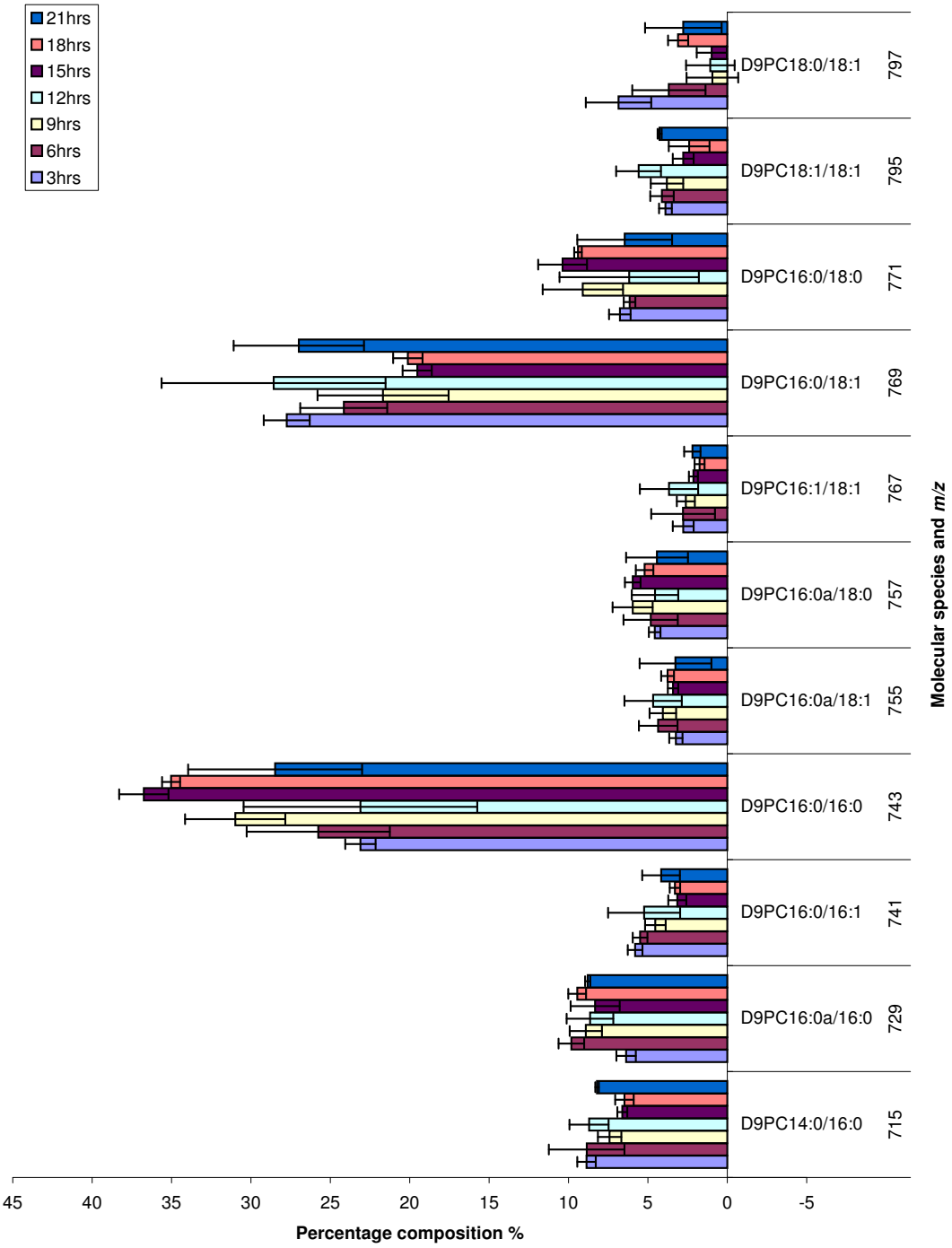

Figure 5.12: Molecular species percentage composition of newly synthesised PC for synchronised nuclei extracted with Maltopyranoside

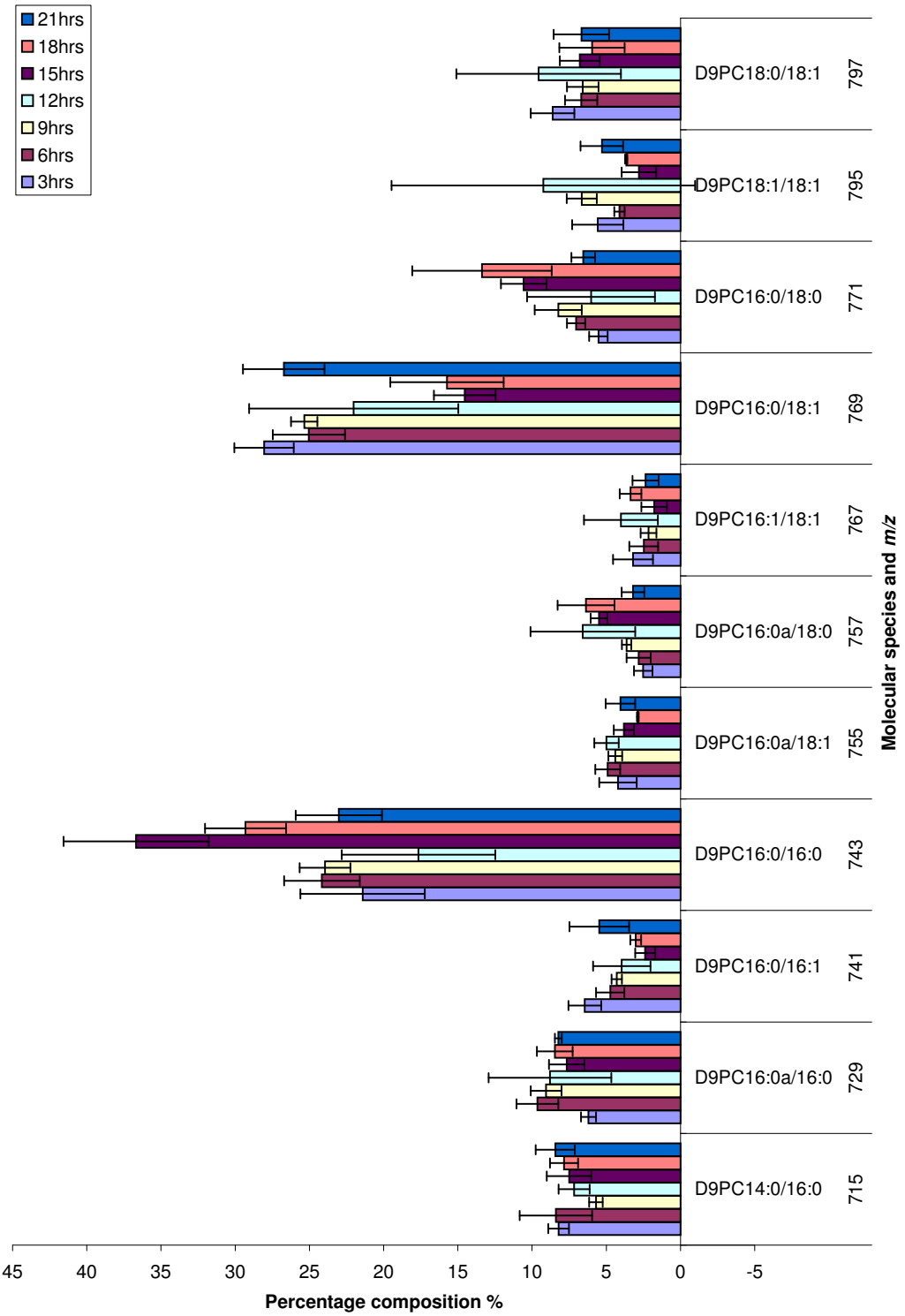

Figure 5.13: Molecular species percentage composition of newly synthesised PC for synchronised nuclei extracted with Maltopyranoside repeat

Figures 5.14 to 5.16 show the result of comparing this data from synchronised cells to that of the non-synchronised cells. The error bars represent the combined standard deviation of the synchronised and asynchronous results. This combined standard deviation is determined by calculating the square root of the sum of the squared standard deviations for each equivalent data point. This combined standard deviation therefore includes the error of instrument instability from the asynchronous data and the biological variability and systematic errors from both data sets.

The saturated species (Figure 5.14) generally show no change or an increase relative to the non-synchronised control. The most significant increases in each data set are for species 16:0/16:0 (m/z 743). In sets 1 and 3 the greatest increase is in the 15hr time point, however, this is not true for set 2 which instead shows no change at 15hrs but a large increase at 18hrs. This variation between the data-sets may represent a slight shift in the cell cycle position. At 15hrs to 18hrs post cell cycle block removal, a high proportion of the cell population are undergoing mitosis or entering the G1 phase (Figure 3.10). Species 16:0/18:0 (m/z 771) also shows the greatest increase relative to the non-synchronised cells at either the 15hr or 18hr time point. This suggests that the increase at these time points may be related to the cell cycle position. These results are very similar to that of endogenous nuclear PC (Figure 4.12). In both cases species 16:0/16:0 shows the greatest increase particularly at the later time points.

The monounsaturated species generally show no change or a decrease relative to the non-synchronised control. Species 16:0/18:1 (m/z 769) shows the largest decrease in all three data-sets, particularly at the 15hr time point in set 1 and 3 and the 18hr time point in set 2. Again this may indicate a link to the cell cycle position. Species 18:0/18:1 (m/z 797) shows a decrease in set 1 but this is not apparent in the other data sets. This data is also similar to that of the endogenous PC (Figure 4.13), however species 16:0/18:1 showed the greatest decrease at 6hrs rather than 15/18hrs and species 16:0a/18:1 showed a more significant decrease for endogenous PC than newly synthesised. Species 16:0/16:1 (m/z 741) shows a decrease at 15hrs and 18hrs in set 1 and 3 and at 18hrs and 21hrs in set 2. The endogenous PC data, however, shows very little change relative to the non-synchronised control except a small decrease at 6hrs and 15hrs in set 1, 6hrs and 18hrs in set 2 and 15hrs in set 3.

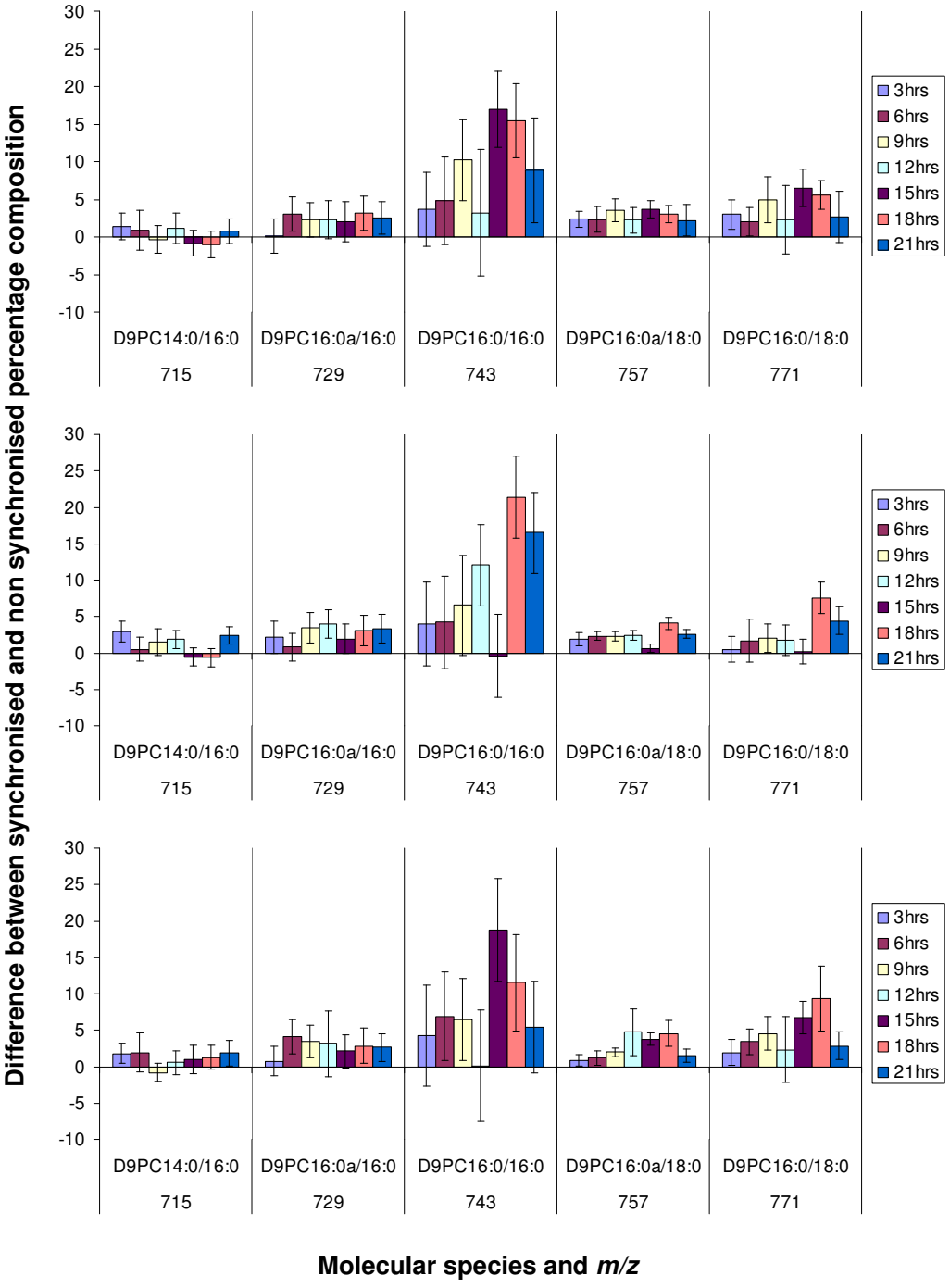

Figure 5.14: Difference between synchronised and non-synchronised percentage composition for endonuclear saturated d9PC species. Set 1 (nuclei extracted with Triton-X-100) is shown at the top followed by set 2 (nuclei extracted with maltopyranoside) and set 3 (independent repeat of nuclei extracted with maltopyranoside)

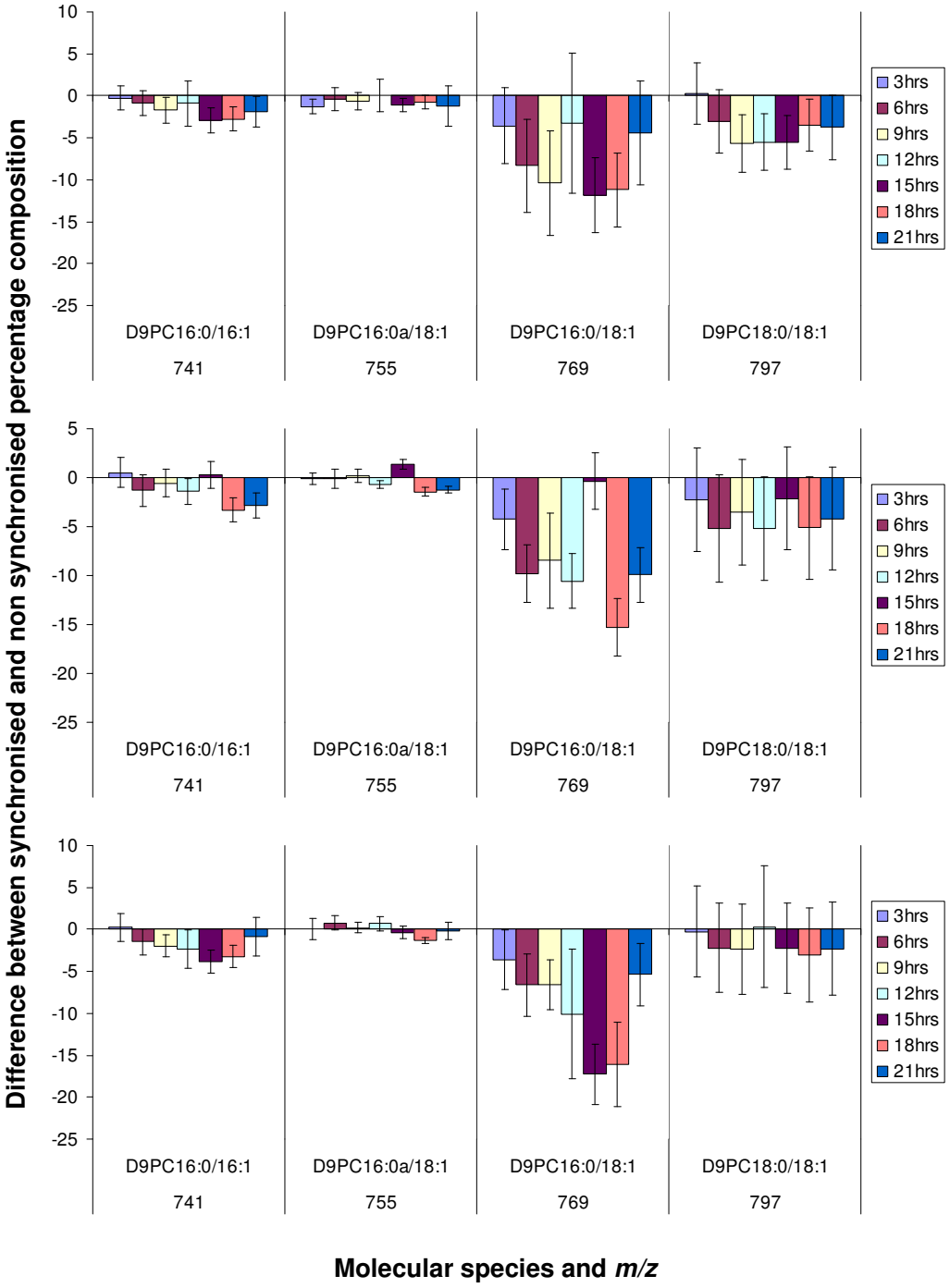

Figure 5.15: Difference between synchronised and non-synchronised percentage composition for endonuclear monounsaturated d9PC species. Set 1 (nuclei extracted with Triton-X-100) is shown at the top followed by set 2 (nuclei extracted with maltopyranoside) and set 3 (independent repeat of nuclei extracted with maltopyranoside)

The di-monounsaturated and highly unsaturated species (Figure 5.16) show very little change relative to the asynchronous control except for species 18:1/18:1 (m/z

795) which shows a significant decrease in all three data sets. Species 18:1/18:2a (m/z 722) shows a significant increase relative to the asynchronous control at the 6hr time point in set 2. Although the equivalent endogenous species does not appear in the analysis presented in Figure 4.14, species 18:1/24:5a (m/z 848) is also significantly increased relative to the asynchronous control at the 6hr time point in both set 1 and 2. This may indicate a link between highly unsaturated species and the start of the S-phase of the cell cycle (Figure 3.10). As this increase is not found in all data-sets the possibility that this is an artefact should also be noted. As described for whole cells in section 5.2, there does not appear to be an obvious correlation between the changes in DAG relative to the asynchronous control (Figure 4.25) and the changes in newly synthesised PC. The newly synthesised PC molecular species which show the greatest change, in all three data sets, are 16:0/16:0 (m/z 743) and 16:0/18:1 (m/z 848). As noted for whole cells, these are the most abundant endonuclear newly synthesised PC molecular species (Figures 5.11 to 5.13).

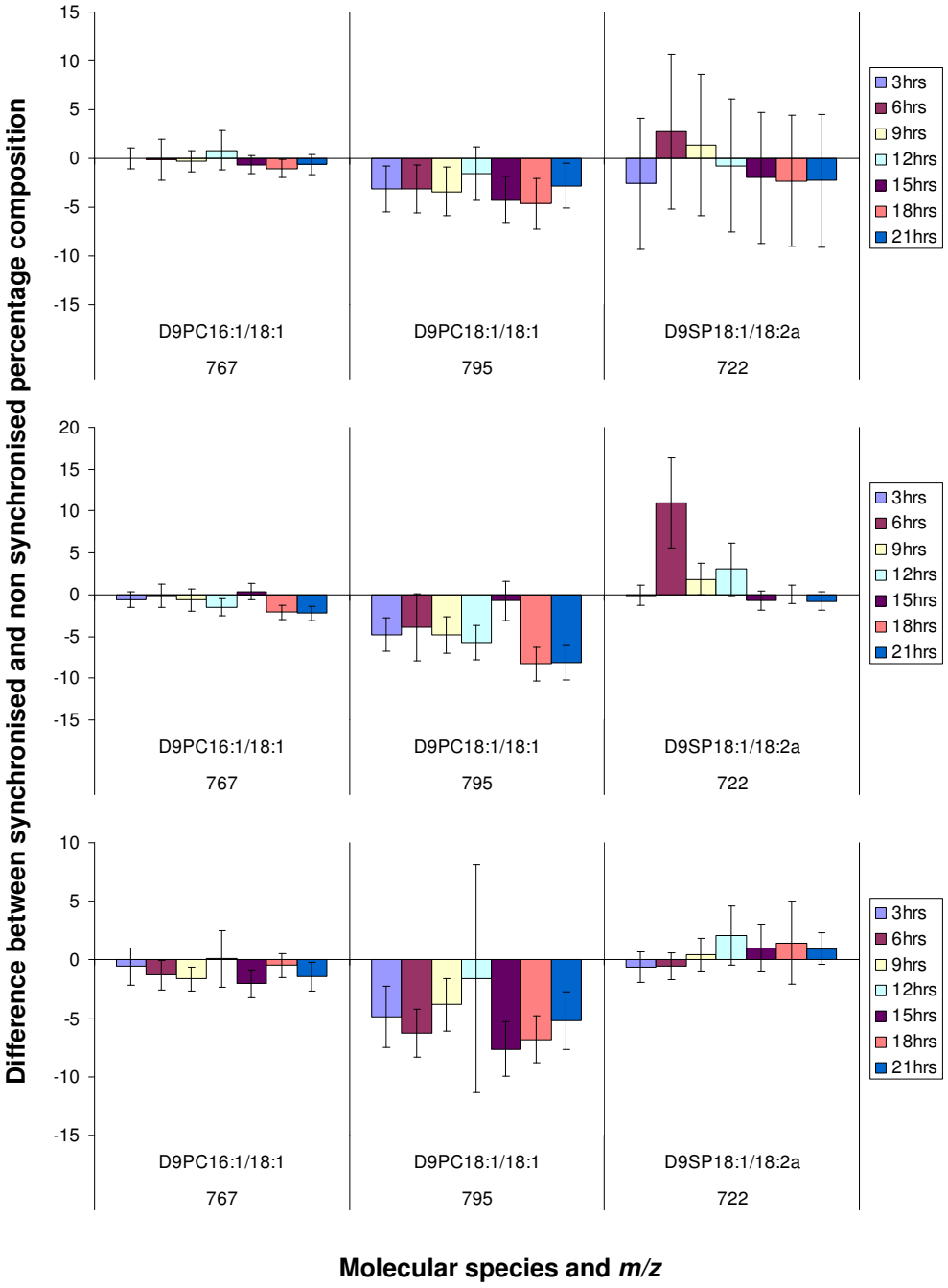

Figure 5.16: Difference between synchronised and non-synchronised percentage composition for unsaturated endonuclear d9PC species. Set 1 (nuclei extracted with Triton-X-100) is shown at the top followed by set 2 (nuclei extracted with maltopyranoside) and set 3 (independent repeat of nuclei extracted with maltopyranoside)

Figure 5.17 shows the amount of newly synthesised PC per nucleus over the cell cycle. The data presented for each time point is an average of the results from three phospholipid samples. The error bars on this data represent the first standard de-

viation of the three measurements. Each sample was obtained from separate flasks of cells, therefore, the reported standard deviation includes biological variability in addition to systematic errors. This is quantified data and therefore also includes any error resulting from cell counting and internal standard addition.

The values obtained for each data set are quite similar except for the 15hr and 21hr time points. At these time points the nuclei extracted with maltopyranoside data set shows a value approximately three times greater than the other data sets. This does not appear to be detergent related as the repeat does not show the same trend. The newly synthesised PC is quantified from the same internal standard as the endogenous PC however the endogenous PC (Figure 4.40) does not show an equivalent result at these time points. This suggests that the result is not simply due to incorrect internal standard addition, however, it is unclear why this increase is only seen in one data set.

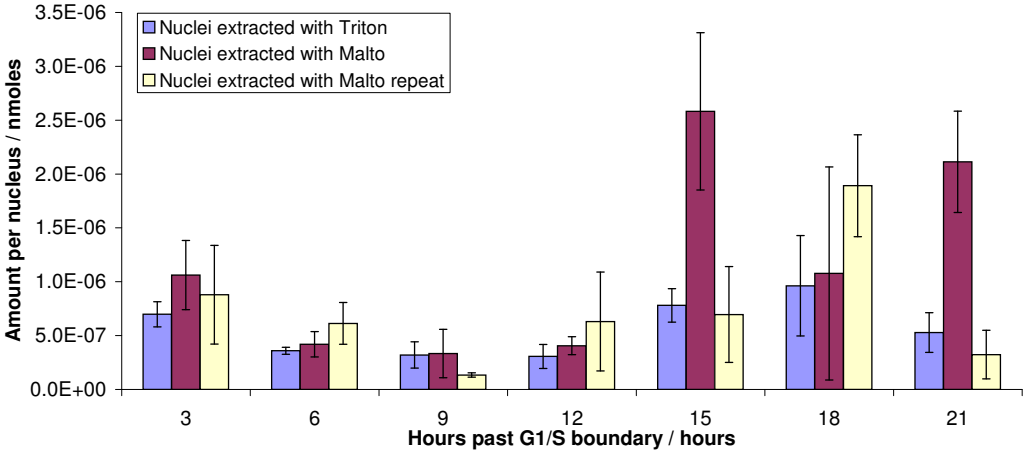

Figure 5.17: Absolute amount per cell of d9PC for synchronised nuclei. The reported standard deviation includes biological variability in addition to systematic errors. This is quantified data and therefore also includes any error resulting from cell counting and internal standard addition.

The newly synthesised PC as a percentage of the total endonuclear PC is shown in Figure 5.18. There is a considerable variation between the data sets at some time points (up to 20% at the 21hr time point), however, most of these values fall within the error of the non-synchronised results. The 18hr time point has the most consistently high percentage of newly synthesised PC although the variation

between the data sets prevents a more detailed analysis of any link between the cell cycle position and proportion of newly synthesised PC.

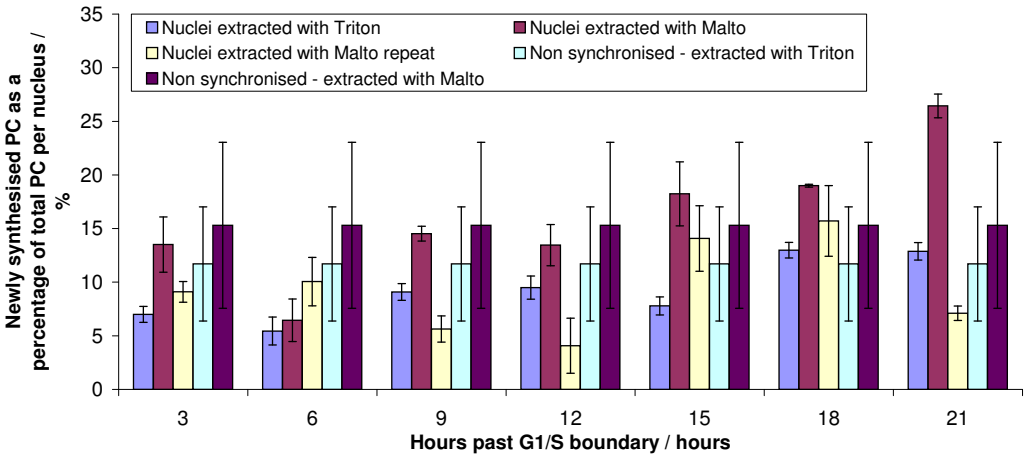

Figure 5.18: Newly synthesised PC as a percentage of the total PC per cell.

5.4 Radiochemical study of PC synthesis

Phosphatidylcholine synthesis can also be determined by monitoring the incorporation of radiolabelled choline [11, 12]. Figure 5.19 shows the amount of newly synthesised PC in synchronised whole cells following a three hour incubation with methyl-[^{14}C]choline chloride. The data presented for each time point is an average of measurements on three separate phospholipid samples. The error bars represent the first standard deviation of this data and therefore include biological variability in addition to systematic errors. This data is directly comparable to that obtained by mass spectrometry and provides an independent means of assessing trends in PC biosynthesis.

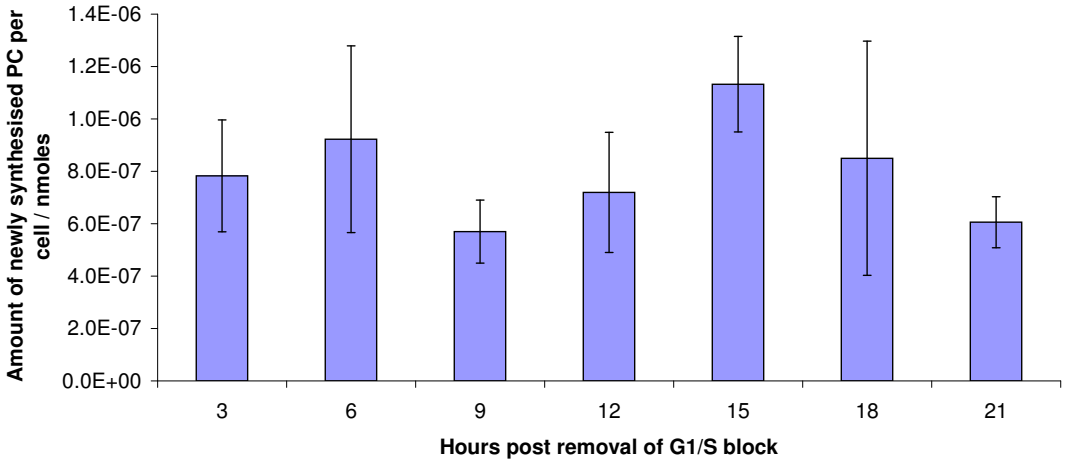

Figure 5.19: Radiochemical study of PC synthesis. This figure shows the amount of newly synthesised PC per whole cell at various cell cycle points following a three hour incubation with methyl-[^{14}C]choline chloride. The error bars represent the first standard deviation of this data and therefore include biological variability in addition to systematic errors.

The amount of newly synthesised PC per cell determined by the radiochemical method is less than that determined by mass spectrometry (Figure 5.8). There is however a very similar trend over the cell cycle between set 2 of the mass spectrometry results and the radiochemical results.

5.5 Phospholipid synthesis within naked nuclei

The results presented in section 5.3 show that the biosynthesis of endonuclear PC occurs whilst the cell remains intact. A preliminary investigation was undertaken to determine if PC biosynthesis could occur in naked nuclei. Naked nuclei were prepared as previously described (section 7.3) and incubated with excess d9-choline in D-MEM for 3 hours at 37°C.

Figure 5.20C shows that newly synthesised PC was detected by ESI-MS in naked nuclei prepared with n-Decyl β-D-Maltopyranoside. Newly synthesised PC was also detected in nuclei prepared with Triton-X-100 (Figure 5.20B) although this is difficult to observe due to detergent contamination.

Figure 5.21 shows the molecular species composition of PC synthesised in naked nuclei compared to that synthesised in nuclei whilst they remain part of the intact

cell. It also shows PC synthesised in whole cells (see also Figure 5.10). The composition of PC synthesised within naked nuclei extracted with maltopyranoside more closely resembles that of the whole cell than the nucleus and does not show the enrichment of saturated species as described in section 5.3.

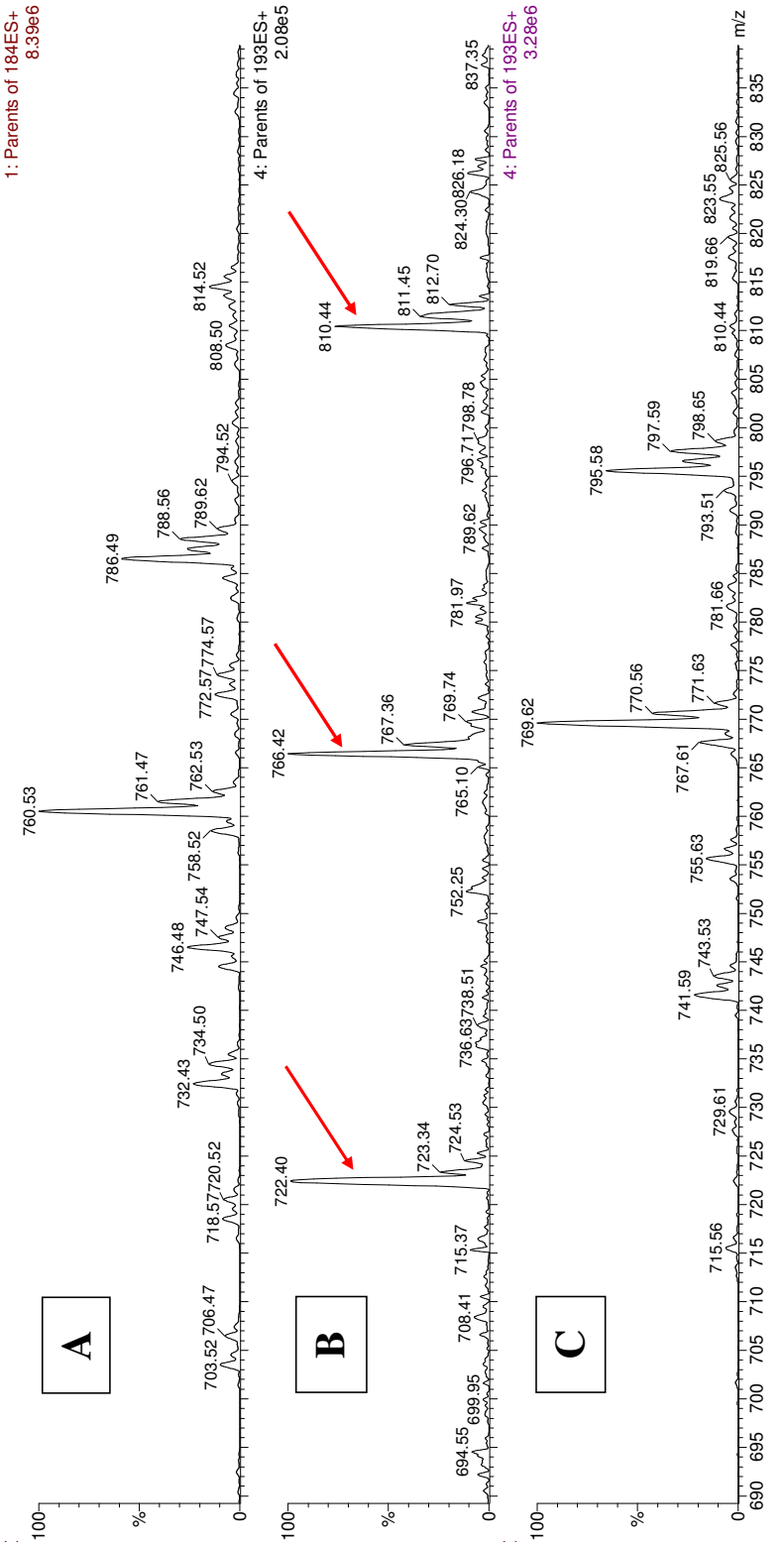

Figure 5.20: Synthesis of PC was detected in naked nuclei after isolation from the intact cell. **A;** Typical P184 spectrum of naked nuclei. **B;** Example P193 spectrum (newly synthesised PC) from nuclei extracted with Triton X-100. The peaks marked with arrows arise from detergent contamination. **C;** Example P193 spectrum from nuclei extracted with n-Decyl β-D-Maltopyranoside

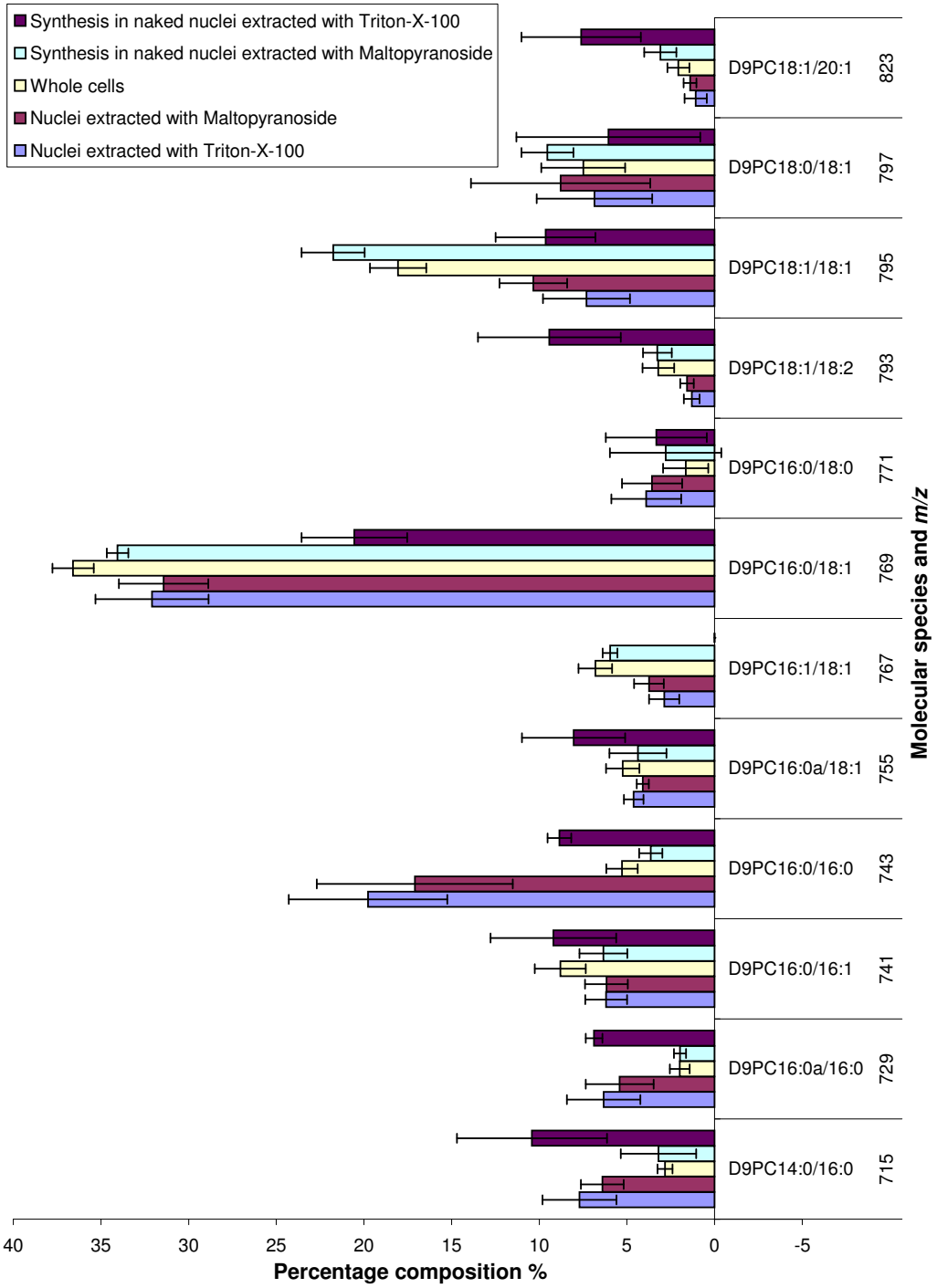

Figure 5.21: Molecular species composition of PC synthesised in naked nuclei compared to the composition of endonuclear PC synthesised whilst the cell remains intact and the composition of newly synthesised PC in whole cells.

The total amount of newly synthesised PC per cell is shown in Figure 5.22 and summarised in Table 5.3. The phospholipid composition from three separate flasks of cells was measured. The error bars represent the first standard deviation of this data and therefore include biological variability in addition to systematic errors. The amount of newly synthesised PC is less for nuclei extracted with Triton-X-100 than with maltopyranoside. This is most likely due to contamination of the extracted phospholipid by Triton-X-100 which is easily detected by ESI-MS (Figure 5.20B). The peak at m/z 767 for example is completely masked by a detergent peak.

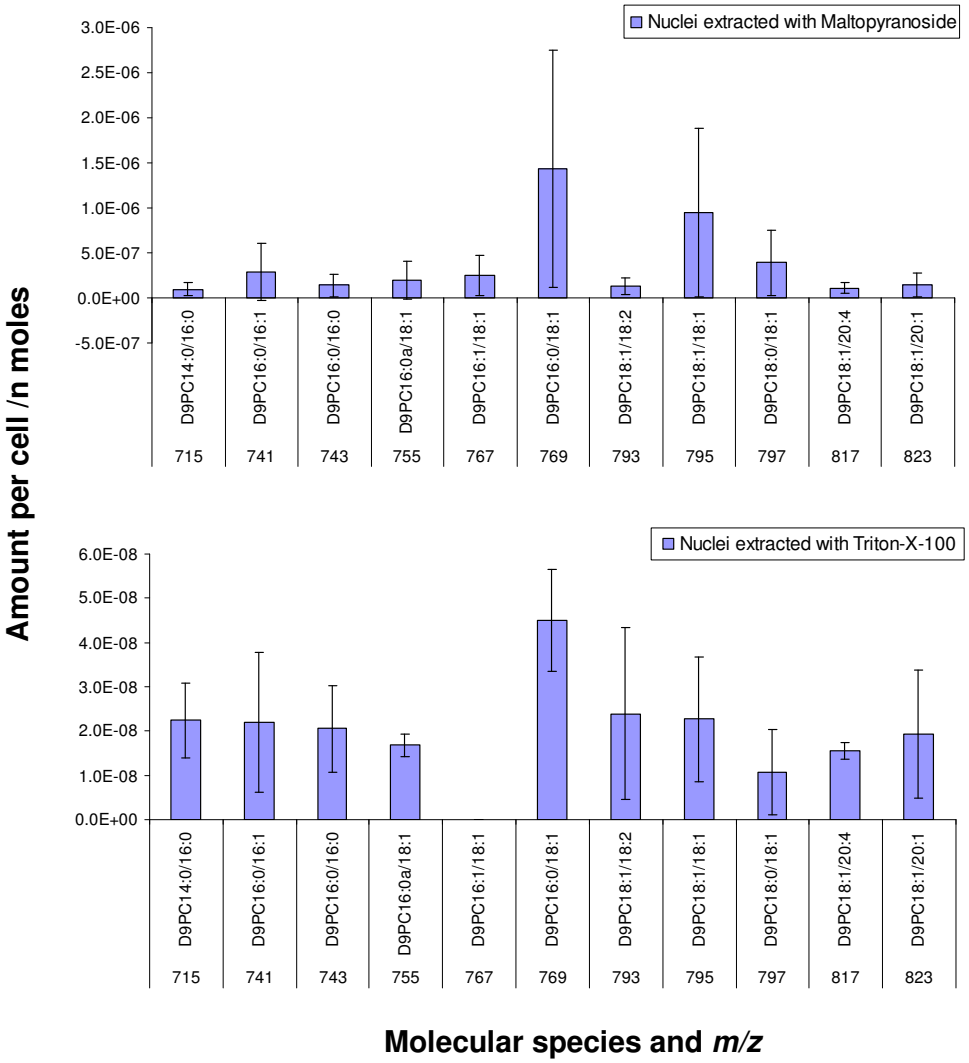

Figure 5.22: Total amount of newly synthesised PC per naked nucleus. Data is shown for nuclei extracted with both Triton-X-100 and n-Decyl β-D-Maltopyranoside. The error bars represent the first standard deviation of this data and include biological variability in addition to systematic errors.

The newly synthesised PC as a percentage of the total PC per nucleus is also shown in Table 5.3. This is less than in intact cells (Table 5.2) however this probably reflects a loss of molecules such as ATP which would normally be present in intact cells. It is possible that addition of molecules such as ATP to the naked nuclei may result in greater synthesis.

Total amount of PC per nucleus /nmoles				
Detergent used for nuclei extraction	**Type of PC**	**Average**	**Standard deviation**	**Coefficient of Variation (%)**
Maltopyranoside	Endogenous	8.2×10^{-5}	2.8×10^{-5}	34.3
	Newly synthesised	4.1×10^{-6}	3.8×10^{-6}	91.9
	Total	3.4×10^{-4}	4.6×10^{-5}	13.2
Triton-X-100	Endogenous	1.4×10^{-5}	5.5×10^{-6}	39.7
	Newly synthesised	2.2×10^{-7}	7.9×10^{-8}	36.3
	Total	4.2×10^{-5}	8.3×10^{-6}	19.5
Newly synthesised PC as percentage of total PC				
Maltopyranoside nuclei		1.2		
Triton-X-100 nuclei		0.5		

Table 5.3: Total amount of endogenous and newly syntheised PC in naked nuclei. The newly synthesised PC as a percentage of the total PC is also shown.

These results strongly indicate that naked nuclei are indeed capable of PC biosynthesis. It is however widely accepted that the catalytic activity of CCTα is mediated by membrane interaction [13, 14, 15, 16]. Naked nuclei have been shown to be free of nuclear envelope (NE) and endoplasmic reticulum (ER) contamination (section 2.2.1 and a study on IMR-32 nuclei by Hunt *et al* [2]). These results therfore indicate that the NE is not required for endonuclear CCTα activity.

It has been suggested that nuclei contain tubular membrane bound invaginations, termed neoplasmic reticulum, which may provide a site for endonuclear PC biosynthesis [17, 18, 19, 20]. The presence of membranous structures within naked nuclei, however, has not yet been demonstrated [2, 21]. Endonuclear phospholipid may form aggregate structures (such as liquid crystal phases) which are able to interact with CCTα and mediate its activity.

These preliminary findings raise many interesting questions; What is the endonuclear phospholipid structure which could mediate CCTα activity? Could the pres-

ence of detergent from the extraction procedure effect CCTα activity and therefore the rate of PC biosynthesis? Are there any substances present in intact cells which would improve synthesis in naked nuclei? Are naked nuclei also capable of synthesising other phospholipid species? What is the effect of cell cycle phase?

5.6 Summary

This chapter describes the use of ESI-MS to analyse newly synthesised PC in whole cells (section 5.2) and nuclei (section 5.3). The molecular species composition of newly synthesised PC in whole cells was found to be very similar to that of endogenous whole cell PC. As also described for endogenous PC, the molecular species composition was also similar to that of DAG. It was suggested that the involvement of DAG in the synthesis of PC via the Kennedy pathway may explain such a similarity. Whole cell newly synthesised PC was found to account for approximately 5.7% of the total PC per cell.

Unlike endogenous PC, the saturated molecular species of newly synthesised PC in synchronised whole cells showed very little change relative to the non-synchronised control. The monounsaturated molecular species 16:0/18:1 was decreased at most time points. The other monounsaturated species, however, showed little consistent change. This similarity to the non-synchronised data was also found for dimonounsaturated and highly unsaturated molecular species. Several differences between the endogenous and newly synthesised PC results were noted. As mentioned earlier DAG is involved in the synthesis of PC, however, no correlation between the changes, relative to the non synchronised control, were found between DAG and the newly synthesised PC. As described for endogenous PC, the species which showed the greatest change is also the most abundant molecular species in the cell.

The amount of newly synthesised PC per whole cell was found to remain very stable at all time points except 3hrs. Set 2, however, showed the largest amount of newly synthesised PC at 18hrs. The pattern of these results over the time points closely resembled that of the endogenous PC. Newly synthesised PC as a percentage of the total PC per cell was generally found to be very similar to the non-synchronised value in both data sets. The 3hr and 15hr time points of set 1 and

the 18hr time point of set 2 show the greatest difference to the non synchronised value. It was suggested that this may agree with a previous study that showed an increase in PC synthesis associated with the M and early G1 phase of the cell cycle.

As found for endogenous PC, the proportion of saturated molecular species is higher in newly synthesised endonuclear PC than in newly synthesised whole cell PC. Disaturated molecular species were found to total 37.7% in nuclei extracted with Triton-X-100 and and 32.5% in nuclei extracted with maltopyranoside. This contrasts with only 11.7% in the whole cell. The composition of newly synthesised PC in the nucleus was very similar to that of the endogenous PC for nuclei extracted with both detergents. Newly synthesised PC as a percentage of the total PC per nucleus was approximatly 15% for nuclei extracted with maltopyranoside and 12% for nuclei extracted with Triton-X-100. These results suggest that the type of detergent does not influence the rate of PC synthesis or the composition of newly synthesised PC.

The saturated molecular species of newly synthesised endonuclear PC show either no change or an increase relative to the non-synchronised control. The monounsaturated species generally show a decrease or no change relative to the non-synchronised control. The di-monounsaturated and highly unsaturated species show very little change relative to the non-synchronised control, except species 18:1/18:1 which shows a significant decrease in all three data sets. Unlike whole cells, the results for newly synthesised endonuclear PC are very similar to that of endogenous PC. As found for whole cells, there was no obvious correlation between the changes in DAG, relative to the non-synchronised control, and the changes in newly synthesised PC. The molecular species that showed the greatest change were again those that were most abundant.

The total amount of newly synthesised PC per nucleus is quite similar for each data set except at the 15hr and 21hr time points. At these time points, the maltopyranoside extracted nuclei data is approximately three times larger than the other time points. The value of newly synthesised PC as a percentage of the total endonuclear PC varies between the data sets at some time points. Most of the values, however, fall within the standard deviation of the non-synchronised result.

Section 5.4 describes the use of radiolabelled choline to monitor the synthesis of PC. The amount of newly synthesised PC per cell was found to be less than that determined by mass spectrometry. The trend over the cell cycle was, however, similar to data set 2 of the whole cell mass spectrometry results.

Section 5.5 describes the results of a preliminary experiment to determine if PC biosynthesis can occur in naked nuclei. Newly synthesised PC was detected by ESI-MS in nuclei extracted with both maltopyranoside and Triton-X-100. The composition of PC synthesised in naked nuclei extracted with maltopyranoside more closely resembles that of the whole cell than the nucleus and does not show an enrichment of saturated molecular species. The newly synthesised PC as a percentage of the total PC per nucleus was 1.2% for nuclei extracted with maltopyranoside and 0.5% for nuclei extracted with Triton-X-100. This is less than in the nuclei of intact cells and it was suggested that loss of molecules such as ATP may cause this decrease in synthesis.

References

[1] E. Albi and M.P. Viola Magni. The role of intranuclear lipids. *Biology of the Cell*, 96:657–667, 2004.

[2] A. Hunt, G. T. Clark, G. S. Attard, and A. D. Postle. Highly saturated endonuclear phosphatidylcholine is synthesized in situ and colocated with CDP-choline pathway enzymes. *The Journal of Biological Chemistry*, 276(11):8492–8499, 2001.

[3] C.S D'Santos, J.H. Clarke, and N. Divecha. Phospholipid signalling in the nucleus. *Biochemica et Biophysica Acta*, 1436:201–232, 1998.

[4] A. Hunt. Completing the cycles; the dynamics of endonuclear lipidomics. *BBA*, 1761:577–587, 2006.

[5] A. Hunt. *Nuclear Matrix phosphatidylcholine biosynthesis: Why is it essential, why is there so much and why is it so saturated?*, pages 47–61. Research Signpost, 2003.

[6] S. Henry and L. Hodge. Evidence for a unique profile of phosphatidylcholine synthesis in late mitotic cells. *The Journal of Cell Biology*, 97:166–172, 1983.

[7] C. Kent. CTP:phosphocholine cytidyltransferase. *Biochemica et Biophysica Acta*, 1348:79–90, 1997.

[8] S. Jackowski and P. Fagone. CTP:phosphocholine cytidyltransferase: Paving the way from gene to membrane. *The Journal of Biological Chemistry*, 280(2):853–856, 2005.

[9] C. DeLong, L. Qin, and Z. Cui. Nuclear localization of enzymatically active green fluorescent Protein-CTP:phosphocholine cytidyltransferase α fu-

sion protein is independent of cell cycle conditions and cell types. *The Journal of Biological Chemistry*, 275(41):32325–32330, 2000.

[10] L. Pegoraro, N. Galanti, G. Stein, and R. Baserga. The synthesis of phospholipids in the nucleus and nuclear membrane of synchronized HeLa cells. *Cell Tissue Kinetics*, 5:65–77, 1972.

[11] P. Caesar, S. Wilson, C. Normand, and A. D. Postle. A comparison of the specificity of phosphatidylcholine synthesis by Human fetal lung maintained in either organ or organotypic culture. *Biochemical Journal*, 253(2):451–457, 1988.

[12] P. Antony, J. N. Kanfer, and L. Freysz. Phosphatidylcholine metabolism in nuclei of phorbol ester-activated LA-N-1 Neuroblastoma cells. *Neurochemical Research*, 25:1073–1082, 2000.

[13] G. Attard, R. Templer, W. Smith, A. Hunt, and S. Jackowski. Modulation of CTP:phosphocholine cytidyltransferase by membrane curvature elastic stress. *PNAS*, 97(16):39032–9036, 2000.

[14] R. Cornell and I. Northwood. Regulation of CTP:phosphocholine cytifyltransferase by amphitropism and relocalization. *TIBS*, 25:441–447, 2000.

[15] A. Lykidis, P. Jackson, and S. Jackowski. Lipid activation of CTP:phosphocholine cytifyltransferase: Characterization and identification of a second activation domain. *Biochemistry*, 40(2):494–503, 2001.

[16] S. Taneva, M. Dennis, Z. Ding, J. Smith, and R. Cornell. Contribution of each membrane binding domain of the CTP:phosphocholine cytifyltransferase-α dimer to its activation, membrane binding and membrane cross-bridging. *The Journal of Biological Chemistry*, 283(42):28137–28148, 2008.

[17] M. Fricker, M. Hollinshead, N. White, and D. Vaux. Interphase nuclei of many mammalian cell types contain deep, dynamic, tubular membrane-bound invaginations of the nuclear envelope. *The Journal of Cell Biology*, 136(3):531–544, 1997.

[18] W. Echevarria, M. Leite, M. Guerra, W. Zipfel, and M. Nathanson. Regulation of calcium signals in the nucleus by a nucleoplasmic reticulum. *Nature Cell Biology*, 5:440–446, 2003.

[19] T. Lagace and N. Ridgway. The rate-limiting enzyme in phosphatidylcholine synthesis regulates proliferation of the nucleoplasmic reticulum. *Molecular Biology of the Cell*, 16:1120–1130, 2005.

[20] K. Gehrig, R. Cornell, and N. Ridgway. Expansion of the nucleoplasmic reticulum requires the coordinated activity of lamins and CTP:Phosphocholine Cytidyltransferase α. *Molecular Biology of the Cell*, 19:237–247, 2008.

[21] J. D. Lewis and D. Tollervey. Like attracts like: Getting RNA processing together in the nucleus. *Science*, 288:1385–1389, 2000.

Chapter 6

Conclusions

6.1 Introduction

As described in section 1.1, the main aim of the neonuclei project was to produce synthetic analogues of cell nuclei. To guide the preparation of these neonuclei it was important to study and understand the components and processes of real nuclei. Previous studies (see sction 1.2.1) indicated that nuclei from Human cells contain a pool of endonuclear phospholipid, distinct from the nuclear membrane, which is potentially involved in nuclear processes such as transcription [1, 2, 3]. The aim of this study was to elucidate the composition and role of this endonuclear phospholipid in eukaryotic cells. Tandem electrospray mass spectrometry was utilised to determine the phospholipid content of cultured HeLa cells and their isolated nuclei throughout the cell division cycle.

Section 6.2 gives a brief summary of the work undertaken and the main findings that are detailed in each chapter of this thesis. This is followed in section 6.3 by a discussion of the significant findings which were observed for both whole cells and nuclei and the conclusions that can be drawn from these. Finally, the future perspectives for this work are presented in section 6.4.

6.2 Summary of findings

6.2.1 Method development

Throughout this investigation several biological and instrumental protocols were developed and optimised to best address the requirements of this study.

Analysis of endonuclear phospholipids requires the preparation of nuclei that are free from nuclear envelope contamination. The detergent Triton-X-100 successfully removes nuclear envelope but residual detergent contamination of the nuclei can lead to artefactual peaks in the P193 spectrum. Alternative detergents to Triton-X-100 were therefore investigated. The non-ionic detergent n-Decyl β-D-Maltopyranoside was found to be a suitable alternative to Triton-X-100 as it allowed isolation of naked nuclei without causing detergent peaks when analysed by mass spectrometry. TEM was used to confirm that n-Decyl β-D-Maltopyranoside effectively removed the nuclear enverlope.

Phospholipid quantification by mass spectrometry requires an accurate estimate of the number of cells per sample. Haemocytometer counting is a simple and quick method for such analysis. Naked nuclei, however, can occasionally become clumped, making an accurate assessment of their number challenging by this method. An alternative method based on using DNA content as an indicator of cell number was therefore investigated. The preliminarly results did not show any significant improvement over the haemocytometer method. It is possible that further development of the procedure may lead to a viable alternative although this was beyond the scope of this study.

Using a carefully prepared mixture of phospholipids at known concentrations, termed the standard mixture, the correction procedures applied to raw mass spectrometry data and instrument stability were assessed. It was determined that intersession variability of mass spectrometry results can occur even when identical samples are measured (standard mixture). This variability tends to be larger for results obtained over longer time periods.

Several molecular species of a particular phospholipid class can have the same mass. Q-TOF mass spectrometry was therfore used to determine the correct molec-

ular species assignments for each phospholipid class.

6.2.2 Phospholipid composition of intact HeLa cells

The phospholipid composition of intact HeLa cells was determined to provide a basis for comparison with the endonuclear phospholipid composition.

Asynchronous populations were found to contain a total phospholipid content of $1.17\times10^{-4}\pm7.72\times10^{-5}$ nmoles per cell. The largest proportion of this phospholipid was found to be PC and PE at 44% and 29% of the total respectively. PC, DAG and PA/PG were found to be composed mainly of monounsaturated molecular species. PE, PI and PS were composed of both monounsaturated and polyunsaturated molecular species.

The relationship between cell cycle phase and phospholipid content was also investigated. HeLa cell populations were treated with mimosine to give a cell population with a higher degree of cell cycle synchronicity than an untreated population. Flow cytometry was used to assess the DNA replication cycle of these synchronised cell populations. The application of mimosine resulted in cell cycle arrest prior to DNA replication. On release of the cell cycle block, the synchronised HeLa cell population was enriched by over 20% in the G1 phase relative to the asynchronous population. The HeLa cell cycle was estimated to last for approximately 21 hours.

Using ESI-MS the phospholipid composition of synchronised HeLa cell populations was determined at three hour intervals following release of the mimosine cell cycle block. The data from asynchronous cell populations was used as a control to allow direct comparison of different data sets and a detailed analysis of the compositional variation between time points.

- Saturated and monounsaturated PC molecular species showed either no change or an increase relative to the non-synchronised data.
- Di-monounsaturated PC molecular species showed a reduction relative to the non-synchronised data.
- Highly unsaturated PC molecular species, PE molecular species and PI molecular species remained very similar, within error, to the non-synchronised

results.

- DAG molecular species containing an alkyl link were increased relative to the non-synchronised control.
- PS molecular species did not show a consistent trend across the data sets.

The total amount of each phospholipid class per cell was also determined at three hour intervals following release of the mimosine cell cycle block. The proportion of PC in synchronised cells was similar to that of non-synchronised cells in set 1 but up to 30% greater in set 2. The proportions of DAG and PI were also higher but only in data set 2. The proportion of PA/PG was the same as the value for non synchronised cells in set 2 but more than twice this value in set 1. The proportion of PE was, however, more than 10% less in synchronised cells than asynchronous cells in both data sets. The total amount of phospholipid per cell did not double as would be expected for the formation of two daughter cells, instead remaining stable across the time points in set 1 and following a wave like pattern in set 2.

6.2.3 Endonuclear phospholipid composition

The endonuclear phospholipid content of HeLa cells was determined by ESI-MS following isolation of the naked nuclei.

The molecular species composition was found to be the same, within error, for nuclei extracted both with Triton-X-100 and maltopyranoside. Endonuclear PC, DAG and PI was found to be enriched in saturated molecular species with respect to the whole cell composition. Disaturated PC molecular species total 34.4% in nuclei extracted with Triton-X-100 and 22% in nuclei extracted with maltopyranoside. Such species total only 12.3% in the whole cell. The total amount of endonuclear phospholipid was found be 12% of that in the whole cell for nuclei extracted with maltopyranoside and 14% of that in the whole cell for nuclei extracted with Triton-X-100. The proportion of each phospholipid class within the nucleus was the same as within the whole cell.

As found for whole cells, the molecular species composition of endonuclear phospholipid was found to differ between nuclei from asynchronous populations and nuclei from synchronised populations.

- Saturated PC molecular species showed an increase relative to the non-synchronised control. The magnitude of these changes was up to 25% compared to only 1.5% in whole cells.
- Monounsaturated PC molecular species showed either no change or a decrease relative to the non-synchronised control which contrasts with the whole cell results.
- Di-monounsaturated PC molecular species showed either no change or a decrease relative to the non-synchronised control.
- Saturated and highly unsaturated PE molecular species, PI molecular species and PA molecular species showed little consistent change relative to the non-synchronised control.
- Monounsaturated and di-monounsaturated PE molecular species showed no change or a decrease which contrasts with the whole cell results.
- Data sets 1 and 2 show an increase in most saturated DAG species and a decrease in unsaturated DAG species relative to the non-synchronised control.
- Set 3 only shows an increase in DAG species containing an alkyl link and either no change or a decrease in the remaining species. This is similar to the whole cell data.
- Most PS molecular species show little change relative to the non-synchronised control. Species 18:0/18:1, however was decreased in all three data sets.

The total amount of phospholipid per nucleus, as found for whole cells, showed no doubling as would be expected prior to mitosis. The proportion of DAG per nucleus was higher in nuclei from synchronised cell populations than in nuclei from asynchronous cell populations.

6.2.4 Phosphatidylcholine biosynthetic dynamics

Using a combination of stable isotope labeling and ESI-MS, the synthesis of PC in whole cells and nuclei was determined.

Whole cell newly synthesised PC was found to account for approximately 5.7% of the total PC per cell after a three hour incubation with d9-choline. The molecular species composition of this newly synthesised PC was found to be similar to that of endogenous whole cell PC.

Unlike endogenous PC, most newly synthesised PC molecular species in synchronised whole cells showed little consistent change relative to the non-synchronised control. As a percentage of the total PC per cell, newly synthesised PC in synchronised cells was very similar to that of non-synchronised cells.

As found for endogenous PC, the proportion of saturated molecular species in endonuclear newly synthesised PC is higher than in whole cell newly synthesised PC. Disaturated molecular species were found to total 37.7% in nuclei extracted with Triton-X-100 and and 32.5% in nuclei extracted with maltopyranoside. This contrasts with only 11.7% in the whole cell.
Newly synthesised PC as a percentage of the total PC per nucleus was approximately 15% for nuclei extracted with maltopyranoside and 12% for nuclei extracted with Triton-X-100. The saturated molecular species of newly synthesised endonuclear PC show either no change or an increase relative to the non-synchronised control. The monounsaturated species generally show a decrease or no change relative to the non-synchronised control. The di-monounsaturated and highly unsaturated species show very little change relative to the non synchronised control, except species 18:1/18:1 which shows a significant decrease in all three data sets. The value of newly synthesised PC as a percentage of the total endonuclear PC falls within the standard deviation of the non-synchronised result.

Biosynthesis of PC was found to continue in nuclei which had been removed from the cell and stripped of their nuclear envelope. The molecular species composition of this newly synthesised PC in nuclei extracted with maltopyranoside more closely resembled that of the whole cell than endonuclear newly synthesised PC (endonuclear synthesis whilst the cell is intact). The newly synthesised PC as a percentage of the total PC was 1.2% for nuclei extracted with maltopyranoside and 0.5% for nuclei extracted with Triton-X-100. This is less than in nuclei of intact cells but loss of molecules such as ATP may account for this.

6.3 Key findings and conclusions

6.3.1 Endonuclear and whole cell phospholipid composition

The detergent n-Decyl β-D-Maltopyranoside was found to be a suitable alternative to Triton-X-100 as it allowed isolation of naked nuclei without causing artefactual detergent peaks in mass spectrometry analysis. Throughout this study, no significant difference was observed between results from nuclei extracted with each detergent. This indicates that the endonuclear phospholipid composition determined by ESI-MS is not an artefact of the detergent used to strip the nuclear envelope.

Endonuclear PC was found to be enriched in disaturated molecular species with respect to whole cell PC. In contrast, diunsaturated PC molecular species were found in a higher proportion in the whole cell than the nucleus. The finding that endonuclear PC is enriched in saturated molecular species agrees with previous study of IMR-32 cells [3] and gives further evidence that this is a generalised phenomenon across a variety of Human cell lines [4]. An increase in disaturated molecular species was also observed for DAG and PI. DAG and PI are known to be involved in cell signalling [5, 6, 7], indicating that this increase in saturated molecular species may play a role in endonuclear phospholipid signalling.

6.3.2 Effects of synchronisation

The molecular species composition of both whole cells and nuclei from cell populations that have been treated with mimosine differs to those which have not. These differences were particularly apparent for PC and DAG molecular species and appeared to be related to the saturation level of the molecular species. There were indications of similar, saturation dependent, changes in other phospholipid classes. These were not always consistent in all data sets, however, probably due to the larger error on these results. DAG molecular species with an alkyl link showed an increase relative to the non-synchronised control in whole cells and one set of the endonuclear data.

As discussed in section 3.3.2 it possible that these changes are an artefact of

treatment with mimosine. Mimosine can cause cellular changes that correlate with the apoptotic process [8, 9]. A study of the neuronal cell line HN2-5 found an increase in saturated fatty acid containing phospholipids associated with apoptosis. This increase in saturated species was attributed to the changes in membrane morphology such as shrinkage and fluidity that occur during apoptosis [10, 11]. It was also found that redistribution of arachidonate containing molecular species could lead to cellular changes associated with apoptosis [12]. In whole cells (section 3.3.2) the arachidonate containing species PE16:0/20:4 and PE20:4/22:5 are visible in the synchronised data but not in the non-synchronised data.

Certain molecular species show a greater change, relative to the non synchronised control, than other species of the same saturation level. These molecular species tend to also be those which are most abundant in the cell. It seems plausible that these species are preferentially remodelled due to their high abundance.
It was observed that the increase in certain DAG molecular species may correlate with the decrease in other DAG molecular species. This would suggest that the molecular species that are decreased, relative to the control, are remodelled into the species that increase, relative to the control. There is, however, an increase in species containing the 16:0a fatty acid but no decrease in species containing this. There is also no obvious correlation between the molecular species that show an increase and those that decrease for other phospholipid classes. This indicates that several remodelling mechanisms may be involved in this process.

A distinction between the compositional changes of certain molecular species in the whole cell and nucleus was observed (section 4.3.1). It is possible that endonuclear lipid may be affected in a different way to whole cell phospholipid during apoptosis. Previous studies indicated that endonuclear phospholipids may interact with DNA and be involved with DNA synthesis [13, 14]. Mimosine may interfere with this lipid-DNA interaction and thus lead to alterations in endonuclear phospholipid composition that are different to the whole cell.

Several differences were noted between the compositional changes of newly synthesised PC and endogenous PC in the whole cell (section 5.2). For example, all endogenous PC di-monounsaturated species were reduced, relative to the non-synchronised control, but little change was observed for newly synthesised PC

molecular species. The results for newly synthesised and endogenous PC, however, were very similar in the nucleus. It is possible that the effects of mimosine are longer lasting in the nucleus than the whole cell.

It has been shown that the biophysical characteristics of a membrane, its curvature elastic stress, could regulate CTP:phosphocholine cytidyltransferase and thus PC synthesis [15]. This curvature elastic stress is determined by the phospholipid composition of that membrane. It is possible that changes in molecular species composition following synchronisation might alter the value of curvature elastic stress and thus alter PC synthesis. Newly synthesised PC as a percentage of the total PC was not, however, significantly different in synchronised cells than non-synchronised cells.

There were some indications that the position of the cell in the cell cycle, following release from the cell cycle block, may influence the magnitude of changes relative to the non-synchronised control. In section 4.3.1 for instance, the 18 hour time point of species PC16:0/16:0 consistently shows the greatest increase over all three data sets. Apoptosis has been linked to the cell cycle, with certain cell cycle regulators influencing both proliferation and cell death [16, 17]. If addition of mimosine is causing an apopotopic response this may provide an explanation for these results.

In both whole cells and nuclei the total phospholipid content was not found to double, as would be expected prior to mitosis, at any time point after release of the cell cycle block. As discussed in section 3.3.3 this may be because phospholipids are not fully synchronised with DNA following treatment with the cell cycle block [18, 19, 20, 21]. The cell population is not 100% synchronised following treatment with mimosine (section 3.3.1). A proportion of the cell population may therfore be halving their mass whilst others are doubling leading to only a small net increase in the total phospholipid.

6.3.3 Variation between data sets

The molecular species composition and amount per cell of each phospholipid class was often found to vary between independent data sets. Curvature elastic stress, or torque tension, of a membrane is likely to be under homeostatic control as it is intrinsically linked to properties such as membrane fluidity and permiability

[22]. As discussed in section 3.3.3 the variations between data sets may represent different phospholipid compositions that maintain a similar value of torque tension.

6.3.4 PC biosynthesis

Biosynthesis of PC was found to continue in nuclei which had been removed from the cell and stripped of their nuclear envelope. This gives compelling evidence of a separate PC synthesis pathway within the nucleus. The newly synthesised PC as a percentage of the total PC was less than in the nuclei of intact cells, however, this may be due to the loss of molecules such as ATP. The composition of PC synthesised in naked nuclei extracted with maltopyranoside did not show an enrichment in saturated molecular species like PC synthesised in the nuclei of intact cells. It is possible that there is also a loss of substances such as acyl-CoA, preventing the remodelling of newly synthesised PC.

6.3.5 Summary of key findings

- Intersession variability of mass spectrometry results should be taken into account when comparing samples measured on different occasions.
- Endonuclear phospholipid composition is not an artefact of the detergent used to strip the nuclear envelope.
- Endonuclear PC, DAG and PI are enriched in saturated molecular species with respect to the whole cell.
- The molecular species composition of cells treated with mimosine differs to untreated cells. It appears that many of these differences are related to the saturation level of the species.
- Treatment with mimosine does not lead to a doubling of phopsholipid content prior to mitosis. Phopspholipids may not be synchronised with DNA following treatment with a cell block such as mimosine.
- The molecular species composition was found to vary between independent data sets. This may be due to similar values of membrane torque tension resulting from different phospholipid compositions.

- Biosynthesis of PC was found to continue in naked nuclei after removal from the cell.

6.4 Perspectives

This study has raised many interesting questions which could form the basis of further studies into this area.

6.4.1 Continuation of the current study

The work presented in this report has highlighted some important questions regarding cell cycle analysis following synchronisation using methods such as cell cycle inhibitors and serum starvation (section 3.3.3). If the synchronisation method causes changes in the molecular species compostion, it can become difficult to distinguish those changes that arise due to position in the cell cycle from those that are artefacts of the synchronisation method.
The next step in determining the effect of cell cycle position on phospholipid composition therefore relies on the assessment of suitable synchronisation techniques. Ideally the synchronisation technique should not perturb the natural cellular physiology and should produce a highly synchronous population. It is possible that a technique that relies on selecting cells from an asynchronous population based on their phase, rather than arresting the whole population in a certain phase, may offer results which better reflect real cellular events. Methods which select cells of a certain phase based on their size have been reported [23] however these could result in a small sample size and poor synchronisation.

The current study provides a comparison of the endonuclear phospholipid composition with that of the whole cell. This work could be extended by determining the composition of the nuclear envelope and comparing this to the endonuclear composition.

The molecular species composition of cell populations that have been treated with mimosine differs to those which have not. It may be possible to design a computer based approach to assess the increase or decrease of molecular species, following treatment with mimosine, and the resulting effect on predicted stored elastic

stress. This would allow further investigation into the apparent differences between certain data sets.

Preliminary results suggested that naked nuclei were capable of PC biosynthesis. The effect of adding molecules such as ATP should be investigated as these may increase the rate of synthesis. The rate of synthesis could also be assessed with respect to the cell cycle. An important extension to this work would be to determine the biosynthesis of phospholipids other than PC in both the naked nuclei and also in the endonuclear compartment whilst the cell remains intact.

Section 2.3.5 highlighted the issue of intersession reproducibility for mass spectrometry analysis [24]. As with all lipidomic studies, a large amount of data is generated, however this can lead to extremely complicated data analysis [25, 26, 27]. This work could be extended to fully explore the variability of results and design experiments that are appropriate for a detailed statistical analysis.

6.4.2 Future work

This thesis has described the composition of endonuclear phospholipids. The nucleus is not however a homogenous compartment containing a mixture of nucleic acids, proteins and lipids. Although not separated by membrane structures, the nucleus contains several distinct structures such as the nucleolus [28, 29]. Some studies using gold-conjugated phospholipases indicated that endonuclear phospholipids are mainly localised in the interchromatin spaces and the nucleolus [1, 30]. A study of the composition and biosynthetic dynamics of these differentially located endonuclear phospholipids would provide a challenging area for future research. Such a study could potentially give a more detailed insight into the roles of endonuclear phospholipid.

The current study has focused on the phospholipid content of the nucleus. The same techniques could, however, be applied to other organelles such as the mitochondria.

Some difficulties regarding the design of reproducible and accurate mass spectrometry studies were highlighted in this work. A vital area for future research is therefore the investigation of new approaches to the design and analysis of

lipidomic studies. Such studies have the potential to open up many exciting avenues of research in this field. They may also provide novel methods for the analysis of current data.

References

[1] N. M. Maraldi, G. Mazzotti, S. Capitani, R. Rizzoli, N. Zini, S. Squarzoni, and F. Manzoli. Morphological evidence of function-related localisation of phospholipids in the cell nucleus. *Advan. Enzyme Regul.*, 32:73–90, 1992.

[2] E. Albi, M. Mersel, M.L Tomassoni, and M.P. Viola Magni. Rat liver chromatin phospholipids. *Lipids*, 29(10):715–719, 1994.

[3] A. Hunt, G. T. Clark, G. S. Attard, and A. D. Postle. Highly saturated endonuclear phosphatidylcholine is synthesized in situ and colocated with CDP-choline pathway enzymes. *The Journal of Biological Chemistry*, 276(11):8492–8499, 2001.

[4] A. Hunt. *Nuclear Matrix phosphatidylcholine biosynthesis: Why is it essential, why is there so much and why is it so saturated?*, pages 47–61. Research Signpost, 2003.

[5] K. Tamiya-Koizumi. Nuclear lipid metabolism and signalling. *Journal of Biochemistry*, 132:13–22, 2002.

[6] C.S D'Santos, J.H. Clarke, and N. Divecha. Phospholipid signalling in the nucleus. *Biochemica et Biophysica Acta*, 1436:201–232, 1998.

[7] A.M.Martelli, G. Tabellini, P. Borgatti, R. Bortul, S. Capitani, and L.M. Neri. Nuclear lipids: New functions for old molecules? *Journal of Cellular Biochemistry*, 88:455–461, 2003.

[8] F. Reno, A. Tontini, S. Burattini, S. Papa, E. Falcieri, and G. Tarzia. Mimosine induces apoptosis in HL60 Human tumor cell line. *Apoptosis*, 4:469–477, 1999.

[9] A. E. Greijer and E. van der Wall. The role of hypoxia inducible factor 1 (HIF-1) in hypoxia induced apoptosis. *J. Clin. Pathol.*, 57:1009–1014, 2004.

[10] J. K. Singha, A. Dasguptab, T. Adayeva, S. A. Shahmehdia, D. Hammondc, and P. Banerjee. Apoptosis is associated with an increase in saturated fatty acid containing phospholipids in the neuronal cell line, HN2-5. *Biochimica et Biophysica Acta (BBA) - Lipids and Lipid Metabolism*, 1304:171–178, 1996.

[11] S. Franz, K. Herrmann, B. Fuhrnrohr, A. Sheriff, B. Frey, U.S. Gaipl, R.E. Voll, J.R. Kalden, H-M. Jack, and M. Herrmann. After shrinkage apoptotic cells expose internal membrane-derived epitopes on their plasma membranes. *Cell Death and Differentiation*, 14:733–742, 2007.

[12] M.E Surette, J.D Winkler, A.N Fonteh, and F.H Chilton. Relationship between arachidonate-phospholipid remodeling and apoptosis. *Biochemistry*, 35:9187–9196, 1996.

[13] E. Albi, M. Micheli, and M.P. Viola Magni. Phospholipids and nuclear RNA. *Cell Biology International*, 20(6):407–412, 1996.

[14] V.V. Kuvichkin. DNA-lipid interactions in vitro and in vivo. *Bioelectrochemistry*, 58:3–12, 2002.

[15] G. Attard, R. Templer, W. Smith, A. Hunt, and S. Jackowski. Modulation of CTP:phosphocholine cytidyltransferase by membrane curvature elastic stress. *PNAS*, 97(16):39032–9036, 2000.

[16] G. Evan, L. Brown, M. Whyte, and E. Harrington. Apoptosis and the cell cycle. *Current Opinion in Cell Biology*, 7:825–834, 1995.

[17] K. Vermeulen, Z. Berneman, and D. Van Bockstaele. Cell cycle and apoptosis. *Cell Proliferation*, 36:165–175, 2003.

[18] L. Urbani, S. Sherwood, and R. Schimke. Dissociation of nulcear and cytoplasmic cell cycle progression by drugs employed in cell synchronization. *Experimental Cell Research*, 219:159–168, 1995.

[19] S. Cooper. Rethinking synchronisation of mammalian cells for cell cycle analysis. *Cell. Mol. Life Sci*, 60:1099–1106, 2003.

[20] S. Cooper, G. Lyer, M. Taruini, and P. Bissett. Nocodazole does not synchronize cells: implications for cell-cycle control and whole-culture synchronization. *Cell Tissue Res*, 324:237–242, 2006.

[21] S. Cooper, K. Z. Chen, and S. Ravi. Thymidine block does not synchronize L1210 mouse leukemic cells: implications for cell cycle control, cell cycle analysis and whole-culture synchronization. *Cell prolif.*, 41:155–167, 2008.

[22] J. Beard, G. S. Attard, and M. J. Cheetham. Integrative feedback and robustness in a lipid biosynthetic network. *Journal of the Royal Society Interface*, 5:533–543, 2008.

[23] U. Kim, C. Shu, K. Dane, P. Daugherty, J. Wang, and H. Soh. Selection of mammalian cells based on their cell-cycle phase using dielectrophoresis. *PNAS*, 104(52):20708–20712, 2007.

[24] R. Pelikan, W. Bigbee, D. Malehorn, J. Lyons-Weiler, and M. Hauskrecht. Intersession reproducibility of mass spectrometry profiles and its effect on accuracy of multivariate classification models. *Bioinformatics*, 23:3065–3072, 2007.

[25] M.R. Wenk. The emerging field of lipidomics. *Nature Reviews*, 4:594–610, 2005.

[26] N. Navas-Iglesias, A. Carrasco-Pancorbo, and L. Cuadros-Rodriguez. From lipids analysis towards lipidomics, a new challenge for the analytical chemistry of the 21st century. part II: analytical lipidomics. *Trends in Analytical Chemistry*, 28(4):393–403, 2009.

[27] J.O. Lay Jr, S. Borgmann, R. Liyanage, and C.L. Wilkins. Problems with the "omics". *Trends in Analytical Chemistry*, 25(11):1046–1056, 2006.

[28] A. I. Lamond and W. C. Earnshaw. Structure and function in the nucleus. *Science*, 280:547–553, 1998.

[29] M. Dundr and T. Misteli. Functional architecture in the cell nucleus. *Biochem. J*, 356:297–310, 2001.

[30] N. M. Maraldi, S. Santi, N. Zini, A. Ognibene, R. Rizzoli, G. Mazzotti, R. Di Primio, R. Bareggi, V. Bertagnolo, and C. Pagliarini. Decrease in nuclear phospholipids associated with DNA replication. *Journal of Cell Science*, 104:853–859, 1993.

Chapter 7

Experimental

7.1 Cell culture

HeLa-GFP cells were obtained from Dr D. Zink (LMU Munich) [1]. Cells were cultured at 37 °C and 5% CO_2 in 50mL D-MEM (Dulbecos modified Eagles medium, Gibco) containing 4 mM L-glutamine and HEPES buffer but no pyruvate. It was supplemented with 10% foetal calf serum (Gibco, Heat inactivated South American origin) and 5% antibiotic/ antimycotic (Gibco).
A cell confluence of approximately 70% was maintained by regular splitting. To detach cells from the side of the flask, Trypsin-EDTA, 5 mL (0.25%, Gibco) was added to the flask following removal of medium, and incubated at 37 °C for 5 minutes. Further action of the trypsin was prevented by addition of 10 mL D-MEM. Cells were then removed from the resulting suspension.

7.2 Cell synchronisation

A stock solution of 200 mM L-mimosine (Sigma) in 1 M NH_4OH was prepared. For each 1 mL of medium, 1 μL of stock solution was added (final concentration 200 μM). Cells were incubated with the mimosine for 16hrs causing the population to remain near the G_1/S boundary of the cell cycle. The mimosine cell cycle block was removed by washing with PBS and supplementing with fresh medium. [1]

7.3 Isolation of naked nuclei

Extraction buffer containing 0.5% (w/v) detergent and 4 mM EDTA in HBSS (without Ca^{2+} or Mg^{2+}) was prepared. A solution of 30% sucrose in the extraction buffer was also prepared. Cells were removed from the side of the flask by tripsinisation and washed with D-PBS (Gibco, without Ca^{2+} or Mg^{2+}). The D-PBS was removed and the cells re-suspended in 500 μL of extraction buffer. This was kept on ice for 15 minutes with occasional mixing. The cells were then carefully layered over 400 μL 30% sucrose in extraction buffer. This was centrifuged at 9000g for 3 minutes. Cell debris was removed from the sucrose solution with a tissue. The supernatant was removed and the nuclear pellet (found at the bottom of the tube) washed with HBSS [2].

7.4 Preparation of samples for phospholipid analysis by Mass Spectrometry

7.4.1 Deuterated PC

An excess of deuterated phosphocholine was added to the cells to assess the rate of PC synthesis by mass spectrometry. Deuterated phosphocholine (d_9-PC, HD Isotopes) in HBSS (2 mg/mL), 500 μL, was added to the flask of cells and incubated at 37 °C for three hours.

7.4.2 Cell counting

Cells were counted on a haemocytometer by the dye exclusion method using 0.4% Trypan blue solution (Sigma) [3]. The cell pellet was suspended in 5 mL of HBSS and a 10 μL sample removed for counting. To this, 40 μL of trypan blue was added, mixed by pipetting and loaded onto the haemocytometer. The number of cells in the original sample was estimated using the following formula:

(number of cells counted/number of squares) × dilution factor × dilution factor of volume

7.4.3 Phospholipid extraction and internal standards

Phospholipid was extracted from whole cell and nuclear samples using a chloroform/methanol extraction protocol first described by Bligh and Dyer [4]. Each sample was made up to 800 μL with saline (0.9% NaCl) and transferred to a glass centrifuge tube. A known volume of each internal standard was added (see section 7.4.4). 1 mL of chloroform was added followed by 2 mL of methanol, 1 mL of chloroform and finally 1 mL of water. After each addition the sample was vortexed. The sample was then centrifuged for 10 minutes at 1500 rpm. The lower organic layer containing the phospholipid was removed and dried under nitrogen. Samples were stored at -20 °C until analysis by mass spectrometry.

7.4.4 Internal standards

Known concentrations of non-physiological phospholipids (internal standards) were used to allow sample quantification by mass spectrometry. A known amount of each internal standard species was accurately measured from the stock (for stock solutions in chloroform, the concentration given by the manufacturer (Avanti Polar Lipids) was assumed to be correct). This was made up to a known volume with chloroform and aliquoted into several vials. The vials were dried under nitrogen and stored at - 20 °C until needed. Internal standards were made up to a known concentration with chloroform before use. The amount of internal standard added to each sample was chosen to give a peak height similar to that of the other species when measured by mass spectrometry.

7.4.5 Standard mixture preparation

A mixture of phospholipids (purchased from Avanti Polar Lipids) was prepared to give a number of identical samples for the assessment of mass spectrometry protocols. The appropriate amount of each molecular species was carefully prepared from stock (Table 7.1) to give enough for 200 identical samples each containing 10 nmoles of PC molecular species and 2 nmoles of all other molecular species (Table 2.2). This mixture was made up to 5 mL with chloroform to give a single stock from which 25 μL aliquots were transferred into 2 mL brown glass screw cap vials.

All solutions were prepared as accurately as possible using volumetric glassware and Drummond positive displacement microdispensers, taking care to minimise evaporation of chloroform. The samples were dried under nitrogen and stored in the freezer until use.

Phospholipid	Original stock	Method of preparation
PC 18:1/18:1	solution in chloroform	aliquoted from stock
PC 16:0/16:0	stock from G.Koster	made up to 1 ml in chloroform and aliqoted
PC 16:0/14:0	stock from G.Koster	made up to 1 ml in chloroform and aliqoted
PC 20:0/20:0	stock from G.Koster	made up to 1 ml in chloroform and aliqoted
DG 16:0/18:1	solution in chloroform	aliquoted from stock
DG 12:0/12:0	solution in chloroform	aliquoted from stock
PS 16:0/16:0	solution in chloroform	aliquoted from stock
PS 18:1/18:1	powder	weighed accurately to make solution in chloroform
PS 14:0/14:0	stock from G.Koster	made up to 1 ml in chloroform and aliqoted
PA 18:1/18:1	solution in chloroform	aliquoted from stock
PA 16:0/16:0	solution in chloroform	aliquoted from stock
PA 14:0/14:0	stock from G.Koster	made up to 1 ml in chloroform and aliqoted
PE 18:1/18:1	powder	weighed accurately to make solution in chloroform
PE 14:0/14:0	stock from G.Koster	made up to 1 ml in chloroform and aliqoted

Table 7.1: Standard mixture compostition and preparation. This mixture was prepared as accurately as possible to give many identical samples. All phospholipids were purchased from Avanti Polar Lipids. Some phospholipid species were obtained from G. Koster - these had been aliquoted from chloroform solution and dried down.

7.5 Internal standard quantification

Ferric chloride (27g, $FeCl_36H_2O$) and ammonium thiocyanate (30g, NH_4SCN) were made up to 1 Litre in water. Phospholipid samples were dissolved in 2 mL chloroform and 1 mL of ammonium ferrothiocyanate reagent was added. This was vortexed for 1 minute and then centrifuged at low speed. The lower layer was removed and the absorbance of this solution measured at 488 nm. A calibration curve was constructed by measuring the absorbance of known phospholipid concentrations and the absorbance of internal standard solutions compared to this [5].

7.6 Mass Spectrometry

ESI-MS of phospholipids extracted from whole cells or nuclei was performed on a Micromass Quatro Ultima triple quadrupole mass spectrometer (Micromass, Wythenshaw, UK) equipped with an electrospray ionisation interface. Samples were dissolved in butanol:methanol:water:ammonia (conc) (2:6:1.6:0.4) and introduced into the mass spectrometer by syringe pump at a flow rate of 5 μL/min. Nitrogen was used as the cone and desolvation gas and argon as the collision gas (3.5 x 10^{-3} mbar). Table 7.2 shows the scan settings used for each phospholipid species. Data was acquired and processed using MassLynx NT software. An Excel Visual Basic macro written by Dr Grielof Koster was used for the correction of ^{13}C isotope effects and subsequent analysis.

Phospholipid species	Fragment	Ionisation mode	Collision energy (eV)	Cone voltage (V)
PC	P184	positive	32	90
d9PC	P193	negative	32	90
PE	NL141	positive	28	90
PS	NL87	negative	22	80
PA	P153	negative	34	90
DAG	NL35	positive	15	50
PI	P241	negative	39	100

Table 7.2: ESI-MS settings for the analysis of phospholipid composition. Following fragmentation with argon gas, sequential scans of the appropriate fragment permit determination of each phospholipid species present. 'P' represents parent scans and 'NL' a constant neutral loss scan.

7.7 TOF mass spec

The PC, PE, acidic and neutral phospholipid fractions were separated on Bond Elute solid phase extraction columns as described in section 7.7.1. TOF-MS was performed on a Micromass Q-TOF spectrometer.

The neutral, acidic and PE sampes were dissolved in MeOH:$CHCl_3$:H_2O:NH_3(conc), 70:20:80:20 (v/v) for introduction into the mass spectrometer. The PC fraction was dissolved in MeOH:NH_3:H_2O:$CHCl_3$:CH_3COOH, 70:2:8:20:0.2 (v,v) to allow it to be run under negative ionisation. Data was aquired using Mass-Lynx software and analysed using an Excel macro designed by Dr. G. Koster.

7.7.1 Bond-elute

Bond Elute NH2 disposable solid phase extraction columns (Varian) were equilibrated with 1 mL chloroform under gravity. Dried phospholipid samples were dissolved in 1 mL of chloroform and applied to the columns. The columns were washed with chloroform (2 x 1 mL) under low pressure nitrogen. This neutral fragment was collected. The PC fraction was collected using 1 mL chloroform:methanol (60:40) under low pressure nitrogen. The PE fraction was eluted with 1 mL methanol un-

der low pressure nitrogen. The acidic fraction was collected after washing with 3 x 1 mL of methanol: water: phosphoric acid (96:4:1). The acidic fraction was dried under nitrogen and back extracted by adding 100 μl of water, 200 μl methanol and 200 μl chloroform and collecting the lower chloroform layer.

7.8 Flow cytometry

Cells were washed with 5-10 ml of PBS and resuspended in 500 μL of cold PBS containing 0.1% glucose. 5 mL of 70% ethanol (kept at -20 °C) was added and the sample left overnight at 4 °C. The cells were then spun down and washed with 10 mL of PBS. Residual PBS was removed following centrifugation. The sample was incubated at 37 °C for 30-45 minutes with 20 μL of PI solution (69 μM propidium iodide in 3.8 mM Sodium Citrate, pH 7.4) and 20μL of 10 mg/mL RNAse before analysis by FACS. Measurements were obtained with a BD FACS Aria flow cytometer using a 585/42 nm bandpass filter for peak emission. Data collection and analysis was performed using BD FACS Diva software. The percentage of the cell population in each phase of the cell cycle was determined by estimating the area under each part of the curve corresponding to each phase.

7.9 Electron microsopy

Cell samples were fixed overnight in fixative (3% gluteraldehyde and 4% formaldehyde in 0.1M PIPES buffer at pH 7.2). The fixed samples were then embedded in 5% sodium alginate. Approximately 0.75 mL of post fixative (2 mL OsO4 and 2 mL of 0.2 M PIPES) was added to the sample and placed in a rotator for 1 hour. Post fixative was removed and the sample washed twice with 0.1 M PIPES and once with water. The sample was stained with 1 mL of 2% uranyl acetate for 20 minutes. Following removal of the stain the sample was dehydrated in a graded ethanol series (use a series of ethanol concentrations from 30% to absolute). The ethanol was removed from the sample and replaced with acetonitrile for 10 minutes. Following infiltration of 50:50 acetonitrile:resin overnight the sample was left in resin for 6 hours. Finally the sample was embedded in fresh resin and polymerised at 60 °C. Thin sections were cut with a glass knife using an ultrami-

crotome and collected on metal grids. Sample grids were stained using Reynolds lead stain. Electron micrographs were obtained using a Hitachi H7000 TEM at 75 kV [6].

7.10 DNA extraction and quantification

Aqueous and solid fractions from Bligh Dyer phospholipid extraction were dried under nitrogen before use. DNA was isolated using a Promega Wizard SV kit. The sample was suspended in lysis buffer and transferred to minicolumn. DNA was bound to the column using centrifugation and washed four times with wash solution. The DNA was eluted from the column with nuclease free water. Detailed instructions included with the Wizard SV kit were followed. DNA concentration was quantified by measuring absorbance at 260 nm with a Thermo scientific nanodrop 1000 spectrophotometer using the DNA-50 setting. The nucleic acid concentration in ng/microlitre is calculated using the Beer-Lambert equation with an extinction coefficient of 50 mg-cm/μL. This calculation is performed automatically by the nanodrop 1000 software.

7.11 Radiochemical assessment of newly synthesised PC

An appropriate volume of methyl ^{14}C choline was added to each flask of cells to give an isotopic diultion of 5% and incubated at 37 °C for three hours. The phospholipid was extracted by the Bligh and Dyer method and the chloroform layer dried under nitrogen. The activity in counts per minute was measured by liquid scintillation counting on a Beckman LS 6500 scintillation counter.

References

[1] D. Zink, N. Sadoni, and E. Stelzer. Visualizing chromatin and chromosomes in living cells. *Methods*, 29:42–50, 2003.

[2] A. Hunt and A.D. Postle. Mass spectrometry determination of endonuclear phospholipid composition and dynamics. *Methods*, 39:104–111, 2006.

[3] J. M. Davis, editor. *Basic Cell Culture*. Oxford University Press, second edition, 2002.

[4] E.G. Bligh and W.J. Dyer. A rapid method of total lipid extraction and purification. *Can. J. Biochem. Physiol*, 37:911–917, 1959.

[5] J.C.M. Stewart. Colorimetric determination of phospholipids with ammonium ferrothiocyanate. *Biochemistry*, 104:10–14, 1980.

[6] Southampton University Hospital Biomedical Imaging Unit. Transmission Electron Microscopy. Postgraduate course handbook, 2008.

Appendix A

Appendices

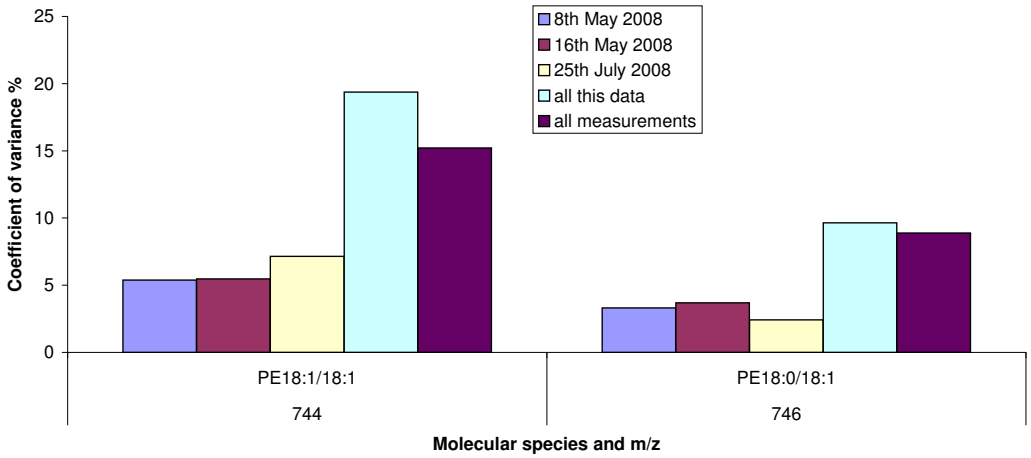

Figure A.1: Coefficient of variance for the standard mixture PE percentage composition results

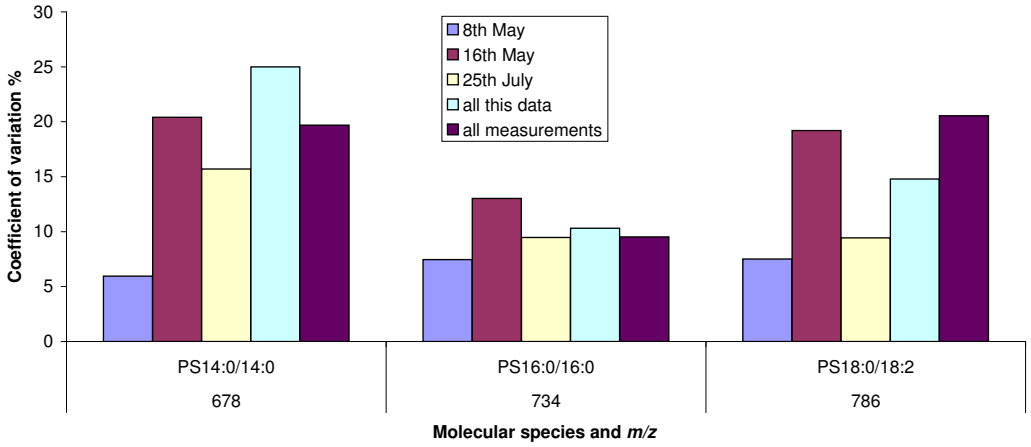

Figure A.2: Coefficient of variance for the standard mixture PS percentage composition results

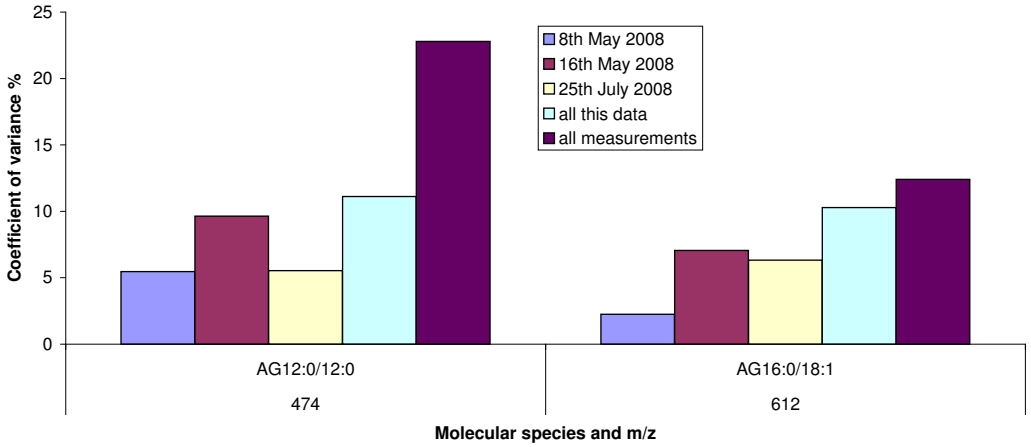

Figure A.3: Coefficient of variance for the standard mixture DAG percentage composition results

mass	Originally assigned species	Species found to be present by TOF analysis. In order of intensity					
		whole cells			nuclei		
716	PE16:0/18:2	16:1/18:1	16:0/18:2		18:1/16:1	16:0/18:2	
718	PE16:0/18:1	16:0/18:1	18:0/16:1		16:0/18:1	18:0/16:1	
740	PE16:0/20:4	20:4/16:0			16:0/20:4		
742	PE18:1/18:2	18:1/18:2	18:0/18:3		18:1/18:2	18:0/18:3	
744	PE18:0/18:2	18:1/18:1	18:0/18:2		18:1/18:1	18:0/18:2	16:0/20:2
746	PE18:0/18:1	18:0/18:1			18:0/18:1		
764	PE16:0/22:6	18:1/20:5	22:6/16:0		18:1/20:5	22:6/16:0	
766	PE18:1/20:4	18:1/20:4	22:5/16:0		18:1/20:4	20:5/18:0	16:0/22:5
768	PE18:0/20:4	18:0/20:4	20:3/18:1		18:0/20:4	20:3/18:1	
770	PE18:0/20:3	18:0/20:3			18:1/20:2	18:0/20:3	18:2/20:1
772	PE18:0/20:2	20:1/18:1	18:0/20:2		18:0/20:2	18:1/20:1	16:0/22:2
774	PE18:0/20:1	20:0/18:1	20:1/18:0		18:1/20:0	18:0/20:1	
788	PE18:0a/22:1	22:0a/18:1			22:0a/18:1		
790	PE18:0a/22:0	24:0a/16:0			18:0/22:0a		
792	PE18:0/22:6	18:0/22:6			18:0/22:6	18:2/22:5	
794	PE18:0/22:5	18:0/22:5			18:0/22:5	18:1/22:4	
796	PE18:0/22:4	22:3/18:1			18:1/22:3	18:0/22:4	
798	PE18:0/22:3	22:2/18:1			18:1/22:2		
800	PE18:0/22:2	18:1/22:1			18:1/22:1	18:2/22:0	18:0/22:2

Figure A.4: The NL141 (PE) molecular species composition for whole cells and nuclei. The species are presented in the order of decreasing intensity. The proportion of each species for a particular mass can not be quantified.

mass	Originally assigned species	Species found to be present by TOF analysis. In order of intensity			
		whole cells		nuclei	
572	AG16:0a/16:0				
584	AG16:0/16:1			16:0/16:1	
586	AG16:0/16:0	16:0/16:0		16:0/16:0	
598	AG16:0a/18:1				
600	AG16:0a/18:0				
610	AG16:0/18:2	16:1/18:1	16:0/18:2	16:1/18:1	
612	AG16:0/18:1	16:0/18:1		16:0/18:1	
614	AG16:0/18:0	16:0/18:0		16:0/18:0	
626	AG18:0a/18:1	18:0a/18:1			
636	AG18:1/18:2			18:1/18:2	
638	AG18:0/18:2	18:1/18:1	16:0/20:2	18:1/18:1	16:0/20:2
640	AG18:0/18:1	18:0/18:1	16:0/20:1	18:0/18:1	
642	AG18:0/18:0	18:0/18:0	20:0/16:0	18:0/18:0	
664	AG18:0/20:3				
666	AG18:0/20:2				
668	AG18:0/20:1	LCH18:1	16:0/22:1		
694	AG18:0/22:2	18:0/22:2			

Figure A.5: The NL35 (DAG) molecular species composition for whole cells and nuclei. The species are presented in the order of decreasing intensity. The proportion of each species for a particular mass can not be quantified.

mass	Originally assigned species	Species found to be present by TOF analysis. In order of intensity					
		whole cells			nuclei		
647	PA16:0/16:0	16:0/16:0			16:0/16:0	14:0/18:0	
673	PA16:0/18:1	16:0/18:1			16:0/18:1		
675	PA16:0/18:0	16:0/18:0			16:0/18:0		
695	PA16:0/20:4				18:1/18:3		
699	PA18:0/18:2	18:1/18:1	16:1/20:1	16:0/20:2	18:1/18:1	18:0/18:2	
701	PA18:0/18:1	18:0/18:1	16:0/20:1		18:1/18:0	16:0/20:1	
747	PA18:0/22:6	PG16:0.18:1			PG16:0/18:1		
759	PA18:0/22:0	PG18:1a/18:1			PG18:1a/18:1	PG18:0a/18:2	
773	PA20:0a/22:0	PG18:1/18:1	PG18:018:2		PG18:1/18:1	PG16:0/20:2	18:0/24:0a
775	PA20:0/22:6	PG18:0/18:1			PG18:0/18:1	PG16:0/20:1	PG16:1/20:0
781	PA20:3/22:0				PG16:0/22:5a		
789	PA22:0a/22:6	PG20:1a/18:0	26:6a/18:0		PG20:0a/18:1		
809	PA22:0/22:3	18:1/26:2			18:1/26:2		

Figure A.6: The P153 (PA) molecular species composition for whole cells and nuclei. The species are presented in the order of decreasing intensity. The proportion of each species for a particular mass can not be quantified.

mass	Originally assigned species	Species found to be present by TOF analysis. In order of intensity							
		whole cells				nuclei			
760	PS16:0/18:1	18:1/16:0	16:1/18:0			16:0/18:1	16:1/18:0		
774	PS18:0a/18:1	18:0a/18:1				18:0a/18:1	16:0/20:1a		
784	PS18:1/18:2	18:2/18:1				18:1/18:2	18:0/18:3		
786	PS18:0/18:2	18:1/18:1	18:0/18:2			18:1/18:1	18:2/18:0		
788	PS18:0/18:1	18:1/18:0				18:1/18:0			
802	PS18:0a/20:1	20:1a/18:0	18:0a/20:1			18:0/20:1a	18:1/20:0a	18:0a/20:1	
810	PS18:0/20:4	20:4/18:0	20:3/18:1			18:0/20:4			
812	PS18:0/20:3	20:3/18:0	20:2/18:1	18:2/20:1		18:0/20:3			
814	PS18:0/20:2	18:1/20:1	18:0/20:2	22:2/16:0		18:1/20:1	18:0/20:2		
816	PS18:0/20:1	20:1/18:0	20:0/18:1			18:0/20:1	18:1/20:0		
828	PS18:0a/22:2	22:1a/18:1	22:2a/18:0			18:1/22:1a	20:0a/20:2	20:1a/20:1	22:2a/18:0
834	PS18:0/22:6	22:6/18:0				18:0/22:6			
836	PS18:0/22:5	22:5/18:0				18:0/22:5			
838	PS18:0/22:4	22:4/18:0				20:0/20:4			
840	PS18:0/22:3	22:2/18:1	22:1/18:2			18:1/22:2	18:0/22:3	18:2/22:1	20:1/20:2
842	PS18:0/22:2	22:2/18:0	18:1/22:1			22:2/18:0	22:1/18:1	20:0/20:2	20:1/20:1
844	PS18:0/22:1	18:1/22:0				18:1/22:0	18:0/22:1		

Figure A.7: The NL87 (PS) molecular species composition for whole cells and nuclei. The species are presented in the order of decreasing intensity. The proportion of each species for a particular mass can not be quantified.

mass	Originally assigned species	Species found to be present by TOF analysis. In order of intensity					
		whole cells			nuclei		
833	PI16:0/18:2	16:1/18:1	18:2/16:0		16:1/18:1		
835	PI16:0/18:1	16:0/18:1	16:1/18:0		16:0/18:1	16:1/18:0	
837	PI16:0/18:0	16:0/18:0			16:0/18:0		
849	PI18:0a/18:1	18:1a/18:0	18:0a/18:1		18:0a/18:1	18:1a/18:0	
859	PI18:1/18:2	18:2/18:1	16:0/20:3		18:2/18:1	18:3/18:0	
861	PI18:0/18:2	18:1/18:1	18:2/18:0	20:2/16:0	18:1/18:1	18:2/18:0	
863	PI18:0/18:1	18:1/18:0			18:0/18:1		
865	PI18:0/18:0	18:0/18:0			18:0/18:0		
875	PI18:0a/20:2	20:1a/18:1	20:2a/18:0	18:0a/20:2	20:1a/18:1	20:2a/18:0	
883	PI18:1/20:4	20:4/18:1	20:5/18:0		18:1/20:4	22:5/16:0	
885	PI18:0/20:4				18:0/20:4	20:3/18:1	
887	PI18:0/20:3	18:1/20:2	20:3/18:0		20:2/18:1	20:3/18:0	
889	PI18:0/20:2	18:0/20:2	20:1/18:1		18:0/20:2	20:1/18:1	
891	PI18:0/20:1	20:1/18:0	20:0/18:0		20:1/18:0		

Figure A.8: The P241 (PI) molecular species composition for whole cells and nuclei. The species are presented in the order of decreasing intensity. The proportion of each species for a particular mass can not be quantified.

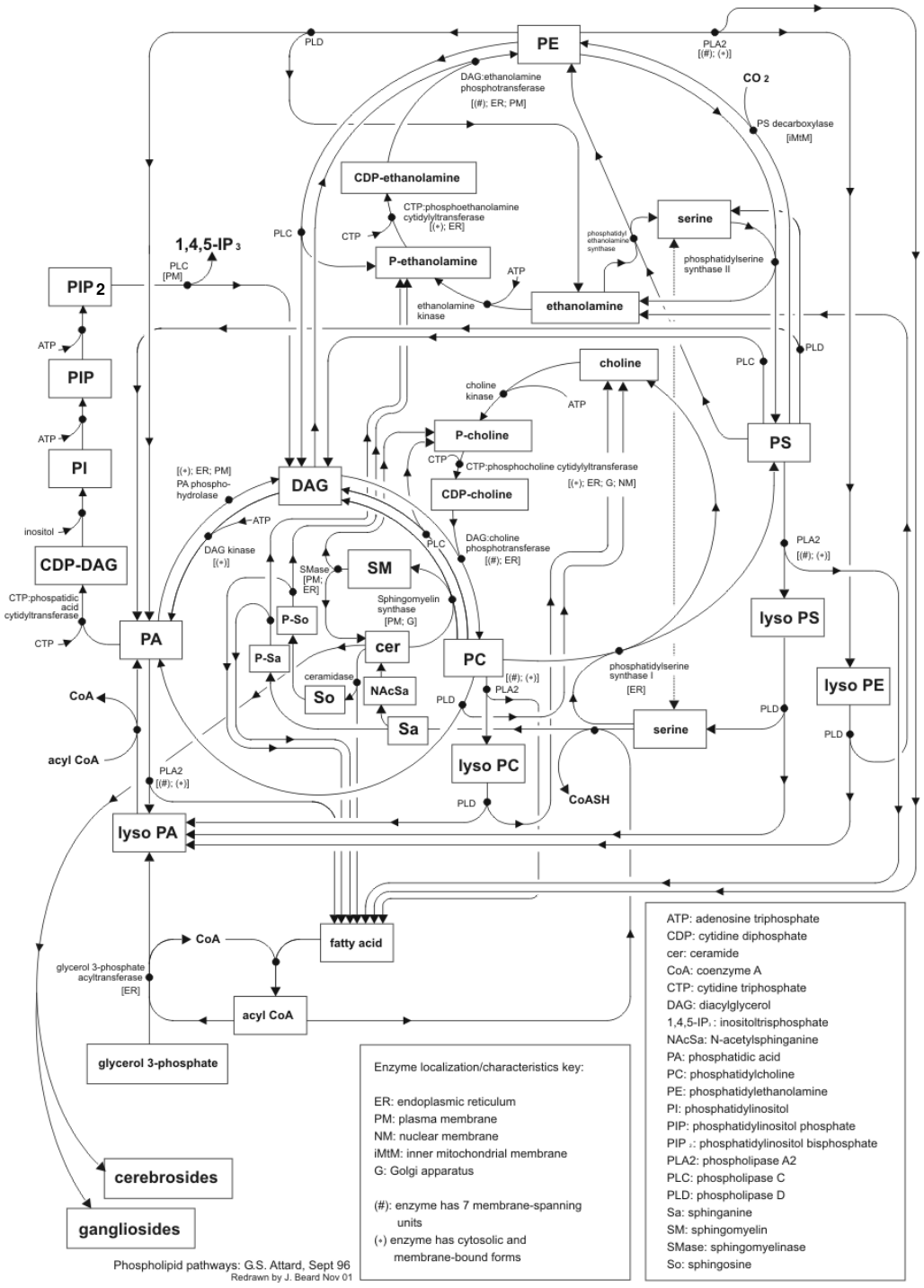

Figure A.9: Phospholipid biosynthetic pathways. (Diagram by G.S Attard, Sept 96 and redrawn by J. Beard, Nov 01)

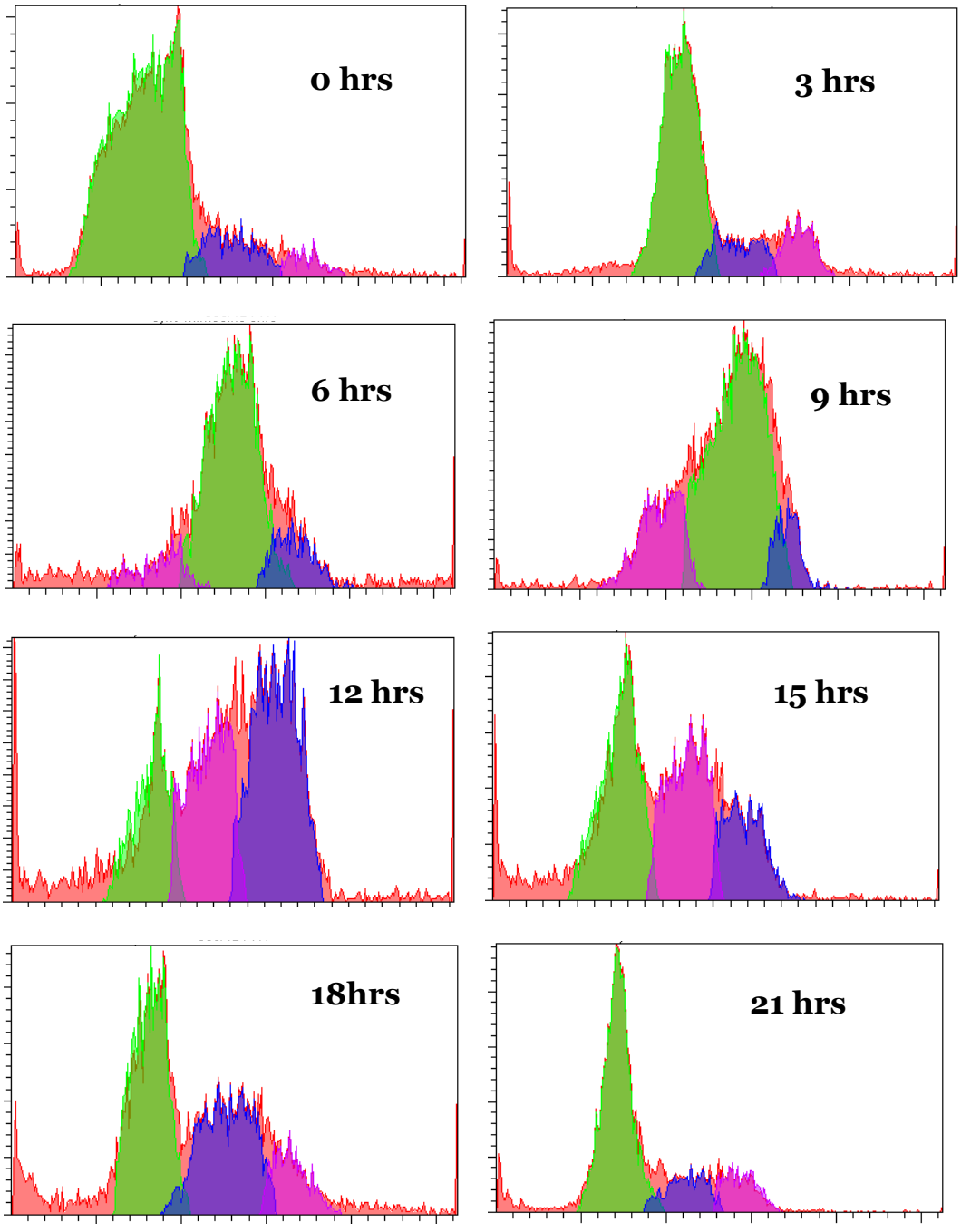

Figure A.10: Typical FACS plots at time points following synchronisation with mimosine

Appendix B

Mass spectrometry data

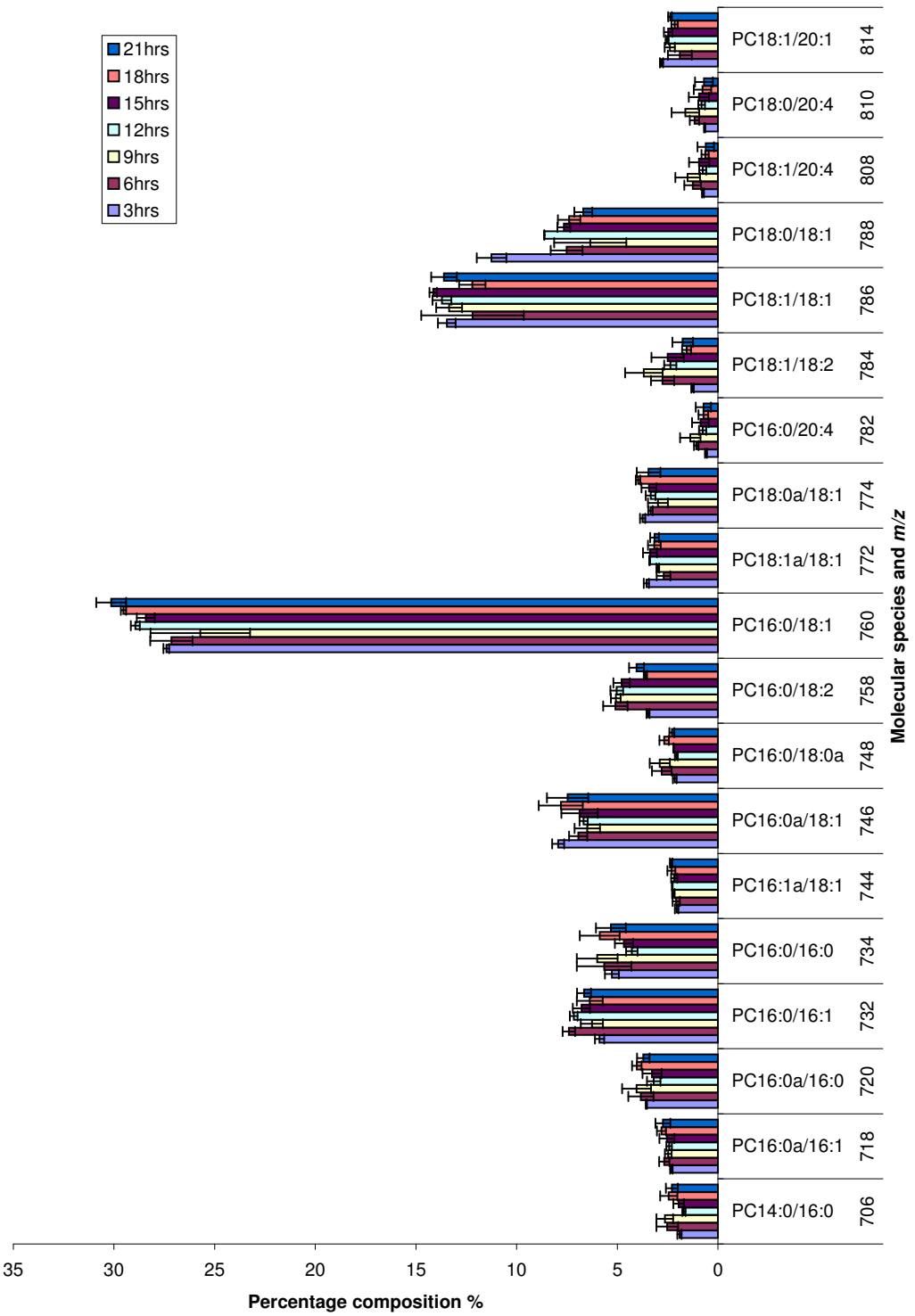

Figure B.1: Molecular species percentage composition of PC for synchronised whole cells (data set 1)

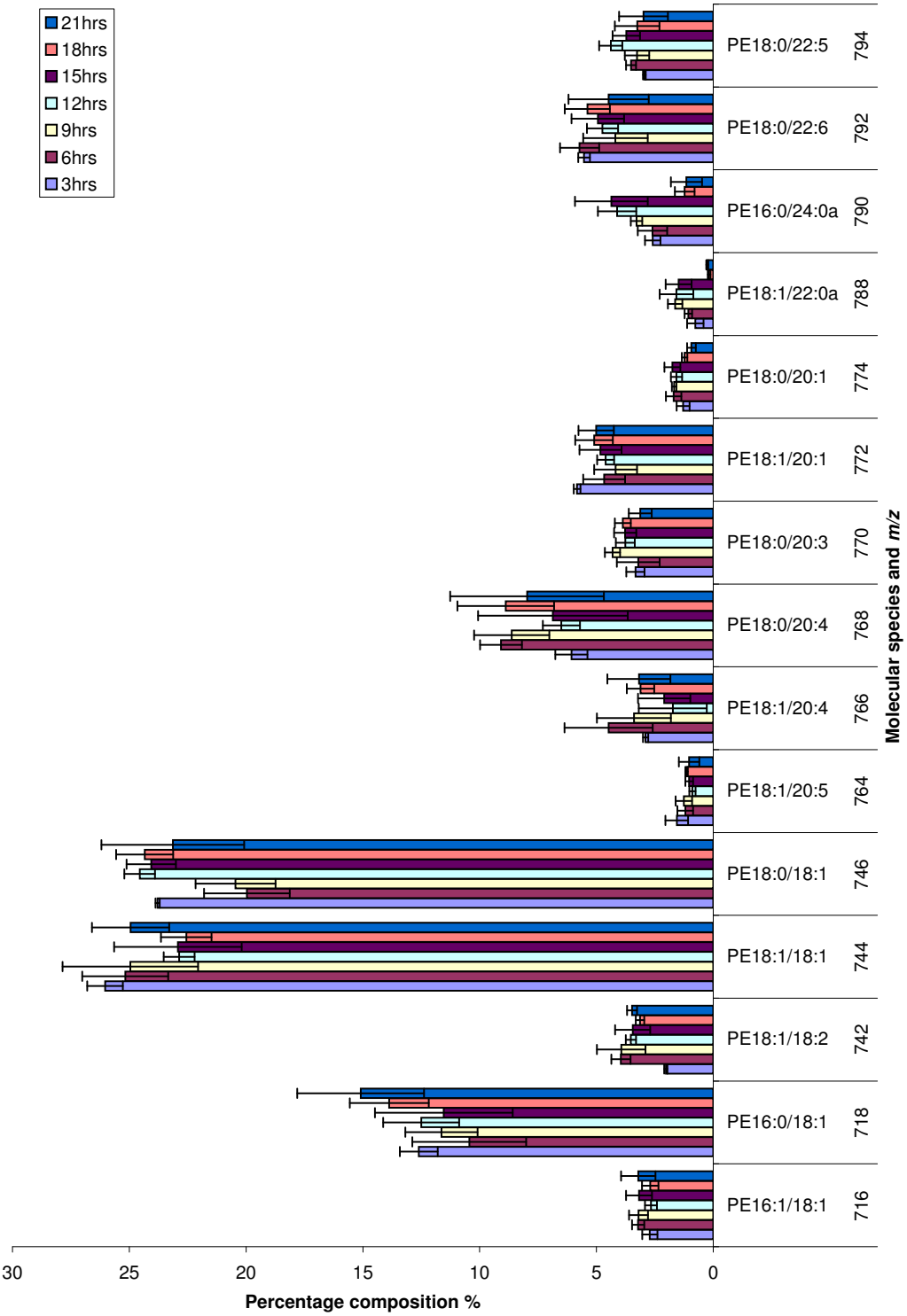

Figure B.2: Molecular species percentage composition of PE for synchronised whole cells (data set 1)

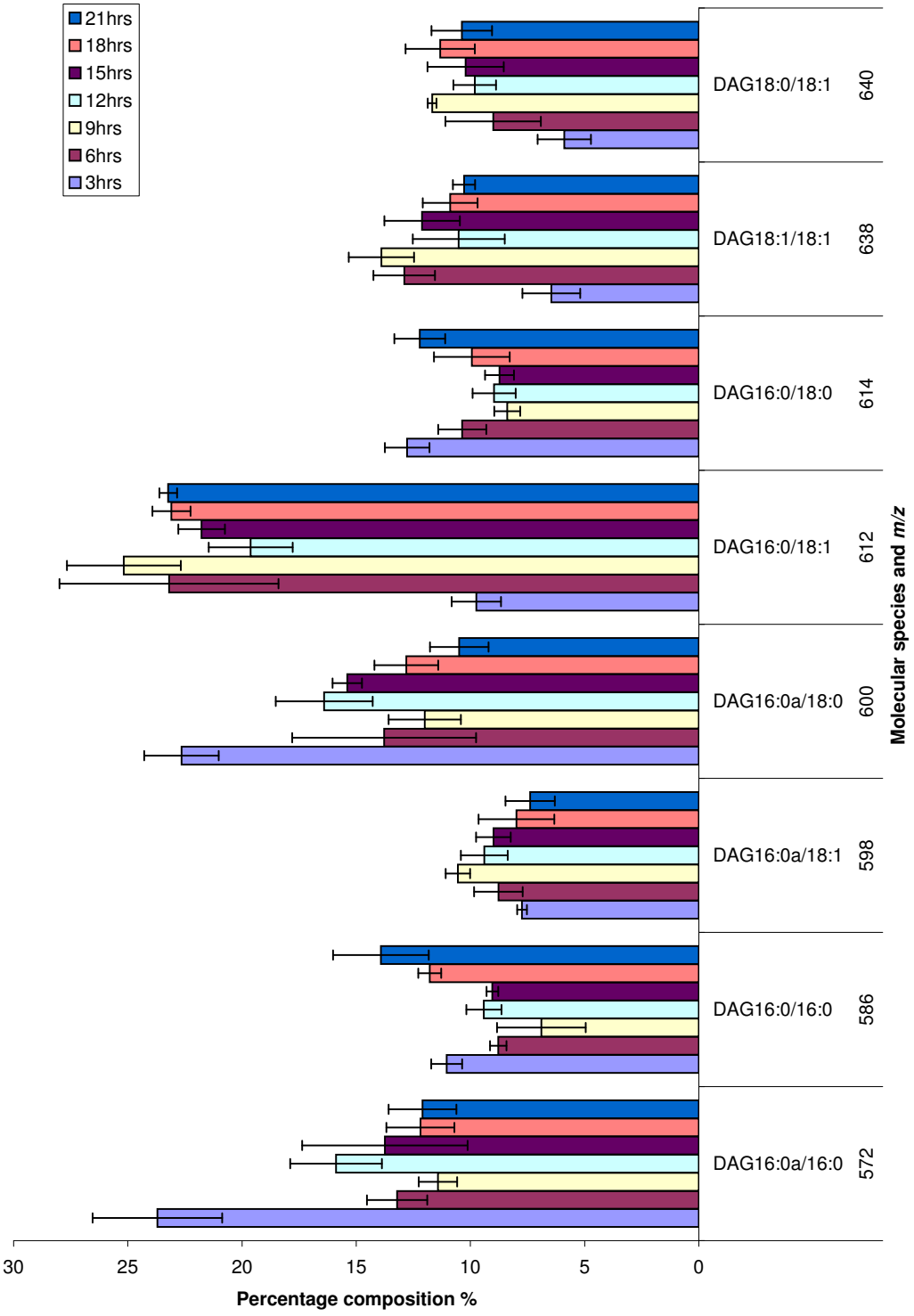

Figure B.3: Molecular species percentage composition of DAG for synchronised whole cells (data set 1)

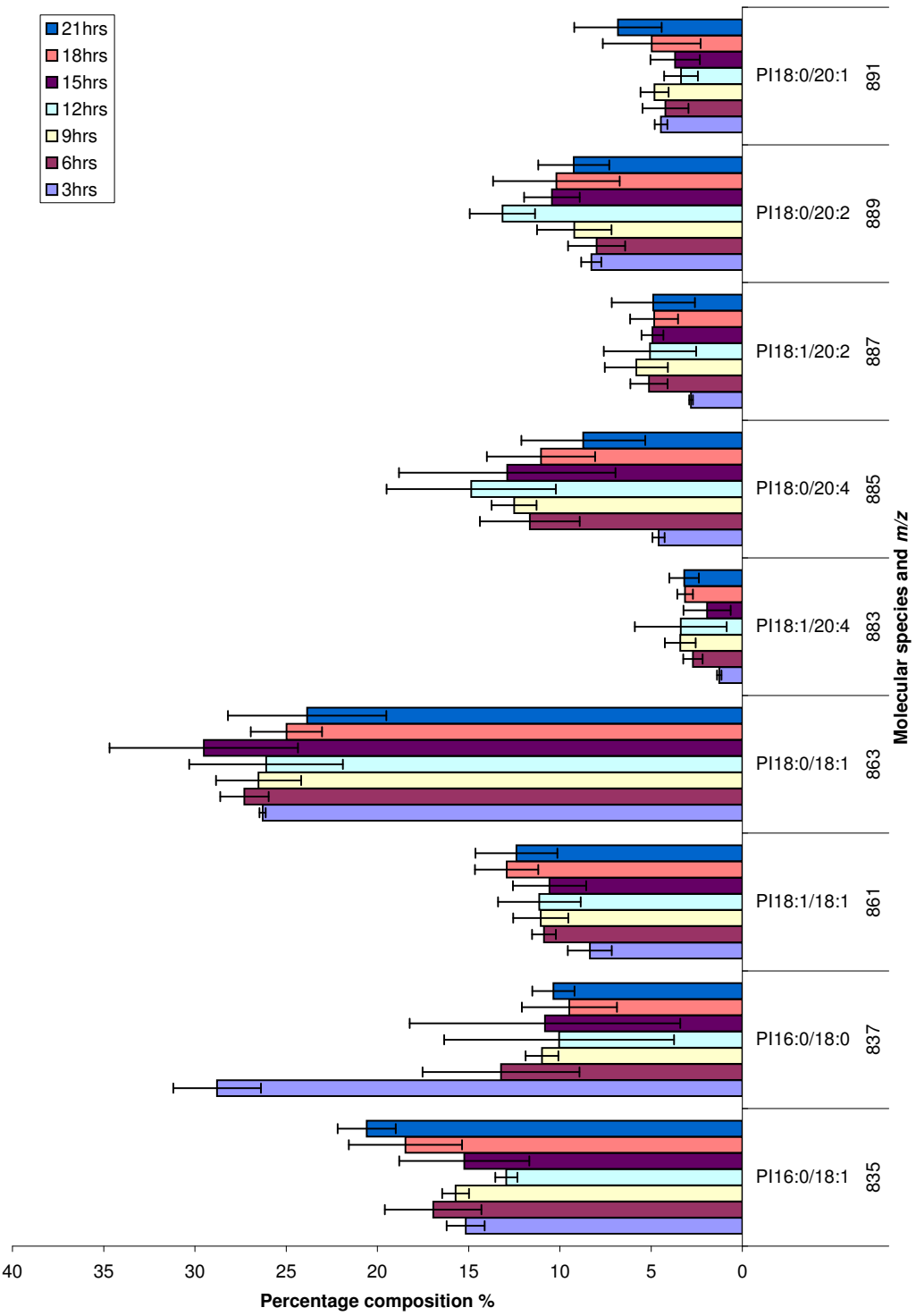

Figure B.4: Molecular species percentage composition of PI for synchronised whole cells (data set 1)

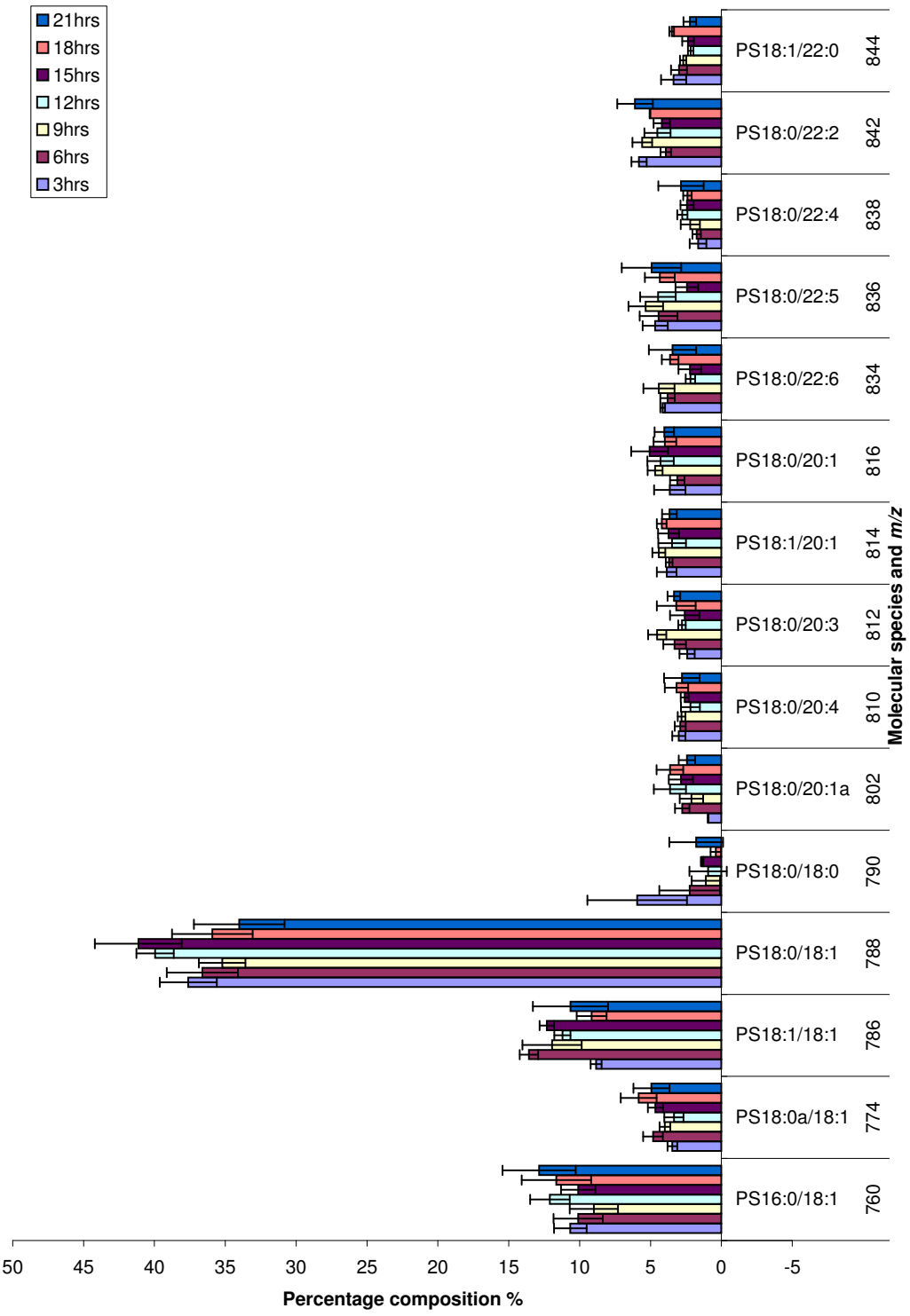

Figure B.5: Molecular species percentage composition of PS for synchronised whole cells (data set 1)

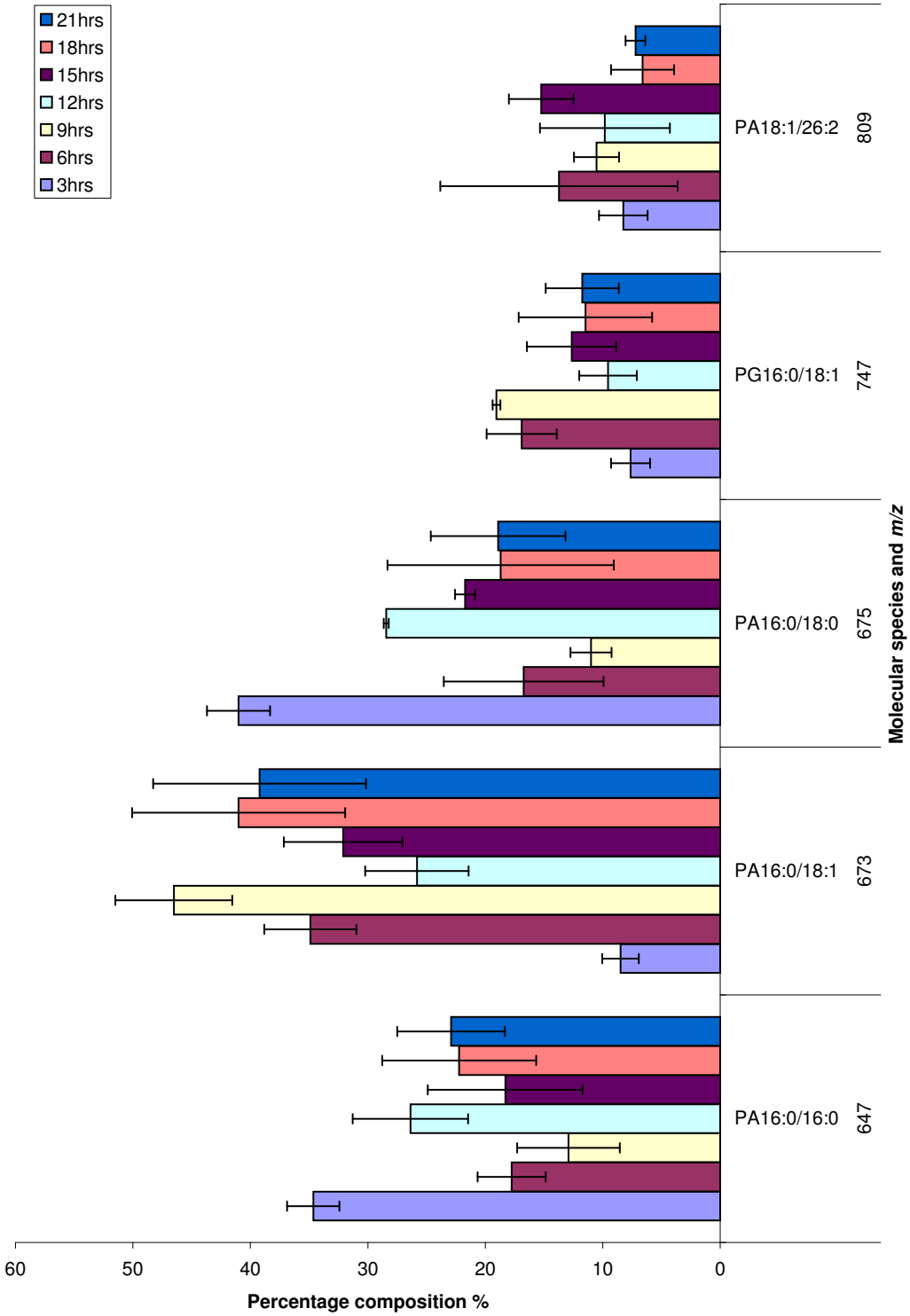

Figure B.6: Molecular species percentage composition of PA for synchronised whole cells (data set 1)

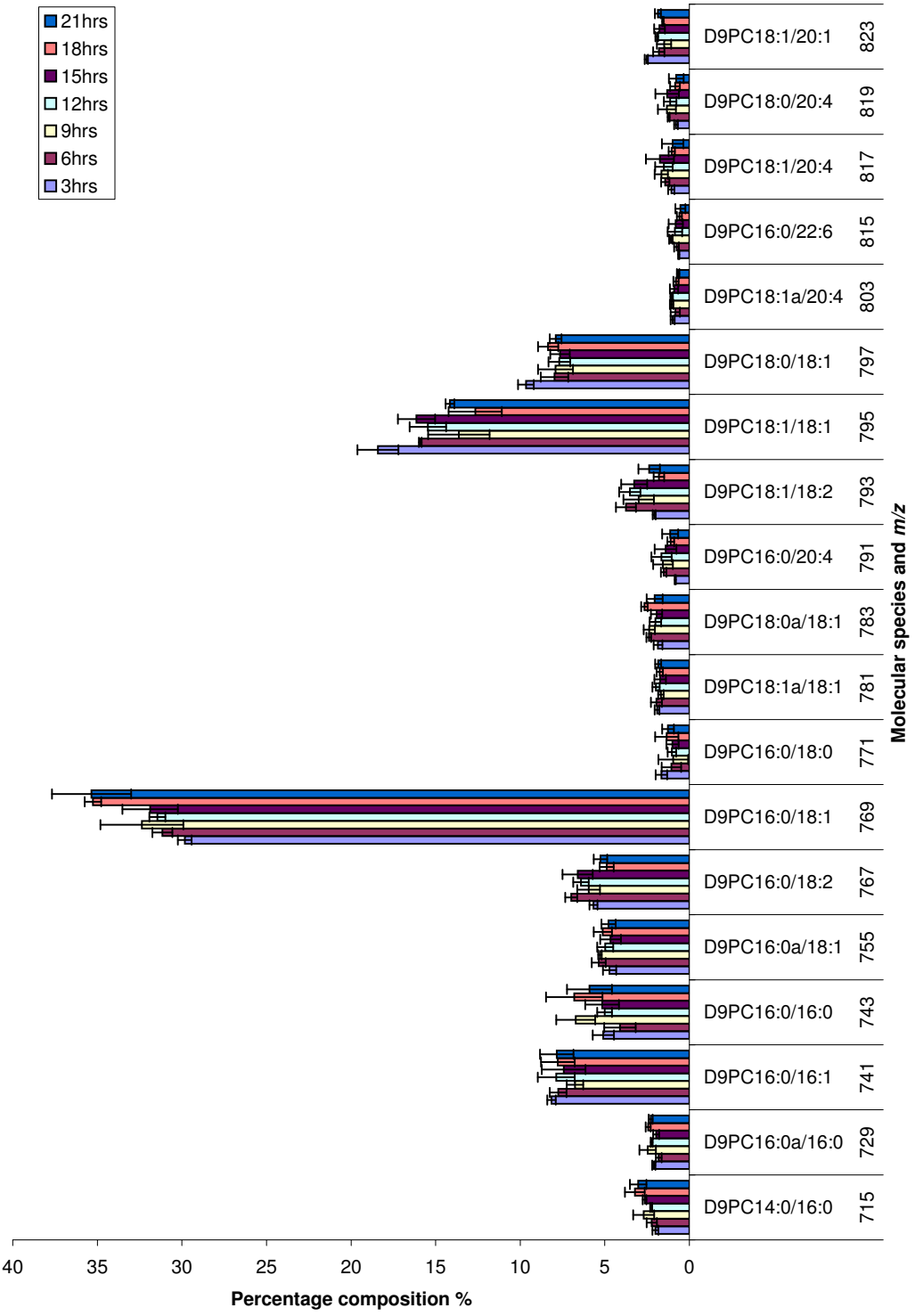

Figure B.7: Molecular species percentage composition of d9PC for synchronised whole cells (data set 1)

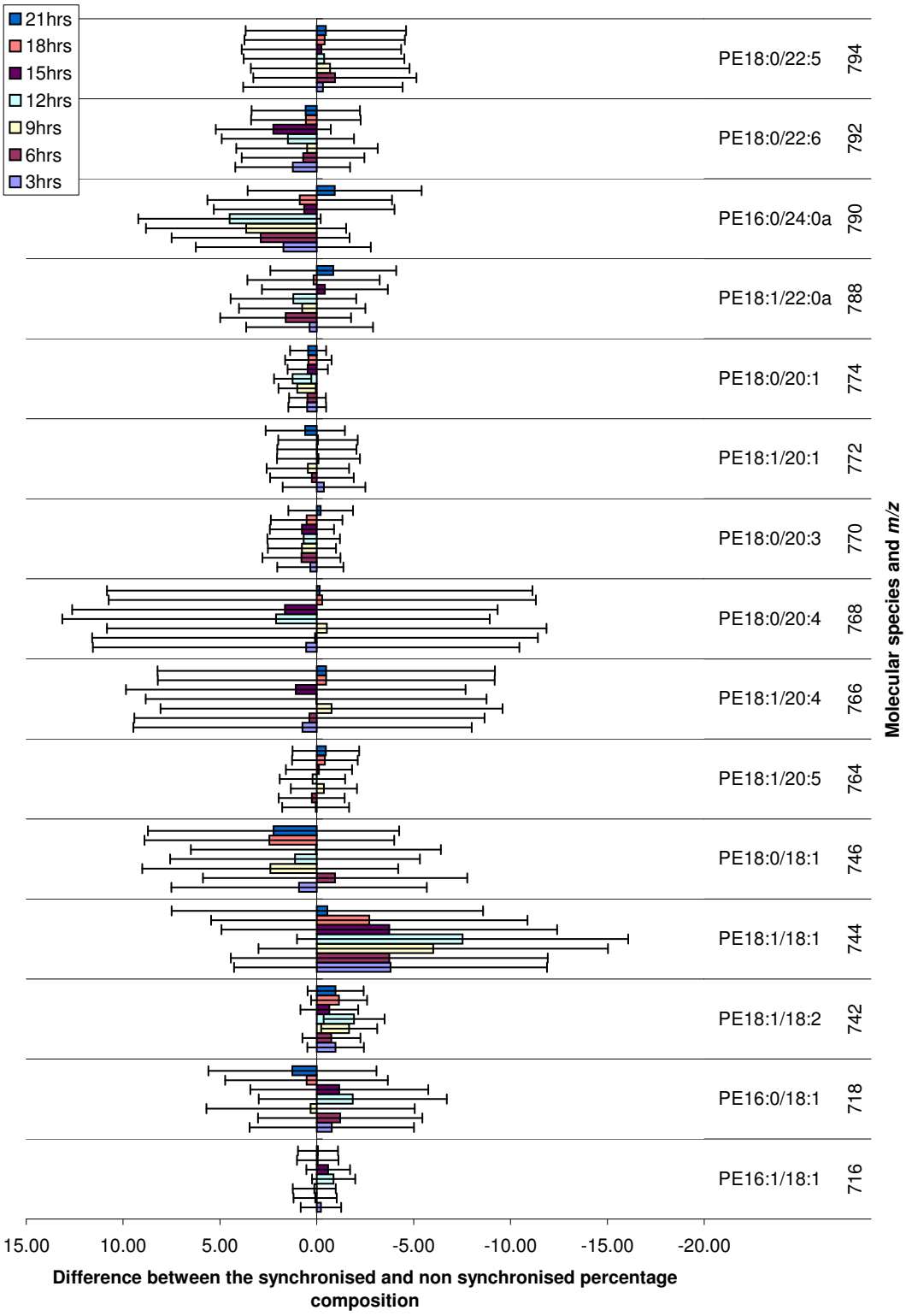

Figure B.8: Difference between synchronised and non synchronised percentage composition PE. Data set 2